

**UNIVERSITY OF NAPLES "FEDERICO II"**



**PhD Program in Neuroscience**

**XXXII Cycle**

***ROLE OF MITOCHONDRIA IN THE  
ACTIVATION OF NEUROINFLAMMATION IN  
ANIMAL MODELS OF  
ALPHA-SYNUCLEINOPATHIES***

**Coordinator:**

**Prof. Maurizio Tagliatela**

**Tutor:**

**Prof. Antonella Scorziello**

**PhD Student:**

**Rossana Di Martino**

**ACADEMIC YEAR 2018-2019**

# SUMMARY

LIST OF ABBREVIATION.....	3
1. BACKGROUND .....	7
2. PATHOGENESIS OF PARKINSON'S DISEASE	
2.1. Mitochondrial dysfunction during Parkinson's Disease.....	13
2.2. Calcium homeostasis and neurodegeneration .....	22
2.3. Role of $\alpha$ -synuclein in the pathogenesis of Parkinson's Disease.....	29
2.4. Neuroinflammation in Parkinson's Disease.....	39
3. SODIUM CALCIUM EXCHANGER (NCX)	
3.1. Structural and functional features of NCXs.....	48
3.2. Role of NCXs in physiological and pathological condition.....	53
4. AIM OF THE STUDY .....	57
5. EXPERIMENTAL PROCEDURES	
5.1 <i>In vivo and in vitro models</i>	
5.1.1 PrP- A53T $\alpha$ -synuclein transgenic mice.....	62
5.1.2 PDGF- h- $\alpha$ -synuclein Transgenic mice .....	62
5.1.3 Primary neurons from PrP-A53T $\alpha$ -synuclein transgenic mice.....	64
5.1.4 Primary astrocytes from PrP-A53T $\alpha$ -synuclein transgenic mice.....	65
5.1.5 Microglia from PDGF-h- $\alpha$ synuclein transgenic mice.....	65
5.2 Western Blot analysis .....	67
5.3 Mitochondrial $[Ca^{2+}]_{mit}$ , cytosolic $[Ca^{2+}]_{cit}$ calcium concentrations and mitochondrial membrane potential measurements .....	68

<b>5.4 Mass Spectrometry</b>	
5.4.1 Preparation of the isolated microglial cells for Mass Spectrometry.....	70
5.4.2 Proteomic profile of isolated microglia from transgenic PDGF- h- $\alpha$ -synuclein mice.....	71
<b>5.5 Statistical Analysis .....</b>	<b>72</b>
<b>6. RESULTS</b>	
6.1. The decrease of NCX3 expression is correlated to mitochondrial dysfunction in mesencephalic neurons in A53T $\alpha$ -synuclein transgenic mice.....	73
6.2. The onset of neuroinflammation in transgenic A53T $\alpha$ -synuclein mice is associated with differences in NCXs expression during ageing .....	77
6.3. Microglial proteomic profile from young and adult PDGF-h- $\alpha$ -synuclein transgenic mice reveals a relationship between mitochondrial dysfunction and impairment in synaptic plasticity.....	85
<b>7. DISCUSSION .....</b>	<b>118</b>
<b>8. BIBLIOGRAPHY .....</b>	<b>124</b>

## ***LIST OF ABBREVIATION***

6-OHDA: 6-hydroxydopamine

AD: Alzheimer's Disease

AMP: Antimicrobial Peptides

ASC: Adaptor molecule Apoptosis-associated speck-like protein containing a CARD

ATP: Adenosine Triphosphate

CaM: calmodulin

CB-28: Calbindin K28

CNS: Central Nervous System

CR: calretinin

CSF: Cerebrospinal Fluid

CYT-C: Cytochrome-c

DA: Dopamine

DAT: Dopamine Transporter

DIV: days in vitro

DLB: Dementia with Lewy Bodies

DRP1: Dynamin-1-like

ER: Endoplasmic Reticulum

ETC: Electron Transport Chain

FADH: Flavin Adenine Dinucleotide

Fis1: Mitochondrial Fission-1

GFAP: Glial Fibrillary Acidic Protein

HLA-DR: Human leukocyte antigen

HSV-1: Herpes Simplex virus 1

IBA-1: Ionized Calcium-Binding Adapter molecule 1

ICAM-1: Intracellular Adhesion Molecule 1

IFN- $\gamma$ : Interferon-gamma

IL-10: Interleukin-10

IL-12: Interleukin-12

IL-13: Interleukin-13

IL-18: Interleukin-18

IL-1 $\beta$ : Interleukin- 1 beta

IL-4: Interleukin-4

IL-6: Interleukin-6

IMM: Inner Mitochondrial Membrane

iNOS: Inducible Nitric oxide synthases

LB: Lewy Body

LC3-II: Microtubule-associated protein light chain 3

L-DOPA: L- 3,4-DiOxyPhenylAlanine

LPS: Lipopolysaccharides

MAM: Mitochondrial Associated Membrane

MAOA and MAOB: Monoamine oxidase A or B

Mfn: Mitofusin

MnSOD: Manganese Superoxide Dismutase

MPTP: 1-methyl-4-phenyl- 1,2,3,4-tetrahydropyridine

mPTP: Mitochondrial Membrane Permeability Transition Pore

MS: Mass Spectrometry

MSA: Multiple System Atrophy

mtDNA: mitochondrial DNA

MV: Micro Vesicles

MVB: Multivesicular Body

NADH: Nicotinamide Adenine Dinucleotide

NCX1: sodium-calcium Exchanger isoform 1  
NCX2: sodium-calcium Exchanger isoform 2  
NCX3: sodium-calcium Exchanger isoform 3  
NLRP3 or cryopyrin: NACHT, LRR and PYD domains Protein 3  
nNOS: Neuronal Nitric oxide synthases  
NO: Nitrogen oxide  
Omi/HTRA2: Mitochondrial serine protease 2  
OMM: Outer Mitochondrial Membrane  
OPA-1: Mitochondrial dynamin-like GTPase  
P62: sequestosome-1  
PARK1-4 or SNCA: gene  $\alpha$ -synuclein  
PARK2 or PARKIN: E3 ubiquitin ligase  
PARK6 or PINK1: PTEN-induced kinase 1  
PARK7 or DJ-1: Protein deglycase DJ-1 or Parkinson disease protein 7  
PARK8 or LRRK2: Leucine-rich repeat kinase  
PD: Parkinson's Disease  
PDGF- $\beta$ : Platelet-Derived Growth Factor- $\beta$   
PET: Positron Emission Tomography  
PMCA: Plasma Membrane Calcium ATPase  
PrP<sup>Sc</sup>: Prion Protein  
PV: parvalbumin  
ROS: Reactive Oxygen Species  
RyR: Ryanodine receptor  
SERCA: Sarco-Endoplasmatic reticulum ATPase  
SNARE: Complex of syntaxin, VAMP and SNAP-25  
SNCB: gene  $\beta$ -synuclein  
SNCG: gene  $\gamma$ -synuclein

SNpc: Substantia nigra Pars Compacta

SPCA: Secretory Pathways Ca<sup>2+</sup>- ATPase

TCA: tricarboxylic acid

TG: Transgenic

TGF-  $\beta$ : Transforming Growth Factor beta

TNF- $\alpha$ : Tumour Necrosis Factor-alpha

TNT: Tunnelling Nanotube

TSPO: Translocator protein 18KDa

VDAC: Voltage-dependent Anion Channel

VTA: Ventral Tegmental area

WT: Wild Type

## 1. **BACKGROUND**

Parkinson's Disease (PD) is a chronically progressive, age-related neurodegenerative pathology characterized by resting tremor, rigidity, bradykinesia, gait disturbance, postural instability and dementia (Hausdroff, 2009). The major neuropathological feature of PD is degeneration of dopamine neurons in the *substantia nigra pars compacta* (SNpc) and in other brainstem regions (Scalzo et al., 2010; Obeso et al., 2000). Lewy bodies and Lewy neurites are a second neuropathological feature of PD. These are eosinophilic cellular inclusions comprising a dense core of filamentous material which mainly consists of  $\alpha$ -synuclein (Cookson, 2005; Burch and Sheerin, 2005; Spillantini et al., 1997)

The annual incidence rate of the disease has been estimated to range from 16 to 19 per 100.000 persons affected, mainly over 50 years, with prevalence and incidence rates increasing with age (Pahwa and Lyons, 2010). Incidence of the disease is approximately 1.8 times higher in men versus women (Twelves et al., 2003; Van Den Eeden et al., 2003). Age is the greatest risk factor for PD with the number of worldwide cases increasing from an estimated 4.1 million in 2005 to nearly 8.7 million within 2030 (Dorsey et al., 2007).

PD was described for the first time in 1817 by James Parkinson as the "shaking palsy", but only in 1912, Fritz Heinrich Lewy demonstrated the presence of intracellular inclusions in the brains of patients affected by PD (Rodrigues et al., 2010; Engelhardt et al., 2017). However, the identity of these inclusions was revealed by Konstantin Tretiakoff who coined the term "corps de Lewy" as a tribute to Lewy's first observation. Moreover, the studies performed by Tretiakoff and those performed by Foix and Nicolesco allowed identifying SNpc as the brain region affected by neurodegeneration responsible for PD (Lees et al., 2008; Gonzalez-Hernandez et al., 2010). In the following years, Arvid Carlsson and



colleagues identified dopamine as a neurotransmitter enriched in the basal ganglia (Carlsson et al., 1957; Bertler and Rosengren, 1959). All these discoveries were further confirmed by the studies from Oleh Hornykiewicz who demonstrated the loss of dopamine in PD brains (Ehringer and Hornykiewicz, 1998) and more interestingly, that the replacement of dopamine, by administering the precursor, levodopa (L-DOPA), was able to alleviate PD symptoms (Birkmayer and Hornykiewicz, 1961). Since then L-DOPA still represents the first pharmacological support for treating this disease.

By a clinical point of view, PD is a heterogeneous disease which develops in different ways patient to patient, but only some time is associated with dementia. Subtypes may be recognized on the basis of age of onset, predominant clinical features and progression rate. There are two principal clinical subtypes: a tremor predominant form that is often found in young people, and a type, often observed in elder people (>70 years old), characterized by a postural imbalance, gait disorders, akinesia and rigidity. The first subtype leads to a slow decline of motor function, whereas the second subtype worsens more rapidly (Obeso et al., 2010). The clinical diagnosis of PD is typically based on the presence of cardinal motor features, absence of atypical findings suggestive of an alternative diagnosis, and response to levo-3, 4-dihydroxyphenylalanine (L-DOPA) (Perfeito et al., 2013).

Nowadays, it is possible to identify two kinds of symptoms in patients affected by PD: the “Non-Motor Manifestations of Parkinson disease” and the classical “Motor Manifestations of Parkinson disease”. The Non-Motor symptoms include autonomic, behavioural, cognitive, olfactory, sensory, sleep and visual deficits which occur in the 80–90% of patients affected by PD (Shulman et al., 2002). They may manifest before, coincident with, or

after the classic motor symptoms of the disease and are important to recognize patients in the early phase of their disease (Gallagher et al., 2010). Lewy pathology has been extensively studied in different clinical stages of typical idiopathic PD using  $\alpha$ -synuclein immunohistochemistry (Braak and Braak, 2000; Braak et al., 2002, 2003, 2004, 2006; Braak and Del Tredici, 2008). In particular, the observations reported by Braak in 2003, suggest that  $\alpha$ -synuclein deposition follows a *caudo-rostral* distribution with an initial localization in the olfactory bulb, in the enteric nervous system and in the brainstem, the areas mainly involved in early pre-motor stage of disease, and a final accumulation in the locus coeruleus (Braak et al., 2003). The SNpc, most often associated with the motor symptoms of PD, becomes involved later at approximately stage 3 of 'Braak and Braak' classification (Braak and Braak, 2003). Finally, the cortical involvement is most evident at the terminal stage of the disease and is characterized by intracytoplasmic  $\alpha$ -synuclein-positive neuronal inclusions, dystrophic  $\alpha$ -synuclein-positive Lewy neurites and astrocytic inclusions. According to Braak 's hypothesis, PD might be considered as "prion-like-disease", in term of propagation in the brain, with an environmental/pathogenic factor represented by misfolded  $\alpha$ -synuclein deposition at the level of the olfactory bulb and/or gut and, with a slowly progressing to the CNS.

It is believed that many cellular mechanisms may be involved in the pathogenesis of PD. They may take place inside the degenerating neurons and are identified as cell-autonomous processes, or outside the degenerating neurons and are identified as non-cell-autonomous processes. Cell-autonomous mechanisms leading to PD include oxidative stress, protein aggregation, defects in the ubiquitin-proteasome pathway, autophagy, and, in the last decade, the alterations in mitochondrial function. In particular, mutations in three proteins encoded by genes, namely parkin (PARK2), DJ-1 (PARK7), and PINK1 (PARK6), are

associated with recessive early-onset forms of PD, whereas mutations in  $\alpha$ -synuclein (PARK1-4) and LRRK2 (PARK8) are responsible for dominant forms of familial PD. The activity and cellular distribution of the proteins encoded by these genes are different and still not completely elucidated. PINK1 and LRRK2 are kinases, DJ-1 is a multifunctional protein that acts as peptidase, chaperone, redox/oxidative sensor, transcriptional modulator, and oncogene. Parkin is an E3-ubiquitin ligase and,  $\alpha$ -synuclein, in addition to being the principal component of Lewy bodies, plays an important role in the regulation of vesicles trafficking (Bueler, 2009). Among these proteins, PINK1 and Parkin play crucial roles in the regulation of mitochondrial dynamics and function in PD (Gandhi et al., 2009; Perier and Vila, 2012). Mutations in DJ-1 and Parkin render animals more susceptible to oxidative stress (Chang et al., 2014; Thomas et al., 2011). Moreover, a mitochondrial association of  $\alpha$ -synuclein was also linked to impairment of respiratory complex I activity, oxidative modification of mitochondrial proteins, and increased levels of  $\text{Ca}^{2+}$  (Cannon et al., 2013; Liu et al., 2009; Li et al., 2013). Alterations in the mitochondrial complex I are also found in autaptic samples of substantia nigra from patients affected by PD in which the activity of complex I was shown to be reduced (Parker et al., 2008). As mentioned above, many pieces of evidence described in the literature seem to converge on mitochondria as a primary target in the process of dopaminergic neuronal loss observed in PD. Any alteration in the mitochondrial functionality seems to deeply affect the ability to support cellular stresses, thus making the cells more susceptible to additional insults. Therefore, dysfunction in mitochondria results in a deficit supply of cellular energy and in a failure in maintaining cellular homeostasis with particular regards to calcium homeostasis. These events play a central role in apoptotic and necrotic cell death pathway leading to neurodegeneration in PD (Ghosh et al., 1999; Banerjee et al., 2009).

Among the cell-autonomous mechanisms underlining the onset and progression of this disease, the electrophysiological characteristics of the nigral dopaminergic neurons play a fundamental role (Chan et al., 2007; Guzman et al., 2010). Dopaminergic neurons are autonomously active, being characterized by a pace making activity responsible to generate action potentials also in the absence of synaptic input. This activity exposes dopaminergic neurons to large  $Ca^{2+}$  influx (Surmeier et al., 2009). Furthermore, it has been reported that increased activity of several classes of  $Ca^{2+}$  channels including L-type voltage-dependent and cyclic nucleotide-sensitive channels seems to play a key role in the pathogenesis of PD, leading to an alteration of intracellular  $Ca^{2+}$  homeostasis. Moreover, the recent observation that cells deficient in Complex-I showed an alteration in the cytosolic calcium handling, reduced mitochondrial calcium accumulation and consequent ATP synthesis (Guzman et al., 2010) suggested a possible relationship between mitochondrial dysfunction and perturbation of intracellular calcium homeostasis in the pathogenesis of PD.

Among the non-cell-autonomous processes leading to PD, the interactions between neuronal and non-neuronal cells are considered as the pathogenic mechanism involved in neurodegeneration observed in the disease progression. In fact, PD post-mortem brains also display increased gliosis (McGeer et al., 1988; McGeer and McGeer, 2008). Gliosis refers either to an increase in the number or in the activation state of astrocytes and microglial cells. Both of these glial cell types can respond to injury with changes in their morphology and with the production and secretion of inflammatory molecules (Colton and Wilcock, 2010; Klegeris et al., 2007; Lee et al., 2009; Olson, 2010). McGeer et al. (McGeer et al., 1988) have reported an increase in the human class II major histocompatibility complex antigen, HLA-DR, positive microglia within the SNpc of post-mortem PD brains (Przedborski

et al., 2007). Finally, several studies demonstrate that misfolded forms of  $\alpha$ -synuclein can directly activate microglia, further linking  $\alpha$ -synuclein and neuroinflammation to PD progression (Zhang et al., 2005; Klegeris et al., 2008; Su et al., 2008, 2009). However, post-mortem studies do not allow the determination of whether neuroinflammation participates in neuronal degeneration or merely represents a consequence of it. Therefore, the molecular mechanisms responsible for microglial activation as well as its role in the pathogenesis of neurodegeneration occurring in PD progression is still a matter of debate (Benner et al., 2004).

In the light of these premises, the present study has been undertaken in order to clarify the molecular and cellular events leading to neuronal dysfunction in PD with particular regard to the role played by mitochondria in the triggering neuroinflammation as the pathogenic mechanism involved in disease progression.

## 2. PATHOGENESIS OF PARKINSON'S DISEASE

### *2.1 Mitochondrial dysfunction during Parkinson's Disease*

Mitochondria are ubiquitous organelles found in most eukaryotic cells, which plays several important cellular functions, such as the production of energy by oxidative phosphorylation, the regulation of calcium homeostasis, and the control of programmed cell death.

Mitochondria are the only structures within the cells that are surrounded by a double membrane. The two membranes differ in protein and lipid composition and in their functional roles. The outer mitochondrial membrane (OMM) is characterized by the presence of  $\beta$ -barrel pore-forming proteins (named porins) that make it permeable to solute up to 5 kDa, while the inner mitochondrial membrane (IMM) is highly selective since it is impermeable to ions and to most hydrophilic molecules. In term of composition, the IMM is characterized by an elevated proteins content, in fact, in addition to carrier proteins, it includes also the proteins of the electron transport chain (ETC) and the ATP synthase. The IMM surface is enormously enhanced by a process of membrane invagination called cristae, which can host a large number of ETC complexes and ATP synthases, thus expanding the capacity of the cells to generate ATP in an extremely confined space. (Perier and Vila, 2012; Fernandez-Vizarra et al., 2009) (Fig. 1).

The ETC complex is composed to five multi-subunits proteins: three of them, the complexes I, III and IV, which pump protons ( $H^+$ ) across the inner membrane thus establishing an electrochemical gradient that is responsible for a membrane potential negative inside. Along with ETC complexes, electrons are transported from the reduced substrates (NADH and  $FADH_2$ ) to the oxygen that is converted in  $H_2O$ . Complex V, the ATP synthase, uses

the electrochemical gradient generated across the IMM to produce ATP, by coupling the entry of protons to ADP phosphorylation. The electron transport, especially at complex I and III levels, also generates the free radical superoxide ( $O_2^-$ ), which, by the large majority, is converted to hydrogen peroxide by Manganese Superoxide Dismutase (MnSOD) that in turn is converted to water by glutathione peroxidase and catalase. Free radicals may be also generated by the activity of mitochondrial Monoamine Oxidase (MAOA and MAOB), enzymes involved in the metabolism of serotonin, norepinephrine and dopamine. All these reactive species are potentially dangerous because they could cause membrane lipid peroxidation and damage of protein and DNA. However, it is worth to note that the free radical superoxide ( $O_2^-$ ) and  $H_2O_2$  also serve important signalling functions in physiological processes, thus their generation has not exclusively detrimental consequences (Angelova et al., 2016)

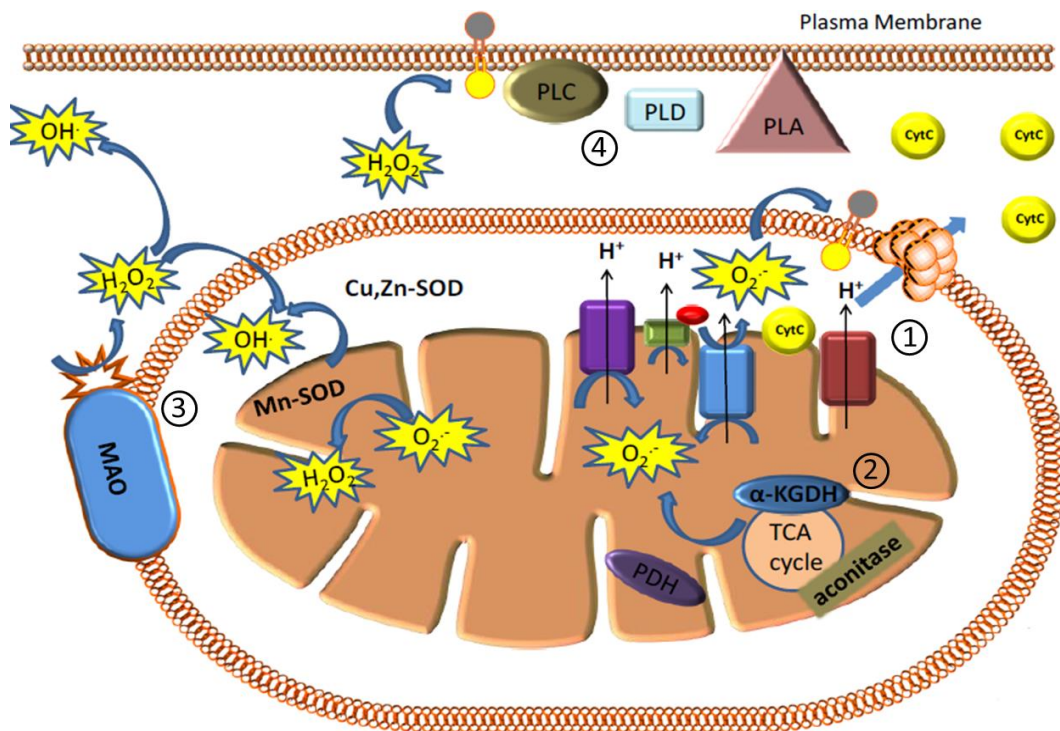


**Figure 1: Different mechanisms of ROS production in Mitochondria.** 1) The main source of ROS in the mitochondria is the electron transport chain (ETC). 2) ROS production in mitochondria takes place also outside the electron transport chain, in the matrix through  $\alpha$ -ketoglutarate dehydrogenase or pyruvate dehydrogenase complexes (PDHC). 3) MAO catabolises dietary monoamines through oxidative deamination. 4) ROS production outside mitochondria through ROS-activated phospholipases. (Angelova et al., 2016)

Mitochondria are the only organelles of the cell besides the nucleus that contain their own DNA (mitochondrial DNA, mtDNA), and their own machinery for synthesizing RNA and proteins. The human mitochondrial genome consists of a 16.6 kb multi-copy, a double-stranded, circular molecule containing 37 genes, which encodes for 13 mitochondrial proteins, all of which are subunits of respiratory chain complexes: seven subunits of complex I, one subunit of complex III, three subunits of complex IV and two of ATP synthase (DiMauro and Schon, 2003). In addition, mtDNA codes for 22 tRNAs and two rRNAs that are necessary for mitochondrial protein synthesis (Reeve et al., 2008). Another important feature of the mtDNA is that it replicates independently (1000–10.000 copies for mitochondrion) from the cell cycle and nuclear DNA replication. The majority of proteins required to build and maintain functional mitochondria are therefore encoded by nuclear DNA, synthesized in the cytosol, and imported into mitochondria (Bolender et al., 2008; Neupert et al., 2007).

MtDNA is characterized by an increased vulnerability to mutations, based on less efficient DNA repair mechanisms and on the absence of protective histones. In addition, the proximity to the respiratory chain has been suggested to favour mtDNA damage by reactive oxygen species (Fig. 2).



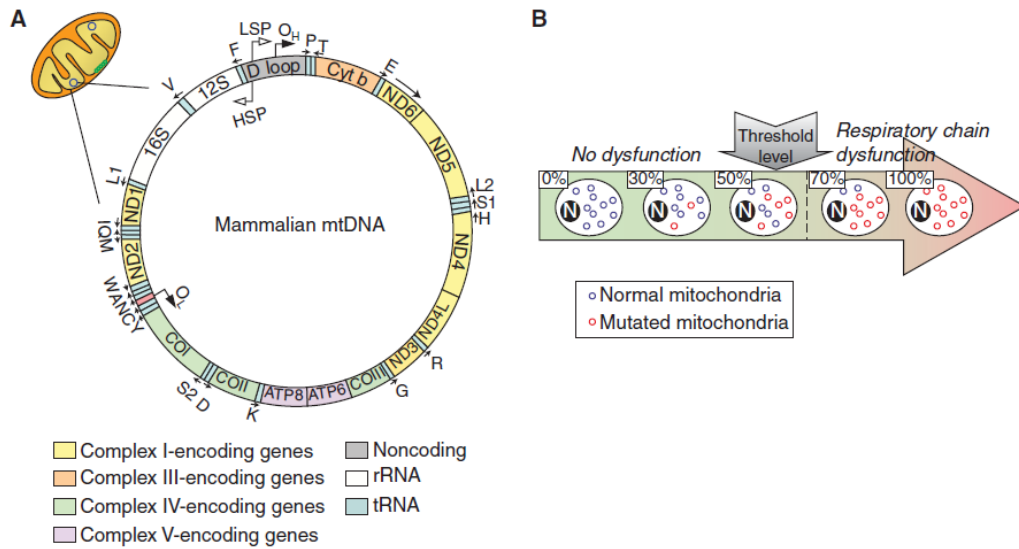


**Figure 2: Mitochondrial DNA (mtDNA).** (A) Mammalian mtDNA is a double-stranded circular molecule containing 37 genes: two ribosomal RNAs (12S and 16S rRNAs), 22 transfer RNAs (tRNAs: F, V, L1, I, M, W, D, K, G, R, H, S1, L2, T, P, E, S2, Y, C, N, A, Q), and 13 encoding subunits of the respiratory chain, including seven subunits of complex I (ND1, 2, 3, 4L, 5, and 6), one subunit of complex III (cytochrome b), three subunits of cytochrome c oxidase (COX I, II, and III) and two subunits of ATP synthase (ATP6 and ATP8). (B) In a normal situation, all mtDNA within a cell are identical (homoplasmy). In a pathological situation linked to pathogenic mtDNA mutations, cells can harbour both normal and mutant mtDNA (heteroplasmy). In the latter case, a minimal number of mutated mtDNA is required to cause mitochondrial dysfunction and clinical signs (threshold effect). (Perier-Vila, 2012).

Evidence for the involvement of the mitochondria in PD emerged following the observation that accidental exposure to 1-methyl-4-phenyl- 1,2,3,4-tetrahydropyridine (MPTP), an inhibitor of complex I (NADH/ubiquinone oxidoreductase), resulted in an acute and irreversible parkinsonian syndrome almost indistinguishable from PD (Langston et al., 1983). A biochemical link between MPTP toxicity and sporadic PD was subsequently established when several groups described a reduced complex I activity in the brain, platelets and skeletal muscle of patients with PD (Parker et al., 1989; Schapira et al., 1990).

Furthermore, MPTP intoxication in mice leads to the peroxidation of the IMM phospholipid cardiolipin, thereby disrupting the normal binding of cytochrome-c to the IMM, facilitating its pro-apoptotic release into the

cytosol (Perier et al., 2005). Mitochondria-derived ROS have also been shown to damage lysosomal membranes in MPTP-intoxicated mice, leading to an impairment of lysosomal function and defective autophagic degradation (Dehay et al., 2010). In addition to proteins and lipids peroxidation, MPTP-intoxicated mice also exhibit oxidative damage to nuclear and mitochondrial DNA (Hoang et al., 2009). Moreover, oxidative damage to proteins, lipids, and DNA have been observed also in post-mortem brain samples from PD patients (Dauer and Przedborski, 2003).

Given that mitochondria are a significant source of intracellular ATP and given that the neurons are characterized by high rates of metabolic activity it is now well accepted that defects in the processes on mitochondrial function leads to a neurodegenerative disorder like PD (Vives-Bauza and Przedborski, 2011; Devoto and Falzone, 2017; Exner et al., 2012).

Mitochondria are also dynamic organelles which actively divide (fission processes), fuse with one another (fusion processes), branch and fragment, swell and extend, exist in clusters or as individual entities and have a regulated turnover, all of them are important for the maintenance of mitochondrial function and for quality control. Importantly, they move from the cell body to regions of the cell to deliver ATP and other metabolites where they are most required. The direction from the cell body outwards it is called anterograde movement, instead of in the opposite direction is known as a retrograde movement. The movement of the mitochondria is seen most strikingly in highly elongated cells such as neurons: mitochondria are enriched at presynaptic terminals at the ends of axons and at postsynaptic terminals at the ends of dendrites, where bioenergetics demand is particularly high.

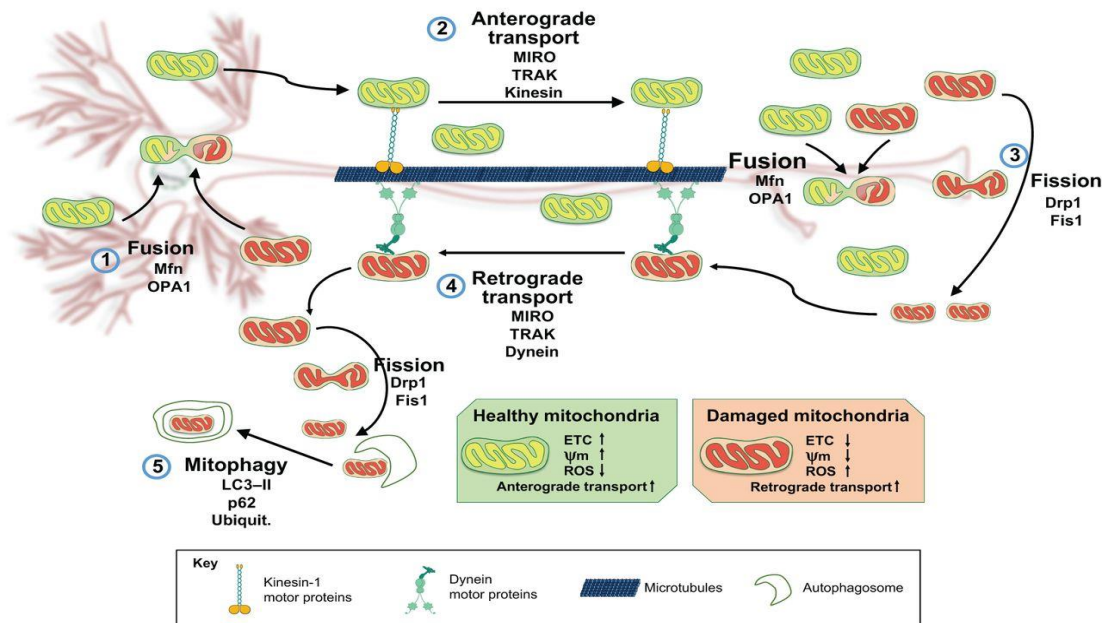


**Figure 3: Neuronal mitochondrial dynamics.** Mitochondrial dynamics in neurons are orchestrated by regulated rates of mitochondrial fusion and fission, transport and mitophagy. Damaged mitochondria (red) can be restored by fusion (1) with healthy mitochondria (green), a process that mainly occurs in the neuronal soma and is driven by Mfn and OPA1. Healthy mitochondria are transported along the axon from soma to synapses by the anterograde axonal transport system (2), which delivers mitochondria to distant. Aged or damaged mitochondria (red) can undergo fission (3) driven by Drp1 and Fis1, and are taken back to the soma by the retrograde axonal transport machinery (4). Once these mitochondria reach the cell body, they may be cleared by mitophagy (5) (p62 and LC3-II are involved in regulating this process). (Devoto et al., 2017).

The subsequent discovery of hereditary forms of PD caused by dominant and recessive mutations in nuclear genes encoded proteins functionally related to mitochondria has added importance to the study of mitochondrial dysfunction in PD. The products of two dominantly inherited genes,  $\alpha$ -synuclein and LRRK2, and of several autosomal recessive inherited genes, DJ-1, parkin, PINK1 and Omi/HTRA2, have been found to be localized in, and/or to interfere with mitochondria (Liu et al., 2009).

Mutations in the *parkin* gene (*PARK2*) were originally identified in five Japanese patients with autosomal recessive juvenile parkinsonism (Kitada et al., 1998). *Parkin* encodes a 465-amino acid E3-ubiquitin ligase (Shimura et al., 2000), thus, loss-of-function of this ligase activity would be expected to result in disruption of the proteasome system.

Mutations in the gene encoding for PINK1 (*PARK6*, *PINK1*) were initially identified by Valente and colleagues (Valente et al., 2004) in families with PD that displayed an earlier age of onset, slower progression and more favourable L-DOPA response. PINK1 is a 581-amino acid protein mitochondrial kinase with unknown substrates, but this protein is known to be upstream of *parkin* in the mitophagy pathway. There is evidence that wild type PINK1, in contrast to mutant PINK1, may protect neurons from stress-induced mitochondrial dysfunction and apoptosis (Perfeito et al., 2013). Work by Narendra et al. (Narendra et al., 2010) suggests that the selective retention of the PINK1 protein on damaged/depolarized mitochondria leads to recruitment and ubiquitination of parkin followed by mitophagy. Thus, both *parkin* and PINK1 are important for normal mitochondria dynamics and loss of function of both of them can lead to mitochondrial impairment, dopamine neuron loss and parkinsonism.

Mutations in the gene encoding the protein DJ-1 (*PARK7*, *DJ-1*) were first identified in two European families (Bonifati et al., 2003). The DJ-1 protein is ubiquitously expressed with strong localization in astrocytes and occasionally to Lewy bodies in sporadic PD (Bandopadhyay et al., 2004; Kumaran et al., 2009). It is clear that DJ-1 is a redox sensor that can play multiple roles such as peroxidase (Andres-Mateos et al., 2007), chaperone (Shendelman et al. 2004), RNA-binding protein (Blackinton et al., 2009) and regulator of mitochondrial integrity (Hao et al., 2010; Larsen et al., 2011). Its deficiency in mutant mice results in increased mitochondrial ROS production (Perier and Vila, 2012). While the exact mechanisms of action remain unknown, recent evidence suggests that DJ-1 acts in parallel with the PINK1/parkin pathway in modulating mitophagy (Thomas et al., 2011). Mutations in the gene encoding the LRRK2 (Leucine-rich repeat kinase 2, or *PARK8*) protein are the most common in both familial and sporadic PD (Berg et al., 2005; Goldwurm et al., 2005). *LRRK2* encodes for a 2527-amino

acid protein with both kinase and GTPase activity. Little is currently known about the native substrates or normal function of this protein, although studies suggest roles in process outgrowth, synaptic vesicle dynamics and the autophagy/ lysosomal pathway (Greggio et al., 2011; Kuar and Cookson, 2011).

Moreover, a mitochondrial association of  $\alpha$ -synuclein is also linked to impairment of respiratory complex I activity, oxidative modification of mitochondrial proteins, and increased levels of  $\text{Ca}^{2+}$  (Cannon et al., 2013; Liu et al., 2009; Li et al., 2013). Alterations in the mitochondrial complex I are also found in autaptic samples of *SNpc* from patients affected by PD in which the activity of complex I was shown to be reduced (Parker et al., 2008).

There is evidence that  $\alpha$ -synuclein modulates  $\text{Ca}^{2+}$  influx (Buttner et al., 2013), suggesting that its oligomers promote alterations in calcium dynamics via interference with intracellular buffering mechanisms. Furthermore,  $\text{Ca}^{2+}$  accumulation in the mitochondrial matrix results at an energetic cost, as it dissipates the electrochemical gradient created by ETC (Chan et al., 2010) and also leads to a disruption of mitochondrial membrane integrity, permeability transition, irreversible oxidative damage and consequently cell death (Calì et al., 2012) (Fig. 4).

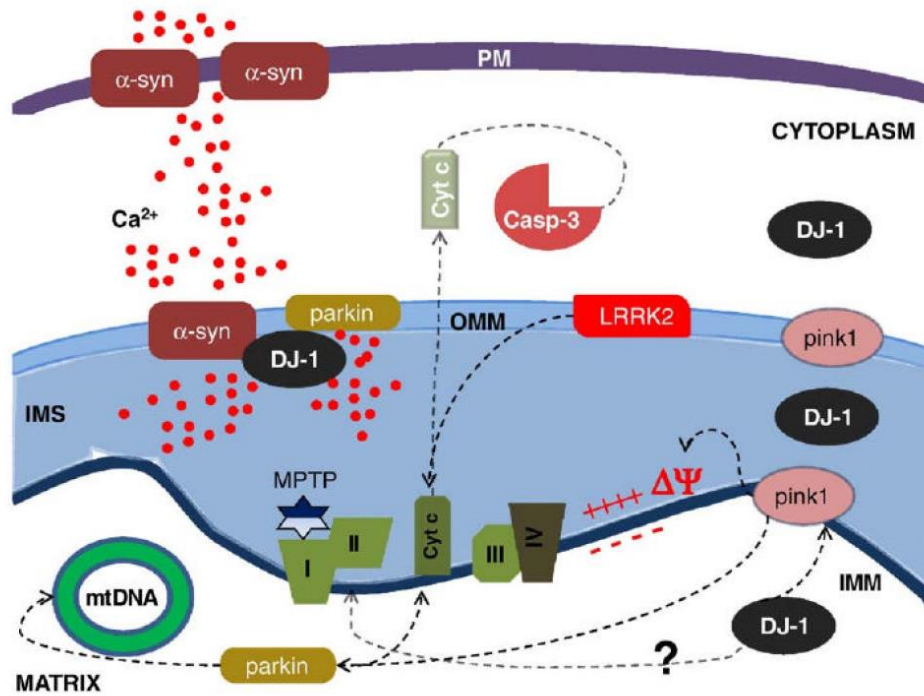


**Figure 4: Mutations in familial PD-linked genes encoding  $\alpha$ -synuclein, parkin, pink1, DJ-1 and LRRK2 cause mitochondrial dysfunctions through common intersecting pathways.** Mutant  $\alpha$ -synuclein promotes  $\text{Ca}^{2+}$  influx and mitochondrial  $\text{Ca}^{2+}$  overload and mutant parkin exacerbate this effect. DJ-1, PINK1 and Parkin may act in series on the same protein targets: genetic data suggest that pink1 is upstream of parkin and that all of them exert a protective role preserving mitochondrial functions, morphology and preventing mitochondrial-induced apoptosis. LRRK2 mutations induce apoptotic death through cytochrome c release and activation of caspase-3. Complex I activity is reduced in PD and its inhibition by MPTP or rotenone causes dopaminergic degeneration. Mutations in mtDNA-encoded complex I subunits also cause PD. PM, plasma membrane; OMM outer mitochondrial membrane; IMS, intermembrane space; IMM, inner mitochondrial membrane. (Celsi et al., 2009)

## ***2.2 Calcium homeostasis and neurodegeneration***

Recently, several indications have argued in favour of the possibility that dysregulation in calcium ( $\text{Ca}^{2+}$ ) homeostasis participates in the pathogenesis of PD (Surmeier et al., 2012). Thus, the study of the characteristics of  $\text{Ca}^{2+}$  handling in dopaminergic neurons and of the possible role of PD-related proteins in the control of intracellular  $\text{Ca}^{2+}$  homeostasis has recently received great interest (Cali et al., 2011).

$\text{Ca}^{2+}$  is universal second messenger regulating a wide range of important eukaryotic cells functions such as differentiation, proliferation, growth, survival, apoptosis, gene transcription, membrane excitability (Capiod et al., 2016; Clapham et al., 2007; La Rovere et al., 2016; Toth et al., 2016), control of dendritic responses to neurotransmitters, signalling to the nucleus to regulate gene expression, and initiation of neurotransmitter release from presynaptic axon terminals (Gleichmann and Mattson, 2011).

Neurons express various types of voltage-dependent  $\text{Ca}^{2+}$  channels including the following: the low-voltage activated T-type channels (Cav3 family channels); the dihydropyridine-sensitive L-type (Cav1.2 and Cav1.3), which are important in the regulation of gene expression, integration of synaptic input, and initiation of neurotransmitter release; the P/Q-type (Cav2.1), N-type (Cav2.2), and R-type (Cav2.3) channels, which are activated after the rising phase of the action potential and sustain large  $\text{Ca}^{2+}$  currents during the falling phase (Bean, 2007). Once  $\text{Ca}^{2+}$  is in, it must be rapidly extruded or buffered to avoid its excessive accumulation and toxicity (Gleichmann and Mattson, 2011). High-affinity ATP-driven pumps in the plasma membrane (PMCA) and in the ER membrane (SERCA) cooperate with the  $\text{Na}^+/\text{Ca}^{2+}$  exchanger, which uses the  $\text{Na}^+$  gradient generated by the  $\text{Na}^+/\text{K}^+$  ATPase, to restore basal  $\text{Ca}^{2+}$  levels. Several  $\text{Ca}^{2+}$  binding proteins are expressed in the nervous system, calmodulin (CaM),

Calbindin D-28 k (CB-28 k), calretinin (CR), and parvalbumin (PV) are differentially expressed in various brain regions and their differences in  $\text{Ca}^{2+}$  affinity account for their specific role (Schwaller, 2012) (Fig.5).

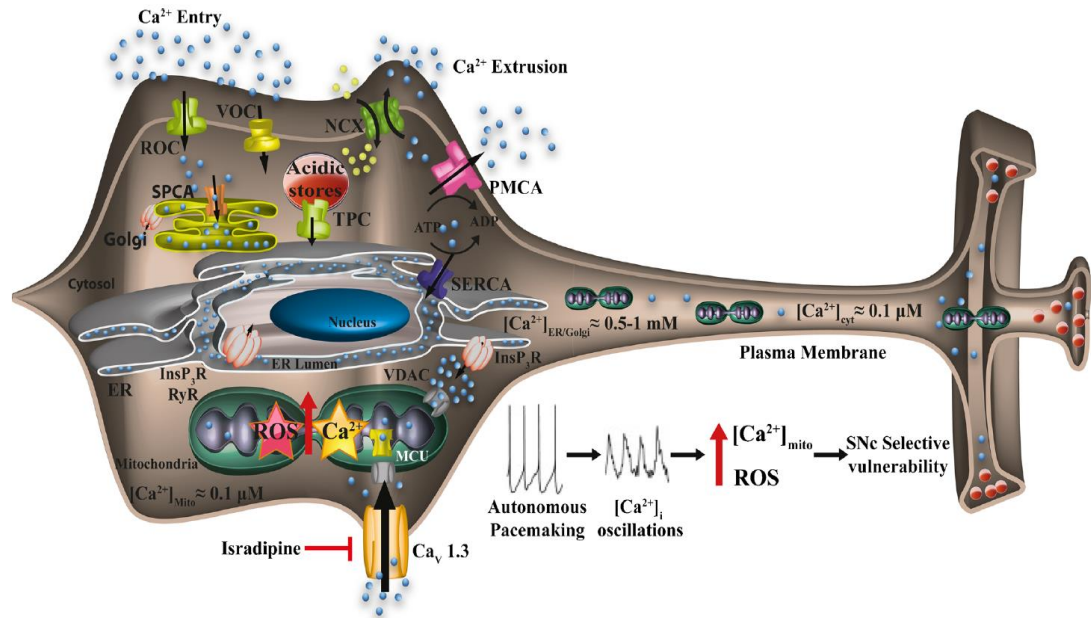


**Figure 5: The main  $\text{Ca}^{2+}$  transport systems in dopaminergic neurons.** SNpc neurons engage Cav1.3 L-type  $\text{Ca}^{2+}$  channels during their constitutive pacemaking. The activity of these channels generates  $\text{Ca}^{2+}$  influx that, on one side, has the advantage of sustaining pacemaking activity and thus dopamine production, and on the other requires the enhanced action of mitochondria in buffering  $\text{Ca}^{2+}$  entry, thus exposing them to increased oxidant stress by enhanced reactive oxygen species (ROS) production. Thus, the final outcome of this activity appears responsible for the selective vulnerability of SNpc neurons when additional stresses (environmental or genetic) are added. Many other  $\text{Ca}^{2+}$  transport proteins contribute to  $\text{Ca}^{2+}$  handling: the inositol 1,4,5-trisphosphate receptor (InsP<sub>3</sub>R), the ryanodine receptor (RyR) at the Sarco/endoplasmic reticulum (SR/ER) membranes, and the voltage (VOC) and the receptor (ROC)-activated  $\text{Ca}^{2+}$  channels of the plasma membrane.  $\text{Ca}^{2+}$  extrusion depends on the activity of the plasma membrane  $\text{Ca}^{2+}$  ATPase (PMCA) and the plasma membrane  $\text{Na}^+/\text{Ca}^{2+}$  exchanger (NCX).  $\text{Ca}^{2+}$  reuptake in the intracellular stores is operated by the ER/SR  $\text{Ca}^{2+}$  ATPase (SERCA) and the secretory pathway  $\text{Ca}^{2+}$  ATPase (SPCA) of the Golgi apparatus. Recently, acid compartments, e.g., endo-lysosomes, have been proposed to act as  $\text{Ca}^{2+}$  stores: the nicotinic acid/adenine dinucleotide phosphate (NAADP)-sensitive two-pore channels (TPC) have been suggested to be responsible for their  $\text{Ca}^{2+}$  release (Cali et al., 2014)

Mitochondria and the endoplasmic reticulum (ER) are the principal organelles involved in sequestering  $\text{Ca}^{2+}$  in neurons (Rizzuto and Pozzan, 2006; Verkhratsky, 2005). As this store fills up,  $\text{Ca}^{2+}$  triggers the opening of ER  $\text{Ca}^{2+}$  channels that let the  $\text{Ca}^{2+}$  flow back into the cytoplasm. These channels are often found in close apposition to mitochondria and their



opening creates a region of high-local  $\text{Ca}^{2+}$  concentration (microdomains) that drives an influx of  $\text{Ca}^{2+}$  into the matrix of mitochondria through  $\text{Ca}^{2+}$  uniporters (Rizzuto and Pozzan, 2006). An important feature of the mitochondrial  $\text{Ca}^{2+}$  transport pathway is that this organelle contains low calcium in resting cells, but is able to accumulate large amounts of calcium in condition stimulating  $\text{Ca}^{2+}$  entry and to release this calcium loaded during the recovery phase (Nicholls, 2005). This is due to the ability of specific transporters localized on the inner mitochondrial membrane that allow calcium to cycle from the mitochondrial matrix to the cytosol and from the cytosol to the mitochondrial matrix.  $\text{Ca}^{2+}$  is removed from the matrix through the mitochondrial sodium-calcium exchanger NCX (Kim and Matsuoka, 2008; Rizzuto and Pozzan, 2000), the  $\text{Ca}^{2+}$  proton exchanger (Williams and Fry, 1979), and the transient opening of the mitochondrial permeability transition pore (mPTP) (Hüser and Blatter, 1999). These events allow the maintenance of mitochondrial calcium concentrations within physiological range that are necessary for the neurons to adjust aerobic ATP production, to regulate synaptic transmission and excitability, to promote organelle dynamics and trafficking, to mediate signalling to nucleus, to control the generation of ROS, and to preserve neuronal survival (Nicholls, 2005; Starkov, 2002; Chinopoulos and Adam-Vizi, 2010; Duchen, 2004; Mattson et al., 2008). The possibility that mitochondria dysfunction is also related to mitochondrial  $\text{Ca}^{2+}$  mishandling and defects in ER-mitochondria communication now represent an additional intriguing hypothesis for PD pathogenesis (Cali et al., 2012, 2013; Exner et al., 2012; Schapira, 2011). The crucial question is whether or not the disease begins with the dysfunction of these organelles.

SNpc dopaminergic neurons are autonomously active: they differ from most neurons in the brain because they generate action potentials in the absence of conventional synaptic input (Grace and Bunney, 1983). Their

basal activity is innately generated by multichannel activity and is supported by the voltage-dependent L-type  $\text{Ca}^{2+}$  channels containing a distinctive Cav1.3 pore-forming subunit, which opens at relatively hyperpolarized potentials (Xu and Lipscombe, 2001; Wilson and Callaway, 2000). Thus, these channels are open much of the time ensuring also a continuous supply of DA to the connected brain areas, e.g., the striatum, and thus the control of coordinated movement (Surmeier, 2007). Interestingly, VTA neurons, which are more resistant to neurodegeneration, have also slow pacemaker's activity, but because of their relatively low expression of the Cav1.3 subunits (Khaliq and Bean, 2010) do not manifest  $\text{Ca}^{2+}$  oscillations (Chan et al., 2007). We should mention that, in spite of PD pathology displaying extreme selectivity within dopaminergic neuronal subtypes, other non-mesencephalic neurons are involved, e.g., olfactory and some hypothalamic neurons. Curiously, these neurons do not share a common neurotransmitter, but all of them are characterized by spontaneously high activity associated with conspicuous  $\text{Ca}^{2+}$  currents and low buffering capacity (Surmeier and Schumacker, 2013). On the basis of these observations, an intriguing hypothesis has been formulated by Surmeier and co-workers, who have proposed and documented that the constant and long-lasting elevations of cytosolic  $\text{Ca}^{2+}$  occurring in SNpc neurons are directly linked to mitochondrial stress, impaired mitochondrial bioenergetics, and increased ROS production, thus augmenting cell death sensitivity (Guzman et al., 2010, Surmeier et al., 2012) Consistent evidence accounts for the role of  $\text{Ca}^{2+}$  signalling in PD pathogenesis and suggests that altered  $\text{Ca}^{2+}$  homeostasis is an early feature of PD rather than a consequence of neuronal derangements. In particular,  $\text{Ca}^{2+}$  entry during the pacemaking activity of SNpc neurons can amplify the effects of genetic defects or of environmental factors (Fig. 6).

A new hypothesis considers the possibility that also  $\alpha$ -synuclein exerts its toxicity through the engagement of the  $\text{Ca}^{2+}$  homeostatic machinery. Because of  $\alpha$ -synuclein is an aggregation-prone protein, it forms fibrillar oligomers that enhance plasma membrane permeability to  $\text{Ca}^{2+}$  and mediate exaggerated  $\text{Ca}^{2+}$  influx with consequent toxicity (Schmidt et al., 2012; Tsigelny et al., 2012; Danzer et al., 2007). In fact, two mutant forms of  $\alpha$ -synuclein, A53T and A30P, enhance the formation of pore-like fibrils by inducing conformational protein changes (Lashuel et al., 2002) and further induce membrane permeabilization, leading to increases in the intracellular  $\text{Ca}^{2+}$  level (Furukawa et al., 2006). Other reports have shown that  $\alpha$ -synuclein is secreted into the extracellular medium and contributes to the progression of the PD pathology by modulating the activity of voltage-gated or other types of  $\text{Ca}^{2+}$  influx channels of the plasma membrane (Emmanouilidou et al., 2010; Melachroinou et al., 2013). The investigation of this aspect is particularly relevant, since  $\text{Ca}^{2+}$  binding to  $\alpha$ -synuclein has been shown to favour its propensity to aggregate in vitro and in cultured cells overexpressing  $\alpha$ -synuclein (Follett et al., 2013; Lowe et al., 2004; Nath et al., 2011), suggesting that enhanced basal  $\text{Ca}^{2+}$  levels contribute to the progression of the disease by also enhancing  $\alpha$ -synuclein aggregation in vivo. According to this possibility, the stress induced by  $\text{Ca}^{2+}$  might increase SNpc neuron susceptibility by stimulating ROS production in the cytosol (Dryanovski et al., 2013; Marongiu et al., 2009; Melachroinou et al., 2013; Parihar et al., 2008,2009).

In addition to the aforementioned considerations, further support for a  $\text{Ca}^{2+}$  dyshomeostasis link in PD comes from the rapidly expanding literature on genetic mutation associated with familial forms of PD. As matter of fact, DJ-1 is a multifunctional protein and, despite its predominant role as antioxidant (Taira et al., 2004), it has been shown essential to maintain cytosolic basal  $\text{Ca}^{2+}$  concentration values and to permit depolarization-

induced  $\text{Ca}^{2+}$  release from the sarcoplasmic reticulum in muscle cells (Shtifman et al., 2011) as well as to protect dopaminergic neurons by  $\text{Ca}^{2+}$ -induced mitochondrial uncoupling and ROS production during physiologic pacemaking (Guzman et al., 2010). An augmented phospholipase C activity with consequent increase of cytosolic basal  $\text{Ca}^{2+}$  concentration and increased vulnerability to 6-hydroxydopamine (6-OHDA) have also been shown in parkin-deficient human neuroblastoma cells (Sandebring et al., 2009). As to PINK1, its direct role in regulating cellular, and most specifically mitochondrial  $\text{Ca}^{2+}$  fluxes, has been recently proposed starting by the seminal observation that the coexpression of mutant, but not WT, PINK1 in a cellular model of PD expressing mutated A53T  $\alpha$ -synuclein exacerbated the observed mitochondrial defects leading to loss of mitochondrial membrane potential, increased mitochondrial size with loss of cristae and reduced ATP levels. The proposed mechanisms of PINK1 action was based on dysregulation of mitochondrial  $\text{Ca}^{2+}$  influx, as by blocking mitochondrial  $\text{Ca}^{2+}$  uptake, it was possible to restore the original phenotype (Marongiu et al., 2009), thus suggesting that mutant PINK1 could reinforce  $\alpha$ -synuclein pathology by acting on converging pathways affecting mitochondrial function.

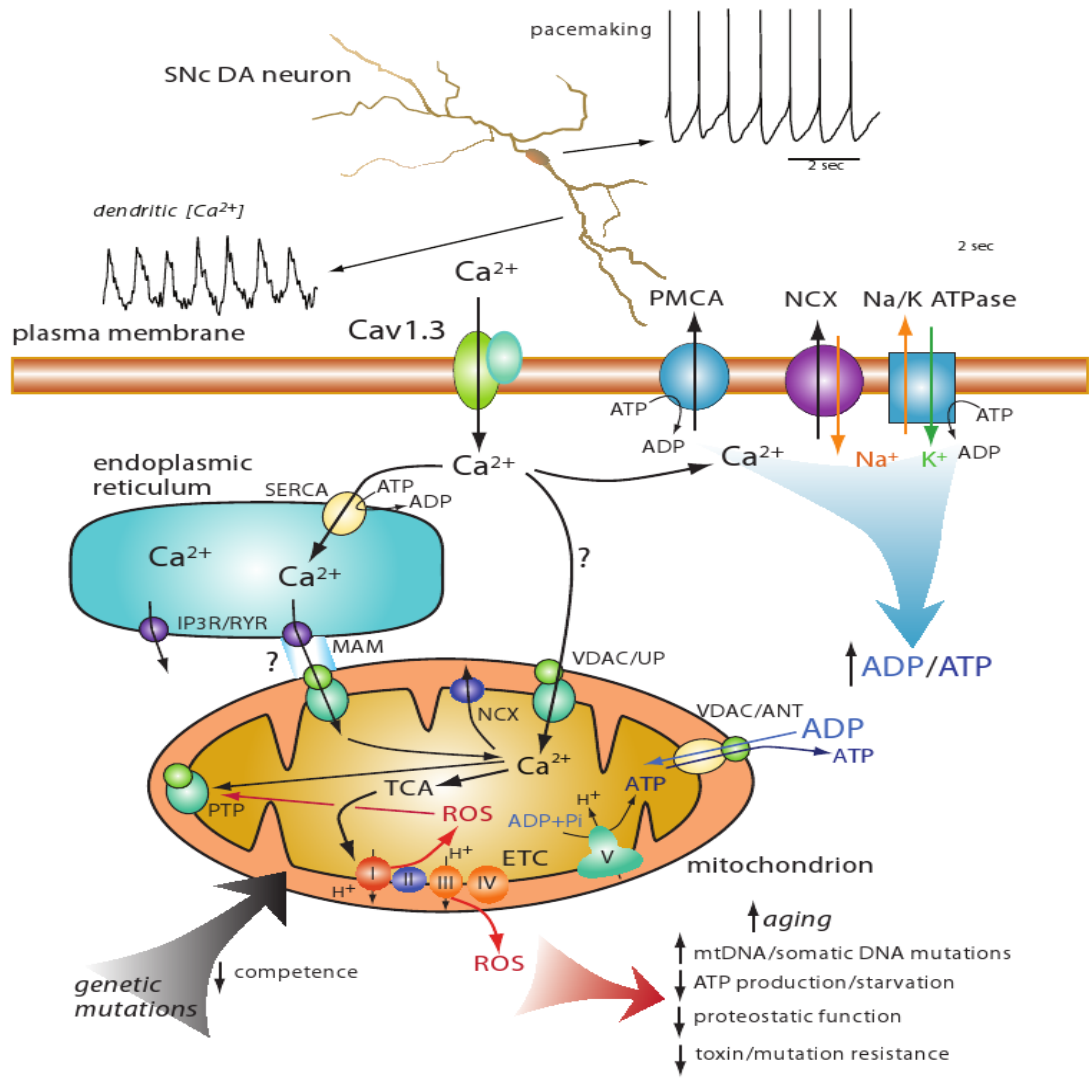


**Figure 6: Schematic model of how  $Ca^{2+}$  entry during pacemaking in SNpc DA neurons might lead to mitochondrial oxidative stress, accelerated ageing and eventual cell death.** At the top is an image of a reconstructed SNpc DA neuron showing the pacemaker drive somatic spiking and dendritic  $Ca^{2+}$  oscillations associated with pacemaking. This dendritic  $Ca^{2+}$  influx is attributable almost entirely to flux through Cav1.3  $Ca^{2+}$  channels.  $Ca^{2+}$  influx through Cav1.3 channels is either sequestered in the endoplasmic reticulum by uptake through smooth endoplasmic reticulum  $Ca^{2+}$  (SERCA) pumps or taken up by mitochondria through channels created by voltage-dependent anion channels (VDAC) and  $Ca^{2+}$  uniporter (UP).  $Ca^{2+}$  could also enter mitochondria through this VDAC/UP channel at points of apposition between the ER and mitochondria in the specific area called mitochondrial associated membrane (MAM).  $Ca^{2+}$  entering through Cav1.3 channels are moved back across the plasma membrane through either the  $Ca^{2+}$ -ATPase (PMCA) or through a Na<sup>+</sup>/ $Ca^{2+}$  exchanger (NCX) that relies upon the Na<sup>+</sup> gradient maintained by the Na/K ATPase at energetic cost; leading to the conversion of ATP to ADP.  $Ca^{2+}$  entering the mitochondrial matrix can stimulate enzymes of the tricarboxylic acid (TCA) cycle that produces reducing equivalents for the electron transport chain (ETC). Electron movement along the ETC generates superoxide, leading to the production of reactive oxygen species (ROS) that can produce a variety of deleterious effects that can be viewed as accelerated ageing (red arrow at the bottom). One other action of ROS is to promote the opening of the mitochondrial permeability transition pore (mPTP); that leads to the release of pro-apoptotic factors into the cytosol.  $Ca^{2+}$  is removed from mitochondrial through mitochondrial Na<sup>+</sup>/ $Ca^{2+}$  exchangers (NCX). (Surmier et al., 2010)

### ***2.3 Role of $\alpha$ -synuclein in the pathogenesis of Parkinson's disease***

$\alpha$ -synuclein is a small acid protein of 14.5 kDa, 140 amino-acid, belonging to the synuclein superfamily that also includes  $\beta$ -synuclein ( $\beta$ -synuclein) and  $\gamma$ -synuclein ( $\gamma$ -synuclein), codified from three highly expressed human genes (SNCA, SNCB and SNCG) (Lavedan et al., 1998).

$\alpha$ -synuclein is highly conserved in vertebrates and is expressed mainly in presynaptic nerve terminals in several regions of the brain (Jain et al., 2013, Maroteaux et al., 1988). In physiological condition, it can be found mainly into the cytoplasm; however, it has also been reported to be located in the nucleus, attached to mitochondria or at the endoplasmic reticulum (Pinho et al., 2019; Goers et al., 2003; Cole et al., 2008; McLean et al., 2000b; Li et al., 2007; Devi et al., 2008; Guardia-Laguarta et al., 2014, 2015; Kahle et al., 2000; Davidson et al., 1998; Jo et al., 2000). While it is clear that  $\alpha$ -synuclein can modulate synaptic activity, the function and presence of the protein within the organelles, the action on ER-Golgi transport are still subjects of debate. (Zhou et al., 2010).

Current knowledge suggests that  $\alpha$  -synuclein is involved in maintaining homeostasis of neurotransmitter release by interacting with proteins involved in synaptic vesicle fusion and transportation, SNARE complexes (Soluble N-ethylmaleimide-sensitive factor attachment protein receptor) (Calo et al., 2016; Burre et al., 2018, 2010; Abeliovich et al., 2000; Larsen et al., 2006; Chandra et al., 2005). This is supported by the observation that changes in SNARE complex are seen in the brains of patients with  $\alpha$ -synucleinopathies like PD (Bellucci et al., 2008; Calo et al., 2016). Aggregation of misfolded  $\alpha$  -synuclein is thought to interfere with the formation of the SNARE complex, specifically resulting in problems with vesicle docking and fusion that ultimately lead to decreased

neurotransmitter release and synaptic dysfunction (Calo et al., 2016). Consistent with this notion, two recent studies have found that the absence of normally functioning  $\alpha$ -synuclein correlates to a decrease in the number of dopaminergic neurons observed in the substantia nigra (Garcia-Reitboeck et al., 2013; Calo et al., 2016). Moreover, in the brains of patients with dementia with Lewy bodies,  $\alpha$ -synuclein aggregates were located at presynaptic terminals and resulted in severe synaptic pathology, leading to almost complete loss of dendritic spines at the postsynaptic area (Kramer et al., 2007).

The role of  $\alpha$ -synuclein in neurotransmitter release is mainly based on its regulation of synaptic vesicle recycling. Dopamine transporter (DAT) functions are also controlled by  $\alpha$ -synuclein as mice not expressing  $\alpha$ -synuclein show impairment of DAT functions and reduction of striatal DAT levels (Bellucci et al., 2011; Chadchankar et al., 2011). A direct interaction between  $\alpha$ -synuclein and DAT has been reported in PD patients as well as in experimental models (Butler et al., 2015), in which has been shown that  $\alpha$ -synuclein controls the trafficking of DAT by modulating the cytoskeleton DAT anchoring. In physiological conditions,  $\alpha$ -synuclein binds the C-terminal tail of DAT, increasing its levels at the plasma membrane with a consequently enhanced uptake of extracellular dopamine (DA) (Lee et al., 2001), instead mutant forms of  $\alpha$ -synuclein decreases the trafficking of DAT at the plasma membrane (Wersinger et al., 2003). Similarly,  $\alpha$ -synuclein controls the trafficking of serotonin and norepinephrine through their transporters (Buddhala et al., 2015). The monoaminergic transporters are modulated by the interaction with synuclein that removes them from the plasma membrane increasing their compartmentalization (Wersinger et al., 2006a, 2006b; Jeannotte et al., 2007). Another *in vivo* study showed that lack of  $\alpha$ -synuclein leads to a permanent increase of the vesicle refilling rate in the DA readily releasable pool,

maintaining stable DA release during stimulation in contrast to the decline of DA release observed in normal conditions (Yavich et al., 2004). Together, these findings suggest that  $\alpha$ -synuclein is an activity-dependent negative regulator of DA neurotransmission.

In PD,  $\alpha$ -synuclein is found as a major component of Lewy bodies and Lewy neurites, the hallmark protein inclusions made up primarily of insoluble and fibrillar  $\alpha$ -synuclein protein (Spillantini et al., 1998).  $\alpha$ -synuclein also accumulates in dementia with Lewy bodies (DLB) and MSA (Multiple System Atrophy) and as a component of amyloid from brain tissues of Alzheimer's Disease (AD) patients (Ueda et al., 1993).

The conformational plasticity of  $\alpha$ -synuclein, which depends on its primary amino acid sequence, reflects the ability of the protein to interact with multiple ligands, including proteins and lipids, and to exert chaperone-like functions (Ahn et al., 2006). The primary sequence of  $\alpha$ -synuclein can be divided into three main regions: N-terminal domain, central region (NAC region) and C-terminal domain.

The N-terminal domain (aa 1–60), containing four highly conserved 11 repeats with a KTKGEV consensus sequence, involved in the formation of amphipathic  $\alpha$ -helices, which are essential for membrane binding (Vamvaca et al., 2009). These helices are stabilized by interaction with high-curvature membranes enriched in phospholipids, similarly to synaptic vesicles (SV) (Zhu et al., 2003; Davidson et al., 1998). This part of the protein can also form  $\alpha$ -helical oligomers following acetylation, suggesting that this post-translational modification affect the structural and functional properties of  $\alpha$ -synuclein (Dikiy et al., 2014; Trexler et al., 2012). These repeated sequences are very highly conserved, in fact, the motif is unique, with no similar sequence identified outside the synuclein family (Bussell et al., 2005). Remarkably, all of the mutations associated with PD, A30P, E46K, A53T, A53E, G51D, H50Q (Appel-Cresswell et al., 2013; Kruger et al., 1998;



Lesage et al., 2013; Polymeropoulos et al., 1997; Proukakis et al., 2013; Zarranz et al., 2004; Giasson et al., 2002), cluster within this N-terminal domain. It is also interesting to note that rodent synuclein normally contains a threonine at position 53, which instead causes PD in humans. The A53T mutation, thus, appears to be pathogenic specifically within the human context (Cabin et al., 2005).

The  $\alpha$ -synuclein mutants A53T and E46K exhibit increased membrane-binding affinity and flatten micelle surface curvature, whereas the A30P  $\alpha$ -synuclein mutant has a decreased membrane affinity and does not alter the surface curvature of the micelles (Auluck et al., 2010). A study using computer modelling and membrane simulations investigated the course of penetration of WT and A53T mutant  $\alpha$ -synuclein in the membranes and pore formation activity, showing that the penetration of the A53T mutant  $\alpha$ -synuclein across the membrane is 20% faster than WT  $\alpha$ -synuclein (Tsigelny et al., 2012).

The central region of  $\alpha$ -synuclein (aa 61–95) comprises the hydrophobic non-amyloid component (NAC) domain: a sequence that is highly aggregation-prone and results necessary and sufficient for  $\alpha$ -synuclein filament formation (Mor et al., 2016; Giasson et al., 2001). When  $\alpha$ -synuclein is in a disordered state, this region is protected from the cytoplasm via transient intramolecular interactions, in order to prevent aggregation (Theillet et al., 2016).

The C-terminal domain of  $\alpha$ -synuclein (aa 96–140) is highly enriched in negatively charged amino acids and proline residues (Ulmer et al., 2005). This region seems to interact with the N-terminal region of  $\alpha$ -synuclein in order to protect the NAC residues thus resulting in compact aggregation-resistant monomeric structures (Bertoncini et al., 2005; Dedmon et al., 2005). Post-translational modifications of the C-terminal domain can enhance  $\alpha$ -synuclein aggregation propensity and affect its molecular interactions.

Phosphorylation at Ser129 or nitration at Tyr125, Tyr133 and Tyr136 have been reported to promote the formation of  $\alpha$ -synuclein fibrils or oligomers (Giasson et al., 2000), to alter its conformational state and to reduce its membrane-binding affinity (Sevcsik et al., 2011). Moreover, C-terminally truncated forms of  $\alpha$ -synuclein aggregate faster than full-length protein (Li et al., 2005; Crowther et al., 1998).

The process of  $\alpha$ -synuclein aggregation has been studied in detail in an attempt to identify the toxic species responsible for neuronal dysfunction and death.

In intracellular inclusions,  $\alpha$ -synuclein is detected as large beta-sheet-enriched fibrils (Spillantini et al., 1998) which are formed in a multistep process involving numerous intermediate states including proto-fibrils, large oligomers and small oligomers process called nucleation (Fig. 7) (Hoyer et al., 2002; Munishkina et al., 2003; Mehra et al., 2019).

Initially, it was hypothesized that accelerated fibrillation of  $\alpha$ -synuclein was responsible for early-onset PD pathogenesis and this was supported by the discovery that A53T, A30P and E46K mutations, showed early oligomerization and enhanced fibrillation of  $\alpha$ -synuclein (Conway et al., 2000; Greenbaum et al., 2005; Narhi et al., 1999).

There is evidence showing that inhibition of  $\alpha$ -synuclein aggregation process is associated with a decrease of  $\alpha$ -synuclein toxicity (Hashimoto et al., 2001; Periquet et al., 2007). However, similarly to the case of amyloid-beta ( $A\beta$ ) plaques in AD, it was suggested that the fibrillar forms of  $\alpha$ -synuclein might not represent the most toxic  $\alpha$ -synuclein species. Instead, pre-fibrillar, soluble oligomer species (comprising multiple  $\alpha$ -synuclein molecules) are now suggested to be the main toxic  $\alpha$ -synuclein species, with amyloid aggregates possibly serving as a reservoir for these oligomer species. The neurotoxic effects of  $\alpha$ -synuclein oligomers were also studied in vivo, using animal models of synucleinopathies.

Together, these studies provide evidence for the importance of soluble oligomers as the prominent toxic species in synucleinopathies, although the precise size and type of the toxic oligomer species remain to be determined (Danzer et al., 2007; Winner et al., 2011).

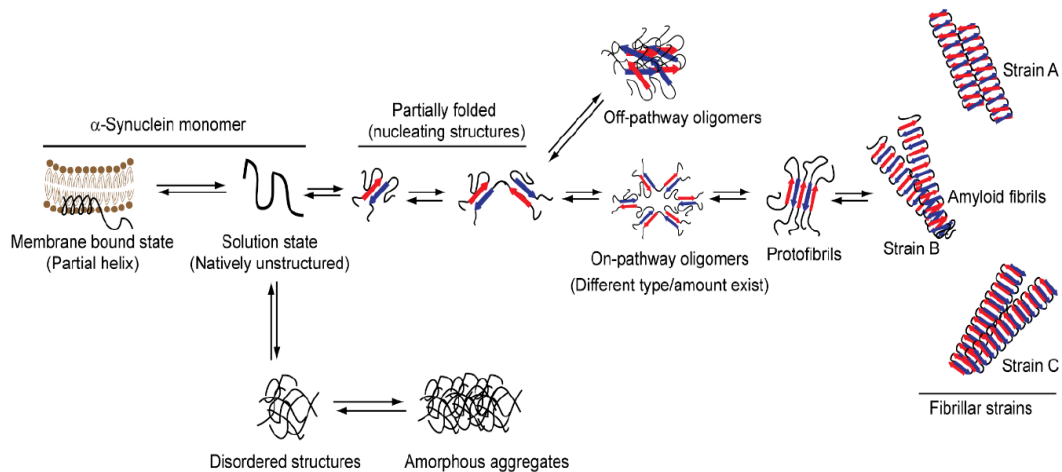


**Figure 7: Conformational states of  $\alpha$ -Synuclein.**  $\alpha$ -Synuclein monomer exists in two states, i.e., solution (natively unstructured) and membrane-bound state (partially helical conformation). Upon incubation, the natively unstructured monomer converts into oligomers (on-pathway or off-pathway) via partially folded nucleating structures. The on-pathway oligomers eventually convert into highly ordered cross- $\beta$ -sheet amyloid fibrils whereas the fate of off-pathway is unclear. Natively unstructured protein can also form some disordered structures in the beginning, which results in the formation of amorphous aggregates. Under different assembly/solution conditions, native protein can form different types of amyloid fibrils, i.e., fibrillar strains. (Mehra et al., 2019)

Once a cell contains aberrant  $\alpha$ -synuclein, there are three possibilities for managing it: degradation, deposition in a specialized compartment or release into the extracellular space. Both deposition inside the cell and release into the extracellular space are tightly related to the failure of proper degradation. Degradation of  $\alpha$ -synuclein can occur both via autophagic clearance and by the proteasome system (Cuervo et al., 2004; Rideout et al., 2004; Emmanouilidou et al., 2010). Moreover, it has been demonstrated that, depending on the conformation,  $\alpha$ -synuclein can be targeted to the proteasome or to the lysosome (Lee et al., 2004, 2008). Failure of clearance promotes the extracellular release of aggregated  $\alpha$ -synuclein (Alvarez-Erviti et al., 2011). Interestingly, the amount of released

$\alpha$ -synuclein appears to correlate directly with the levels of intracellular  $\alpha$ -synuclein (Reyes et al., 2015), how demonstrated by measurable quantities of  $\alpha$ -synuclein in CSF, plasma and cell culture supernatant (El-Agnaf et al., 2006; Mollenhauer et al., 2008). Several active mechanisms have been demonstrated for the release of monomeric, oligomer and aggregated  $\alpha$ -synuclein: ER-Golgi-dependent exocytosis and non-classical exocytosis, as well as in association with vesicles exosome-like (Fig. 8) (Lee et al., 2005; Emmanouilidou et al., 2010; Jang et al., 2010; Alvarez- Erviti et al., 2011; Danzer et al., 2011). Exosomes, in fact, have been proposed to participate in the spreading of  $\alpha$ -synuclein within the brain as already described for PrP<sup>Sc</sup> in prion diseases and for  $\beta$ -amyloid peptide (A $\beta$ ) in AD. Exosomes are small membrane vesicles derived from the endocytic pathway and are released from cells into the environment. A wide range of cells secretes exosomes *in vitro*, including neurons and astrocytes (Angot and Brundin, 2009). Danzer et al. (Danzer et al., 2012) provided evidence that  $\alpha$ -synuclein oligomers are present in the exosome fractions from both neuronal and non-neuronal cells. According to their results, exosome-associated  $\alpha$ -synuclein oligomers are more prone to be taken up by the cells than free  $\alpha$ -synuclein oligomers and they confer more cytotoxicity when compared to the increase in Caspase 3/7 activation (Emmanouilidou et al., 2010; Alvarez- Erviti et al., 2011; Danzer et al., 2012) (Fig. 8).

Recently, tunnelling nanotubes (TNTs) have been proposed to be involved in intercellular propagation of  $\alpha$ -synuclein (Abounit et al., 2016). TNTs are actin-containing membrane bridges between cells (Angot and Brundin, 2009) acting as conduits for the exchange of cytosolic and membrane-bound molecules and organelles, as well as for the spreading of pathogens (Costanzo and Zurzolo, 2013). Moreover, the TNTs have been demonstrated to connect neurons/astrocytes (Cavaliere et al., 2017; Wang et al., 2012; Lee et al., 2010) or astrocytes/astrocytes (Rostami et al., 2010) or

neuron/neuron (Desplats et al., 2009), suggesting a possible mechanism of interactions/communications between these two cell population. Through the TNT Rostami and colleagues, hypothesised that neurons and glial cells are able to change materials and organelles such as exosome or mitochondria. (Rostami et al., 2010; Gao et al., 2019).

As with release, uptake of extracellular  $\alpha$ -synuclein can occur passively (by diffusion), or actively, i.e., by endocytosis (Fig. 9). Otherwise, different types of endocytosis take up extracellular  $\alpha$ -synuclein: pinocytosis (often referred to simply as endocytosis) and phagocytosis. While pinocytosis occurs constitutively in virtually all mammalian cells, mainly professional phagocytes like macrophages and microglia carry out phagocytosis. Thus, the uptake mechanism and fate of extracellular  $\alpha$ -synuclein vary depending on the species of  $\alpha$ -synuclein and on the type of recipient cell. Lee et al. demonstrated that different types of brain cells take up exogenous synuclein with different kinetics (Lee et al., 2008).

In particular, microglia were much more efficient than neurons and astrocytes, both in uptake and degradation of extracellular  $\alpha$ -synuclein. These findings suggest either that the same uptake pathways are differentially regulated in different cell types or that different cell types are equipped with distinct receptors for extracellular  $\alpha$ -synuclein. (Liu et al., 2010; Kim et al. 2013) (Fig. 8).

It has also been reported that the aggregates of  $\alpha$ -synuclein can induce lysosomal rupture which increases reactive oxygen species levels and leads to mitochondrial dysfunction and autophagy (Nakamura et al., 2013; Freeman et al., 2013; Parihar et al., 2008; Ghavami et al., 2014). On the other hand, in PD patients,  $\alpha$ -synuclein impairs autophagy by delaying autophagosomes maturation (Winslow et al., 2010, 2011; Martinez-Vincente et al., 2008) thus leading to mitochondrial respiratory chain damage. This results in the accumulation of reactive oxygen species, calcium

dyshomeostasis, and consequently mitochondrial-dependent apoptosis (Smith et al., 2005; Parihar et al., 2009). However, if  $\alpha$ -synuclein aggregation affects the autophagosomes-lysosome pathway in neurodegenerative disease (Wong et al., 2015), it, in turn, leads to further  $\alpha$ -synuclein accumulation (Gallegos et al., 2015).

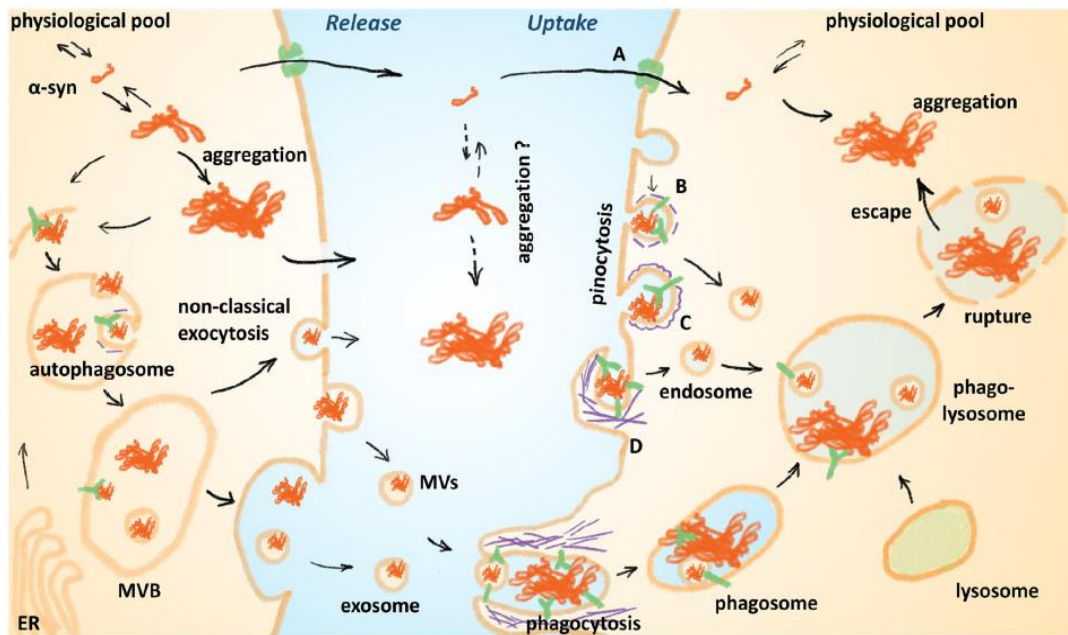


**Figure 8: Schematic model summarizing  $\alpha$ -synuclein release and uptake mechanisms:** Monomeric  $\alpha$ -synuclein can aggregate to different molecular weight species. Aggregated  $\alpha$ -synuclein that fails to be degraded via the autophagic system can be secreted by non-classical exocytosis and by the release of multivesicular bodies' (MVB) contents to the extracellular space.  $\alpha$ -synuclein can also be released in association to vesicles, either through membrane shedding ('microvesicles', MVs) or by incorporation into vesicles of the MVB ('exosomes' when in the extracellular space). Passive release of  $\alpha$ -synuclein can occur through leaky cell membranes or by a putative translocator for monomeric  $\alpha$ -synuclein, which can also facilitate passive uptake of monomeric  $\alpha$ -synuclein (A). In the extracellular space,  $\alpha$ -synuclein can be modified (e.g., by proteases) and/or aggregate further. Extracellular  $\alpha$ -synuclein can be taken up by caveolin-dependent pinocytosis (B), clathrin-dependent pinocytosis (C) or actin-dependent macropinocytosis (D). LAG3 and further binding partners (Na/K-ATPase, neurexin) and receptors can mediate the uptake process. Large  $\alpha$ -synuclein particles and vesicles are also engulfed by actin-mediated phagocytosis in phagocytic cells. Internalized material is routed by the endosomes and phagosomes to the phagolysosome for degradation. Failure of lysosomal degradation and lysosomal rupture can release  $\alpha$ -synuclein into the cytoplasm, where it can seed the aggregation of endogenous  $\alpha$ -synuclein from the physiological pool. (Grozdanov et al., 2018)

Another cellular toxicity pathway is the permeabilization of cellular membranes by oligomers (Stockl et al., 2013). The oligomers might interfere with the normal functions of cellular membranes and form pore-like

structures, resulting in abnormal ions influx with consequent neurodegeneration (Tsigelny et al., 2012). Several studies indicate that  $\alpha$ -synuclein oligomers being able to interact with lipid membranes, increase the conductance and form a pore complex in planar lipid bilayers (Kim et al., 2009; Schmidt et al., 2012; Tosatto et al., 2012). Neurons overexpressing  $\alpha$ -synuclein, in fact, display increased membrane permeability, an effect that is more evident in the cells expressing A53T mutant  $\alpha$ -synuclein (Furukawa et al., 2006) (Fig. 9).

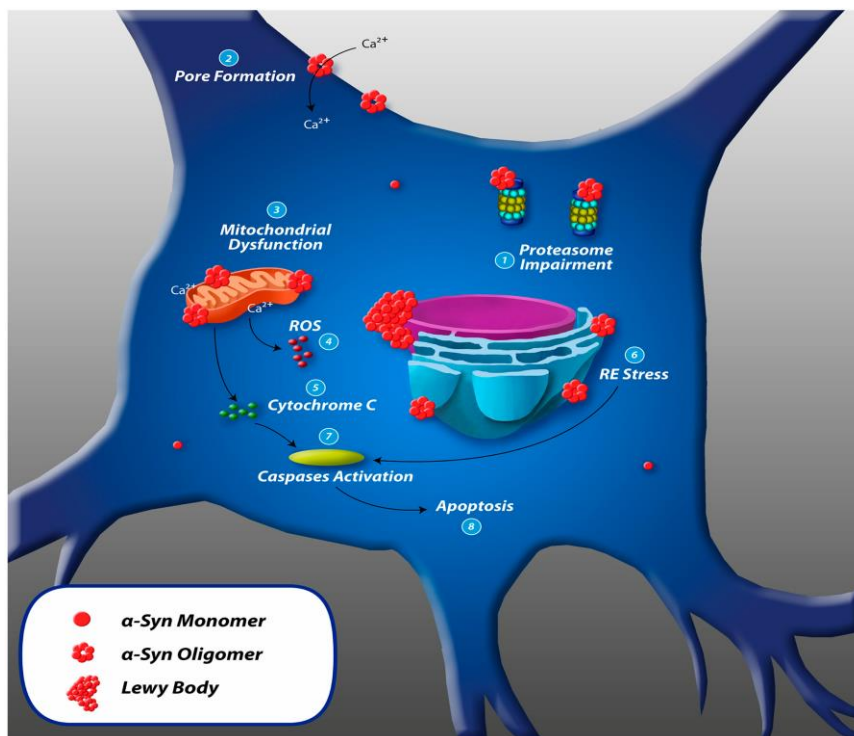


**Figure 9: Toxic mechanisms leading to  $\alpha$ -synuclein aggregation and cell death.** (1) Proteasome impairment: inhibition of chymotrypsin, tryptic and post-acidic proteasome activity leading to further intracellular accumulation of misfolded proteins such as  $\alpha$ -synuclein. (2) Pore-formation:  $\alpha$ -synuclein oligomers penetrate cellular membranes increasing the conductance by forming pore-like structures that could act as non-selective channels, resulting in abnormal calcium influx. (3) Mitochondrial dysfunction:  $\alpha$ -synuclein associates to the mitochondrial inner and outer membrane and (4) increases mitochondrial and intracellular ROS levels. (5) Release of Cytochrome-C: accumulation of intra- mitochondrial ROS and  $\text{Ca}^{2+}$  leads to a reduction in mitochondrial membrane potential and opening of permeability transition pores that could cause the release of Cytochrome-C to the cytosol. (6) RE stress: cellular accumulation of misfolded proteins can lead to chronic endoplasmic reticulum stress.  $\alpha$ -synuclein associates to ER membrane and causes morphologic dysfunction such as dilated cisternae and increases the level of ER chaperones. (7) Cytochrome-C leads to activation of caspase-3 and-9, and ER stress leads to the activation of caspase-12. (8) Caspases initiate apoptosis leading to cell death. (Gallegos et al., 2015)

## 2.4 Neuroinflammation in Parkinson's Disease

Among the many factors related to PD pathology, microglia and neuroinflammation have gained the great attention during the last years, and it has been suggested that the immune system plays an active part in the symptoms and progression of the disease (Doorn et al., 2012; Blandini, 2013; Wang et al., 2015; Caggiu et al., 2019; Tansey et al., 2019; Torres-Odio et al., 2017; Troncoso-Escudero et al., 2018; Zhao et al., 2019; Gelders et al., 2018). Further supporting this, epidemiological studies have revealed that taking ibuprofen anti-inflammatory agent regularly is associated with a 35% lower risk of PD (Chen et al., 2005; Rees et al., 2011).

On the other hand, *in vivo* studies show that the specific early up-regulation of SN microglia in PD correlates with disease severity and dopamine terminal loss (Orr et al., 2005; Ouchi et al., 2005). Studies based on animal models and *in vitro* cell culture indicate that dopaminergic cells are highly sensitive to inflammatory attack (Castano et al., 1998; Fernagut and Chesselet, 2004) and that microglial cells can be strongly activated to lead such an inflammatory response (Austin et al., 2006). Moreover, it has been recently reported that treatment with CSF from PD patients strongly affects cultured microglial cells, resulting in reduced cell growth, morphological changes, as well as increased content and aggregation of  $\alpha$ -synuclein (Schiess et al., 2010).

In parallel, the investigation of  $\alpha$ -synuclein role in PD has added several relevant pieces of evidence regarding the neuroinflammatory process occurring in PD. First: extracellular  $\alpha$ -synuclein is most efficiently cleared by microglia (Lee et al., 2008); second, the efficiency of this process seems to depend on the activation state of microglia and on whether  $\alpha$ -synuclein is in monomeric or oligomer form (Lee et al., 2008; Park et al., 2008). Lastly,  $\alpha$ -synuclein, especially if aggregated, can lead to pro-inflammatory activation of microglia.



Since the first report showing activation of microglia in PD post-mortem brains (McGeer et al., 1988) numerous other studies have been published describing microglial changes, so-called “microgliosis” in humans, as well as in PD animal models (Long-Smith et al., 2009; Halliday and Stevens, 2011). The post-mortem observations have been confirmed by in vivo positron emission tomography (PET) imaging studies of microglial activation, by means of administration of the peripheral benzodiazepine receptor (PBR/TSPO) binding ligand [11C] -(R) PK11195 (Bartels et al., 2010). This ligand gives normally a low signal but it is increased upon neuronal injury due to up-regulation of the TSPO in microglial cells (Weissman and Raveh, 2003). The use of this ligand revealed microglial activation in the midbrain, putamen, pons and cortex of PD patients (Ouchi et al., 2005; Gerhard et al., 2006). These and other studies have confirmed that microgliosis is not only related to those brain areas in which neuronal death occurs, but rather to the appearance of  $\alpha$ -synuclein pathology. Moreover, these studies also demonstrated that although microglial activation is an early event in PD, activated microglial cells are present during all the disease duration (Politis et al., 2012; Sanchez-Guajardo et al., 2010; Barkholt et al., 2012).

The neuron-microglia crosstalk can result from changes in neurons that are subsequently sensed by microglia or vice versa, therefore creating a feed-forward mechanism that contributes to the maintenance of neuroinflammation and progression of the disease. Thus neurons expressing  $\alpha$ -synuclein can activate microglia, but also microglial activation may lead to abnormal handling of  $\alpha$ -synuclein in neurons. Indeed, injection of monomeric or oligomeric  $\alpha$ -synuclein into the substantia nigra leads to microgliosis, supporting  $\alpha$ -synuclein as a direct initiator of inflammation (Wilms et al., 2009; Couch et al., 2011).

Two recent studies have explored the link between neuroinflammation and  $\alpha$ -synuclein dysfunction by LPS injection in rat (Choi et al., 2010) or mice (Gao et al., 2011). In particular, in the second study, the authors evaluated the dopaminergic neurodegeneration, the  $\alpha$ -synuclein pathology and the neuroinflammation in WT and transgenic A53T  $\alpha$ -synuclein - overexpressing mice (Gao et al., 2011). They observed that, while both models initially displayed acute neuroinflammation, only the latter developed persistent neuroinflammation together with chronic progressive degeneration of nigrostriatal dopamine pathway, accumulation of aggregated-nitrated  $\alpha$ -synuclein and formation of LB (Gao et al., 2011). In line with this finding, a rat AAV-based model overexpressing the A53T variant in the SN revealed dramatic changes in cytoskeletal protein levels and activated microglia-mediated neuroinflammation in the striatum (with increased release levels of IL-1 $\beta$ , IFN- $\gamma$ , and TNF- $\alpha$  pro-inflammatory cytokines), well before neuronal loss was evident (Chung et al., 2009; Theodore et al., 2008).

Over the last few years, certain differential functions for non-aggregated extracellular  $\alpha$ -synuclein in glia have been reported. It has been observed that, in contrast to the aggregated form, monomeric  $\alpha$ -synuclein enhances microglial phagocytosis (Park et al., 2008). Interestingly, a comparative study using exogenous non- aggregated  $\alpha$ -synuclein has recently shown to induce higher TNF- $\alpha$ , IL-1 $\beta$  and ROS release levels than aggregated  $\alpha$ -synuclein in microglia (Lee et al., 2010). These and other recent findings point at the importance of exploring the effects on the immune response of aggregated as well as non-aggregated  $\alpha$ -synuclein.

Recently, a possible role of  $\alpha$ -synuclein as a natural antimicrobial peptide (AMP) has been outlined. AMPs belong to an ancient family of proteins able to generate oligomers and fibrils, similar to  $\alpha$ -synuclein, and constitute the first line of defence against pathogens acting as potent broad-spectrum

antibiotics and immunomodulators (Wiesner et al., 2010). However, when dysregulated, the protective action of AMPs may lead to various toxic effects (Yamaguchi et al., 2007; Paulsen et al., 2002) (Fig. 10).

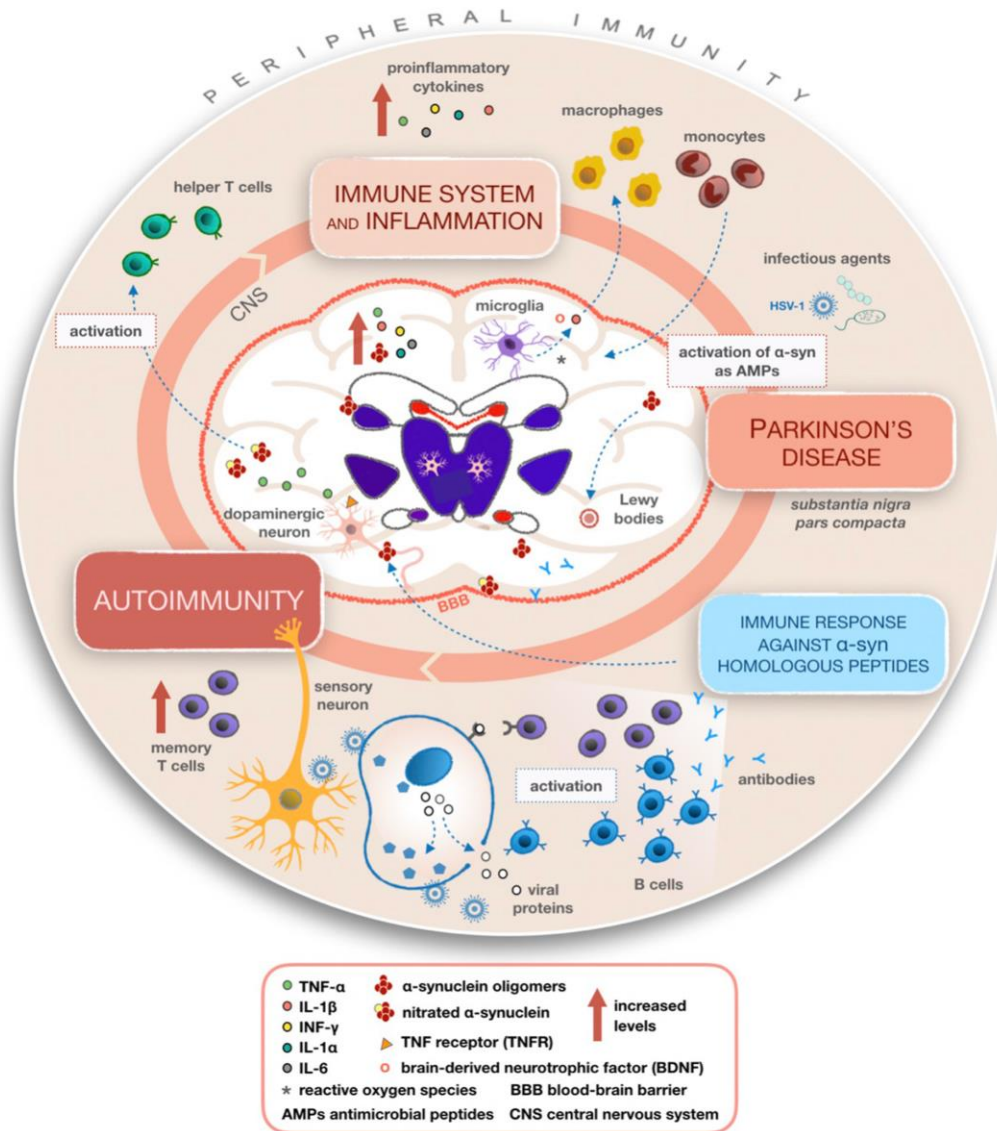


**Figure 10: Mechanisms summarizing the involvement of inflammatory and immune processes in Parkinson's disease (PD).** Once activated, microglial cells produce cytokines able to recruit macrophages and monocytes from peripheral compartments to the CNS, leading to altered peripheral immunity and various inflammatory processes within the CNS in PD patients. A possible mechanism of action giving rise to autoimmunity involves the reactivation of latent HSV-1 on infected sensory neurons and production of antibodies targeting  $\alpha$ -synuclein (fragments homologous to viral proteins). It is plausible that  $\alpha$ -synuclein acting as an AMP becomes dysregulated during recurring infections with its consequent accumulation in the CNS. (Caggiu et al, 2019)

Mounting evidence indicates that microglia has two alternative phenotypes the M1 pro-inflammatory phenotype and the alternative M2 anti-inflammatory phenotype. These different activation statuses of microglia are characterized by the secretion of different arrays of cytokines (Pisanu et al., 2014; Hu et al., 2012). The classical M1 activation of microglia is featured by the production of pro-inflammatory cytokines, including TNF- $\alpha$ , IL-1 $\beta$ , IL-6, IL-12, and other cytotoxic molecules such as superoxide, NO and reactive oxygen species (ROS), contributing to the amplification of the pro-inflammatory responses during injuries and infections. Conversely, M2 microglia plays an immunosuppressive role by antagonizing the classic M1 microglia and promoting tissue repair. The M2 microglia produces a variety of cytokines with anti-inflammatory property, such as IL-4, IL-13, IL-10, and TGF- $\beta$ . Previous investigations indicated that a majority of the activated microglia expresses M2 associated genes at the early stages following injury in various models. However, long-term over-activation of microglia in the PD brain significantly up-regulates the expression of a large group of pro-inflammatory cytokines including TNF- $\alpha$ , IL-1 $\beta$ , interleukin-6 (IL-6) and IFN- $\gamma$ , which contribute to the acceleration of nigral DA neuron degeneration (Ferrari et al., 2006; McCoy et al., 2006). As the disease progresses, molecules such as  $\alpha$ -synuclein, ATP and metalloproteinase-3 (MMP-3) released from the degenerating DA neurons will further enhance microglia activation, amplify the neuroinflammatory responses in the brain forming a vicious cycle of neurodegeneration (Saijo et al., 2009; Zhang et al., 2005). These interesting observations suggest a promising strategy to intervene in the progression of PD by manipulating the transition of microglia activation status (Delgado and Ganea, 2003; Gao and Hong, 2008; Halliday and Stevens, 2011; Sanchez-Pernaute et al., 2004; Vila et al., 2001; Wu et al., 2002; Wyss-Coray and Mucke, 2002).

Several recent studies have identified a dynamic role for mitochondria in cell death, especially the role of mitochondria and mitochondrial products in the execution of an inflammatory form of cell death, referred as pyroptotic cell death that is mediated by Nod-like receptor family pyrin domain containing 3 (NLRP3) inflammasome activation.

The NLRP3 inflammasome is a molecular platform activated upon signs of cellular 'danger' to trigger innate immune defences through the maturation of pro-inflammatory cytokines such as interleukin IL-1 $\beta$ . Key components of a functional NLRP3 inflammasome are NLRP3, the adaptor protein ASC and caspase-1 (Schroder et al., 2010). Upon detecting cellular stress, NLRP3 recruits ASC and procaspase-1, which results in caspase-1 activation and processing of cytoplasmic targets, including the pro-inflammatory cytokines IL-1 $\beta$  and IL-18 (Fig. 11).

Several distinct pathways activated by dysfunctional mitochondria have been proposed to modulate NLRP3 inflammation activation. For example, inhibition of mitochondrial complex I by rotenone or complex-III by antimycin A induces robust ROS production by mitochondria (Huang et al., 2005; Li et al., 2013) which is sufficient to drive NLRP3 inflammasome activation, indicating mitochondrial ROS as a direct activator of the NLRP3 inflammasome (Zhou et al., 2011). Interestingly, a role for Ca<sup>2+</sup> influx to the cytoplasm in NLRP3 inflammasome activation is also hypothesized (Brough et al., 2003; Lee et al., 2012).

Like microglia, astrocytes respond to inflammatory stimulations such as LPS, IL-1 $\beta$  and TNF- $\alpha$  by producing pro-inflammatory cytokines both in vitro and in vivo (Saijo et al., 2009; Tanaka et al., 2013). Reactive astrogliosis, characterized by the increased expression levels of glial fibrillary acidic protein (GFAP) and hypertrophy of cell body and cell extensions, has been described in various PD animal models.

Because they have been shown to produce both pro-inflammatory and anti-inflammatory agents, these cells are thought to have opposite effects in the pathogenesis of PD (McGeer & McGeer, 2008). In fact, if on the one hand  $\alpha$ -synuclein has been shown to be capable to stimulate astrocytes to produce IL-6 and ICAM-1 (Klegeris et al., 2008) on the other hand, astrocytes have been shown to secrete a number of neurotrophic factors that protect dopaminergic neurons in some models of PD (McGeer & McGeer, 2008), even if the mechanisms underlying most of these functions are not yet known.

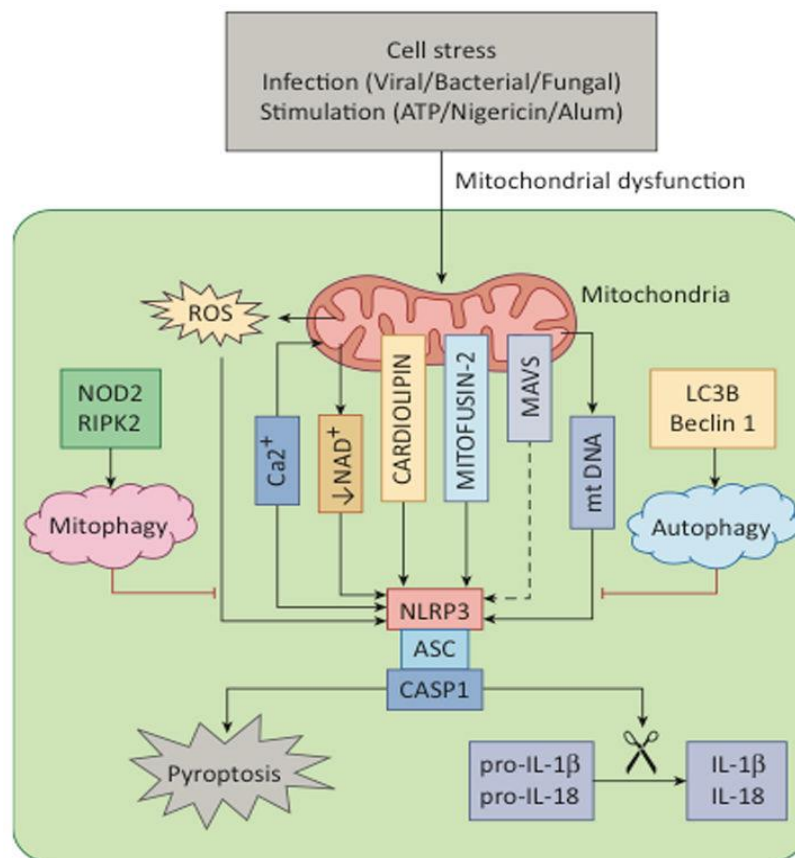


**Figure 11: Schematic model showing mitochondria at the centre of NLRP3 inflammasome activation.** NLRP3 inflammasomes are activated by a myriad of stimuli that ranges from virus, bacteria, and fungi to danger-associated molecular patterns (DAMPs) such as ATP, nigericin and alum. Once activated, NLRP3 forms a multimeric protein complex with associated speck-like protein containing a CARD (ASC) and caspase-1 (CASP1) termed the inflammasome. Caspase-1 is activated in the inflammasome complex, which cleaves pro-IL1 $\beta$  and pro-IL-18 into their bioactive mature forms. Mitochondria are central regulators of NLRP3 inflammasome activation. Mitochondrial reactive oxygen species (ROS), Ca<sup>2+</sup> overload, reduced NAD<sup>+</sup>, cardiolipin, mitofusin, mitochondrial antiviral signalling protein (MAVS) and mitochondrial DNA (mtDNA) have all been shown to promote NLRP3 inflammasome activation. NOD2/RIPK2-dependent mitophagy and LC3B/Beclin 1-mediated autophagy are involved in the clearance of damaged mitochondria, and thus negatively regulate NLRP3 inflammasome activation. (Gurung et al., 2015)

Astrocytes have been shown to express  $\alpha$ -synuclein (Tanji et al., 2001; Braak et al., 2007; Terada et al., 2003; Wakabayashi et al., 2000). It has been observed that astrocytic responses are relatively slower than microglial activation after stimulations. Microglia may initiate the inflammatory responses after immune stimulations such as LPS treatment and  $\alpha$ -synuclein aggregation. Astrocytes are then activated by a variety of molecules including pro-inflammatory mediators released from activated microglial cells and this immune signal are further amplified by astrocytes (Saijo et al., 2009). It has been proposed that uncontrolled neuroinflammation caused by the synergic activation of microglia and astrocytes ultimately might contribute to the enhanced death of DA neurons in the SNpc during neurodegeneration (Saijo et al., 2009; Glass et al., 2010). The expression levels of TNF- $\alpha$  and IL-6 by primary cultured astrocytes are increased significantly after  $\alpha$ -synuclein treatment in vitro (Fellner et al., 2013) (Fig.12).

Specific overexpression of mutant A53T  $\alpha$ -synuclein in astrocytes causes widespread astrogliosis, strong microglial activation, development of progressed paralysis and degeneration of DA neurons and motor neurons in mice (Gu et al., 2010).

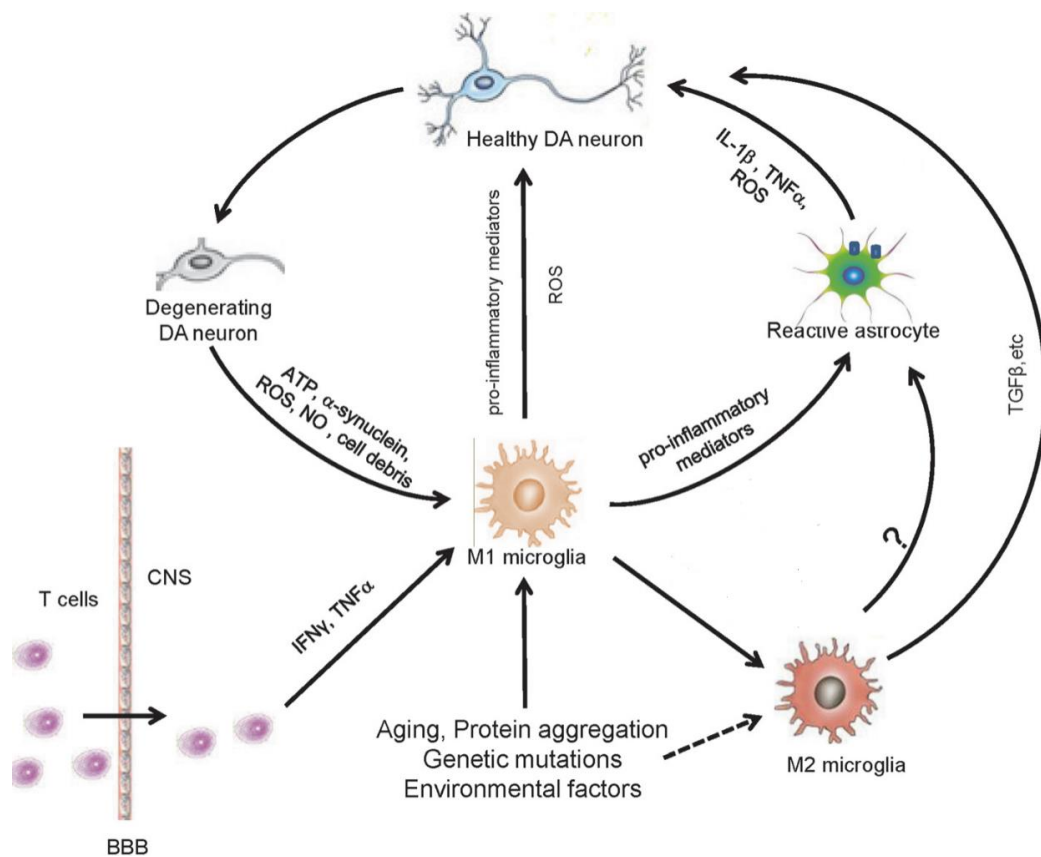


**Figure 12: Diagrammatic representation of inflammatory mechanisms involved in PD pathogenesis.** Microglia become activated, M1 phenotype, in PD under pathological conditions such as protein aggregation, gene mutations, environmental factors and cytokines released from infiltrated T cells. The pro-inflammatory mediators from M1 microglia activate astrocytes leading to elevated production of proinflammatory factors, nitric oxide and superoxide radicals, contributing to the degeneration of DA neurons. The molecules released from degenerative DA neurons can further cause activation of glia and enhanced inflammatory response. At a certain stage of PD, sub-population of microglia may become activated, M2 phenotype, releasing anti-inflammatory factors, including TGF- $\beta$ , and exert a neuroprotective effect in PD (Wang *et al.*, 2015)



### 3. SODIUM/CALCIUM EXCHANGER

#### 3.1 Structural and functional features of NCXs

Na<sup>+</sup>/Ca<sup>2+</sup> exchanger (NCX) represents a major transporter assuring Ca<sup>2+</sup> efflux from mammalian cells (Blaustein and Lederer, 1999). Under physiologic conditions, NCX provides the exchange of 3Na<sup>+</sup>/1Ca<sup>2+</sup> between the cytoplasm and extracellular medium. In most tissues, it operates in a “forward” way corresponding to inward current and thus to calcium exit from the cell (Blaustein and Lederer, 1999). Under some conditions, however, a reverse mode of Na<sup>+</sup>/Ca<sup>2+</sup> exchange can be activated coupling the extrusion of three Na<sup>+</sup> ions with the influx of one Ca<sup>2+</sup> ion (Blaustein and Lederer, 1999; Philipson and Nicoll, 2000; Annunziato et al., 2004).

NCX belongs to a multigene family comprising three isoforms, named NCX1, NCX2, and NCX3. To fulfil the physiological demands of various cell types, the Na<sup>+</sup>/Ca<sup>2+</sup>exchanger isoforms and their splice variants are expressed in a tissue-specific manner (Philipson and Nicoll, 2000; Khananshvili, 2012). NCX expression is highest in cardiac muscle, skeletal muscle, and brain tissue and has also been reported in vascular smooth muscle and urinary bladder smooth muscle (Murata et al., 2010). NCX1 localizes at the presynaptic and postsynaptic sites and in the endoplasmic reticulum membrane of neurons (Canitano et al., 2002), in axons, dendrites, and growth cones (Luther et al., 1992). NCX1 also localizes to the inner membrane of the nuclear envelope and complexes with GM1 (Ledeen and Wu, 2007; Secondo et al., 2018). NCX2 and NCX3 are highly expressed in brain tissue and skeletal muscles (Li et al., 1994; Nicoll et al., 1996; Quednau et al., 1997) and all three NCX proteins are widely expressed throughout the rat CNS (Canitano et al., 2002) (Table 1).

NCX1 and NCX3 give rise to several splicing variants that appear to be selectively expressed in different regions and cellular populations of the

brain (Quednau et al., 1997; Yu and Colvin, 1997). In fact, NCX1 mRNA can be detected in the midbrain and in basal ganglia in which dopaminergic cell bodies are localized. Moreover, NCX1 protein isoform is present in the striatum, where the terminal projection fields of dopaminergic nigrostriatal neurons are present (Canitano et al., 2002; Papa et al., 2003).

The NCX3 gene is composed of 9 exons numbered from 1 to 9. The exons 2 and 3, also named A and B, are mutually exclusive (Quednau et al. 1997). Exon 4, also called exon C, is optional. Thus, in the rat, three splice variants can be detected. A variant containing exon A and C is present in skeletal muscle (NCX3-AC), while variants expressing the exon B are expressed in the brain (NCX3-B and NCX3-BC). Additionally, three truncated forms of NCX3 are expressed in humans. Two truncated variants are expressed in the fetal brain and appear to contain exons 4 to 9 and 6 to 9 (Lindgren et al. 2005). The third truncated variant is expressed in skeletal muscle and comprises exons 2 and 6 to 9 (Gabellini et al., 2002). Importantly, it has been observed that the splice variants of NCX3 have different affinity for  $\text{Ca}^{2+}$  and different binding sites in their CBD2 (calcium-binding domain 2), three for NCX3-B and two for NCX3-AC (Breukels et al., 2012) (Fig. 13).

**TABLE 1. Distribution of NCX1, NCX2, and NCX3 mRNA in the CNS**

	NCX1	NCX2	NCX3
<b>Olfactory system</b>			
Olfactory bulb	+	++	++
Anterior olfactory nucleus	++	++	+
<b>Cerebral cortex</b>			
Cingulate cortex	++	++	++
Motor cortex: layers III/V	+++	+	+
Motor cortex: layers V/VI	++	++	+
Sensory cortex: layers I/III	+	+++	+
Sensory cortex: layers V/VII	+	+++	+/-
Piriform cortex	+++	+++	++
<b>Hippocampus</b>			
Pyramidal cell layer, CA 1	++	++	+
Pyramidal cell layer, CA 2	+++	+++	+
Pyramidal cell layer, CA 3	+++	+++	+
Granule cell layer, dentate gyrus	++	+++	+++
Polymorph layer, dentate gyrus	++	+	-
<b>Amygdala</b>			
Lateral nucleus	++	+	++
Basolateral/basomedial nuclei	++	+/-	+++
Central nucleus	++	+	++
<b>Basal ganglia</b>			
Nucleus accumbens/core	+	+++	+
Nucleus accumbens/shell	-	+++	+
Caudate putamen	+/-	+++	+/-
Globus pallidus	+/-	+++	+/-
<b>Thalamus</b>			
Habenula	++	++	+/++
Anterodorsal thalamic nuclei	++	++	++
Ventromedial nucleus	+++	++	++
Ventrolateral	++	++	+/++
Ventroposterior (VP)	+	+++	+/++
Dorsolateral thalamic nuclei	++	+++	+++
Reticular nucleus	+	++	++
Geniculate nucleus	+	++	-
<b>Hypothalamus</b>			
Magnocellular preoptic nucleus	+++	-	+/-
Supraoptic nucleus	+++	+	+
Lateral hypothalamic nuclei	++	+	+
Mammillary nuclei	+/-	++	+
<b>Brainstem</b>			
Substantia nigra, pars compacta, VTA	+++	+/-	+/-
Reticular formation	++	++	++
Raphe nuclei	++	++	+++
<b>Cerebellum</b>			
Granular cell layer	+	+	++
Purkinje cells	+++	+	++
Molecular cell layer	-	-	-
Cerebellar nuclei	++	++	-
<b>Medulla and spinal cord</b>			
	+	++	++

(According to Canitano et al., 2002)

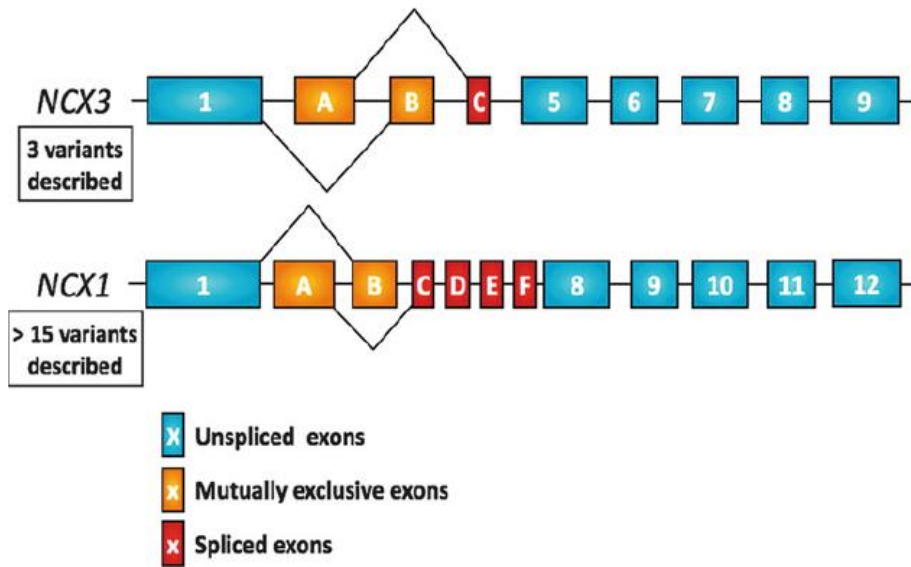
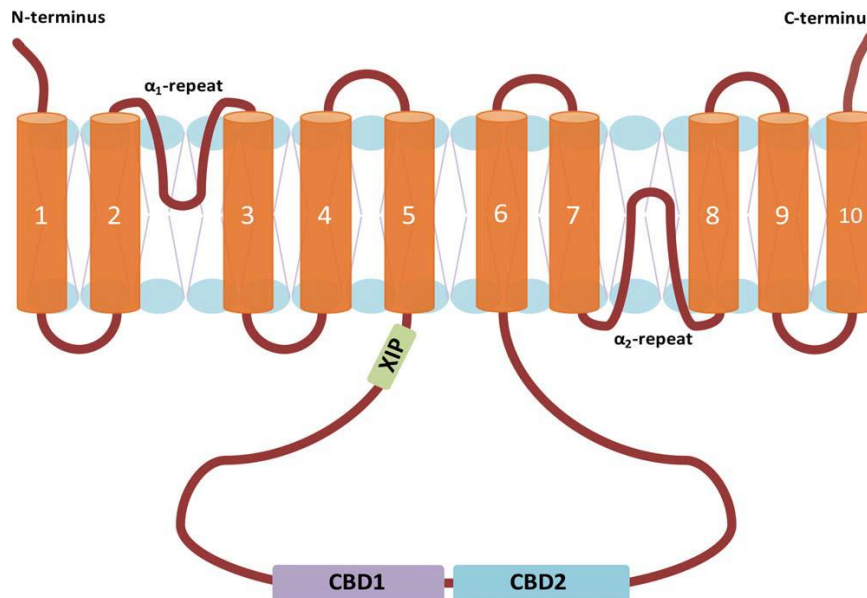


Figure 13: Schematic view of the exons constituting NCX3 (upper) and NCX1 (bottom) gene sequence and presenting the exons giving rise to multiple variants after alternative splicing event (Michel et al., 2015)

The NCX proteins have a general topology composed of 10 transmembrane domains (TM) (Ren and Philipson, 2013), with a large intracellular loop between TM5 and TM6. This loop contains the calcium-binding domain 1 (CBD1) and calcium-binding domain 2 (CBD2), which are regulatory domains required for intracellular ion sensing and binding. Binding of four calcium ions to the CBD1 domain triggers a conformation change from disordered to a more rigid structure, resulting in activation of the NCX transporter (Hilge et al., 2006, 2009). Calcium has a low affinity for CBD2 and binds it at elevated concentration, therefore CBD2 may play a more selective role than CBD1 (Hilge et al., 2009, Weber et al., 2001; Nicoll et al., 2007; Reeves and Condrescu, 2008; Boyman et al., 2011). Within the same intracellular loop that includes CBD1 and CBD2, there is the XIP motif, a 20 amino acid sequence located on the N-terminus of the cytosolic loop that confers sodium-dependent inactivation to the exchanger protein (Matsuoka et al., 1997). Domain linker between TM2 and TM3 forms the  $\alpha$ 1-repeat, and the linker between TM7 and TM8 forms the  $\alpha$ 2-repeat. The  $\alpha$ -repeats

domains contain residues essential for cation ligands and transport (Winkfein et al., 2003) (Fig. 14).



**Figure 14: The general topology of the NCX protein.** The NCX protein is composed of 10 transmembrane domains, two  $\alpha$ -repeats, and a large intracellular loop that contains ion sensing and binding regulatory domains. (Sharma et al., 2013)

Several factors are involved in the regulation of NCXs activity. Among them, the two transported ions,  $\text{Na}^+$  and  $\text{Ca}^{2+}$  play a crucial role. Indeed, a rise in cytosolic  $[\text{Na}^+]$  rapidly stimulates and then inactivates the exchanger, whereas a rise in cytosolic  $[\text{Ca}^{2+}]$  activates NCX and relieves the  $\text{Na}^+$ -dependent inactivation (Hilgemann et al., 1992). Moreover, NCX is extremely sensitive to cytosolic acidification, redox status and metabolic state (DiPolo and Beauge, 1982; Doering and Lederer, 1994, 1996). These factors imply, in some cases, modifications of the exchange activity and, in others, alterations of the protein expression and docking into the membrane where, associated with other transporters such as  $\text{Na}^+/\text{K}^+$ -ATPase and  $\text{Na}^+/\text{H}^+$  exchanger as well as enzymes like kinases and phosphatases, they form functional supramolecular complexes (Bers and Despa, 2009; Schulze et al., 2003; Berberian et al., 2009).

### ***3.2 Role of NCXs in physiological and pathological conditions***

The activity of NCX is important, especially in some neurophysiological conditions.

The level of expression of NCX in neurons is predominantly high in those sites where a large movement of  $\text{Ca}^{2+}$  ions occurs across the plasma membrane, as it happens at the level of synapses (Juhaszova et al., 1996; Canitano et al., 2002). Specifically, during an action potential or after glutamate-activated channel activity,  $\text{Ca}^{2+}$  massively enters the plasma membrane. Such phenomenon triggers the fusion of synaptic vesicles with the plasma membrane and promotes neurotransmitter exocytosis. After this event, outward  $\text{K}^+$  currents repolarize the plasma membrane, thus leading to voltage-gated calcium channels closure. According to the diffusion principle,  $\text{Ca}^{2+}$  ions are distributed in the cytosolic compartment, reversibly interacting with  $\text{Ca}^{2+}$ -binding proteins. Residual  $\text{Ca}^{2+}$  ions are then rapidly extruded by the plasma membrane  $\text{Ca}^{2+}$  ATPase and by NCX activation. The  $\text{Na}^+/\text{Ca}^{2+}$ -exchanger becomes the dominant  $\text{Ca}^{2+}$  extrusion mechanism when  $[\text{Ca}^{2+}]_i$  is higher than 500nM, as it happens when a train of action potentials reaches the nerve terminals. It has been calculated that for these  $[\text{Ca}^{2+}]_i$  value, more than 60% of  $\text{Ca}^{2+}$  extrusion is mediated by  $\text{Na}^+/\text{Ca}^{2+}$ -exchanger families. In such physiological conditions, NCX activation is consistent with its low-affinity ( $K_d$  500nM) and high-capacity ( $5 \times 10^3 \text{Ca}^{2+}/\text{s}$ ) function. In contrast, in resting conditions or after a single action potential, when  $[\text{Ca}^{2+}]_i$  slightly increases, requiring, therefore, a subtler control, the high-affinity ( $K_d$  100 nM) and low-capacity ( $10^2 \text{Ca}^{2+}/\text{s}$ ) pump, the plasma membrane  $\text{Ca}^{2+}$ -ATPase, assumes a predominant function, thus making the involvement of NCX less relevant (Blaustein and Lederer, 1999).

On the other hand, dysregulation of  $[Ca^{2+}]_i$  and  $[Na^+]_i$  homeostasis is involved in neuronal injury occurring in *vitro* and *in vivo* models of hypoxia-anoxia and in several neurodegenerative diseases. More specifically, in the early phase of neuronal anoxic insult, the  $Na^+/K^+$ -ATPase blockade causes an increase of  $[Na^+]_i$ , which in turn induces NCX to reverse its mode of operation. Although during this phase NCX causes an increase in  $[Ca^{2+}]_i$ , its effect on neurons appears beneficial for two reasons. First, by promoting  $Ca^{2+}$  influx, NCX promotes  $Ca^{2+}$  refilling into the ER, which is depleted by anoxia followed by deoxygenation, thus allowing neurons to delay ER stress (Sirabella et al., 2009). Second, by eliciting the decrease in  $[Na^+]_i$  overload, NCX prevents cell swelling and death (Annunziato et al., 2007). Conversely, in the later phase of neuronal anoxia, when  $[Ca^{2+}]_i$  overload takes place, the NCX forward mode of operation contributes to the lowering of  $[Ca^{2+}]_i$ , thus protecting neurons from  $[Ca^{2+}]_i$  induced neurotoxicity (Annunziato et al., 2004). Moreover, further studies have demonstrated that BHK cells overexpressing NCX1 or NCX2 isoforms are more vulnerable to chemical hypoxia compared to BHK cells expressing NCX3 isoforms, thus suggesting that each of the three isoforms has different functional properties and plays a different role in the pathogenesis of a cellular damage (Secondo et al., 2007; Bano et al., 2005). Another study shows that ischemic rats treated with NCX1 or NCX3 antisense display a remarkable enlargement of the infarct volume (Pignataro et al., 2004) thus suggesting a crucial role of these two isoforms in the pathogenesis of ischemic damage.

It is also demonstrated that NCX plays an important role during ageing since the impairment of  $Ca^{2+}$  homeostasis in neuronal cells is considered to be the major triggering event that leads to the development of brain ageing (Annunziato et al., 2002). Studies performed on the cerebro-cortex nerve endings of aged rats have shown that the activity of NCX is markedly

reduced in the forward and in the reverse mode of action (Michaelis et al., 1984; Canzoniero et al., 1992). NCX decline seems to be the consequence of a reduced affinity of the antiporter for  $\text{Ca}^{2+}$  ions (Michaelis et al., 1984).

In this sense, during ageing and also during neurodegenerative diseases, such as Alzheimer's disease and Parkinson's disease in which a neuronal calcium dysfunction is found, NCX might have a relevant role. In fact, a study performed in the synaptic terminals obtained from the brain cortex of AD patients showed that NCX activity was increased (Colvin et al., 1994). Another study performed in synaptosomes prepared from cryopreserved brain of cognitively normal aged controls and late-stage Alzheimer's disease patients demonstrated that NCX2 protein expression was upregulated whereas, NCX3 native 105 kDa band was downregulated. Moreover, the co-localization of NCX1, NCX2, and NCX3 with  $\text{A}\beta$  in synaptic terminals has been demonstrated (Sokolow et al., 2011). Recently, it was found that in the absence of PINK1,  $\text{NCX}_{\text{mito}}$  activity was severely impaired, leading to mitochondrial calcium overload, permeability transition pore opening and cell death (Gandhi et al., 2009). In fact, it was proposed that  $\text{NCX}_{\text{mito}}$  is entirely distinct from the characterized plasmalemmal NCX isoforms, due to the specific sensitivity of  $\text{NCX}_{\text{mito}}$  to the inhibitor CGP-37157 (Czyz and Kiedrowski, 2003). Recently, it has been shown that among the three isoforms of NCX, the NCX3 isoform is the only one detected on the outer mitochondrial membrane where it plays an important role in cell survival during hypoxia (Scorziello et al., 2013).

Astrocytes possess several molecular entities responsible for  $\text{Ca}^{2+}$  and  $\text{Na}^{+}$  flux across the plasma membrane, including ionotropic receptors, ion channels, transient receptor potential channels and a wide variety of ion transporters and exchangers including NCXs (Verkhratsky et al., 2012). The plasma membrane  $\text{Ca}^{2+}$ -ATPase is a high-affinity/low capacity transporter and is the major  $\text{Ca}^{2+}$  extruder in resting astrocytes. Similarly, the  $\text{Na}^{+}/\text{K}^{+}$ -



ATPase (NKA) is the major Na<sup>+</sup> extruder in resting astrocytes. Plasmalemmal NCX is a high-capacity/low-affinity exchanger which appears to influence resting levels of cytosolic Ca<sup>2+</sup> and Na<sup>+</sup> and plays the major role in the regulation of these ions when they are elevated in an excessive or prolonged manner (Reyes et al., 2012). NCX is highly enriched in perisynaptic astroglial processes, which represent the third component of the tripartite synapse (Araque et al., 1999) and perform glutamate gliotransmission to modulate synaptic transmission and plasticity (Ni et al., 2007; Perea and Araque, 2007).

[Ca<sup>2+</sup>]<sub>i</sub> also regulates many important functional responses in microglia, including phagocytosis, transformation and migration (Pozner et al., 2015). All three NCX isoforms have been documented in cultured microglia, with NCX1 being the predominant form (Annunziato et al., 2013; Matsuda et al., 2001; Nagano et al., 2004; Newell et al., 2007). The microglial NCX expression is up-regulated by inflammatory mediators such as interferon-gamma and NO (Nagano et al., 2004). Moreover, microglial NCX upregulation has also been documented in the inflammatory phase in microglial cultured, obtained from in-vivo stroke model, where this NCX-1 up-regulation was concomitant with down-regulation of NCX2-3, an effect that accompanies post-ischemic microglial activation (Boscia et al., 2009)

#### 4. AIM OF THE STUDY

The purpose of the present study was to investigate the possible role of the mitochondria in the onset of neuroinflammation in *in vitro* and *in vivo* models of PD. In particular, it was investigated the relationship between the dysregulation of mitochondrial calcium content and mitochondrial dysfunction and its consequences on the activation of the neuroinflammatory process. To address this issue experiments were performed in animal models of familial forms of PD, such as mice carrying the human mutation of  $\alpha$ -synuclein A53T under the Prion murine promoter, and mice expressing wild-type human  $\alpha$ -synuclein under the regulatory control of the platelet-derived growth factor- $\beta$  (PDGF- $\beta$ ) promoter. The choice of these models was supported by the evidence that in both of them the accumulation of aggregates of  $\alpha$ -synuclein is in line with the severity of the pathology and with the alteration in the phenotype during ageing, miming the features of the human disease (Masliah et al., 2000; Giasson et al., 2000). Moreover, the choice of the A53T mutation in  $\alpha$ -synuclein was correlated to the evidences that: the mutated protein is more prone to aggregate compared to the WT protein (Ruf et al., 2019), the aggregates of mutated protein interact with the plasma membrane more than the WT  $\alpha$ -synuclein (Ghio et al., 2016), and finally the mutated form of  $\alpha$ -synuclein is able to bind cardiolipin, the principal component of mitochondrial membrane, with a major affinity respect the WT form. In fact, this animal model is characterized by alteration of mitochondrial morphology, reduced activity of the complex IV and mitochondrial DNA damage (Martin et al., 2006) Recent results performed in 12-months-old A53T transgenic mice demonstrated that NCX1 and NCX3 are potential factors contributing to neurodegeneration and neuroinflammation in this

mouse model (Sirabella et al., 2018). Interestingly, these studies also provided evidence that the changes in the expression of these two proteins occurred in neuronal and glial cells although the increase of NCX1 expression was more evident in glial cells and the reduction of NCX3 expression was more pronounced in neurons (Sirabella et al., 2018). To further understand the functional implications of these changes in NCXs expression and their potential role in the pathogenesis of PD, the first part of this study was performed in vitro, in primary neuronal and glial cells obtained from midbrain and striatum of A53T transgenic and wild type mice. In this model, mitochondrial calcium content and membrane potential were measured simultaneously with intracellular calcium concentration by using confocal microscopy and fluorescent dyes. The results obtained showed that in the mesencephalic neurons obtained from A53T transgenic mice an increase of cytosolic calcium concentration  $[Ca^{2+}]_i$  occurred accompanied to an increase of mitochondrial calcium content  $[Ca^{2+}]_m$  and to mitochondrial membrane depolarization. These effects were associated with a decrease of NCX3 expression in A53T transgenic neurons compared to WT without any change in NCX1 expression. Conversely, in the striatal neurons from A53T transgenic mice, in which no changes in the expression of NCX1 and NCX3 were detected,  $[Ca^{2+}]_i$  was similar to WT neurons whereas mitochondrial membrane was hyperpolarized and  $[Ca^{2+}]_m$  was lower compared to WT. To confirm that the changes in NCX3 expression detected in mesencephalic neuron caused mitochondrial dysfunction and in turn mitochondria-activated neuroinflammation in PD, further experiments were performed ex vivo in midbrain and striatum obtained from A53T and WT mice during ageing. Specifically, in these mice, Western blot experiments were first performed to measure  $\alpha$ -synuclein, TH, NCX1 and NCX3 expression during ageing in order to correlate DA neuronal impairment with the abnormal deposition of  $\alpha$ -

synuclein and with the changes of NCX3 and NCX1 protein expression. Furthermore, additional western blotting experiments were performed to evaluate mitochondrial dysfunction and neuroinflammation in A53T transgenic mice during ageing in comparison with WT. The results of these experiments demonstrated a decrease in the expression of NCX3 only in the midbrain of 4 months old transgenic mice, but no variation in the expression of NCX1 in the midbrain and in the striatum. To confirm that the impairment in NCX3 protein expression was associated to mitochondrial dysfunction, the expression of Cytochrome-c (Cyt-c), a marker of mitochondrial damage, and Manganese superoxide dismutase (MnSOD) and Neuronal Nitric oxide synthases (nNOS) two markers of mitochondrial oxidative stress, were measured in 4-12-16- month- old mice. The results of these experiments confirmed that in the midbrain an increase of Cyt-c occurred in transgenic mice already in early-stage of disease (4-month-old mice) while in the striatum of A53T transgenic mice the increase in Cyt-c occurred only in 16-month- old mice. Interestingly, in midbrain of A53T aged mice, the rise up of Cyt-c was associated to a decrease in the expression of MnSOD and to an increase of nNOS, whereas, in the striatum, an increase of nNOS was observed only in A53T 16- month- old mice and no changes in MnSOD expression were observed between transgenic and WT mice. Finally, to correlate mitochondrial dysfunction to neuroinflammation, further experiments were performed *ex vivo* in 4-12-16- months-old A53T and WT mice with the aim to evaluate the expression levels of pro-inflammatory proteins such as the inducible Nitric oxide synthases (iNOS) and Interleukin 1 beta(IL-1 $\beta$ ). Moreover, since previously performed immunohistochemistry experiments in 12-month-old A53T mice demonstrated an increase in Glial Fibrillary Acidic Protein (GFAP) both in midbrain and in striatum and an increase in the Ionized Calcium-Binding Adapter molecule 1(IBA-1) only in the Striatum, Western blot experiments

were performed to evaluate GFAP and IBA1 protein expression in 4 and 16-month-old WT and A53T transgenic mice. Interestingly, the results obtained confirmed the increase of GFAP in transgenic adult mice (16-months-old) both in the midbrain and in the striatum, whereas IBA-1 increased only in the striatum of 16 months old A53T transgenic mice. In this brain area, the increase in IBA-1 was accompanied to an increase in the expression of iNOS and IL-1 $\beta$ , thus confirming the activation of a neuroinflammatory response in the striatum of A53T transgenic mice during ageing.

The last part of the study was addressed to delve deeper into the understanding of the role played by mitochondrial dysfunction in the pathogenesis of neuroinflammation observed in PD. To this aim experiments were performed in collaboration with the “Deutsches Zentrum für Neurodegenerative Erkrankungen” (Centre for Neurodegenerative Disease), with the intent to study the proteomic profile of microglial cells isolated from PDGF-h- $\alpha$ -synuclein mice 2- and -12- month-old, and to correlate the changes in mitochondrial protein expression with the onset of the neuroinflammatory process leading to neurodegeneration occurring in PD. The results of these experiments demonstrated that in 2-month-old PDGF-h- $\alpha$ -synuclein mice the changes in protein profile observed are mainly related to proteins involved in the regulation of mitochondrial dynamics, such as mitofusin-2, or in the protein involved in a mitochondrial oxidative capacity such as the protein belonging to oxidative phosphorylation chain compared to WT mice. These results are suggestive of early involvement of mitochondria in the pathogenic mechanisms leading to neuronal damage observed in PD development. In support of this hypothesis, the results obtained examining the proteomic profile in 12-month-old PDGF-h- $\alpha$ -synuclein mice, which instead demonstrated that the changes occurring are mainly related to proteins involved in neuronal

transmission, such as neurotransmitter release and SNARE complex, as well as to proteins involved in cellular response to the stress, autophagy and endocytosis processes.

To further confirm the role played by glial cells in the pathogenesis of neuroinflammation leading to neuronal dysfunction observed in PD progression, experiments were performed in vitro in astrocytes obtained from A53T transgenic and WT mice, in which NCX1 expression and mitochondrial function were assessed by western blot analysis and confocal microscopy. The results of these experiments demonstrated an increase in NCX1 expression in astrocytes obtained from A53T transgenic mice associated with a reduction in  $[Ca^{2+}]_i$  compared to WT. Interestingly, in astrocytes obtained from A53T transgenic mice mitochondria are hyperpolarized and contain lower calcium concentration compared to WT cells thus confirming that gliosis observed in adult mice is related to preserved mitochondrial function.

## 5. EXPERIMENTAL PROCEDURES

### 5.1 *In vivo and in vitro models*

#### 5.1.1. *A53T $\alpha$ -synuclein transgenic mice*

Mice that express human A53T  $\alpha$ -synuclein under the control of *prion* promoter (PrP-SNCA\*A53T) (Giasson et al., 2002) were obtained from The Jackson Laboratory. Mice hemizygous for the A53T mutation were bred on a mixed C57Bl/6 x C3H background to produce transgenic and non-transgenic littermates. In all cases, 4- 12-16-month- old transgenic mice were directly compared with age-matched wild type littermates. To identify transgenic mice PCR amplifications were performed according to the protocol from The Jackson Laboratory. Mice were group-housed (1-5 animals/cage) in temperature and humidity-controlled rooms under a 12-hours light-/dark cycle and fed ad libitum diet of standard mouse chow. Experiments were performed on male and female mice according to the international guidelines for animal research and approved by the Animal Care Committee of "Federico II" University of Naples, Italy.

#### 5.1.2 *PDGF- h- $\alpha$ -synuclein transgenic mice*

Mice that express human WT  $\alpha$ -synuclein under the control of *PDGF- $\beta$*  promoter (Tg(PDGF $\beta$ -SNCA)4Ema) (Masliah et al., 2002) were obtained from The Jackson Laboratory. The fusion gene, carrying the promoter and the gene of h-  $\alpha$ -synuclein, was freed of vector sequences, purified, and microinjected into one-cell embryos (C57BL/6 x DBA/2 F2) according to standard procedures. Transgenic offspring were identified by polymerase chain reaction (PCR) analysis of tail DNA according to the protocol from The Jackson Laboratory. The expression of h- $\alpha$ -synuclein was confirmed by

western blotting experiments. Briefly, the whole brain was collected, collected was collected and destroyed mechanically and enzymatically until a cell suspension. This cellular suspension was lysed in a buffer containing Tris-HCl (20 mM, pH 7.5); NaF 10 mM; NaCl 150 mM; phenylmethylsulphonyl fluoride (PMSF) 1 mM; NP-40 1%; Na<sub>3</sub>VO<sub>4</sub> 1 mM; aprotinin 0.1%; pepstatin 0.7 mg/ml e leupeptin 1 µg/ml. Homogenates were centrifuged at 14.000 rpm for 20 minutes at 4° C. The supernatant was used to perform Western blot analysis. Protein levels were determined using the BC assay method. (Protein assay kit, Uptima). The total amount of protein used for each sample was 10µg and it was separated on 8% or sodium dodecyl sulfate-polyacrylamide gels with 5% sodium dodecyl sulphate stacking gel (SDS-PAGE) and electro-transferred onto Hybond ECL PVDF paper (Amersham, Milan, Italy). The membranes were blocked in 5% non-fat dry milk in 0.1% Tween 20 (TBS-T; 2mmol/l Tris HCl, 50mmol/l NaCl, pH 7.5) for 1 hour at room temperature (RT) and subsequently incubated overnight at 4°C in the blocked buffer with 1: 1000 antibody for β- Active (SIGMA, A5316), 1:1000 for TH (Millipore, MSB5280). And for h-α-synuclein (Anti-α-Synuclein, 103-108 Antibody, clone 4b12 Biolegend). To increase h-α-synuclein retention on blot membranes, the PVDF membrane was incubated for 30 minutes with PBS plus PFA 4% at room temperature, followed by blocking for 1 hour 5% with no fat milk in 0.1% Tween 20 (Lee et al., 2011; Preterre et al., 2015). Next, all membranes were washed 3 times with a solution containing Tween 20 (0.1%) and subsequently incubated with the secondary antibodies for 1 hour (1:2000) at room temperature. Immunoreactive bands were detected by ECL (Amersham). Discrimination among the distinct types of extracts was ensured by running parallel Western blots with the endogenous actin protein. The signal was detected by the ChemiDoc Imaging System (Bio-



Rad, Milan, Italy) and the optical density of the bands was determined by Image J program.

Experiments were performed on female and male PDGF- $\alpha$ -synuclein transgenic mice according to the Bavarian Government (Art. 55.2-1-54-2532-163-13) and performed according to the animal protection law. All animals were housed in groups under pathogen-free conditions and bred in the animal housing facility at the Centre for Neurodegenerative Disease (DZNE, Munich), in temperature (21 - 2°C) and humidity-controlled rooms, with food and water provided ad libitum and under 12/12-h light/dark cycle.

### *5.1.3 Primary neurons from Prp- A53T- $\alpha$ -synuclein transgenic mice*

Primary midbrain cultures were isolated from the brains of 15 days-old A53T and wild type mice embryos and prepared by modifying the previously described method of Fath and collaborators (Fath et al., 2009). The tissue was minced and incubated with a dissection medium containing EBSS, DNase, BSA and ovomucoid for 30 minutes at 37°C. After incubation, the suspension was centrifuged and subjected to mechanical dissection in order to obtain a cellular suspension. Then the cells were placed on Poly-D-lysine-coated (100 $\mu$ g/ml) plastic dishes, in MEM/F12 culture medium containing glucose, 5% deactivated fetal bovine serum, and 5% horse serum, glutamine (2mM), penicillin (50 U/ml), streptomycin (50  $\mu$ g/ml). The day after plating, cells were treated with Cytosine- $\beta$ -D-arabinose-furanoside in vitro (10  $\mu$ M) to prevent the non-neuronal cell growth. Neurons were cultured at 37°C in a humidified 5% CO<sub>2</sub> atmosphere and used after 10 days in vitro (DIV) for all experiments described. For confocal experiments, cells were plated on glass coverslips coated with Poly-D-lysine (Scorziello et al., 2007).

#### *5.1.4 Primary astrocytes from A53T- $\alpha$ -synuclein transgenic mice*

Primary striatal astrocyte cultures from A53T mice and wild-type animal were obtained from the midbrain and striatum of new-born mice 1-2 days old. The respective areas of the brain were aseptically dissected and meninges were carefully removed. The tissues were minced finely and enzymatically (0.25% trypsin and DNase/MgSO<sub>4</sub> 37 °C, 30 min) and mechanically dissociated to produce single cells suspension. Then the cell suspension was centrifuged at 1000 r.p.m. for 5 min and suspended in DMEM containing 100U/mL penicillin, 100  $\mu$ g/mL streptomycin and 10% FBS. The cells were plated in tissue flasks, then cultured at 37 °C in a 95% air 5% CO<sub>2</sub> incubator. The medium change occurred once every two days. When cells grew to confluence (7-8 days), the flask was shaken with PBS for three-time to remove the loosely attached contaminated microglia. The attached enriched astrocytes were subsequently detached using trypsin-EDTA and then subjected to different experimental procedures.

For Western blotting experiments astrocytes were cultured in flask T75 at 37°C in a humidified 5% CO<sub>2</sub> atmosphere and used after 14-15 days in culture (DIV). For confocal microscopy experiments, after 14-15 (DIV), cells were plated in glasses pre-coated with Poly-D-Lys and analysed after 24h.

#### *5.1.5 Microglia isolated from PDGF-h-synuclein transgenic mice*

The microglia cells were isolated with the gentleMACS Octo Dissociator (Miltenyi Biotec), following its protocols and using all its kits and reagents. Briefly, the whole brain was collected from transgenic and wild-type 2-and-12-month-old mice after anaesthesia with CO<sub>2</sub> and decapitation. The brain was cut into 8 sagittal slices using a scalpel in a sterile dish. The tissue was

mechanically and enzymatically processed to obtain a cell suspension. This suspension was mixed with an antigen-antibody- magnetic cell-sorting (MACS, Miltenyi Biotec) to positively select microglia. Briefly, the mixed cellular population (neurons and glial cells) was re-suspended in MACS buffer (Miltenyi Biotec) and incubated with CD11b Microbeads (Miltenyi Biotec). The cell suspension was then applied to the LS separation column (Miltenyi Biotec) fitted into a QuadroMACS cell separator (Miltenyi Biotec). Unlabelled cells (neurons, astrocytes and oligodendrocytes) were allowed to pass through the column while labelled cells remained captured in the magnetic field. After washing the column with MACS buffer, the column was then removed from the magnetic separator and flushed with MACS buffer to collect the purified microglia population. For an increased level of purity, the eluted microglia population was passed through a new LS separation column a second time. The purity of microglia used in our study was more than 95% assessed by immunocytochemistry (data not shown). The unlabelled cells were collected and used to confirm the expression of  $\alpha$ -synuclein in transgenic and wt mice, while the microglia were collected, were centrifuged and washed for three-time in HBSS buffer. Then the pellet was frozen, after passage in liquid-ammonium, at main 80°C until the Mass Spectrometry experiments.

## 5.2 Western blot analysis

Mice brain tissue and primary neurons were lysed in a buffer containing Tris-HCl (20 mM, pH 7.5); NaF 10 mM; NaCl 150 mM; phenylmethylsulphonyl fluoride (PMSF) 1 mM; NONIDET P-40 1%; Na<sub>3</sub>VO<sub>4</sub> 1 mM; aprotinin 0.1%; pepstatin 0.7 mg/ml e leupeptin 1 µg/ml. Homogenates were centrifuged at 14.000 rpm for 20 minutes at 4°C. The supernatant was used to perform western blot analysis. Protein levels were determined using the Bradford method. The total protein amount used for each sample was 50µg and it was separated on 8% or 12% sodium dodecyl sulfate-polyacrylamide gels with 5% sodium dodecyl sulphate stacking gel (SDS-PAGE) and electro-transferred onto Hybond ECL nitrocellulose paper (Amersham, Milan, Italy). The membranes were blocked in 5% non-fat dry milk in 0.1% Tween 20 (TBS-T; 2mmol/l Tris HCl, 50mmol/l NaCl, pH 7.5) for 1 hour at room temperature (RT) and subsequently incubated overnight at 4°C in the blocked buffer with the 1 : 1000 antibody for NCX1 (polyclonal rabbit antibody, Swant, Marly, Switzerland), 1 : 5000 antibody for NCX3 (polyclonal rabbit antibody, Philipson's Laboratory, UCLA, Los Angeles, CA, USA), 1:10000 for Tyrosine Hydroxylase (monoclonal mouse antibody), 1:1000 for  $\alpha$ -synuclein (monoclonal, Abcam ab277766) , 1:1000 GFAP (polyclonal, Novus Biologicals, NB300-141), 1:1000 for IBA-1 (polyclonal, Wako 019-19741), 1:1000 for nNOS (monoclonal, Santa Cruz NOS1(R-20)sc-648), 1:1000 for iNOS (monoclonal, NOS2, Santa CRUZ (C-11):sc-7271, 1:1000 for IL-1 $\beta$  (monoclonal, Cell Signaling 12242), 1:1000 for CYT-C ( polyclonal, Cell Signaling 4272), 1:1000 for MnSOD (polyclonal, Merk Millipore 06-984).Next, all membranes were washed 3 times with a solution containing Tween 20 (0.1%) and subsequently incubated with the secondary antibodies for 1 hour (1:2000) at room temperature.

Immunoreactive bands were detected by ECL (Amersham). Discrimination among the distinct types of extracts was ensured by running parallel western blots with the endogenous actin protein. The optical density of the bands was determined by *Image J* program.

### **5.3 Mitochondrial calcium concentration $[Ca^{2+}]_{mit}$ , cytosolic calcium concentrations $[Ca^{2+}]_{cit}$ and mitochondrial membrane potential measurements**

To assess the  $[Ca^{2+}]_m$ , neurons and astrocytes obtained from A53T and wild type mice embryo and pups respectively were loaded with X-Rhod-1 (0.2  $\mu$ M) for 15 min in a medium containing: 156mM NaCl, 3mM KCl, 2mM  $MgSO_4$ , 1.25mM  $KH_2PO_4$ , 2mM  $CaCl_2$ , 10mM glucose, and 10mM HEPES. The pH was adjusted to 7.35 with NaOH. At the end of the incubation, cells were washed 3 times in the same medium. An increase in the mitochondria-localized intensity of fluorescence was indicative of mitochondria  $Ca^{2+}$  overload (Sisalli et al., 2014).

$[Ca^{2+}]_{cit}$  was measured using the fluorescent dye Fluo-3AM acetoxymethyl ester (Fluo-3AM). Cells were loaded with Fluo-3AM (5 nM) for 30 min at room temperature in the same medium described above. At the end of incubation, cells were washed 3 times in the same medium. An increase in  $[Ca^{2+}]_{cit}$  intensity of fluorescence was indicative of cytosolic  $Ca^{2+}$  overload (Secondo et al., 2007). The advantage to use fluo3 was that this calcium indicator can be loaded into the cells together with the mitochondrial calcium indicator X-Rhod-1, thus allowing a simultaneous comparison of calcium levels in the cytoplasmic and mitochondrial compartment. Mitochondrial membrane potential was assessed using the fluorescent dye tetramethylrhodamine ethyl ester (TMRE) in the “redistribution mode”. Cells were loaded with TMRE (20nM) for 30 minutes in the above-

described medium. At the end of the incubation, cells were washed in the same medium containing TMRE (20nM) and allowed to equilibrate. A decline in the mitochondria-localized intensity of fluorescence was indicative of mitochondrial membrane depolarization (Livigni et al., 2006). Confocal images were obtained using Zeiss inverted 510 confocal laser scanning microscopy and a 63X oil immersion objective. The illumination intensity of 543 Xenon laser used to excite X-Rhod-1 and TMRE, and of 488 Argon laser used to excite Fluo-3AM fluorescence, was kept to a minimum of 0.5% of laser output to avoid phototoxicity.

## ***5.4 Mass Spectrometry (MS)***

### ***5.4.1 Preparation of the isolated microglial cells for MS***

After extraction with buffer containing: NaCl (150mM), EDTA pH8 (5mM) Tris-HCl pH8 (50mM) Triton X-100 (1%), Na<sub>3</sub>OV<sub>4</sub> (0.5%), SDS (0.1%) and quantification of protein concentration by BC assay method (Protein assay kit, Uptima) the isolated microglia were prepared with the SP3-protocol, which is specific for the analysis of MS, following the protocol of Hughes and colleagues (Hughes et al., 2014). In all the steps were used the specific tube for MS (LoBind tube). Briefly, in the first step, the samples were treated with MgCl<sub>2</sub> and Benzonase to remove DNA and RNA and incubated for 30 minutes at 37°C in a thermomixer (1200 r.p.m). Reduction and alkylation of the proteins were performed through the addition of DDT and incubated again for 30 min at 37°C in a thermomixer (1200 r.p.m). In the second step, in each sample were added two types of beads used in SP3protocol, Sera-Mag Speed Beads A (ThermoFischer,09-981-121) and Sera-Mag Speed Beads (ThermoFischer,09-981-123) and mixed to generate a homogeneous solution. After incubation for 30 min at room temperature in a thermomixer (1200 r.p.m), tubes were placed on a magnetic rack for 2 minutes. The supernatant was collected while the beads were rinsed three times through the addition of 200 µL of 70% absolute ethanol. Next, Trypsin and LysC were added in the bead-protein mixtures and incubate for 30 minutes at 37°C in a thermomixer (1200 r.p.m) and left over-Night at room temperature. The day after, samples were put them in magnetic support, the supernatant was collected in new Lobind tube and the beads were washed with 0.2% of Formic acid, sonicated twice for 30 seconds. Later on, was measured the concentration of the peptides obtained with the Qubit Protein Assay Kits (Life Technologies, Q33211, Q33212) and collected

only the  $\mu\text{l}$  corresponding at 1.3  $\mu\text{g}$  of peptides for the injection in the column of MS

#### ***5.4.2 Proteomic profile of isolated microglia from transgenic PDGF- $\alpha$ -synuclein mice***

Samples were injected on a trapping column (nanoAquity UPLC column, C18, 180  $\mu\text{m}$   $\times$  20 mm, 5  $\mu\text{m}$ , Waters) and washed with 2 % acetonitrile containing 0.1 % formic acid and a flow rate of 15  $\mu\text{l}/\text{min}$  for 8 min. A C18 UPLC column (nanoAcquity UPLC column, C18, 75  $\mu\text{m}$   $\times$  150 mm, 1.7  $\mu\text{m}$ , Waters) was used for peptide separation. Peptides were eluted using a gradient from 2 to 85 % acetonitrile, 0.1 % formic acid (0 min, 2 %; 2 min, 2 %; 7 min, 6 %; 55 min, 20 %; 73 min, 30 %; 91 min, 40 %; 94 min, 85 %) with a flow rate of 300  $\mu\text{l}/\text{min}$  and a column temperature of 40° C. MS analysis was performed with a spray voltage of 1.8 kV in positive ion mode. The mass spectrometer automatically switched between full-scan MS mode (from 400 to 1.400 m/z, R = 60,000) and MS2 acquisition. Peptide ions exceeding an intensity of 5,000 counts were fragmented within the linear ion trap by collision-induced dissociation (isolation width 4 m/z, normalized collision energy 35, activation time 30 ms, activation Q 0.25). Protein identification and relative quantification were carried out with the software MaxQuant (version 1.2.0.18, Max Planck Institute of Biochemistry, Munich, Germany) which is a quantitative proteomics software designed for analysing large mass-spectrometric data sets, combined with Andromeda, which is a peptide search engine based on probabilistic scoring. (Cox et al., 2009, 2011) This combination allows for improving the identification of peptides. Peptides with the same sequence but different labelling states elute at the same retention time. Heavy to light peptide pairs can be detected by their distinct mass shifts according to the labelling with heavy arginine and lysine. MaxQuant uses the intensity of heavy and



light labelled peptide pairs to calculate relative peptide abundances. The derived peptide intensity ratios belonging to the same protein are the basis for relative protein quantification. Proteins with a log<sub>2</sub> fold change (FC) above 0.5 or below -0.5 were considered to be up or downregulated respectively. For identification of clusters significantly regulated of proteins, the web-based bioinformatics tool STRING was used (Szklarczyk et al., 2019). The analysis of STRING software is based on the correlated databases “Gene Ontology” (GO) which allowed classifying the proteins in 3 categories: Biological process, Molecular function and Cellular component. A deeper analysis is carried out with the Reactome Pathways. Reactome is an open-source database (Croft et al., 2011) which generalizes the concept of a reaction to include transformations of entities such as transport from one compartment to another and interaction to form a complex, as well as the chemical transformations of classical biochemistry. This generalization permits the capture of a range of biological processes that span signalling, metabolism, transcriptional regulation, apoptosis and synaptic transmission in a single computationally format.

### ***5.5 Statistical Analysis***

Data were generated from a minimum of 3 independent experimental sessions for in vitro studies. Calcium and mitochondrial membrane potential measurements were performed at least in 200 cells for each of the 3 independent experimental sessions. Data were expressed as mean ± S.E.M. Statistical comparisons between transgenic and their respective controls during ageing were performed using the one-way ANOVA test followed by Newman Keul’s test. The unpaired T-student test was used to analyse the trend inside the same group corresponding at the single specific age. P-value <0.05 was considered statistically significant.

## 6. RESULTS

### *6.1 Mitochondrial dysfunction in mesencephalic neurons obtained from A53T transgenic $\alpha$ -synuclein mice depends on the decrease of NCX3 protein expression*

To understand the functional implications of changes in NCXs expression detected in 12 months old A53T transgenic  $\alpha$ -synuclein mice (Sirabella et al., 2018) and their role in the pathogenesis of PD, experiments were performed in vitro in primary mesencephalic and striatal neurons obtained from A53T transgenic mice embryos (E15) to evaluate mitochondrial function. Specifically, mitochondrial calcium content and membrane potential were measured simultaneously with intracellular calcium concentration by using confocal microscopy and fluorescent dyes. The results obtained showed that in the mesencephalic neurons obtained from A53T transgenic mice an increase of cytosolic calcium concentration  $[Ca^{2+}]_i$  occurred accompanied to an increase of mitochondrial calcium content  $[Ca^{2+}]_{mit}$  and to mitochondrial membrane depolarization (Fig. 15). These effects were associated with a decrease of NCX3 expression in A53T transgenic neurons compared to WT without any change in NCX1 expression (Fig. 16). Conversely, in the striatal neurons from A53T transgenic mice, in which no changes in the expression of NCX1 and NCX3 were detected (Fig. 17),  $[Ca^{2+}]_i$  was similar to WT neurons whereas mitochondrial membrane was hyperpolarized and  $[Ca^{2+}]_{mit}$  was lower compared to WT (Fig. 18).

## MESENCEPHALIC NEURONS

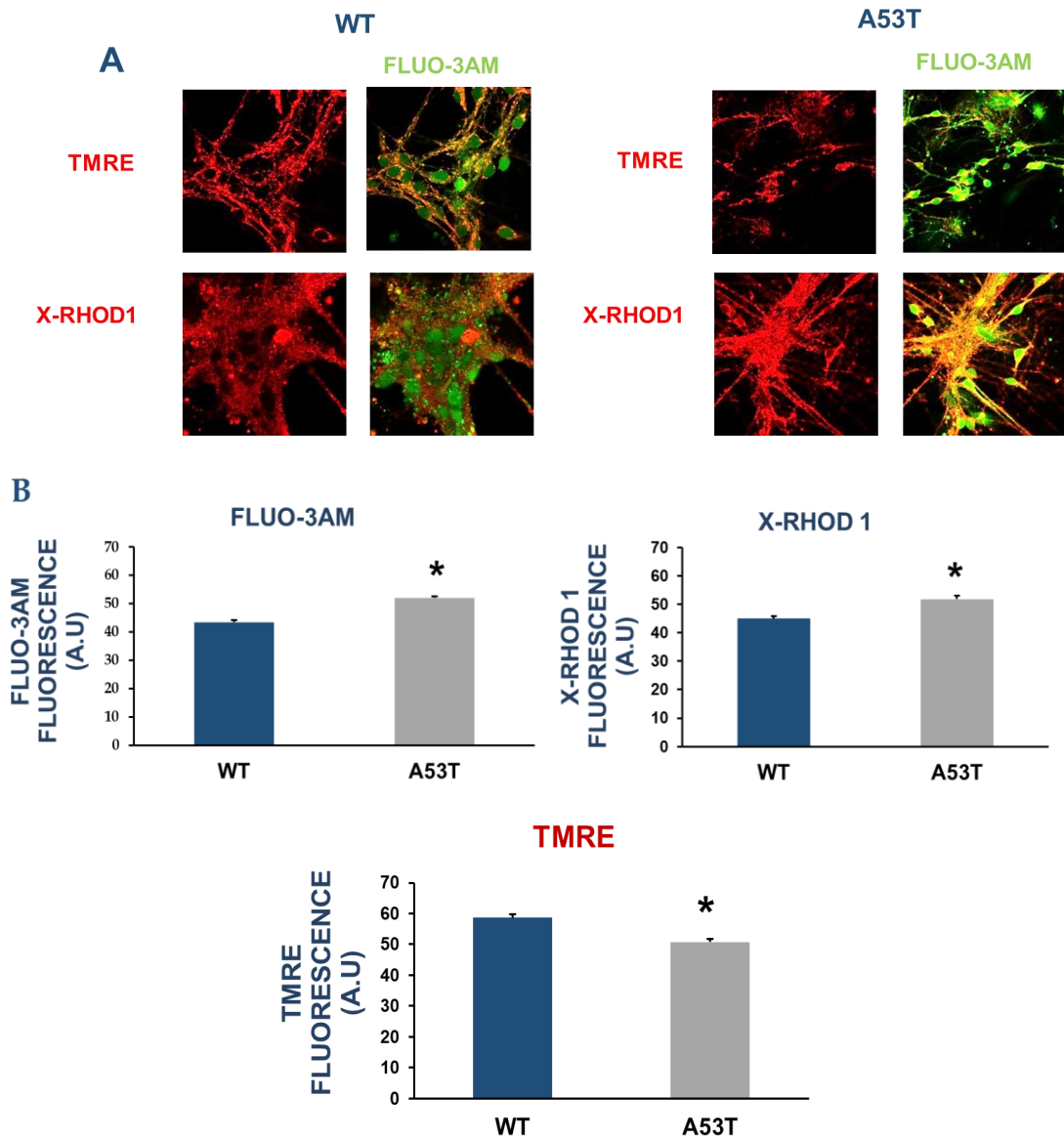


**Figure 15: Mitochondrial dysfunctions in mesencephalic neurons obtained from A53T transgenic and WT embryos.** **A)** Confocal microscopy experiments: simultaneous measurement of mitochondrial membrane potential (TMRE, red) or mitochondrial calcium concentration (XRhod-1, red) and cytosolic calcium concentration (FLUO-3AM, green) in mesencephalic neurons obtained from A53T and WT mouse embryos. **B)** Bar graphs reporting the quantification of the fluorescence intensity in primary midbrain A53T and WT neurons. Values were expressed as the mean of the percentage  $\pm$  S.E.M. Statistical analysis carried out with unpaired T-test student, \* $P < 0.05$  vs WT neurons

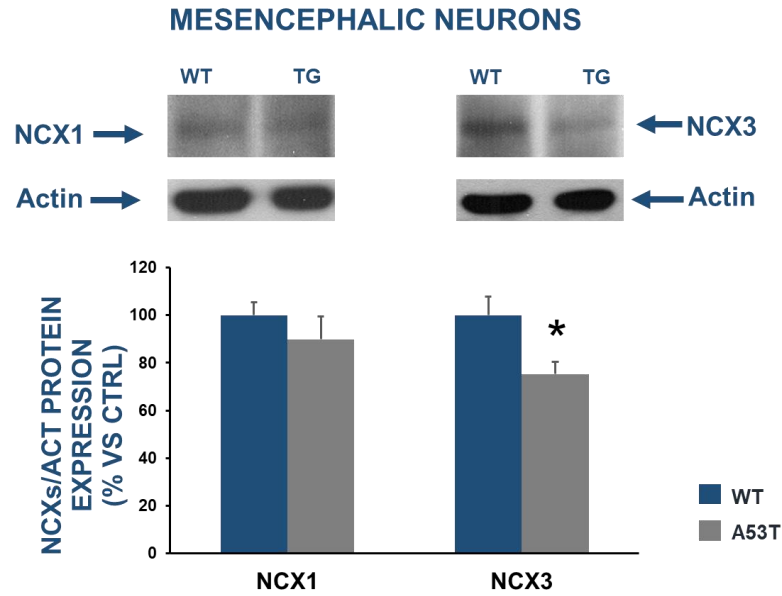


**Figure 16: Expression of NCX1 and NCX3 in mesencephalic neurons obtained from A53T transgenic and WT embryos.** Bar graphs report the densitometric values of NCX1 and NCX3 expression in primary mesencephalic A53T and WT neurons normalized to the respective actin. Values were expressed as the mean of the percentage  $\pm$  S.E.M. Statistical analysis carried out with unpaired T-test student, \*P < 0.05 vs WT neurons

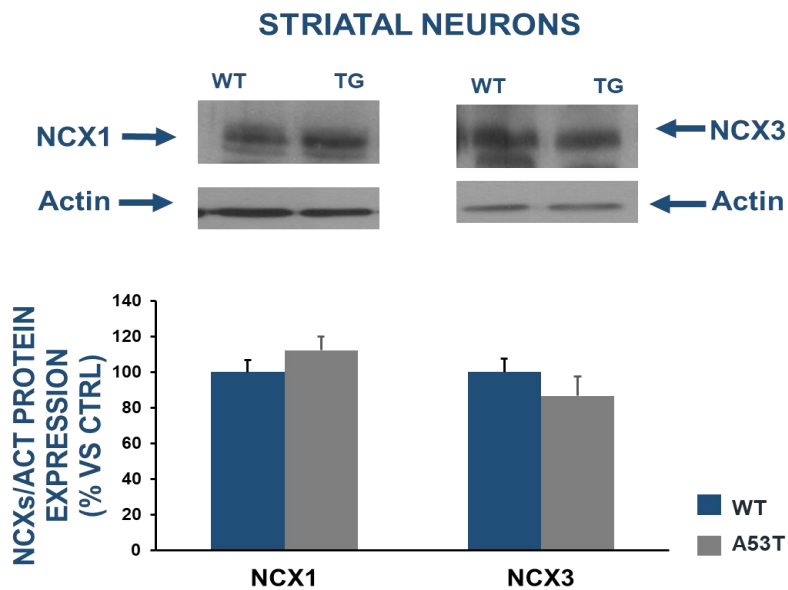


**Figure 17: Expression of NCX1 and NCX3 in striatal neurons obtained from A53T transgenic and WT embryos.** Bar graphs report the densitometric values of NCX1 and NCX3 expression in primary striatal A53T and WT neurons normalized to the respective actin. Values were expressed as the mean of the percentage  $\pm$  S.E.M

## STRIATAL NEURONS

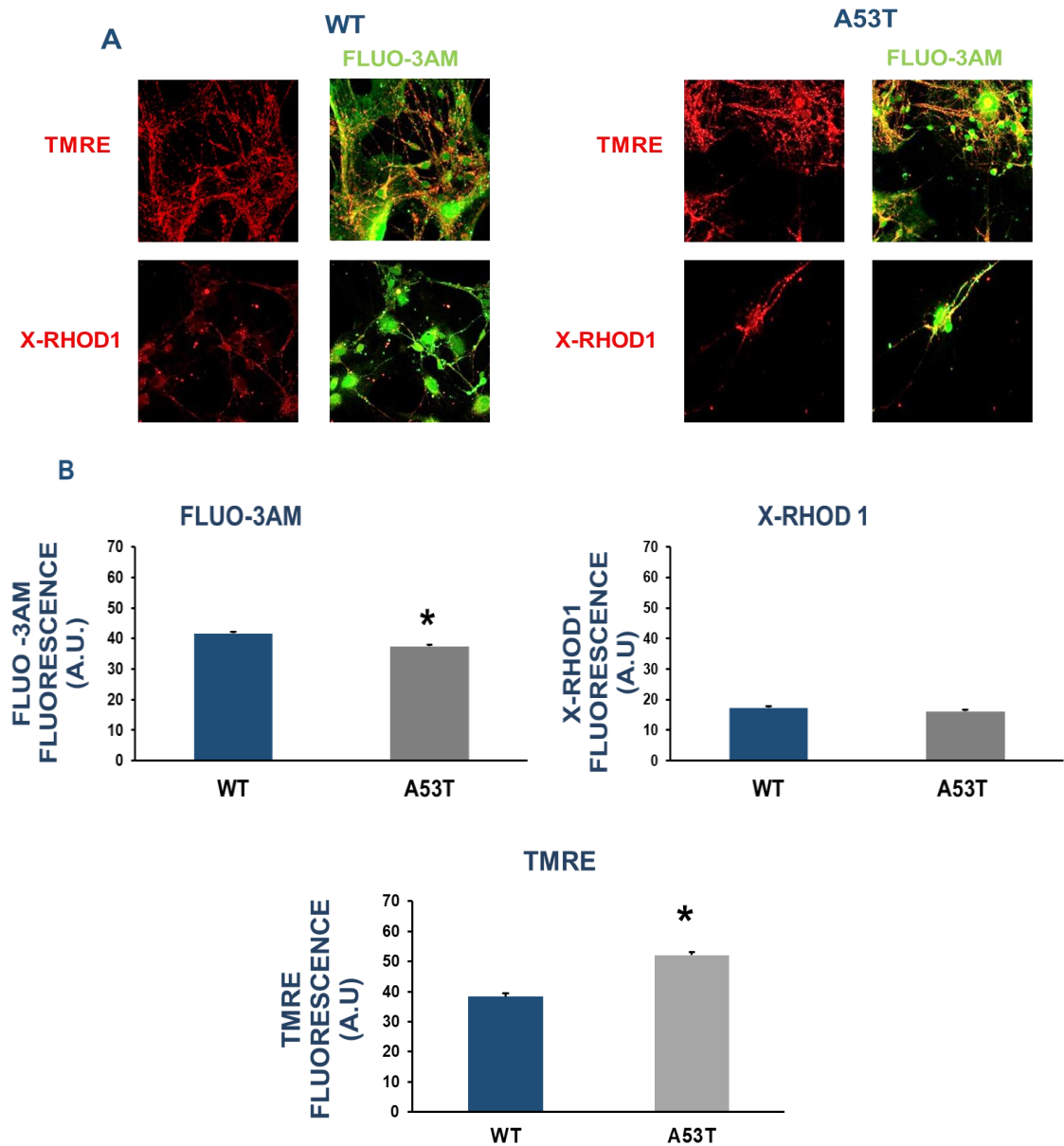


**Figure 18: Mitochondrial dysfunctions in striatal neurons obtained from A53T transgenic and WT embryos.** **A)** Confocal microscopy experiments: simultaneous measurement of mitochondrial membrane potential (TMRE, red) or mitochondrial calcium concentration (XRhod-1, red) and cytosolic calcium concentration (FLUO-3AM, green) in striatal neurons obtained from A53T and WT mouse embryos. **B)** Bar graphs reporting the quantification of the fluorescence intensity in primary midbrain A53T and WT neurons. Values were expressed as the mean of the percentage  $\pm$  S.E.M. Statistical analysis carried out with unpaired T-test student, \*P < 0.05 vs WT neurons.

## 6.2 The onset of neuroinflammation in transgenic A53T $\alpha$ -synuclein mice is associated with differences in NCXs expression during ageing

To confirm that the changes in NCX3 expression detected in mesencephalic neuron caused mitochondrial dysfunction and in turn mitochondria-activated neuroinflammation in PD, further experiments were performed ex vivo in midbrain and striatum obtained from A53T and WT mice during ageing. Specifically, in these mice Western blot experiments were first performed to measure  $\alpha$ -synuclein (Fig. 19), TH (Fig. 20), NCX1(Fig. 21) and NCX3 (Fig. 22) expression during aging in order to correlate DA neuronal impairment with the abnormal deposition of  $\alpha$ -synuclein and with the changes of NCX3 and NCX1 protein expression. The results of these experiments demonstrated a decrease in the expression of NCX3 only in the midbrain of 4-months-old transgenic mice, but no variation in the expression of NCX1 in the midbrain and in the striatum (Fig. 21, 22).

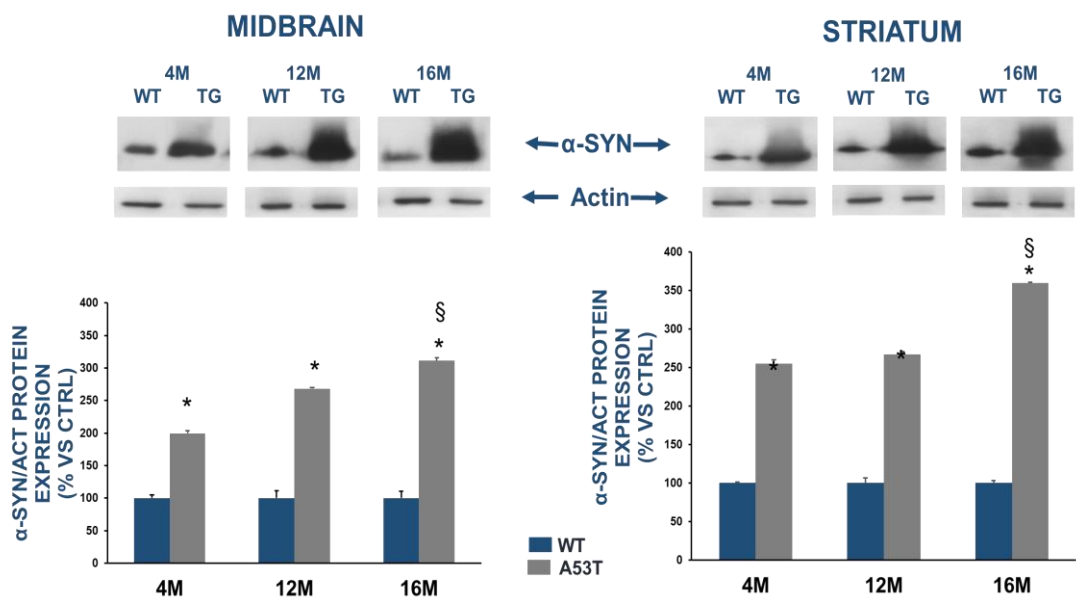


**Figure 19: Expression of  $\alpha$ -synuclein in Midbrain and Striatum obtained from 4-12- and 16 month-old A53T transgenic and WT mice.** Bar graphs report the densitometric values of the  $\alpha$ -synuclein expression in midbrain and striatum from A53T and WT mice normalized to the respective actin. Values were expressed as the mean of the percentage  $\pm$  S.E.M. §P < 0.05 compared to 4 and 12 months TG mice (one-way ANOVA followed by Newman Keul's test); \*P<0.05 compared to WT mice at the same age (un-paired T-test student).

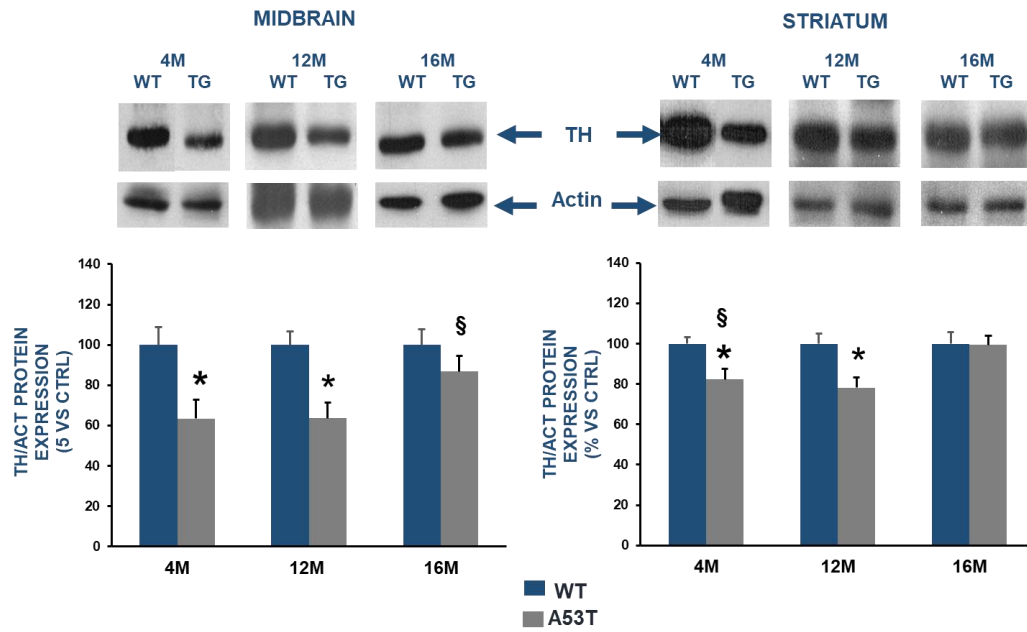


**Figure 20: Expression of TH in Midbrain and Striatum obtained from 4-12- and 16-month- old A53T transgenic and WT mice.** Bar graphs report the densitometric values of the TH expression in midbrain and striatum from A53T and WT mice normalized to the respective actin. Values were expressed as the mean of the percentage  $\pm$  S.E.M. In midbrain  $^{\S}P < 0.05$  compared to 4 and 12 months TG mice (one-way ANOVA followed by Newman Keul's test) and  $*P < 0.05$  compared to WT mice at the same age (un-paired T-test student). In Striatum  $^{\S}P < 0.05$  compared to 12-month-old TG mice (one-way ANOVA followed by Newman Keul's test) and  $*P < 0.05$  compared to WT mice at the same age (un-paired T-test student).

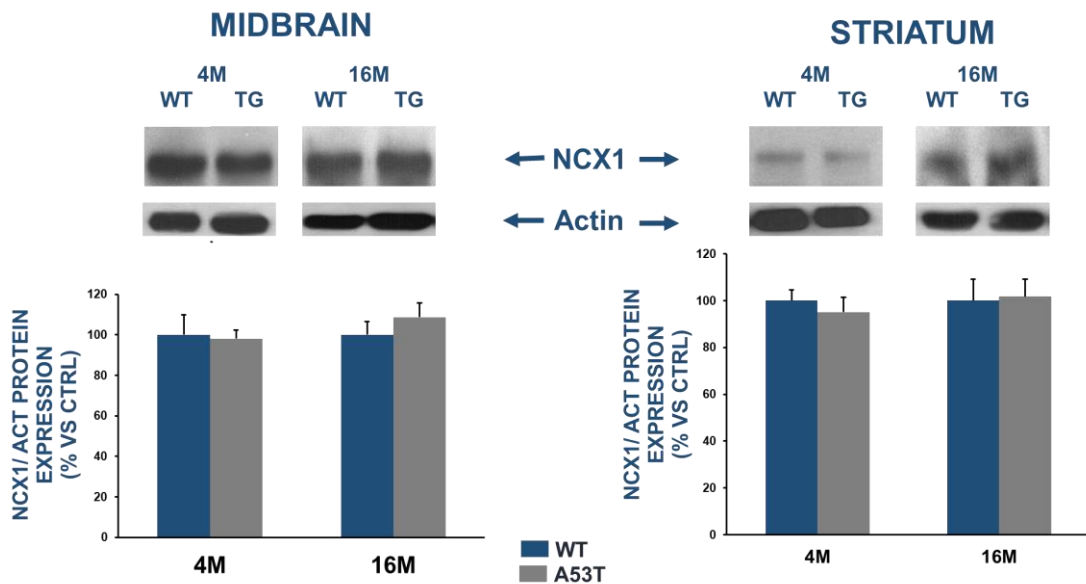


**Figure 21: Expression of NCX1 in Midbrain and Striatum obtained from 4-and 16-months-old A53T transgenic and WT mice.** Bar graphs report the densitometric values of NCX1. Expression in midbrain and striatum from A53T and WT mice normalized to the respective actin. Values were expressed as the mean of the percentage  $\pm$  S.E.M.

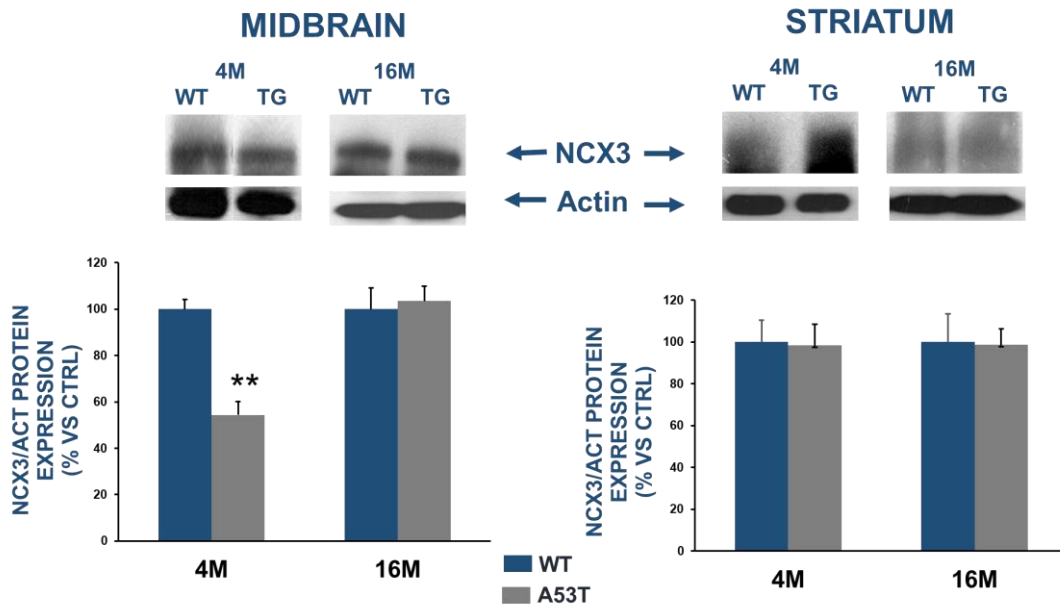


**Figure 22: Expression of NCX3 in Midbrain and Striatum obtained from 4- and 16- month- old A53T transgenic and WT mice.** Bar graphs report the densitometric values of the NCX3 expression in midbrain and striatum from A53T and WT mice normalized to the respective actin. Values were expressed as the mean of the percentage  $\pm$  S.E.M. \*\* $P < 0.05$  compared to WT mice at the same age and to transgenic 16 months old mice (unpaired T-test student)

To confirm that the impairment in NCX3 protein expression was associated to mitochondrial dysfunction, the expression of Cytochrome-c (Cyt-c), a marker of mitochondrial damage, Manganese superoxide dismutase (MnSOD), a marker of mitochondrial oxidative stress, and Neuronal Nitric oxide synthases (nNOS) were measured in 4-12- and 16- month-old mice. The results of these experiments confirmed that in the midbrain an increase of Cyt-c occurred in transgenic mice already in early-stage of disease (4-month-old mice) while in the striatum of A53T transgenic mice the increase in Cyt c occurred only in 16-month-old mice (Fig. 23). Interestingly, in midbrain of A53T aged mice, the rise up of Cyt-c was associated to a decrease in the expression of MnSOD (Fig. 24) and to an increase of nNOS (Fig. 25), whereas, in the striatum, an increase of nNOS (Fig.25) was observed only in A53T transgenic 16- month-old mice and no changes in



MnSOD expression were observed between transgenic and WT mice (Fig. 24).

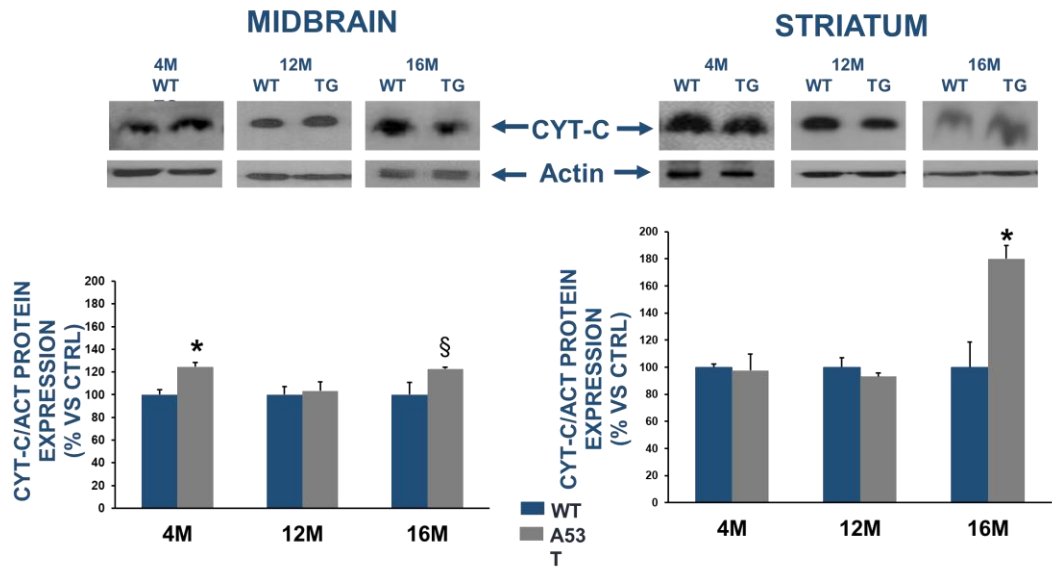


**Figure 23: Expression of CYT-C in Midbrain and Striatum obtained from 4-12- and 16- month- old A53T transgenic and WT mice.** Bar graphs report the densitometric values of the CYT-C expression in midbrain and striatum from A53T and WT mice normalized to the respective actin. Values were expressed as the mean of the percentage  $\pm$  S.E.M. In midbrain  $\S P < 0.05$  compared to 4- and 12-month-old TG mice (one-way ANOVA followed by Newman Keul's test) and  $*P < 0.05$  compared to WT mice at the same age (un-paired T-test student). In Striatum  $*P < 0.05$  compared to WT mice at the same age (un-paired T-test student).

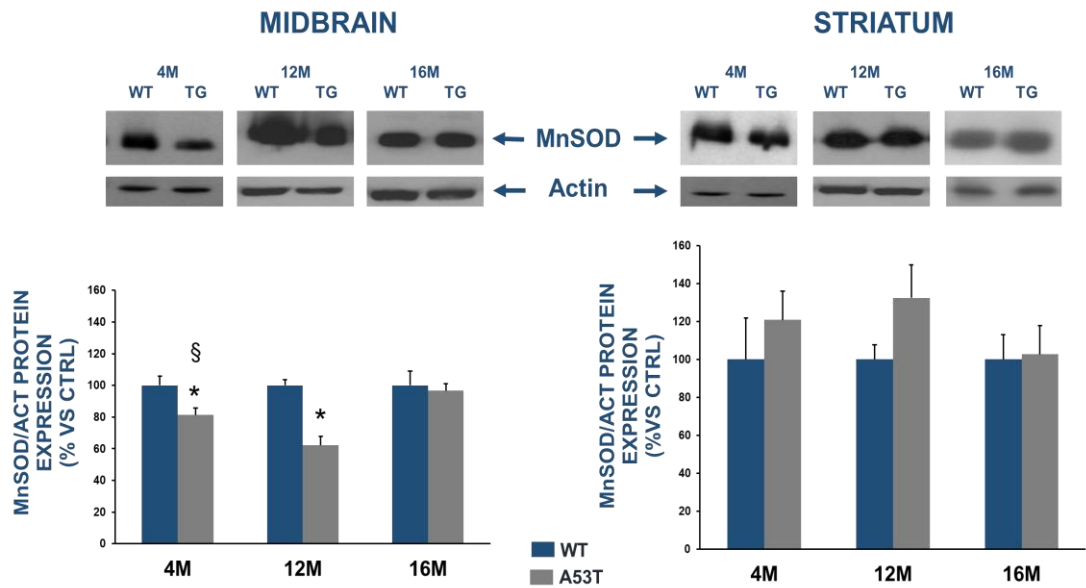


**Figure 24: Expression of MnSOD in Midbrain and Striatum obtained from 4-12- and 1- month- old A53T transgenic and WT mice.** Bar graphs report the densitometric values of MnSOD expression in midbrain and striatum from A53T and WT mice normalized to the respective actin. Values were expressed as the mean of the percentage  $\pm$  S.E.M. In midbrain  $^{\S}P < 0.05$  compared to 12- and 16-month-old TG mice (one-way ANOVA followed by Newman Keul's test) and  $*P < 0.05$  compared to WT mice at the same age (un-paired T-test student).

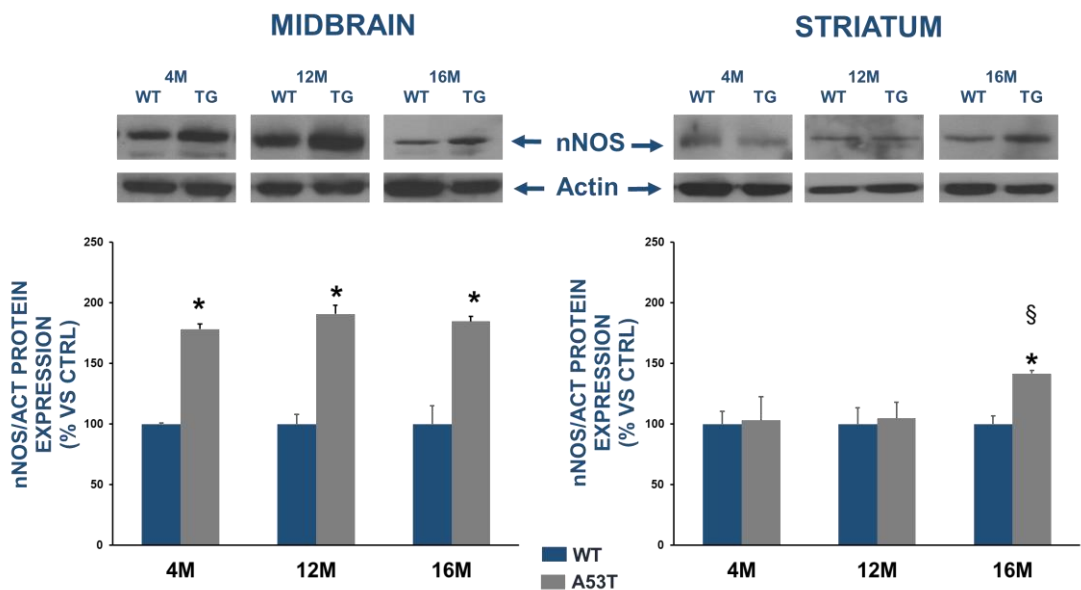


**Figure 25: Expression of nNOS in Midbrain and Striatum obtained from 4-12- and 16- month- old A53T transgenic and WT mice.** Bar graphs report the densitometric values of nNOS expression in midbrain and striatum from A53T and WT mice normalized to the respective actin. Values were expressed as the mean of the percentage  $\pm$  S.E.M. In midbrain  $*P < 0.05$  compared to WT mice at the same age (un-paired T-test student). In Striatum  $^{\S}P < 0.05$  compared to 4- and 12- month-old TG mice (one-way ANOVA followed by Newman Keul's test) and  $*P < 0.05$  compared to WT mice at the same age (un-paired T-test student).

Finally, to correlate mitochondrial dysfunction to neuroinflammation, further experiments were performed *ex vivo* in 4-12- and 16-month-old A53T and WT mice with the aim to evaluate the expression levels of pro-inflammatory proteins such as the inducible Nitric oxide synthases (iNOS) (Fig. 28) and Interleukin 1 beta (IL-1 $\beta$ ) (Fig. 29). Moreover, since previously performed immunohistochemistry experiments in 12 months old A53T mice demonstrated an increase in Glial Fibrillary Acidic Protein (GFAP) (Fig.26) both in midbrain and in striatum and an increase in the Ionized Calcium-Binding Adapter molecule 1 (IBA-1) (Fig. 27) only in the Striatum (Sirabella et al., 2018), Western blot experiments were performed to evaluate GFAP and IBA1 protein expression in 4 and 16 months old WT and A53T transgenic mice. The results obtained confirmed the increase of GFAP in transgenic adult mice (16- month-old) both in the midbrain and in the striatum (Fig. 26), whereas IBA-1 increased only in the striatum of 16-month- old A53T transgenic mice (Fig. 27). In this brain area, the increase in IBA-1 was accompanied to an increase in the expression of iNOS and IL-1 $\beta$  (Fig. 28, 29), thus confirming the activation of a neuroinflammatory response in the striatum of A53T transgenic mice during ageing.

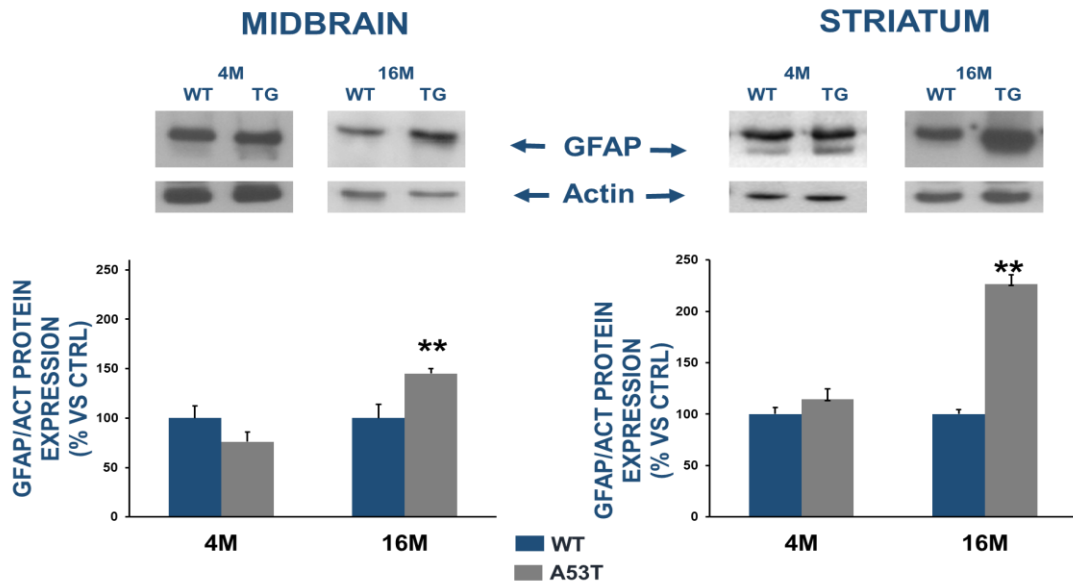


**Figure 26: Expression of GFAP in Midbrain and Striatum obtained from 4- and 16-month-old A53T transgenic and WT mice.** Bar graphs report the densitometric values of GFAP expression in midbrain and striatum from A53T and WT mice normalized to the respective actin. Values were expressed as the mean of the percentage  $\pm$  S.E.M. \*\* $P < 0.05$  compared to WT mice at the same age and to transgenic 4 months old mice (unpaired T-test student)

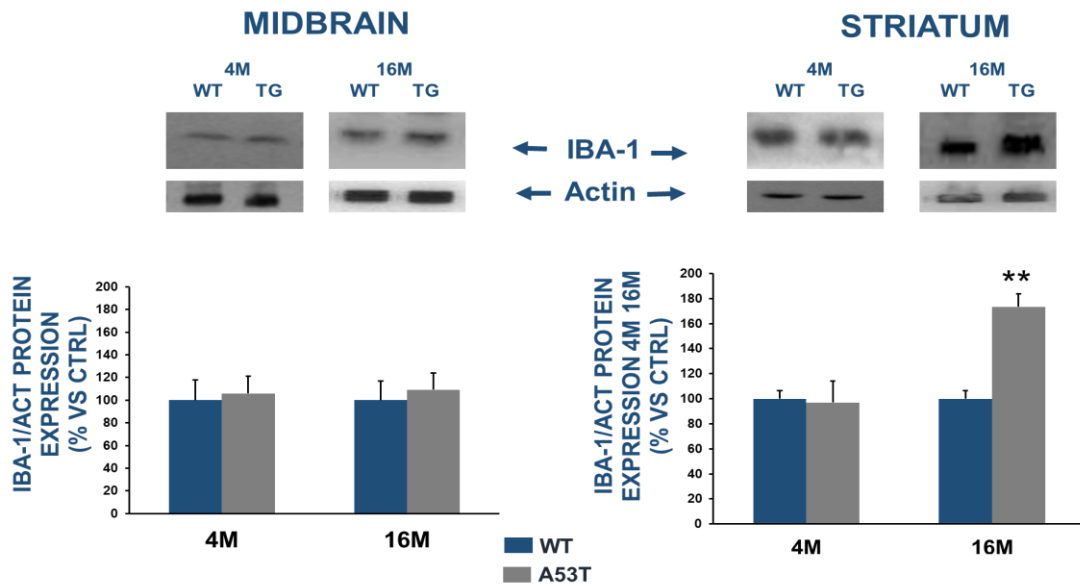


**Figure 27: Expression of IBA-1 in Midbrain and Striatum obtained from 4- and 16-month-old A53T transgenic and WT mice.** Bar graphs report the densitometric values of IBA-1 expression in midbrain and striatum from A53T and WT mice normalized to the respective actin. Values were expressed as the mean of the percentage  $\pm$  S.E.M. \*\* $P < 0.05$  compared to WT mice at the same age and to transgenic 4 months old mice (unpaired T-test student)

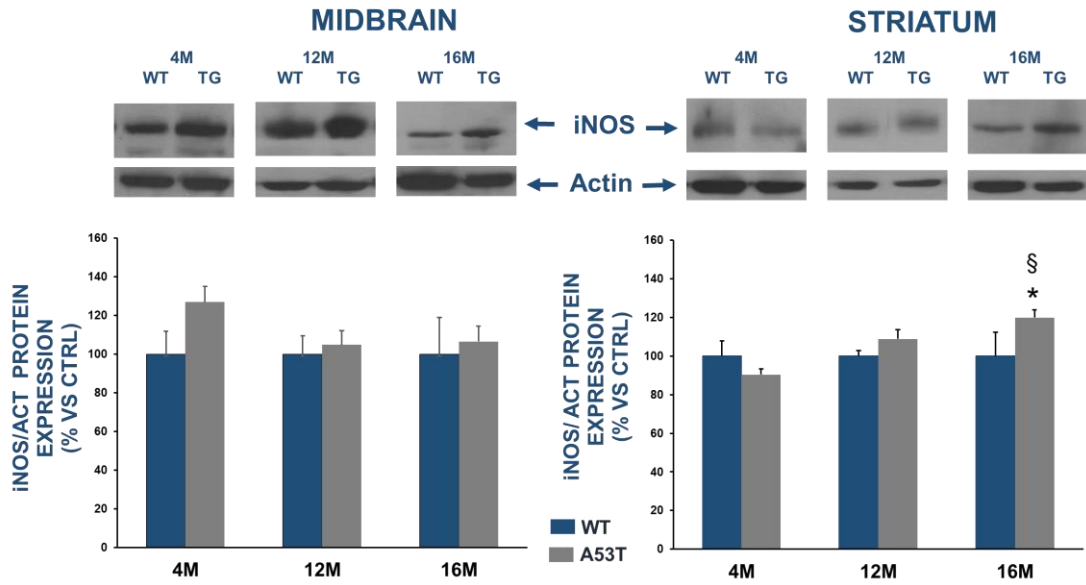


**Figure 28: Expression of iNOS in Midbrain and Striatum obtained from 4-12- and 16- month- old A53T transgenic and WT mice.** Bar graphs report the densitometric values of iNOS expression in midbrain and striatum from A53T and WT mice normalized to the respective actin. Values were expressed as mean of the percentage  $\pm$  S.E.M. \* $P < 0.05$  compared to WT mice at the same age (unpaired T-test student) and  $^{\S}P < 0.05$  compared to 12 months TG mice (one-way ANOVA followed by Newman Keul's test)

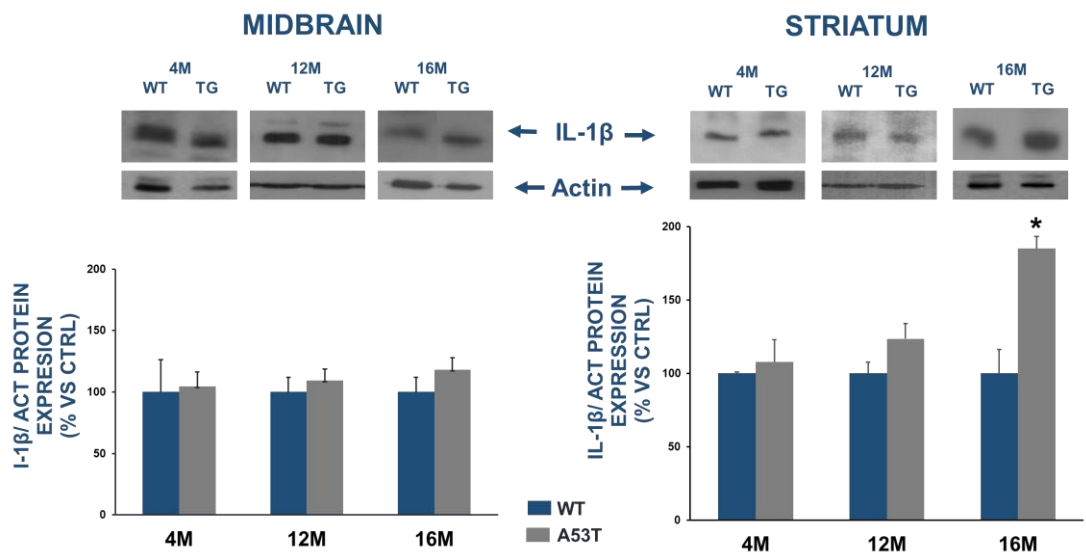


**Figure 29: Expression of IL-1 $\beta$  in Midbrain and Striatum obtained from 4-12- and 16- month-old A53T transgenic and WT mice.** Bar graphs report the densitometric values of IL-1 $\beta$  expression in midbrain and striatum from A53T and WT mice normalized to the respective actin. Values were expressed as the mean of the percentage  $\pm$  S.E.M. \* $P < 0.05$  compared to WT mice at the same age (unpaired T-test student).

### ***6.3 Microglial proteomic profile from young and adult PDGF-h- $\alpha$ -synuclein transgenic mice reveals a relationship between mitochondrial dysfunction and impairment in synaptic plasticity***

The last part of the study was addressed to study deeper into the understanding of the role played by mitochondrial dysfunction in the pathogenesis of neuroinflammation observed in PD. To this aim, experiments were performed *in vitro* in striatal astrocytes obtained from A53T transgenic and WT mice, in which NCX expression and mitochondrial function were assessed by western blot analysis and confocal microscopy. The results of these experiments demonstrated an increase in NCX1 expression (Fig. 30) in astrocytes obtained from A53T transgenic mice associated to a reduction in  $[Ca^{2+}]_i$  and a lower mitochondrial calcium concentration compared to WT (Fig. 31). Interestingly, in astrocytes obtained from A53T transgenic mice mitochondria were hyperpolarized (Fig. 31). These findings let to hypothesize that the overexpression of NCX1 in transgenic astrocytes by maintaining  $[Ca^{2+}]_i$  within physiological range preserves mitochondrial function and promotes gliosis in adult mice.

## STRIATAL ASTROCYTES

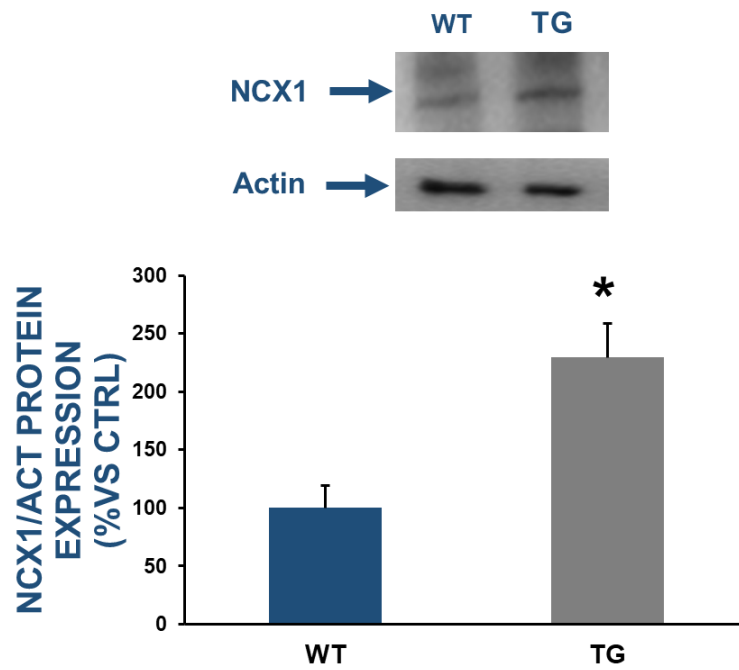


**Figure 30: Expression of NCX1 in striatal astrocytes obtained from A53T transgenic and WT mice.** Bar graphs report the densitometric values of NCX1 expression in primary midbrain A53T and WT astrocytes normalized to the respective actin. Values were expressed as the mean of the percentage  $\pm$  S.E.M. Statistical analysis carried out with unpaired T-test student, \* $P < 0.05$  vs WT astrocytes.

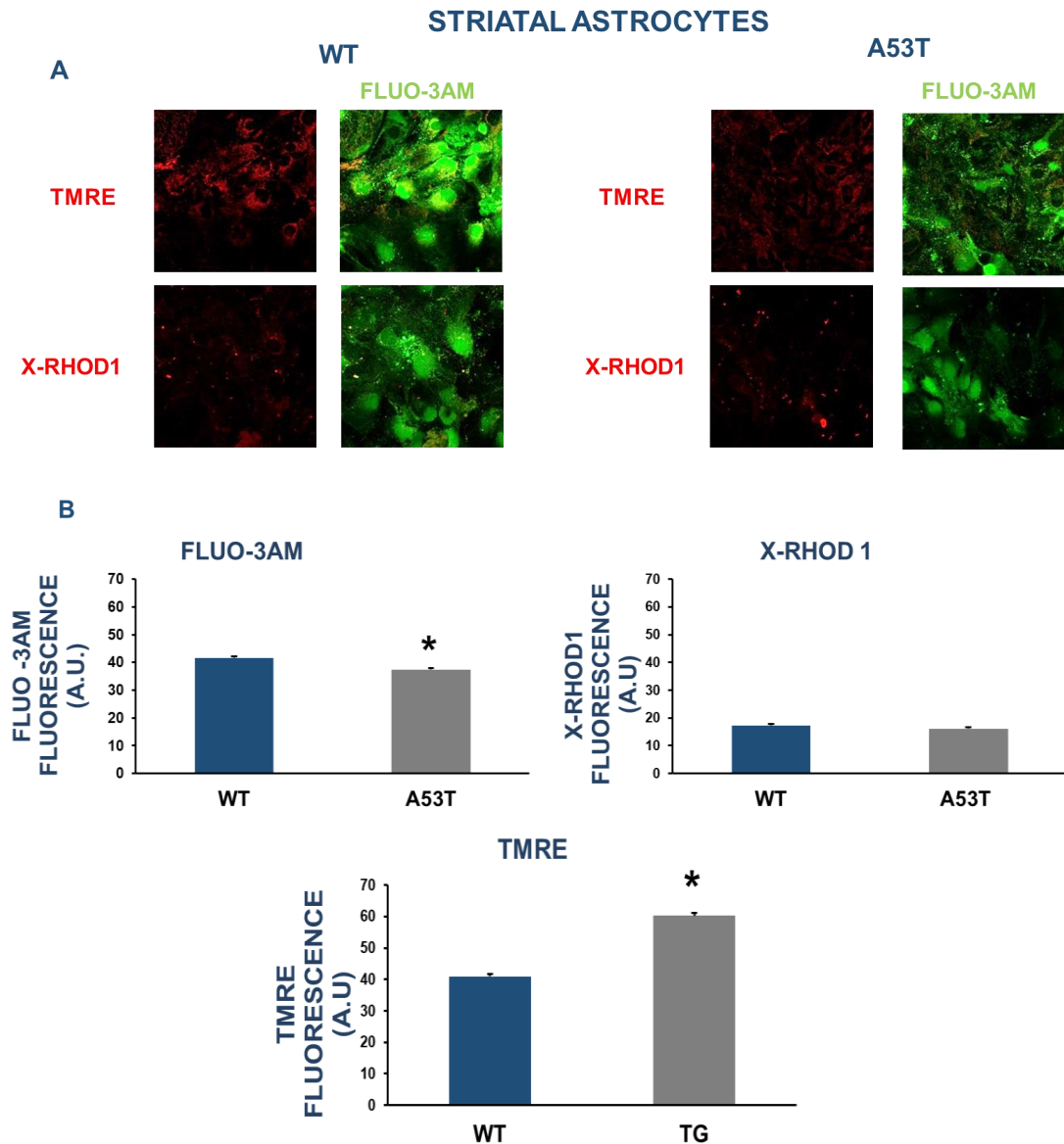


**Figure 31: Mitochondrial dysfunctions in striatal astrocytes obtained from A53T transgenic and WT mice.** A) Confocal microscopy experiments: simultaneous measurement of mitochondrial membrane potential (TMRE, red) or mitochondrial calcium concentration (XRhod-1, red) and cytosolic calcium concentration (FLUO-3AM, green) in astrocytes obtained from A53T and WT mouse pups. B) Bar graphs reporting the quantification of the fluorescence intensity in primary midbrain A53T and WT neurons. Values were expressed as the mean of the percentage  $\pm$  S.E.M. Statistical analysis carried out with unpaired T-test student, \*P < 0.05 vs WT astrocytes

To further confirm the role played by glial cells in the pathogenesis of neuronal dysfunction observed in PD progression, further experiments were performed in collaboration with the “Deutsches Zentrum für Neurodegenerative Erkrankungen” (Centre for Neurodegenerative Disease), with the intent to study the proteomic profile of microglial cells



isolated from PDGF-h- $\alpha$ -synuclein 2- and 12 month- old mice, and to correlate the changes in mitochondrial protein expression with the onset of the neuroinflammatory process leading to neurodegeneration occurring in PD. The analysis of Mass Spectrometry was conducted in 7 animals for each group of 2 months old WT and transgenic mice, and in 5 animals for each group of 12 months old WT and transgenic mice. Only the proteins that have a p-value  $< 0.05$  have been taken into account for the analysis and indicated as red-spot in the Volcano analysis at 2 -and 12 month-old transgenics versus WT mice (Fig. 32, 33). This kind of analysis allowed to obtain a list of the principal proteins down or up-regulated in 2 and 12 months old PDGF- h-  $\alpha$ -synuclein mice compared to WT (Table 2 and Table 3). The list of protein obtained by mass spectrometry analysis was processed by STRING software and analysed by using the correlated databases "Gene Ontology" (GO) which allowed classifying the proteins in 3 categories: Biological process (Fig.34 A, B and C; Fig. 38 A, B and C), Molecular function (Fig.35 A, B and C; Fig.39 A, B and C), Cellular component (Fig.36 A, B and C; Fig.40 A, B and C) and Reactome pathways analysis (Fig. 37 A, B and C; Fig. 41 A, B and C). The results of these experiments demonstrated that in 2 month-old PDGF-h- $\alpha$ -synuclein mice the changes in protein profile observed are mainly related to proteins involved in the regulation of mitochondrial function whose expression resulted downregulated compared to WT mice (Fig. 34 A, B and C, Biological processes).

Very interestingly, the principal down-regulated proteins in the microglial cell of 2 months old PDGF- $\alpha$ -synuclein mice compared to WT are those correlated to different aspects of mitochondrial function. Among them: the S8S ribosomal proteins S2 and S35 (MRPS2, MRPS35) that are required for the mitoribosome formation and mitochondrial translation. An increasing number of gene mutations that impair mitoribosome function and result in

multiple OXPHOS deficiencies linked to human mitochondrial disease. The protein 39S ribosomal and the protein 41L that are components of the mitochondrial ribosome large subunit, involved in the apoptosis and cell cycle regulation. The protein ATP-dependent RNA helicase SUPV3L1, that play a role in the RNA surveillance system in mitochondria, in the removal of aberrantly formed mRNAs, in the rapid degradation of non-coding processing intermediates and in the regulation of apoptosis.

Many other proteins are instead involved in the metabolic and oxidative processes. Among them the Dihydroorotate dehydrogenase (Quinone), DHODH, an enzyme associated with the electron transport chain which plays a role in mitochondrial bioenergetics, cell proliferation, ROS production, and apoptosis in certain cell types. The protein dehydrogenase [ubiquinone] iron-sulfur subunit, SDHB, that is involved in complex II of the mitochondrial electron transport chain and is responsible for transferring electrons from succinate to ubiquinone (coenzyme Q). The mitochondrial 2-oxoglutarate/malate carrier protein that catalyses the transport of 2-oxoglutarate and plays an important role in several metabolic processes, including the malate-aspartate shuttle, the oxoglutarate/isocitrate shuttle, the gluconeogenesis from lactate, and the nitrogen metabolism. It is also able to maintain mitochondrial fusion and fission events, and the organization and morphology of cristae and seem to be involved in the regulation of apoptosis.

Other proteins are involved in the regulation of apoptosis, like the protein DnaJ homolog subfamily A member 3, that affect CYT-C release from the mitochondria and caspase 3 activations. It is also involved in the maintaining of membrane potential and mtDNA integrity, as well as cellular processes such as cell movement, growth, and death. Furthermore, it is associated with a broad range of disease including inflammatory and neurodegenerative disease.

Even, we found some proteins correlated to the formation of the mitochondrial multi-complex proteins, like Acylglycerol kinase, AGK, that acts as a component of TIM22 complex which mediates the import and insertion of multiple transmembrane proteins into the mitochondrial inner membrane by forming a twin-pore translocase that uses the membrane potential as the external driving force (Kang et al., 2017). The mitochondrial inner membrane protein OXA1L, required for the insertion of integral membrane proteins into the mitochondrial inner membrane. It is essential for the activity and assembly of cytochrome oxidase and required for the correct biogenesis of ATP synthase and complex I in mitochondria.

Also Mitofusin-1 a protein involved in mitochondrial fusion is down-regulated in the early stage of the pathology in PDGF-  $\alpha$ -synuclein. Finally, among the protein down-regulated in the early stage of the pathology in PDGF-  $\alpha$ -synuclein we found also NCX1.

The proteomic profile of 12-month-old in PDGF-  $\alpha$ -synuclein mice is radically changed, shifting in favour of proteins involved in the synaptic neuronal transport, neuronal guidance, immune system, metabolic processes and in mitochondrial activity (Fig. 39 A, B and C; Fig. 42 A, B and C). The principal down-regulated protein is the eIF-2-alpha kinase GCN2, a metabolic-stress sensing protein kinase that phosphorylates the alpha subunit of eukaryotic translation initiation factor 2 (eIF-2-alpha/EIF2S1) in response to low amino acid availability. It plays a role as an activator of the integrated stress response (ISR) required for adaptation to amino acid starvation, in the consolidation of synaptic plasticity, learning as well as formation of long-term memory, in neurite outgrowth inhibition, has a role in pro-apoptotic regulation in response to glucose deprivation and in the modulating the adaptive immune response.

Others proteins down-regulated are the calmodulin, synaptogamin, protein Ap2-complex subunit sigma, plexin-A4. The calmodulin mediates many

crucial processes such as inflammation, metabolism, apoptosis, smooth muscle contraction, intracellular movement, short-term and long-term memory, and the immune response.

Synaptotagmin proteins were proposed to function as calcium sensors in the regulation of neurotransmitter release and hormone secretion. Synaptotagmins are involved both in early synaptic vesicle docking to the presynaptic membrane via interaction with  $\beta$ -neurexin or SNAP-25 and in late steps of  $\text{Ca}^{2+}$ -evoked synaptic vesicle fusion with the presynaptic membrane. The protein Ap2-complex subunit sigma, play a role in the recycling of synaptic vesicles membrane from the presynaptic surface. The protein plexin-A4 has a role in axon guidance in the developing of the nervous system.

Some proteins, instead, are linked to the activation of macrophages, like the down-regulated protein TRAF3-interacting-JNK-activating modulator, which together with the coiled-coil protein TRAF3 associates with TLR4 receptor and promotes its translocation to lipid rafts thereby enhancing macrophage-mediated inflammation, while the protein Proteasome activator complex subunit 1, implicated in immunoproteasome assembly and required for efficient antigen processing, is up-regulated.

Among the most down-regulated proteins associated with the mitochondria, the analysis of the proteomic profile detected proteins linked to the complex of the electron transport chain, like NADP-dependent malic enzyme, that generates NADPH for fatty acid biosynthesis; the NADH dehydrogenase [ubiquinone] iron-sulfur protein 6, NDUFS6, that is an accessory subunit of the mitochondrial membrane respiratory chain NADH dehydrogenase (Complex I); the protein Cytochrome b-c1 complex subunit 6, that is a component of the ubiquinol-cytochrome c reductase complex (complex III or cytochrome b-c1 complex) and finally the Superoxide dismutase (MnSOD).

In spite of 175 proteins changed at 2 months and the 286 proteins detected at 12 months PDGF-  $\alpha$ -synuclein old mice, only 10 proteins are in common. Among them, we found protein correlated to the mitochondria, like the NADH dehydrogenase [ubiquinone] 1 alpha sub-complex assembly factor 3, one of the components which forms mitochondrial respiratory chain complex I, the Mitochondrial inner membrane protein OXA1L and 39S ribosomal protein L41. Another protein in common between 2 and 12 months PDGF- h-  $\alpha$ -synuclein old mice compared to WT is the Sinaptogirina-3, which is an integral membrane protein whose function might be associated with the synaptic transmission with particular regard to dopamine transport.

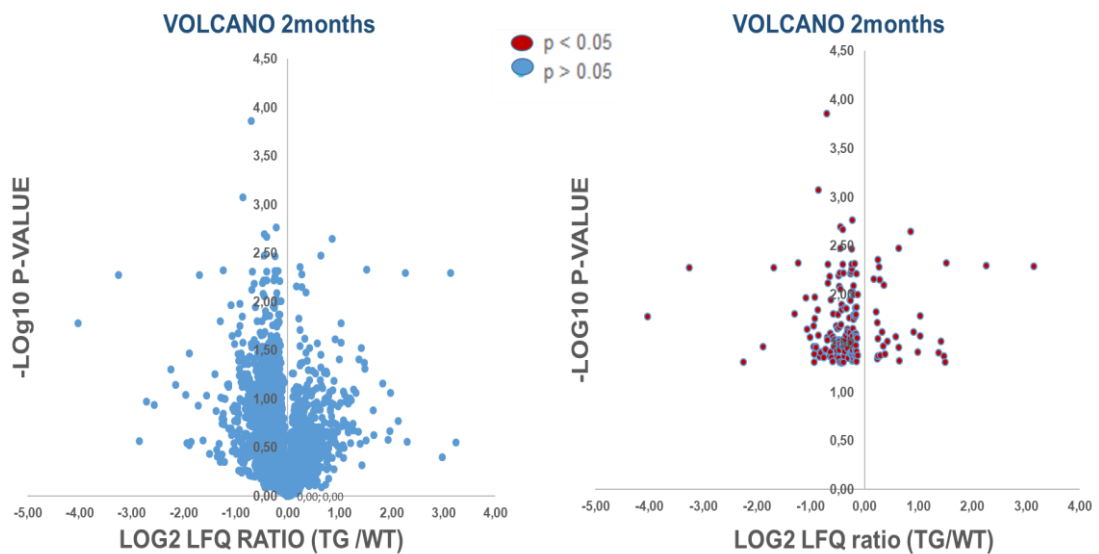


**Figure 32: A representative proteomic profile obtained by isolated microglial cells of 2 months-old PDGF- h-  $\alpha$ -synuclein transgenic mice by applying the Plot VOLCANO analysis.** On the left are represented all the proteins detected in 2 month-old transgenic mice compared to WT, and on the right are reported only the proteins whose expression resulted significantly changed. These changes indicated by the red-spots are expressed as the ratio of protein expression in transgenic and WT mice. The distribution of the red-spots along the axes is indicative of protein down-regulation (negative values) or protein up-regulation (positive values).

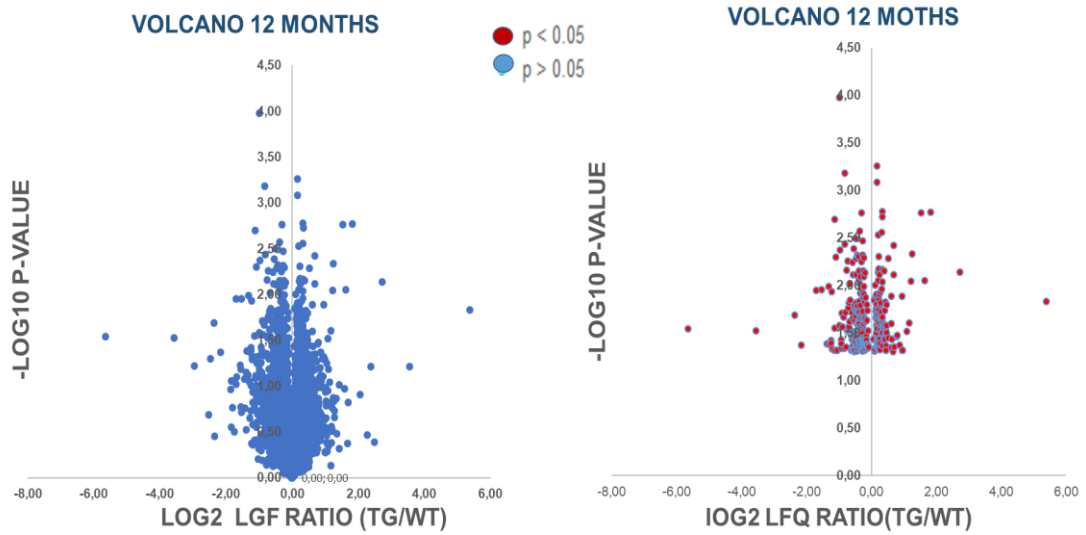


**Figure 33: A representative proteomic profile obtained by isolated microglial cells of 12 month-old PDGF- h-  $\alpha$ -synuclein transgenic mice by applying the Plot VOLCANO analysis. On the left are represented all the proteins detected in 12 months old transgenic mice compared to WT, and on the right are reported only the proteins whose expression resulted significantly changed. These changes indicated by the red-spots are expressed as the ratio of protein expression in transgenic and WT mice. The distribution of the red-spots along the axes is indicative of protein down-regulation (negative values) or protein up-regulation (positive values).**

PG.Gene	PG.ProteinAccession	PG.ProteinDescriptions	log2 (TG/V)
Gopc	Q8BH60	Golgi-associated PDZ and coiled-coil motif-containing protein	-4,03
Oas1a	P11928	2'-5'-oligoadenylate synthase 1A	-3,26
Eppk1	Q8ROW0	Epiplakin	-2,25
Sycp2	Q9CUU3	Synaptonemal complex protein 2	-1,89
Bpgm	P15327	Bisphosphoglycerate mutase	-1,69
Mrps27	Q8BK72	28S ribosomal protein S27, mitochondrial	-1,30
Mfn1	Q811U4	Mitofusin-1	-1,24
Psmf1	Q8BHL8	Proteasome inhibitor PI31 subunit	-1,09
Atp13a2	Q9CTG6	Probable cation-transporting ATPase 13A2	-1,07
Naa40	Q8VE10	N-alpha-acetyltransferase 40	-1,02
Zfyve1	Q810J8	Zinc finger FYVE domain-containing protein 1	-0,95
Scara3	Q8C850	Scavenger receptor class A member 3	-0,95
Mob4	Q6PEB6	MOB-like protein phocein	-0,94
Pi4k2a	Q2TBE6	Phosphatidylinositol 4-kinase type 2-alpha	-0,93
Krit1	Q655J6	Krev interaction trapped protein 1	-0,92
Ifit1	Q64282	Interferon-induced protein with tetratricopeptide repeats 1	-0,92
Ikbkb	O88351	Inhibitor of nuclear factor kappa-B kinase subunit beta	-0,90
Trit1	Q80UN9	tRNA dimethylallyltransferase, mitochondrial	-0,90
Slc8a1	P70414	Sodium/calcium exchanger 1	-0,87
Supv3l1	Q80YD1	ATP-dependent RNA helicase SUPV3L1, mitochondrial	-0,86
Zbtb8os	Q505B7	Protein archease	-0,86
Mrps35	Q8BJZ4	28S ribosomal protein S35, mitochondrial	-0,84
Lgmn	O89017	Legumain	-0,81
Cpsf4	Q8BQZ5	Cleavage and polyadenylation specificity factor subunit 4	-0,81
Esam	Q925F2	Endothelial cell-selective adhesion molecule	-0,75
Mtx2	O88441	Metaxin-2	-0,73
Hgsnat	Q3UDW8	Heparan-alpha-glucosaminide N-acetyltransferase	-0,73
Cog7	Q3UM29	Conserved oligomeric Golgi complex subunit 7	-0,70
Dhodh	O35435	Dihydroorotate dehydrogenase (quinone), mitochondrial	-0,70
Rap2b	P61226	Ras-related protein Rap-2b	-0,69
Vat1	Q62465	Synaptic vesicle membrane protein VAT-1 homolog	-0,68
Fmr1	P35922	Synaptic functional regulator FMR1	-0,68
Mgat1	P27808	Alpha-1,3-mannosyl-glycoprotein 2-beta-N-acetylglucosaminyltransferase	-0,65
Fmn12	A2APV2	Formin-like protein 2	-0,65
Ndufaf3	Q9JKL4	NADH dehydrogenase [ubiquinone] 1 alpha subcomplex assembly factor 3	-0,64
Bst2	Q8R2Q8	Bone marrow stromal antigen 2	-0,64
Dnaja3	Q99M87	DnaJ homolog subfamily A member 3, mitochondrial	-0,62
Cecr5	Q91WWM2	Cat eye syndrome critical region protein 5 homolog	-0,62
Tmem160	Q9D938	Transmembrane protein 160	-0,59
Tmtc3	Q8BRH0	Transmembrane and TPR repeat-containing protein 3	-0,59
Mnt	O08789	Max-binding protein MNT	-0,58
Akap5	D3YVF0	A-kinase anchor protein 5	-0,57
Eri3	Q8C460	ERI1 exoribonuclease 3	-0,57
Fut8	Q9WTS2	Alpha-(1,6)-fucosyltransferase	-0,55
Pla2g15	Q8VEB4	Group XV phospholipase A2	-0,53
Vps45	P97390	Vacuolar protein sorting-associated protein 45	-0,52
Pgs1	Q8BHF7	CDP-diacylglycerol--glycerol-3-phosphate 3-phosphatidyltransferase, mitochondri	-0,51
Ehd1	Q9WVK4	EH domain-containing protein 1	-0,51
Tmem205	Q91XE8	Transmembrane protein 205	-0,50
Itpk1	Q8BYN3	Inositol-tetrakisphosphate 1-kinase	-0,50
P2rx4	Q9JJX6	P2X purinoceptor 4	-0,48
Fuca2	Q99KR8	Plasma alpha-L-fucosidase	-0,48
Alpl	P09242	Alkaline phosphatase, tissue-nonspecific isozyme	-0,48
Atg16l1	Q8COJ2	Autophagy-related protein 16-1	-0,47
Tor1aip2	Q8BYU6	Torsin-1A-interacting protein 2	-0,47
Mrrf	Q9D6S7	Ribosome-recycling factor, mitochondrial	-0,47
Map6	Q7TSJ2	Microtubule-associated protein 6	-0,47
Manba	Q8K2I4	Beta-mannosidase	-0,46
Stx5	Q8K1E0	Syntaxin-5	-0,46
Itm2b	O89051	Integral membrane protein 2B	-0,46
Osbp1a	Q91XL9	Oxysterol-binding protein-related protein 1	-0,45
Arl8b	Q9CQW2	ADP-ribosylation factor-like protein 8B	-0,45
Selt	P62342	Selenoprotein T	-0,45
Nras	P08556	GTPase NRas	-0,44
Rabgap1	A2AWA9	Rab GTPase-activating protein 1	-0,43
Krtcap2	Q5RL79	Keratinocyte-associated protein 2	-0,43
Dennd1a	Q8K382	DENN domain-containing protein 1A	-0,43
Kat7	Q5SVQ0	Histone acetyltransferase KAT7	-0,41
Maoa	Q64133	Amine oxidase [flavin-containing] A	-0,41

Omg	Q63912	Oligodendrocyte-myelin glycoprotein	-0,41
Rars2	Q3U186	Probable arginine--tRNA ligase, mitochondrial	-0,40
Galc	P54818	Galactocerebrosidase	-0,40
Sqrdl	Q9R112	Sulfide:quinone oxidoreductase, mitochondrial	-0,40
Ctage5;Mia	Q8R311;Q91ZV0	cTAGE family member 5;Melanoma inhibitory activity protein 2	-0,40
Vps13c	Q8BX70	Vacuolar protein sorting-associated protein 13C	-0,39
Wrb	Q8K0D7	Tail-anchored protein insertion receptor WRB	-0,39
Zranb2	Q9R020	Zinc finger Ran-binding domain-containing protein 2	-0,38
Sfr1	Q8BP27	Swi5-dependent recombination DNA repair protein 1 homolog	-0,38
Nucks1	Q80XU3	Nuclear ubiquitous casein and cyclin-dependent kinase substrate 1	-0,38
Aldh18a1	Q9Z110	Delta-1-pyrroline-5-carboxylate synthase	-0,37
Dctn5	Q9QZB9	Dynactin subunit 5	-0,36
Atad1	Q9D5T0	ATPase family AAA domain-containing protein 1	-0,36
Tlr7	P58681	Toll-like receptor 7	-0,35
Npc1	O35604	Niemann-Pick C1 protein	-0,34
Zc3h11a	Q6NZF1	Zinc finger CCCH domain-containing protein 11A	-0,32
Gnaq	P21279	Guanine nucleotide-binding protein G(q) subunit alpha	-0,31
Ccdc90b	Q8C3X2	Coiled-coil domain-containing protein 90B, mitochondrial	-0,31
Ap1s2	Q9DB50	AP-1 complex subunit sigma-2	-0,31
	Q8CHH9	Septin-8	-0,30
Creb1	Q01147	Cyclic AMP-responsive element-binding protein 1	-0,29
Raly	Q64012	RNA-binding protein Raly	-0,28
Rps16	P14131	40S ribosomal protein S16	-0,28
Samm50	Q8BGH2	Sorting and assembly machinery component 50 homolog	-0,27
Sdhb	Q9CQA3	Succinate dehydrogenase [ubiquinone] iron-sulfur subunit, mitochondrial	-0,27
Rtn4	Q99P72	Reticulon-4	-0,27
Rap2a	Q80ZJ1	Ras-related protein Rap-2a	-0,26
Unc93b1	Q8VCW4	Protein unc-93 homolog B1	-0,26
Oxa1l	Q8BGA9	Mitochondrial inner membrane protein OXA1L	-0,26
Arl6ip5	Q8R5J9	PRA1 family protein 3	-0,25
Ndufb11	O09111	NADH dehydrogenase [ubiquinone] 1 beta subcomplex subunit 11, mitochondrial	-0,25
Snrnp70	Q62376	U1 small nuclear ribonucleoprotein 70 kDa	-0,24
Vapb	Q9QY76	Vesicle-associated membrane protein-associated protein B	-0,24
Agk	Q9ESW4	Acylglycerol kinase, mitochondrial	-0,24
Sec11a	Q9R0P6	Signal peptidase complex catalytic subunit SEC11A	-0,24
Hnrnpa3	Q8BG05	Heterogeneous nuclear ribonucleoprotein A3	-0,23
Hnrnpab	Q99020	Heterogeneous nuclear ribonucleoprotein A/B	-0,23
Hnrnpul2	Q00PI9	Heterogeneous nuclear ribonucleoprotein U-like protein 2	-0,23
Galnt1	O08912	Polypeptide N-acetylgalactosaminyltransferase 1	-0,22
Srsf5	O35326	Serine/arginine-rich splicing factor 5	-0,22
Syngn3	Q8R191	Synaptogyrin-3	-0,22
Cyp20a1	Q8BKE6	Cytochrome P450 20A1	-0,22
Aldh3a2	P47740	Fatty aldehyde dehydrogenase	-0,21
Tbl1xr1	Q8BHJ5	F-box-like/WD repeat-containing protein TBL1XR1	-0,21
Alg2	Q9DBE8	Alpha-1,3/1,6-mannosyltransferase ALG2	-0,21
Slc25a11	Q9CR62	Mitochondrial 2-oxoglutarate/malate carrier protein	-0,21
Stt3a	P46978	Dolichyl-diphosphooligosaccharide--protein glycosyltransferase subunit STT3A	-0,20
Magoh	P61327	Protein mago nashi homolog	-0,20
Hsd17b12	O70503	Very-long-chain 3-oxoacyl-CoA reductase	-0,19
Lipe	P54310	Hormone-sensitive lipase	-0,19
Ergic1	Q9DC16	Endoplasmic reticulum-Golgi intermediate compartment protein 1	-0,19
Rpl23a	P62751	60S ribosomal protein L23a	-0,19
Phb2	O35129	Prohibitin-2	-0,18
Dnajb6	O54946	DnaJ homolog subfamily B member 6	-0,18
Lpcat3	Q91V01	Lysophospholipid acyltransferase 5	-0,18
Cops7b	Q8BV13	COP9 signalosome complex subunit 7b	-0,18
Eif2a	Q8BJW6	Eukaryotic translation initiation factor 2A	-0,17
Nipbl	Q6KCD5	Nipped-B-like protein	-0,17
Apool	Q78IK4	MICOS complex subunit Mic27	-0,17
Vapa	Q9WV55	Vesicle-associated membrane protein-associated protein A	-0,17
Pds5b	Q4VA53	Sister chromatid cohesion protein PDS5 homolog B	-0,17
Hm13	Q9D8V0	Minor histocompatibility antigen H13	-0,16
Tial1	P70318	Nucleolysin TIAR	-0,16
Acat1	Q8QZT1	Acetyl-CoA acetyltransferase, mitochondrial	-0,16
Stam	P70297	Signal transducing adapter molecule 1	-0,16
Lman1	Q9D0F3	Protein ERGIC-53	-0,16
Glul	P15105	Glutamine synthetase	-0,15
Rps14	P62264	40S ribosomal protein S14	-0,15
Rpl5	P47962	60S ribosomal protein L5	-0,15
Rpl18a	P62717	60S ribosomal protein L18a	-0,15



Mlec	Q6ZQI3	Malectin	-0,15
Pmpcb	Q9CXT8	Mitochondrial-processing peptidase subunit beta	-0,14
Hnrnpu	Q8VEK3	Heterogeneous nuclear ribonucleoprotein U	-0,13
Spcs3	Q6ZWQ7	Signal peptidase complex subunit 3	-0,13
Rpsa	P14206	40S ribosomal protein SA	0,17
Thoc7	Q7TMY4	THO complex subunit 7 homolog	0,22
Irf8	P23611	Interferon regulatory factor 8	0,24
Zfand6	Q9DCH6	AN1-type zinc finger protein 6	0,24
Rprd1b	Q9CSU0	Regulation of nuclear pre-mRNA domain-containing protein 1B	0,24
Ssbp1	Q9CYR0	Single-stranded DNA-binding protein, mitochondrial	0,24
Pfdn1	Q9CWM4	Prefoldin subunit 1	0,25
Cstf1	Q99LC2	Cleavage stimulation factor subunit 1	0,27
Hn1l	Q6PGH2	Hematological and neurological expressed 1-like protein	0,28
	Q8C650	Septin-10	0,29
Slain2	Q8CI08	SLAIN motif-containing protein 2	0,33
Gart	Q64737	Trifunctional purine biosynthetic protein adenosine-3	0,35
Pak1	Q88643	Serine/threonine-protein kinase PAK 1	0,35
Slc9a1	Q61165	Sodium/hydrogen exchanger 1	0,38
Mcee	Q9D1I5	Methylmalonyl-CoA epimerase, mitochondrial	0,42
Eml2	Q7TNG5	Echinoderm microtubule-associated protein-like 2	0,58
Inpp5k	Q8C5L6	Inositol polyphosphate 5-phosphatase K	0,64
	Q9Z2Q6	Septin-5	0,64
Mrpl41	Q9CQN7	39S ribosomal protein L41, mitochondrial	0,64
Slc30a7	Q9JKN1	Zinc transporter 7	0,85
	Q99K99	Uncharacterized protein C4orf19 homolog	0,91
Elof1	P60003	Transcription elongation factor 1 homolog	0,99
Krt1	P04104	Keratin, type II cytoskeletal 1	1,03
Rbp1	Q00915	Retinol-binding protein 1	1,03
Helz2	E9QAM5	Helicase with zinc finger domain 2	1,37
Pcsk1n	Q9QXV0	ProSAAS	1,42
Ngly1	Q9JI78	Peptide-N(4)-(N-acetyl-beta-glucosaminyl)asparagine amidase	1,47
Mmaa	Q8C7H1	Methylmalonic aciduria type A homolog, mitochondrial	1,49
Ampd2	Q9DBT5	AMP deaminase 2	1,52
Sncb	Q91Z73	Beta-synuclein	2,26
Snca	O55042	Alpha-synuclein	3,14

**Table 2: List of analysed proteins in 2-month-old PDGF- h-  $\alpha$ -synuclein transgenic mice obtained by using software MaxQuant associated with Andromeda.** The negative score is indicative of proteins down-regulated while the positive score is indicative of proteins up-regulated. The proteins belonging to the mitochondrial pathways are indicated in red. In blue are reported the proteins associated with other organelles and ion channels; in light-purple are indicate the proteins correlated to the pathways of the immune system; in green are indicated the proteins correlated to the pathways of the cellular cycle; in light-orange, the protein correlated to the pathways of neuronal system.

PG.Gen	PG.ProteinAccession	PG.ProteinDescriptions	log2 FC
Eif2ak4	Q9QZ05	eIF-2-alpha kinase GCN2	-5,65
Gdap1	O88741	Ganglioside-induced differentiation-associated protein 1	-3,56
Lgi3	Q8K406	Leucine-rich repeat LGI family member 3	-2,36
Pan3	Q640Q5	PAB-dependent poly(A)-specific ribonuclease subunit PAN3	-2,16
<b>Calm1</b>	<b>P62204</b>	<b>Calmodulin</b>	-1,70
Atp6v1g2	Q9WTT4	V-type proton ATPase subunit G 2	-1,53
Dnm1	P39053	Dynamin-1	-1,36
Plxna4	Q80UG2	Plexin-A4	-1,32
<b>Me3</b>	<b>Q8BMF3</b>	<b>NADP-dependent malic enzyme, mitochondrial</b>	-1,29
Samd9l	Q69237	Sterile alpha motif domain-containing protein 9-like	-1,25
Ppfibp2	O35711	Liprin-beta-2	-1,23
Enah	Q03173	Protein enabled homolog	-1,22
Rps29	P62274	40S ribosomal protein S29	-1,21
<b>Ndufs6</b>	<b>P52503</b>	<b>NADH dehydrogenase [ubiquinone] iron-sulfur protein 6, mitochondrial</b>	-1,13
Eif4e2	Q8BMB3	Eukaryotic translation initiation factor 4E type 2	-1,13
Siae	P70665	Sialate O-acetyltransferase	-1,12
Napb	P28663	Beta-soluble NSF attachment protein	-1,09
Rap1a	P62835	Ras-related protein Rap-1A	-1,06
Eif1b	Q9CXU9	Eukaryotic translation initiation factor 1b	-0,99
Slc33a1	Q99J27	Acetyl-coenzyme A transporter 1	-0,98
<b>Ndufaf3</b>	<b>Q9JKL4</b>	<b>NADH dehydrogenase [ubiquinone] 1 alpha subcomplex assembly factor 3</b>	-0,97
Aspa	Q8R3P0	Aspartoacylase	-0,94
Arhgef10l	A2AWP8	Rho guanine nucleotide exchange factor 10-like protein	-0,93
Daam1	Q8BPM0	Disheveled-associated activator of morphogenesis 1	-0,93
Eif1a	Q60872	Eukaryotic translation initiation factor 1A	-0,90
Phyhip	Q8K0S0	Phytanoyl-CoA hydroxylase-interacting protein	-0,88
Bnip3l	Q9Z2F7	BCL2/adenovirus E1B 19 kDa protein-interacting protein 3-like	-0,85
Lsm14a	Q8K2F8	Protein LSM14 homolog A	-0,84
Epdr1	Q99M71	Mammalian ependymin-related protein 1	-0,82
Phgdh	Q61753	D-3-phosphoglycerate dehydrogenase	-0,81
Btd	Q8CIF4	Biotinidase	-0,80
Glb1l	Q8VC60	Beta-galactosidase-1-like protein	-0,78
Dpp7	Q9ET22	Dipeptidyl peptidase 2	-0,76
Scrib	Q80U72	Protein scribble homolog	-0,74
Impact	O55091	Protein IMPACT	-0,72
Asrgl1	Q8COM9	Isoaspartyl peptidase/L-asparaginase	-0,72
Syt1	P46096	Synaptotagmin-1	-0,71
Echdc1	Q9D9V3	Ethylmalonyl-CoA decarboxylase	-0,69
Tigar	Q8BZA9	Fructose-2,6-bisphosphatase TIGAR	-0,69
Lancl2	Q9JJK2	LanC-like protein 2	-0,68
Prcp	Q7TMR0	Lysosomal Pro-X carboxypeptidase	-0,67
Syp	Q62277	Synaptophysin	-0,65
Syng3	Q8R191	Synaptogyrin-3	-0,61
Irf2bp2	E9Q1P8	Interferon regulatory factor 2-binding protein 2	-0,60
Ctsl	P06797	Cathepsin L1	-0,60
Guk1	Q64520	Guanylate kinase	-0,59
Rabep1	O35551	Rab GTPase-binding effector protein 1	-0,58
Glmn	Q8BZM1	Glomulin	-0,58
Scpep1	Q920A5	Retinoid-inducible serine carboxypeptidase	-0,58
<b>Szrd1</b>	<b>Q6NXN1</b>	<b>SUZ domain-containing protein 1</b>	-0,58
<b>Uqcrh</b>	<b>P99028</b>	<b>Cytochrome b-c1 complex subunit 6, mitochondrial</b>	-0,58
Cd9	P40240	CD9 antigen	-0,57
Nptxr	Q99J85	Neuronal pentraxin receptor	-0,57
Tubal3	Q3UX10	Tubulin alpha chain-like 3	-0,57
Card19	Q9D1I2	Caspase recruitment domain-containing protein 19	-0,55
Prkca	P20444	Protein kinase C alpha type	-0,54
Spns1	Q8R0G7	Protein spinster homolog 1	-0,54
Tmem19	Q91W52	Transmembrane protein 19	-0,53
Znf740	Q6NZQ6	Zinc finger protein 740	-0,52

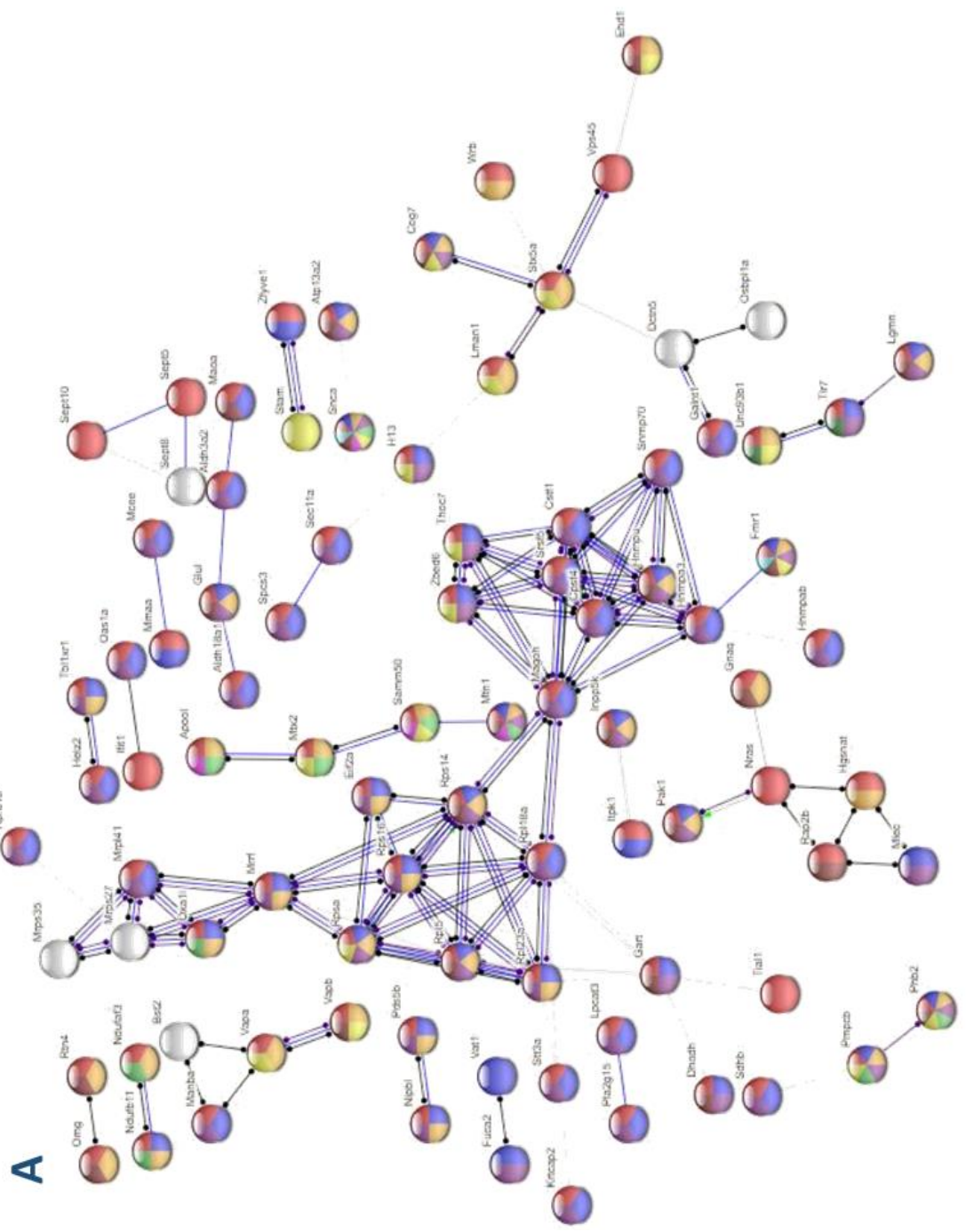
Nptx1	Q62443	Neuronal pentraxin-1	-0,52
Myo5a	Q99104	Unconventional myosin-Va	-0,52
Vps37c	Q8R105	Vacuolar protein sorting-associated protein 37C	-0,52
Ttc5	Q99LG4	Tetratricopeptide repeat protein 5	-0,52
Anxa6	P14824	Annexin A6	-0,52
Prx	O55103	Periaxin	-0,50
Gpd1	P13707	Glycerol-3-phosphate dehydrogenase [NAD(+)], cytoplasmic	-0,50
Ctbs	Q8R242	Di-N-acetylchitobiase	-0,49
Acat2	Q8CAY6	Acetyl-CoA acetyltransferase, cytosolic	-0,49
Tmem65	Q4VAE3	Transmembrane protein 65	-0,49
Phkg2	Q9DB30	Phosphorylase b kinase gamma catalytic chain, liver/testis isoform	-0,48
Ids	Q08890	Iduronate 2-sulfatase	-0,48
Pfkl	P12382	ATP-dependent 6-phosphofructokinase, liver type	-0,48
Memo1	Q91VH6	Protein MEMO1	-0,47
Arsa	P50428	Arylsulfatase A	-0,47
Mfap1	Q9CQU1	Microfibrillar-associated protein 1	-0,46
43718	Q8C650	Septin-10	-0,45
Got2	P05202	Aspartate aminotransferase, mitochondrial	-0,45
Smpdl3a	P70158	Acid sphingomyelinase-like phosphodiesterase 3a	-0,45
Sumf1	Q8ROF3	Sulfatase-modifying factor 1	-0,44
Reep3	Q99KK1	Receptor expression-enhancing protein 3	-0,43
Tmem205	Q91XE8	Transmembrane protein 205	-0,43
Rbm5	Q91YE7	RNA-binding protein 5	-0,43
Chchd6	Q91VN4	MICOS complex subunit Mic25	-0,43
Cpq	Q9WVJ3	Carboxypeptidase Q	-0,42
Manba	Q8K2I4	Beta-mannosidase	-0,42
Gfpt1	P47856	Glutamine--fructose-6-phosphate aminotransferase [isomerizing]	-0,41
Arsb	P50429	Arylsulfatase B	-0,40
Rab33b	O35963	Ras-related protein Rab-33B	-0,39
Rabggta	Q9JHK4	Geranylgeranyl transferase type-2 subunit alpha	-0,39
Phf11	A6H5X4	PHD finger protein 11	-0,39
Cbr2	P08074	Carbonyl reductase [NADPH] 2	-0,39
Dab2	P98078	Disabled homolog 2	-0,38
Gdpd1	Q9CRY7	Glycerophosphodiester phosphodiesterase domain-containing protein	-0,38
Slc25a20	Q922Z6	Mitochondrial carnitine/acylcarnitine carrier protein	-0,37
Smpd1	Q04519	Sphingomyelin phosphodiesterase	-0,37
Mrc1	Q61830	Macrophage mannose receptor 1	-0,36
F13a1	Q8BH61	Coagulation factor XIII A chain	-0,36
Ctsc	P97821	Dipeptidyl peptidase 1	-0,36
Sparc	P07214	SPARC	-0,35
Acap2	Q6ZQK5	Arf-GAP with coiled-coil, ANK repeat and PH domain-containing protein	-0,35
Scamp2	Q9ERN0	Secretory carrier-associated membrane protein 2	-0,35
Irf5	P56477	Interferon regulatory factor 5	-0,34
Dync1i2	O88487	Cytoplasmic dynein 1 intermediate chain 2	-0,34
Atp6v1c1	Q9Z1G3	V-type proton ATPase subunit C 1	-0,34
Dnase2	P56542	Deoxyribonuclease-2-alpha	-0,33
Plbd2	Q3TCN2	Putative phospholipase B-like 2	-0,33
Cask	O70589	Peripheral plasma membrane protein CASK	-0,33
Arsg	Q3TYD4	Arylsulfatase G	-0,33
Ddah2	Q99LD8	N(G),N(G)-dimethylarginine dimethylaminohydrolase 2	-0,32
Mien1	Q9CQ86	Migration and invasion enhancer 1	-0,31
Reep5	Q60870	Receptor expression-enhancing protein 5	-0,31
Aak1	Q3UJH0	AP2-associated protein kinase 1	-0,31
Casp6	O08738	Caspase-6	-0,30
Mrpl41	Q9CQN7	39S ribosomal protein L41, mitochondrial	-0,30
Vps41	Q5KU39	Vacuolar protein sorting-associated protein 41 homolog	-0,30
Anxa5	P48036	Annexin A5	-0,29
Pld3	O35405	Phospholipase D3	-0,29
Mef2c	Q8CFN5	Myocyte-specific enhancer factor 2C	-0,29
Cul4a	Q3TCH7	Cullin-4A	-0,28

Epb41l2	O70318	Band 4.1-like protein 2	-0,28
Sod2	P09671	Superoxide dismutase [Mn], mitochondrial	-0,28
Ywhag	P61982	14-3-3 protein gamma	-0,28
Pdxk	Q8K183	Pyridoxal kinase	-0,28
Npc2	Q9Z0J0	Epididymal secretory protein E1	-0,28
Grhpr	Q91Z53	Glyoxylate reductase/hydroxypyruvate reductase	-0,27
Actb	P60710	Actin, cytoplasmic 1	-0,27
Dnajc2	P54103	DnaJ homolog subfamily C member 2	-0,27
Mob4	Q6PEB6	MOB-like protein phocein	-0,27
Pla2g15	Q8VEB4	Group XV phospholipase A2	-0,27
Psat1	Q99K85	Phosphoserine aminotransferase	-0,27
Pea15	Q62048	Astrocytic phosphoprotein PEA-15	-0,27
Itm2b	O89051	Integral membrane protein 2B	-0,26
Rap2a	Q80ZJ1	Ras-related protein Rap-2a	-0,26
Ptpmt1	Q66GT5	Phosphatidylglycerophosphatase and protein-tyrosine phosphatase	-0,26
Aars	Q8BGQ7	Alanine--tRNA ligase, cytoplasmic	-0,26
Arpc2	Q9CVB6	Actin-related protein 2/3 complex subunit 2	-0,26
Itpa	Q9D892	Inosine triphosphate pyrophosphatase	-0,25
Ankrd17	Q99NH0	Ankyrin repeat domain-containing protein 17	-0,25
Pkm	P52480	Pyruvate kinase PKM	-0,25
Hrsp12	P52760	Ribonuclease UK114	-0,24
Bin1	O08539	Myc box-dependent-interacting protein 1	-0,24
Ctsb		Cathepsin B	-0,24
Merk	Q60805	Tyrosine-protein kinase Mer	-0,23
Ap1m1	P35585	AP-1 complex subunit mu-1	-0,23
Hnrnpa3	Q8BG05	Heterogeneous nuclear ribonucleoprotein A3	-0,23
Ndufs4	Q9CXZ1	NADH dehydrogenase [ubiquinone] iron-sulfur protein 4, mitochondrial	-0,23
Ctsa	P16675	Lysosomal protective protein	-0,22
Ctps2	P70303	CTP synthase 2	-0,22
Lap3	Q9CPY7	Cytosol aminopeptidase	-0,21
Eif3k	Q9DBZ5	Eukaryotic translation initiation factor 3 subunit K	-0,21
P2rx7	Q9Z1M0	P2X purinoceptor 7	-0,20
Ap2s1	P62743	AP-2 complex subunit sigma	-0,20
Hebp1	Q9R257	Heme-binding protein 1	-0,19
Mccc2	Q3ULD5	Methylcrotonoyl-CoA carboxylase beta chain, mitochondrial	-0,19
Dync1li2	Q6PDL0	Cytoplasmic dynein 1 light intermediate chain 2	-0,19
Impa1	O55023	Inositol monophosphatase 1	-0,18
Atp8a1	P70704	Phospholipid-transporting ATPase IA	-0,18
Ube2l3	P68037	Ubiquitin-conjugating enzyme E2 L3	-0,18
Cep170	Q6A065	Centrosomal protein of 170 kDa	-0,17
Dctn1	O08788	Dynactin subunit 1	-0,17
Acp2	P24638	Lysosomal acid phosphatase	-0,16
Ldha	P06151	L-lactate dehydrogenase A chain	-0,15
Pip4k2b	Q80XI4	Phosphatidylinositol 5-phosphate 4-kinase type-2 beta	-0,15
Ap2a1	P17426	AP-2 complex subunit alpha-1	-0,14
Ap2a2	P17427	AP-2 complex subunit alpha-2	-0,13
Smchd1	Q6P5D8	Structural maintenance of chromosomes flexible hinge domain-co	-0,13
Cltc	Q68FD5	Clathrin heavy chain 1	-0,12
Prosc	Q9Z2Y8	Proline synthase co-transcribed bacterial homolog protein	-0,12
Npepl1	Q6NSR8	Probable aminopeptidase NPEPL1	-0,12
Mtpn	P62774	Myotrophin	-0,10
Clta	O08585	Clathrin light chain A	-0,09
Exoc2	Q9D4H1	Exocyst complex component 2	0,06
Rpl17	Q9CPR4	60S ribosomal protein L17	0,07
Rps8	P62242	40S ribosomal protein S8	0,10
Numb	Q9QZS3	Protein numb homolog	0,10
Tfe3	Q64092	Transcription factor E3	0,11
Cct2	P80314	T-complex protein 1 subunit beta	0,12
Rps18	P62270	40S ribosomal protein S18	0,13
Btf3l4	Q9CQH7	Transcription factor BTF3 homolog 4	0,14

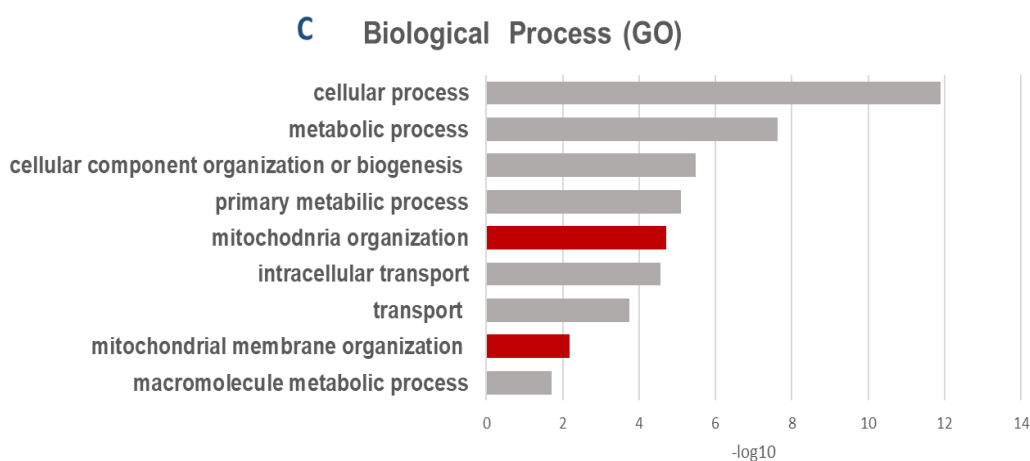
Erbin	Q80TH2	Erbin	0,14
Lypla2	Q9WTL7	Acyl-protein thioesterase 2	0,15
Arhgef2	Q60875	Rho guanine nucleotide exchange factor 2	0,15
Ythdf2	Q91YT7	YTH domain-containing family protein 2	0,15
Nfyc	P70353	Nuclear transcription factor Y subunit gamma	0,15
Rpl26	P61255	60S ribosomal protein L26	0,15
Ap3s1	Q9DCR2	AP-3 complex subunit sigma-1	0,16
Caprin1	Q60865	Caprin-1	0,16
Psme3	P61290	Proteasome activator complex subunit 3	0,16
Lgals9	O08573	Galectin-9	0,16
Ppp1r18	Q8BQ30	Phostensin	0,16
Rpl28	P41105	60S ribosomal protein L28	0,16
Srrt	Q99MR6	Serrate RNA effector molecule homolog	0,16
Kars	Q99MN1	Lysine--tRNA ligase	0,16
Sec31a	Q3UPL0	Protein transport protein Sec31A	0,17
Scaf8	Q6DID3	Protein SCAF8	0,17
Wtap	Q9ER69	Pre-mRNA-splicing regulator WTAP	0,17
Eif4h	Q9WUK2	Eukaryotic translation initiation factor 4H	0,18
Mafg	O54790	Transcription factor MafG	0,18
Pcyt1a	P49586	Choline-phosphate cytidyltransferase A	0,19
Ipo5	Q8BKC5	Importin-5	0,19
Mre11a	Q61216	Double-strand break repair protein MRE11A	0,19
Psmc1	P62192	26S protease regulatory subunit 4	0,19
Ube2g2	P60605	Ubiquitin-conjugating enzyme E2 G2	0,20
Xrn2	Q9DBR1	5'-3' exoribonuclease 2	0,21
Usp10	P52479	Ubiquitin carboxyl-terminal hydrolase 10	0,21
Dicer1	Q8R418	Endoribonuclease Dicer	0,21
Pds5a	Q6A026	Sister chromatid cohesion protein PDS5 homolog A	0,21
Psme1	P97371	Proteasome activator complex subunit 1	0,21
Mbnl1	Q9JKP5	Muscleblind-like protein 1	0,22
Csnk2a1	Q60737	Casein kinase II subunit alpha	0,22
Chmp3	Q9CQ10	Charged multivesicular body protein 3	0,22
Ppie	Q9QZH3	Peptidyl-prolyl cis-trans isomerase E	0,23
Ppp1r10	Q80W00	Serine/threonine-protein phosphatase 1 regulatory subunit 10	0,23
Vps25	Q9CQ80	Vacuolar protein-sorting-associated protein 25	0,23
Rps3a	P97351	40S ribosomal protein S3a	0,23
Top2b	Q64511	DNA topoisomerase 2-beta	0,24
Eif3f	Q9DCH4	Eukaryotic translation initiation factor 3 subunit F	0,24
Nceh1	Q8BLF1	Neutral cholesterol ester hydrolase 1	0,24
Pdia5	Q921X9	Protein disulfide-isomerase A5	0,24
Parvg	Q9ERD8	Gamma-parvin	0,25
Pds5b	Q4VA53	Sister chromatid cohesion protein PDS5 homolog B	0,26
Banf1	O54962	Barrier-to-autointegration factor	0,26
Gosr2	Q35166	Golgi SNAP receptor complex member 2	0,27
Oxa1l	Q8BGA9	Mitochondrial inner membrane protein OXA1L	0,27
Nasp	Q99MD9	Nuclear autoantigenic sperm protein	0,27
Stxbp2	Q64324	Syntaxin-binding protein 2	0,28
Itgb6	Q9Z0T9	Integrin beta-6	0,29
Gpkow	Q56A08	G patch domain and KOW motifs-containing protein	0,29
Ilf3	Q9Z1X4	Interleukin enhancer-binding factor 3	0,30
Supt5h	O55201	Transcription elongation factor SPT5	0,30
Smarcc1	P97496	SWI/SNF complex subunit SMARCC1	0,31
Pdcd4	Q61823	Programmed cell death protein 4	0,32
Bid	P70444	BH3-interacting domain death agonist	0,32
Clptm1l	Q8BXA5	Cleft lip and palate transmembrane protein 1-like protein	0,32
Vsir	Q9D659	V-type immunoglobulin domain-containing suppressor of T-cell act	0,33
Uros	P51163	Uroporphyrinogen-III synthase	0,33
Chd4	Q6PDQ2	Chromodomain-helicase-DNA-binding protein 4	0,33
Sun2	Q8BJS4	SUN domain-containing protein 2	0,33
Psip1	Q99JF8	PC4 and SFRS1-interacting protein	0,33

43723	Q9ERR7	15 kDa selenoprotein	0,33
Fen1	P39749	Flap endonuclease 1	0,34
Ddx46	Q569Z5	Probable ATP-dependent RNA helicase DDX46	0,34
Ckap4	Q8BMK4	Cytoskeleton-associated protein 4	0,34
Haus8	Q99L00	HAUS augmin-like complex subunit 8	0,36
Smad5	P97454	Mothers against decapentaplegic homolog 5	0,38
Lamtor5	Q9D1L9	Ragulator complex protein LAMTOR5	0,39
Ctr9	Q62018	RNA polymerase-associated protein CTR9 homolog	0,39
Nt5dc1	Q8C5P5	5'-nucleotidase domain-containing protein 1	0,39
Fkbp9	Q9Z247	Peptidyl-prolyl cis-trans isomerase FKBP9	0,40
Gxylt1	Q3UHH8	Glucoside xylosyltransferase 1	0,41
Stk17b	Q8BG48	Serine/threonine-protein kinase 17B	0,41
Fmo5	P97872	Dimethylaniline monooxygenase [N-oxide-forming] 5	0,41
Tes	P47226	Testin	0,42
Ktn1	Q61595	Kinectin	0,44
Srpk1	O70551	SRSF protein kinase 1	0,44
Pqbp1	Q91VJ5	Polyglutamine-binding protein 1	0,45
Terf2ip	Q91VL8	Telomeric repeat-binding factor 2-interacting protein 1	0,45
Mfge8	P21956	Lactadherin	0,46
Xrcc1	Q60596	DNA repair protein XRCC1	0,46
Pptc7	Q6NVE9	Protein phosphatase PTC7 homolog	0,47
Hist2h2be;	Q64524;Q8CGP0;Q9D	Histone H2B type 2-E;Histone H2B type 3-B;Histone H2B type 3-A	0,47
Nfkbie	O54910	NF-kappa-B inhibitor epsilon	0,51
Heatr3	Q8BQM4	HEAT repeat-containing protein 3	0,52
Aagab	Q8R2R3	Alpha- and gamma-adaptin-binding protein p34	0,62
Znf326	O88291	DBIRD complex subunit ZNF326	0,62
Med24	Q99K74	Mediator of RNA polymerase II transcription subunit 24	0,62
Traf3ip3	Q8C0G2	TRAF3-interacting JNK-activating modulator	0,64
Igfbp7	Q61581	Insulin-like growth factor-binding protein 7	0,66
Pwwp2a	Q69Z61	PWWP domain-containing protein 2A	0,68
Rnf181	Q9CY62	E3 ubiquitin-protein ligase RNF181	0,69
Man1b1	A2AJ15	Endoplasmic reticulum mannosyl-oligosaccharide 1,2-alpha-manno	0,70
Gstm2	P15626	Glutathione S-transferase Mu 2	0,78
Tspo	P50637	Translocator protein	0,79
Taok2	Q6ZQ29	Serine/threonine-protein kinase TAO2	0,87
Pelo	Q80X73	Protein pelota homolog	0,94
Ccdc94	Q9D6J3	Coiled-coil domain-containing protein 94	0,95
Txlng	Q8BHN1	Gamma-taxilin	0,96
Mtmr3	Q8K296	Myotubularin-related protein 3	1,09
Nid1	P10493	Nidogen-1	1,17
Rdh13	Q8CEE7	Retinol dehydrogenase 13	1,22
Zc3hc1	Q80YV2	Nuclear-interacting partner of ALK	1,25
Src	P05480	Neuronal proto-oncogene tyrosine-protein kinase Src	1,54
Snca	O55042	Alpha-synuclein	1,63
Tmem176l	Q9R1Q6	Transmembrane protein 176B	1,82
Fahd1	Q8R0F8	Acylpyruvase FAHD1, mitochondrial	2,72
Plcb1	Q9Z1B3	1-phosphatidylinositol 4,5-bisphosphate phosphodiesterase beta-1	5,38

**Table 3: List of analysed proteins in 12-month-old PDGF- $\beta$ - $\alpha$ -synuclein transgenic mice obtained by using software MaxQuant associated with Andromeda.** The negative score is indicative of proteins down-regulated while the positive score is indicative of proteins up-regulated. The proteins belonging to the mitochondrial pathways are indicated in red. In blue are reported the proteins associated with other organelles and ion channels; in light-purple are indicated the proteins correlated to the pathways of the immune system; in green are indicated the proteins correlated to the pathways of the cellular cycle; in light-orange, the protein correlated to the pathways of neuronal system.

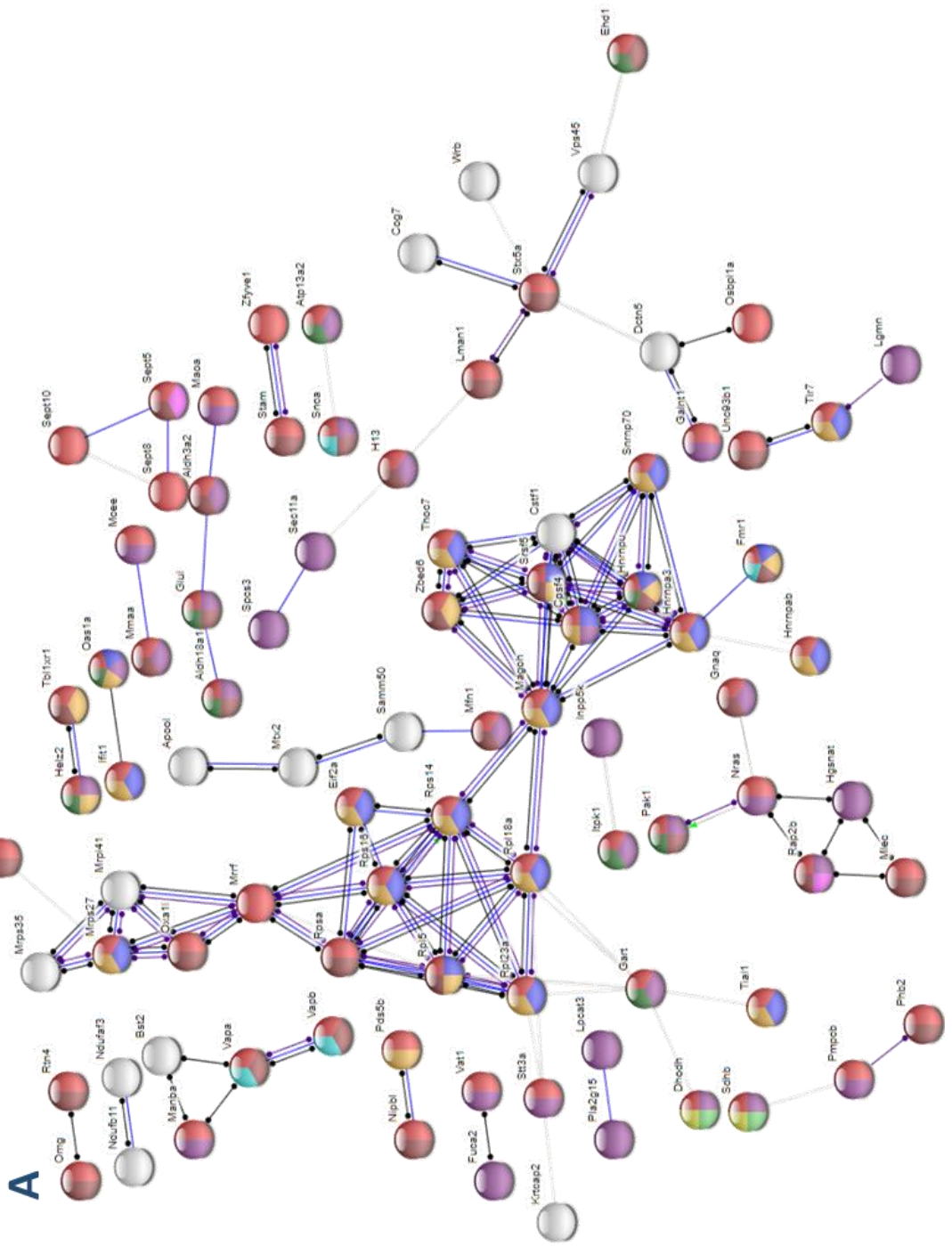


B Biological Process (GO)			
GO-term	description	count in gene set	false discovery rate
GO:0009987	cellular process	147 of 12459	1.29e-12
GO:0008152	metabolic process	107 of 8164	2.37e-08
GO:0071840	cellular component organization or biogenesis	70 of 4730	3.22e-06
GO:0044238	primary metabolic process	93 of 7426	7.93e-06
GO:0007005	mitochondrion organization	16 of 388	1.96e-05
GO:0046907	intracellular transport	26 of 1032	2.70e-05
GO:0006810	transport	49 of 3187	0.00018
GO:0007006	mitochondrial membrane organization	6 of 92	0.0067
GO:0043170	macromolecule metabolic process	69 of 6225	0.0192

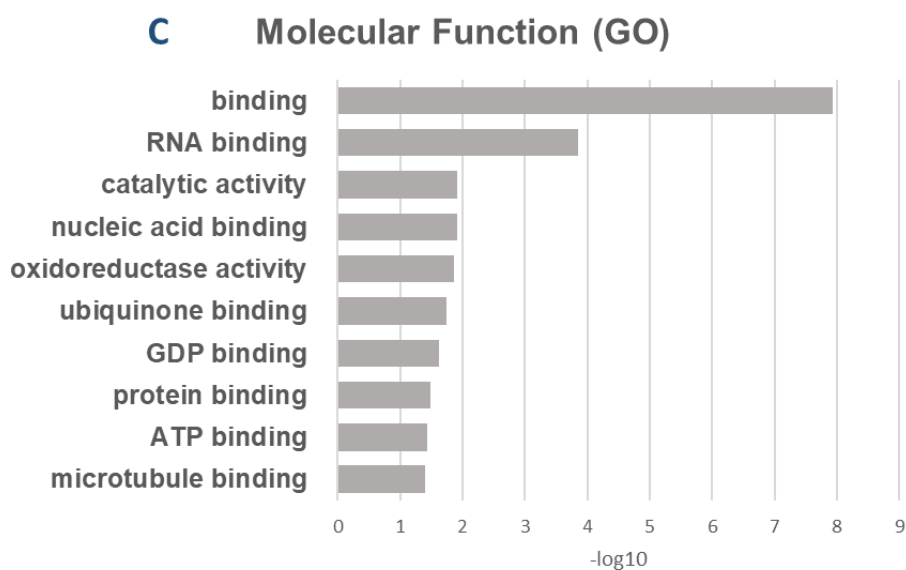


**Figure 34: Representation of the cluster maps of the analysis of the protein obtained with GO respect the Biological Process detected in 2-month-old PDGF- $\alpha$ -synuclein transgenic mice compared to WT. A) Each point in the maps represents one protein. Each protein is coloured respect to its involvement in a specific pathway. The colour is arbitrarily defined but is the same for each protein belonging to the same pathway. The lines linking the different points express the amount of correlation/regulation among the proteins. B) In the corresponding table, the column on the left represents the number of pathways in the GO database. The column called "Count in the gene set" represents the number of the analysed protein respect the number of total proteins present in the database GO which are related to the specific pathway. The column called "False discovery rate" indicates the probability to have false positive in the analysis. C) Graph bars describe the protein expression for each cellular pathway in logarithmic scale. In red are indicate the proteins correlated to the pathways of the mitochondria, in grey all the other pathways.**

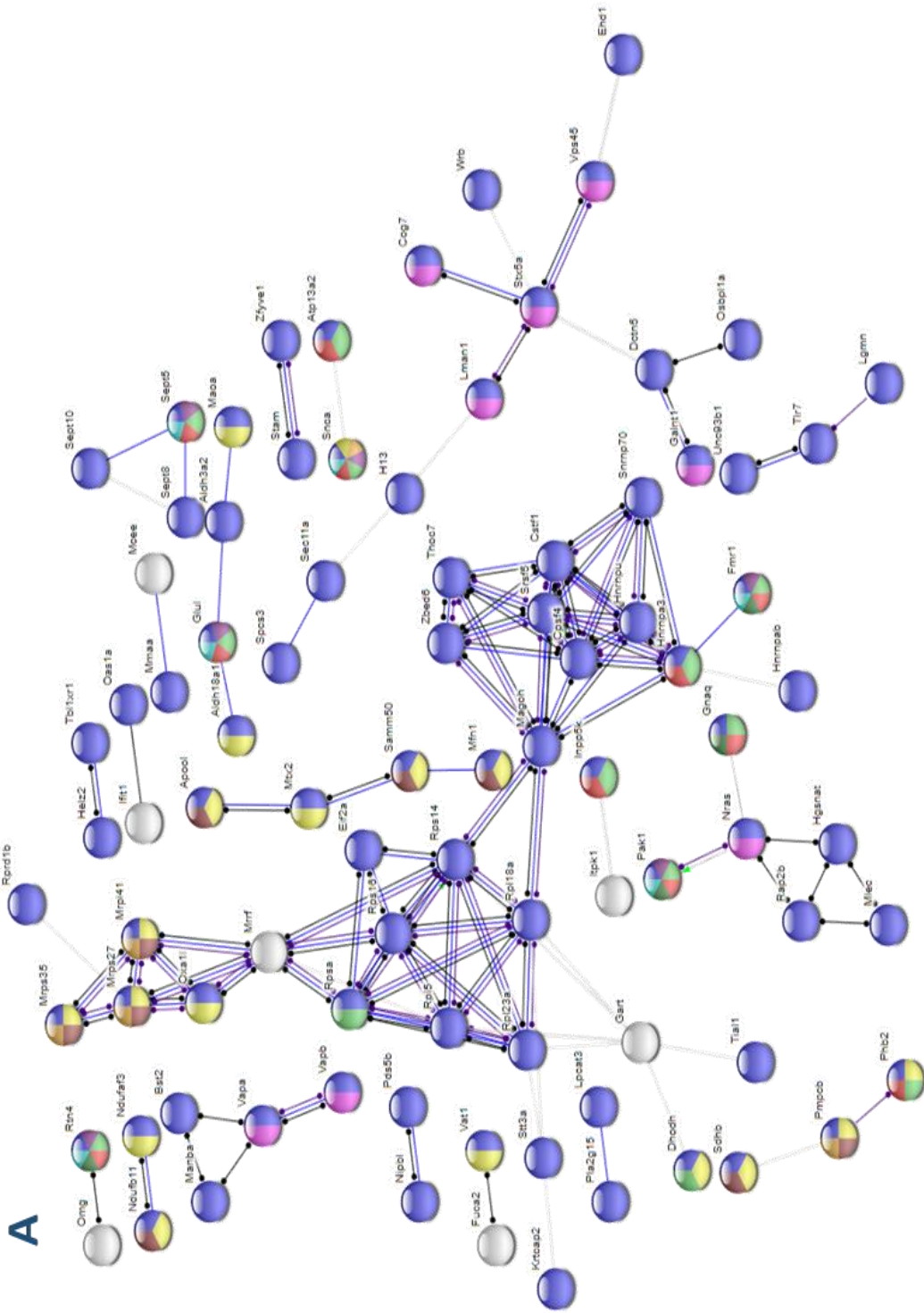














B Molecular Function (GO)			
GO-term	description	count in gene set	false discovery rate
GO:0005488	binding	128 of 10884	1.19e-08
GO:0003723	RNA binding	24 of 986	0.00014
GO:0003824	catalytic activity	60 of 5239	0.0121
GO:0003676	nucleic acid binding	38 of 2868	0.0123
GO:0016635	oxidoreductase activity, acting on the CH-CH group of donor...	2 of 4	0.0139
GO:0048039	ubiquinone binding	2 of 5	0.0183
GO:0019003	GDP binding	4 of 62	0.0240
GO:0005515	protein binding	68 of 6454	0.0331
GO:0005524	ATP binding	21 of 1389	0.0367
GO:0008017	microtubule binding	7 of 245	0.0399



**Figure 35: Representation of the cluster maps of the analysis of the protein obtained with GO respect the Molecular Function detected in 2-month-old PDGF- $\alpha$ -synuclein transgenic mice compared to WT. A)** Each point in the maps represents one protein. Each protein is coloured respect to its involvement in a specific pathway. The colour is arbitrarily defined but is the same for each protein belonging to the same pathway. The lines linking the different points express the amount of correlation/regulation among the proteins. **B)** In the corresponding table, the column on the left represents the number of pathways in the GO database. The column called "Count in the gene set" represents the number of the analysed protein respect the number of total proteins present in the database GO which are related to the specific pathway. The column called "False discovery rate" indicates the probability to have false positive in the analysis. **C)** Graph bars describe the protein expression for each cellular pathway in logarithmic scale.



**B** Cellular Component (GO)

GO:0043229	intracellular organelle	149 of 10645	1.84e-23	
GO:0044429	mitochondrial part	27 of 854	2.86e-08	
GO:0000139	Golgi membrane	16 of 537	9.18e-05	
GO:0098798	mitochondrial protein complex	11 of 255	0.00010	
GO:0005759	mitochondrial matrix	11 of 327	0.00065	
GO:0044456	synapse part	18 of 809	0.00072	
GO:0097458	neuron part	25 of 1732	0.0127	
GO:0043005	neuron projection	21 of 1429	0.0204	
GO:0030425	dendrite	12 of 694	0.0373	
GO:0033267	axon part	9 of 472	0.0468	

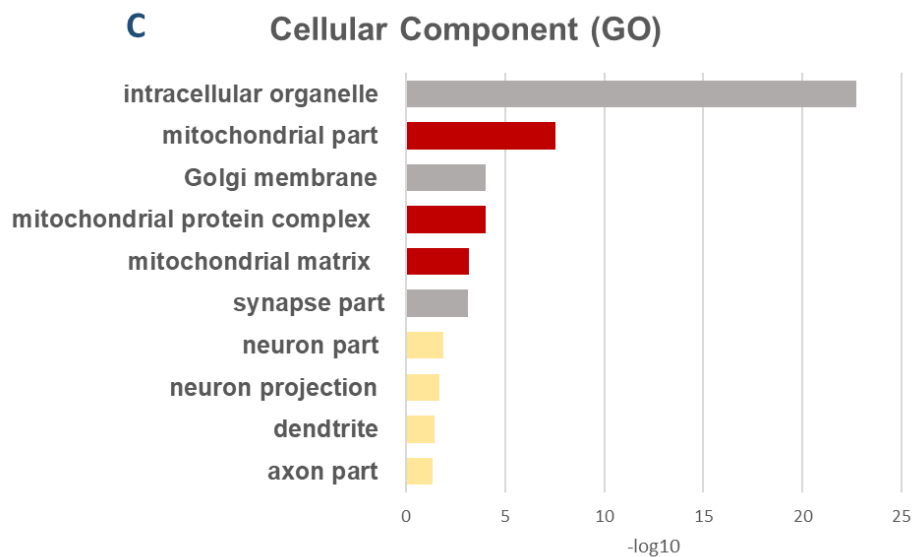
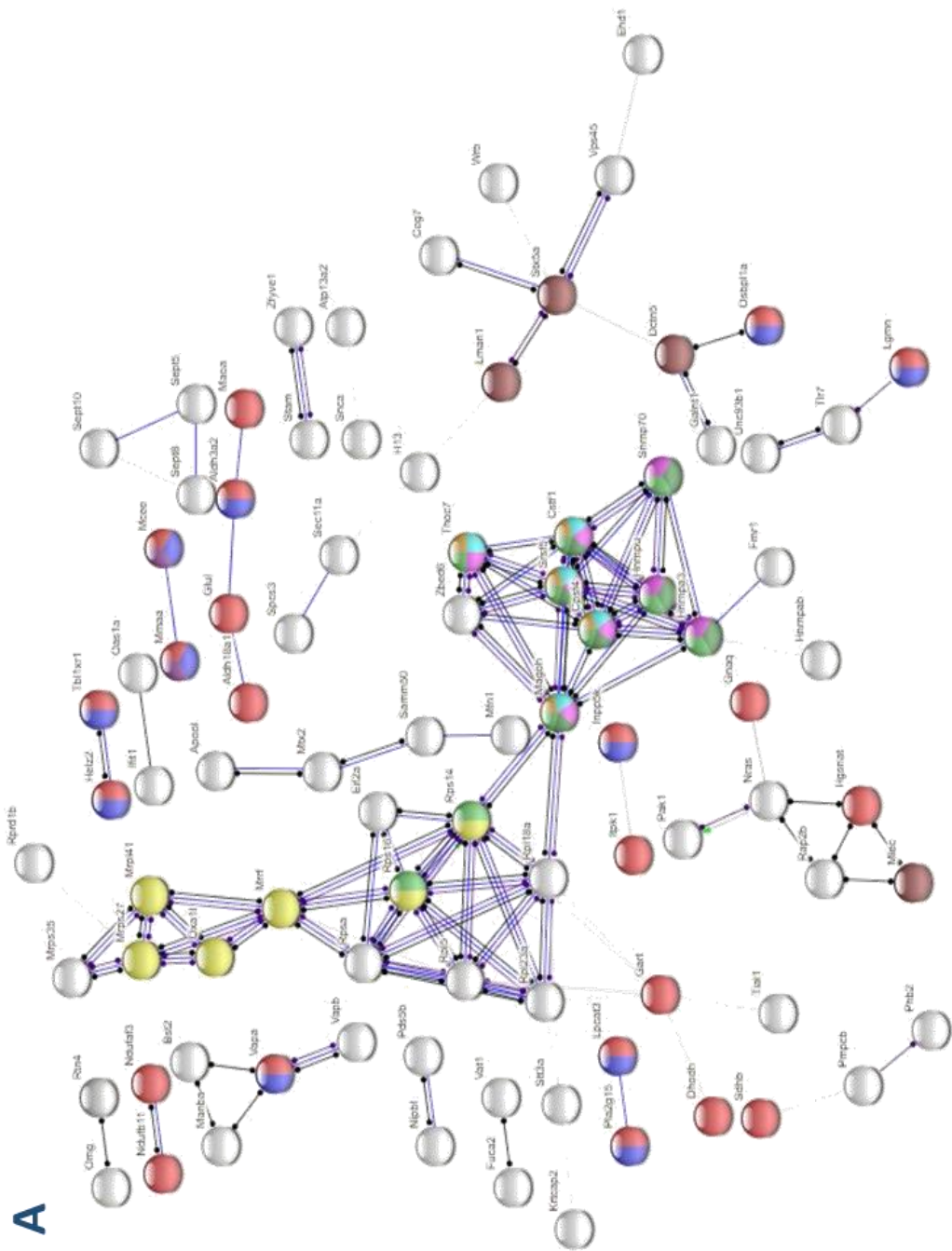


**Figure 36: Representation of the cluster maps of the analysis of the protein obtained with GO respect the Cellular Component detected in 2-month-old PDGF- $\alpha$ -synuclein transgenic mice compared to WT.** **A)** Each point in the maps represents one protein. Each protein is coloured respect to its involvement in a specific pathway. The colour is arbitrarily defined but is the same for each protein belonging to the same pathway. The lines linking the different points express the amount of correlation/regulation among the proteins. **B)** In the corresponding table, the column on the left represents the number of pathways in the GO database. The column called "Count in the gene set" represents the number of the analysed protein respect the number of total proteins present in the database GO which are related to the specific pathway. The column called "False discovery rate" indicates the probability to have false positive in the analysis. **C)** Graph bars describe the protein expression for each cellular pathway in logarithmic scale. In red are indicate the proteins correlated to the pathways of the mitochondria; in light-orange are indicated the protein correlated to the pathways of the neuronal system and in grey all the other pathways.



**B** Reactome Pathways

pathway	description	count in gene set	false discovery rate
MMU-1430728	Metabolism	34 of 1685	0.00012
MMU-556833	Metabolism of lipids	16 of 615	0.0064
MMU-72187	mRNA 3'-end processing	5 of 50	0.0084
MMU-109688	Cleavage of Growing Transcript in the Termination Region	5 of 57	0.0113
MMU-72203	Processing of Capped Intron-Containing Pre-mRNA	8 of 212	0.0180
MMU-72163	mRNA Splicing - Major Pathway	7 of 156	0.0180
MMU-8953854	Metabolism of RNA	11 of 448	0.0392
MMU-72766	Translation	6 of 148	0.0462
MMU-71032	Propionyl-CoA catabolism	2 of 5	0.0462
MMU-446203	Asparagine N-linked glycosylation	8 of 269	0.0462

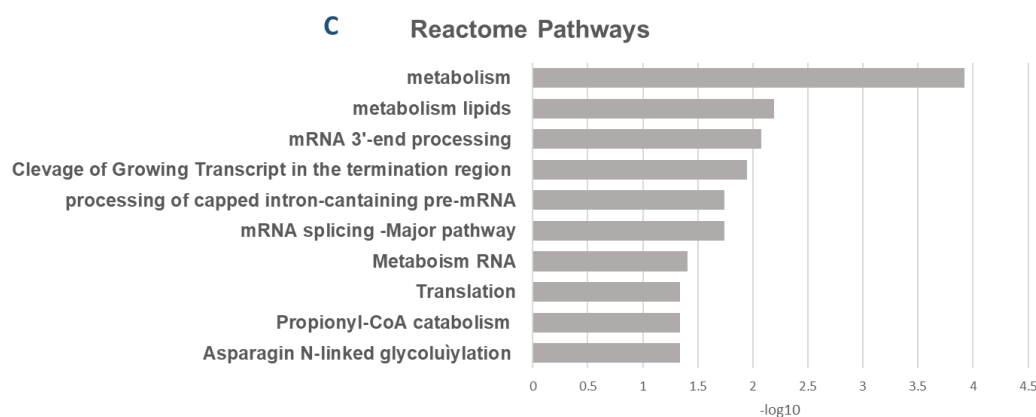
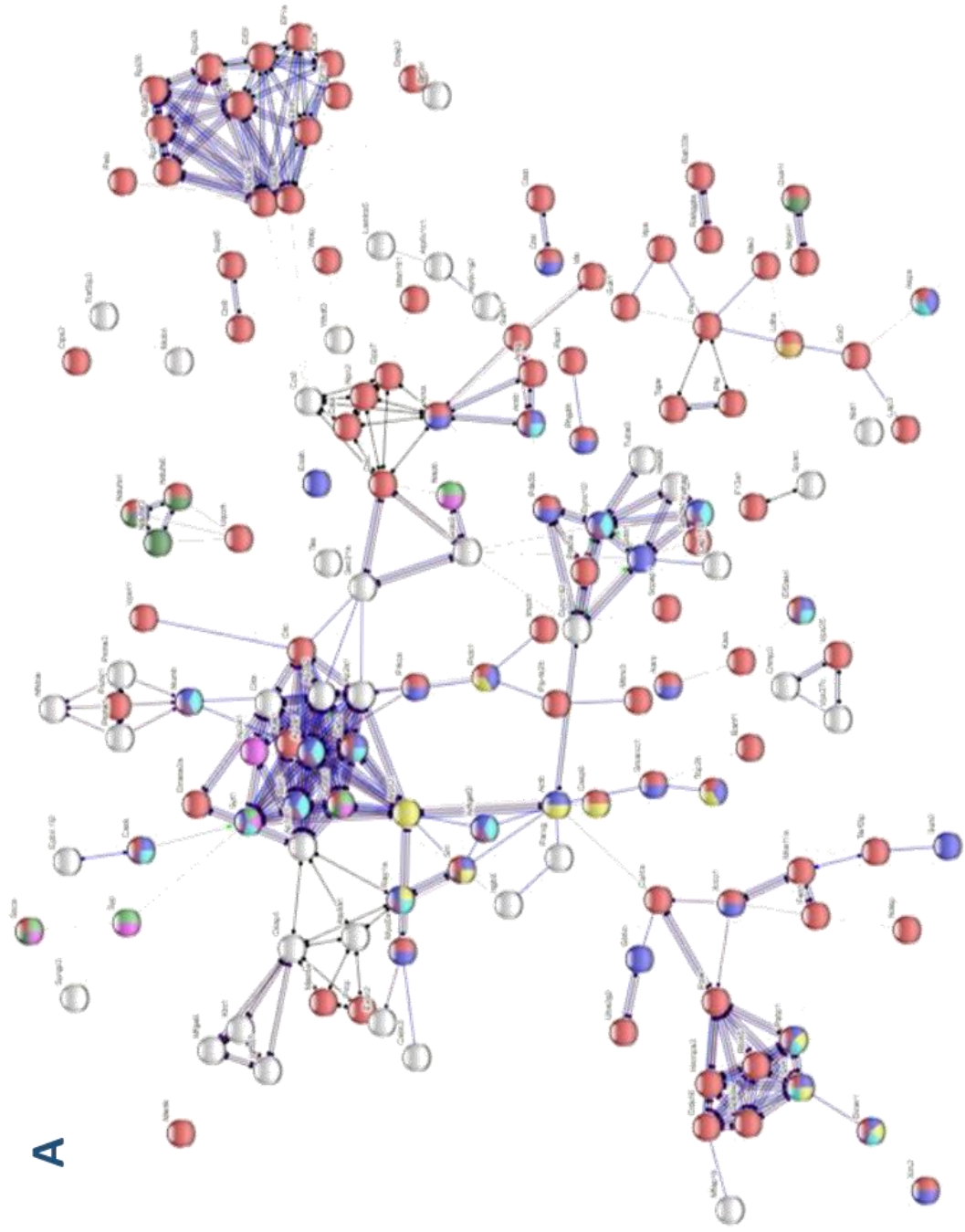


**Figure 37: Representation of the cluster maps of the analysis of the protein obtained with Reactome Pathways analysis detected in 2-month-old PDGF- $\alpha$ -synuclein transgenic mice compared to WT. A)** Each point in the maps represents one protein. Each protein is coloured respect to its involvement in a specific pathway. The colour is arbitrarily defined but is the same for each protein belonging to the same pathway. The lines linking the different points express the amount of correlation/regulation among the proteins. **B)** In the corresponding table, the column on the left represents the number of pathways in the GO database. The column called “Count in the gene set” represents the number of the analysed protein respect the number of total proteins present in the database GO which are related to the specific pathway. The column called “False discovery rate” indicates the probability to have false positive in the analysis. **C)** Graph bars describe the protein expression for each cellular pathway in logarithmic scale.



**B** Biological Process (GO)

GO-term	description	count in gene set	false discovery rate
GO:0009987	cellular process	237 of 12459	2.39e-18
GO:0008152	metabolic process	174 of 8164	3.69e-13
GO:0007399	nervous system development	55 of 2181	0.00015
GO:0048488	synaptic vesicle endocytosis	6 of 30	0.00039
GO:0071407	cellular response to organic cyclic compound	18 of 475	0.0025
GO:0099003	vesicle-mediated transport in synapse	8 of 109	0.0044
GO:0007005	mitochondrion organization	13 of 388	0.0322
GO:0050767	regulation of neurogenesis	22 of 864	0.0344
GO:0045664	regulation of neuron differentiation	19 of 714	0.0399
GO:0051900	regulation of mitochondrial depolarization	3 of 21	0.0456

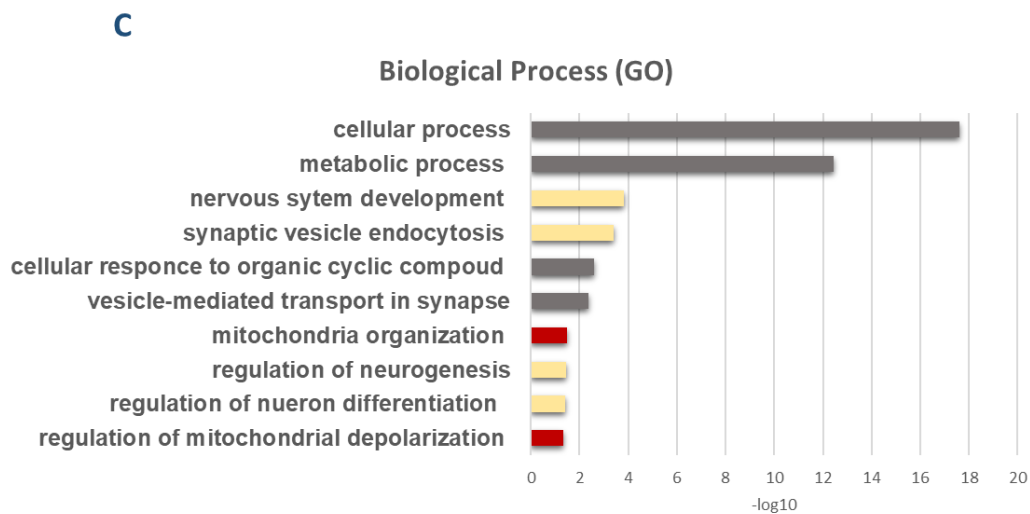
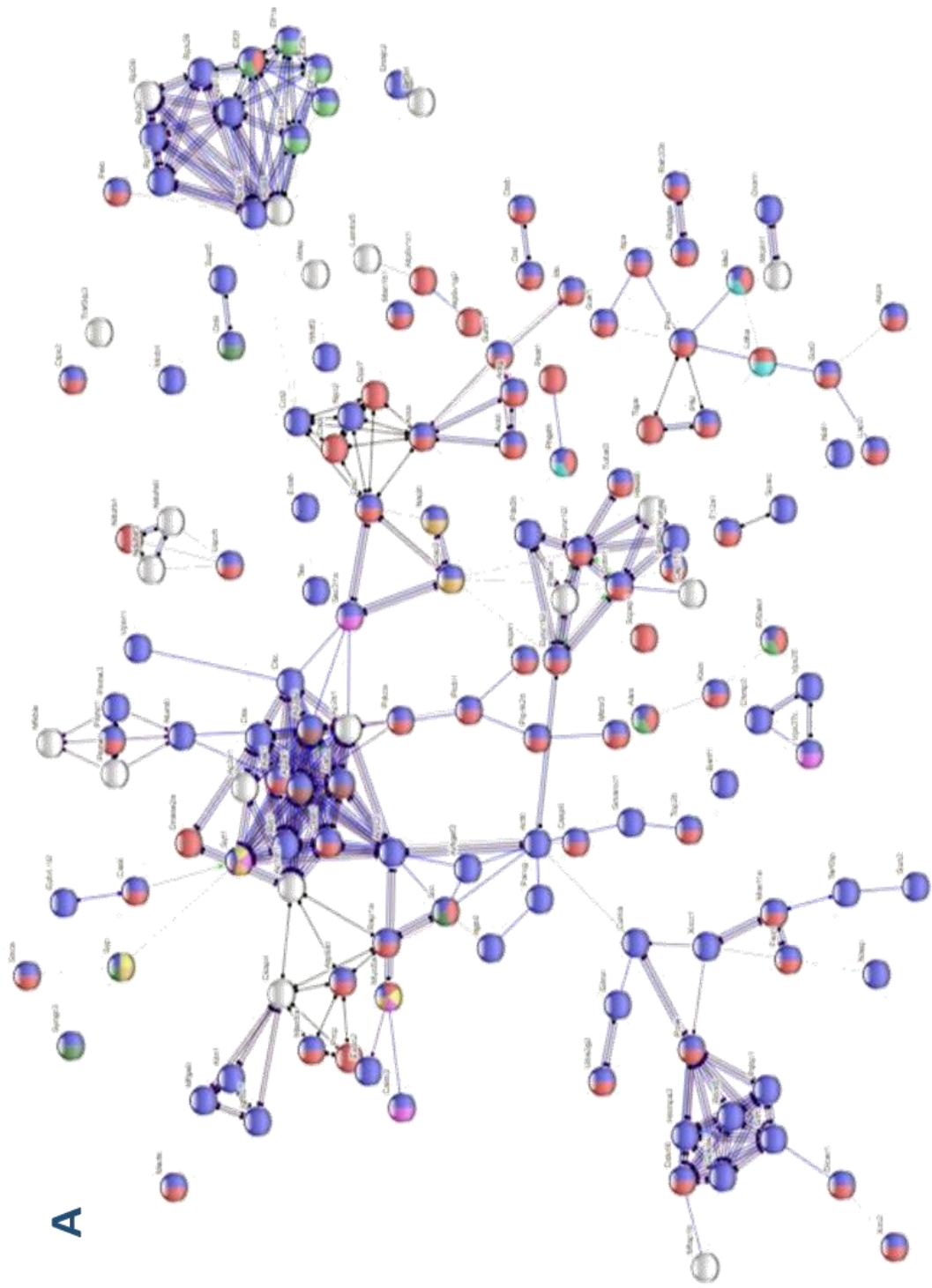


**Figure 38: Representation of the cluster maps of the analysis of the protein obtained with GO respect the Biological Process detected in 12 month-old PDGF- $\alpha$ -synuclein transgenic mice compared to WT. A) Each point in the maps represents one protein. Each protein is coloured respect to its involvement in a specific pathway. The colour is arbitrarily defined but is the same for each protein belonging to the same pathway. The lines linking the different points express the amount of correlation/regulation among the proteins. B) In the corresponding table, the column on the left represents the number of pathways in the GO database. The column called "Count in the gene set" represents the number of the analysed protein respect the number of total proteins present in the database GO which are related to the specific pathway. The column called "False discovery rate" indicates the probability to have false positive in the analysis. C) Graph bars describe the protein expression for each cellular pathway in logarithmic scale. In red are indicate the proteins correlated to the pathways of the mitochondria; in light-orange are indicated the protein correlated to the pathways of the neuronal system and in grey all the other pathways.**





A

**B** Molecular Function (GO)

GO-term	description	count in gene set	false discovery rate
GO:0005488	binding	218 of 10884	3.48e-18
GO:0003824	catalytic activity	125 of 5239	3.22e-11
GO:0045182	translation regulator activity	8 of 117	0.0044
GO:0035615	clathrin adaptor activity	3 of 9	0.0076
GO:0017075	syntaxin-1 binding	4 of 24	0.0076
GO:0048306	calcium-dependent protein binding	6 of 71	0.0077
GO:0000149	SNARE binding	7 of 125	0.0203
GO:0030348	syntaxin-3 binding	2 of 3	0.0205
GO:0042169	SH2 domain binding	4 of 38	0.0243
GO:0016616	oxidoreductase activity, acting on the CH-OH group of dono...	6 of 114	0.0446

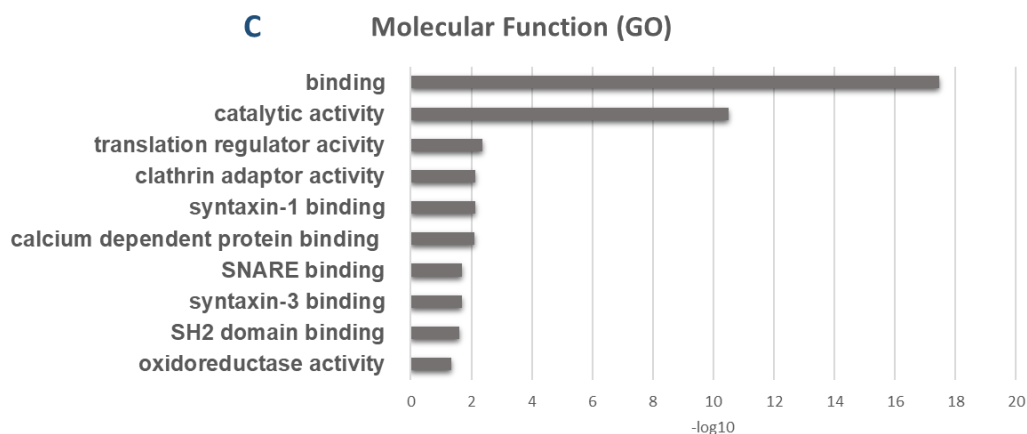
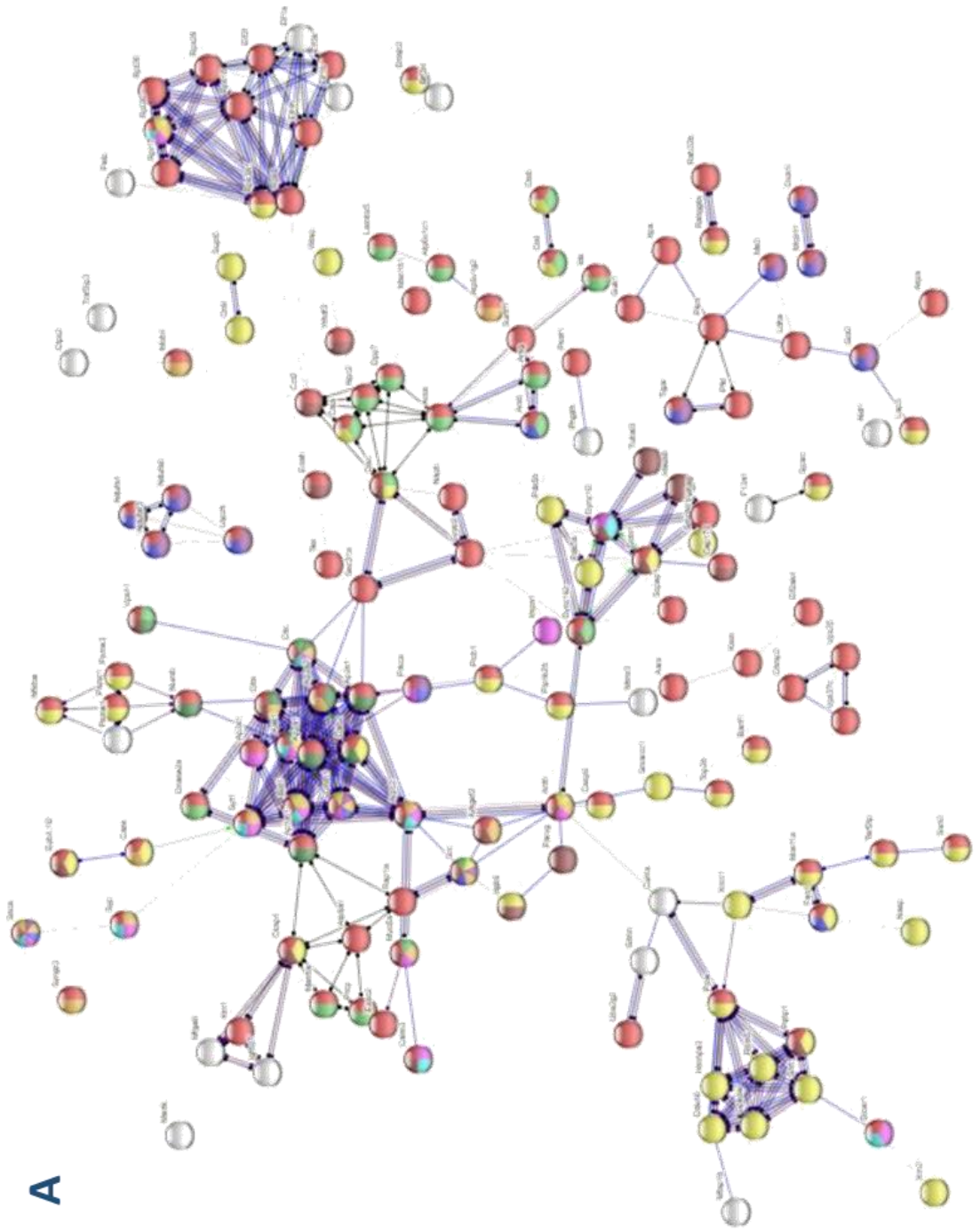


**Figure 39: Representation of the cluster maps of the analysis of the protein obtained with GO respect the Molecular Function detected in 12 month-old PDGF- $\alpha$ -synuclein transgenic mice compared to WT. A)** Each point in the maps represents one protein. Each protein is coloured respect to its involvement in a specific pathway. The colour is arbitrarily defined but is the same for each protein belonging to the same pathway. The lines linking the different points express the amount of correlation/regulation among the proteins. **B)** In the corresponding table, the column on the left represents the number of pathways in the GO database. The column called “Count in the gene set” represents the number of the analysed protein respect the number of total proteins present in the database GO which are related to the specific pathway. The column called “False discovery rate” indicates the probability to have false positive in the analysis. **C)** Graph bars describe the protein expression for each cellular pathway in logarithmic scale.



**B** Cellular Component (GO)

GO-term	description	count in gene set	false discovery rate
GO:0044444	cytoplasmic part	196 of 7673	3.47e-29
GO:0005764	lysosome	31 of 422	9.74e-13
GO:0044428	nuclear part	85 of 3798	2.35e-06
GO:0030136	clathrin-coated vesicle	10 of 113	5.58e-05
GO:0097458	neuron part	45 of 1732	8.87e-05
GO:0044429	mitochondrial part	25 of 854	0.0014
GO:0044456	synapse part	24 of 809	0.0016
GO:0005739	mitochondrion	32 of 1312	0.0038

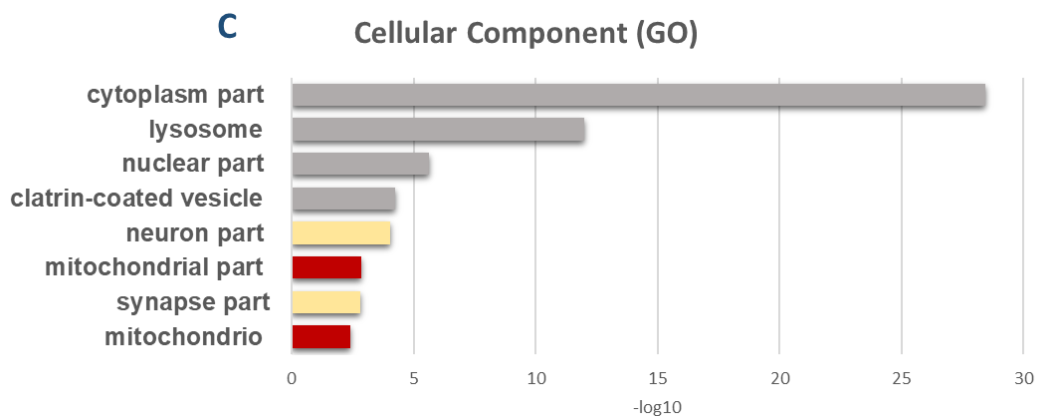
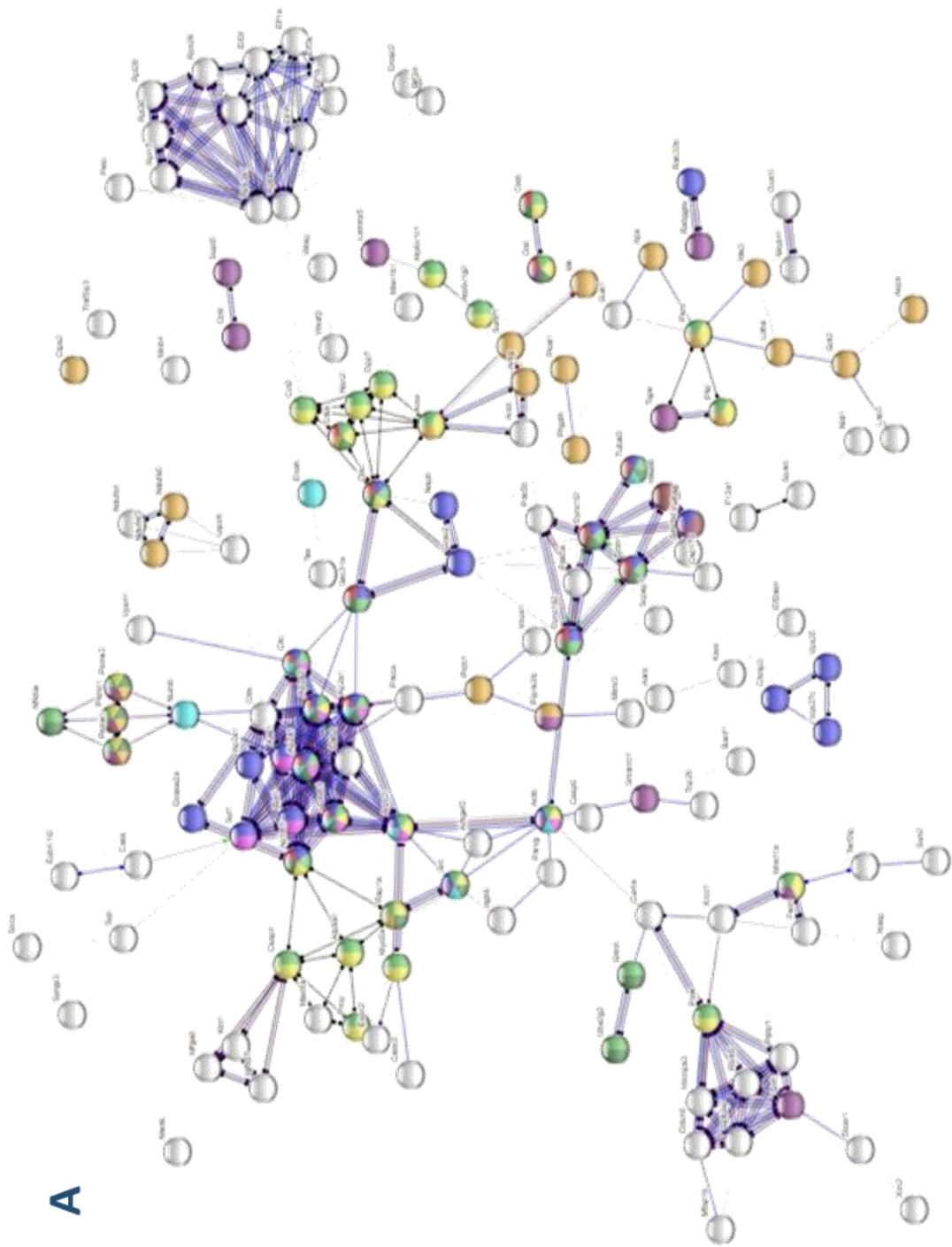


**Figure 40: Representation of the cluster maps of the analysis of the protein obtained with GO respect the Cellular Component detected in 12 month- old PDGF- $\alpha$ -synuclein transgenic mice compared to WT. A)** Each point in the maps represents one protein. Each protein is coloured respect to its involvement in a specific pathway. The colour is arbitrarily defined but is the same for each protein belonging to the same pathway. The lines linking the different points express the amount of correlation/regulation among the proteins. **B)** In the corresponding table, the column on the left represents the number of pathways in the GO database. The column called “Count in the gene set” represents the number of the analysed protein respect the number of total proteins present in the database GO which are related to the specific pathway. The column called “False discovery rate” indicates the probability to have false positive in the analysis. **C)** Graph bars describe the protein expression for each cellular pathway in logarithmic scale. In red are indicate the proteins correlated to the pathways of the mitochondria; in light-orange are indicated the protein correlated to the pathways of the neuronal system and in grey all the other pathways.



B Reactome Pathways			
pathway	description	count in gene set	false discovery rate
MMU-2132295	MHC class II antigen presentation	15 of 114	6.00e-08
MMU-199991	Membrane Trafficking	27 of 523	5.26e-07
MMU-168256	Immune System	45 of 1523	2.27e-05
MMU-168249	Innate Immune System	31 of 879	4.80e-05
MMU-8856828	Clathrin-mediated endocytosis	10 of 117	0.00034
MMU-1280218	Adaptive Immune System	24 of 652	0.00038
MMU-422475	Axon guidance	13 of 248	0.0012
MMU-1430728	Metabolism	40 of 1685	0.0044
MMU-69275	G2/M Transition	8 of 169	0.0229
MMU-74160	Gene expression (Transcription)	21 of 858	0.0399

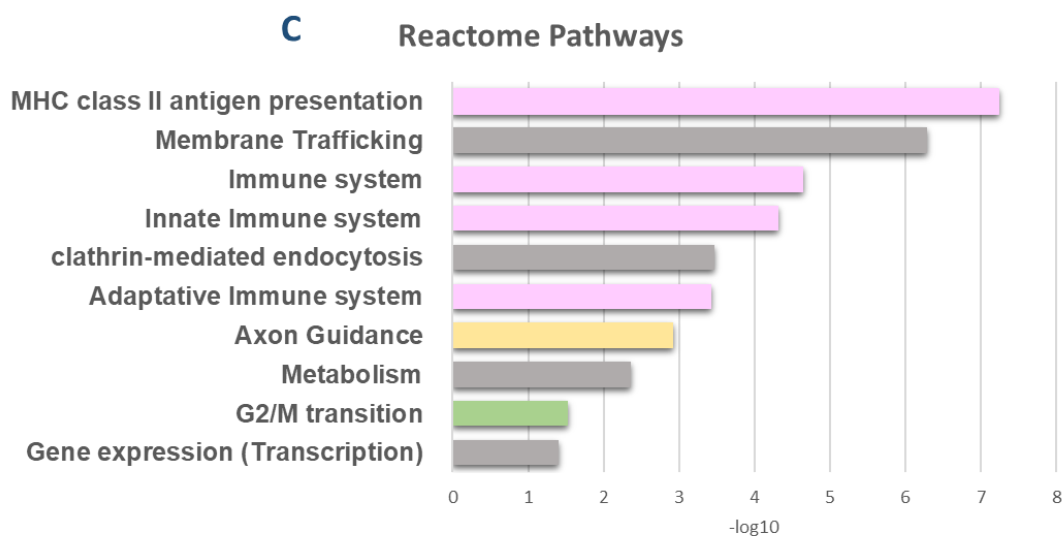


**Figure 41: Representation of the cluster maps of the analysis of the protein obtained with Reactome Pathways detected in 12 month-old PDGF- $\alpha$ -synuclein transgenic mice compared to WT. A) Each point in the maps represents one protein. Each protein is coloured respect to its involvement in a specific pathway. The colour is arbitrarily defined but is the same for each protein belonging to the same pathway. The lines linking the different points express the amount of correlation/regulation among the proteins. B) In the corresponding table, the column on the left represents the number of pathways in the GO database. The column called "Count in the gene set" represents the number of the analysed protein respect the number of total proteins present in the database GO which are related to the specific pathway. The column called "False discovery rate" indicates the probability to have false positive in the analysis. C) Graph bars describe the protein expression for each cellular pathway in logarithmic scale. In light-orange are indicated the protein correlated to the pathways of the neuronal system; in light-purple are indicate the proteins correlated to the pathways of the immune system; in green are indicated the proteins correlated to the pathways of the cell cycle and in grey all the other pathways.**

## 7. DISCUSSION

The results of the present study demonstrate that mitochondrial dysfunction occurring in mesencephalic neurons obtained from A53T transgenic mice is mainly dependent on the reduction of NCX3 expression since in striatal transgenic neurons, in which no changes of NCX3 were detected, mitochondrial function is preserved both in terms of mitochondrial membrane potential and of mitochondrial calcium concentration. This finding is in line with data previously reported by Scorziello et al. (Scorziello et al., 2013) showing that NCX3, apart its localization at plasma membrane level, is also localized on the mitochondria where it promote mitochondrial calcium efflux in physiological and pathological conditions, thus playing a pivotal role in the maintenance of intracellular Na<sup>+</sup> and Ca<sup>2+</sup> homeostasis not only in brain ischemia but also and neurodegenerative diseases (Sisalli et al., 2014; Annunziato et al., 2004; Pignataro et al., 2004; Boscia et al., 2006; Molinaro et al., 2008; Sirabella et al., 2009; Pannaccione et al., 2012). More interesting, the finding that NCX3 expression is differently regulated in dopaminergic neurons in midbrain compared to striatum let to speculate a new potential mechanism contributing to the selective neuronal degeneration in PD. Indeed, due to their pacemaker activity, mesencephalic neurons are more frequently exposed to continue calcium transients that make them more prone to mitochondrial calcium overload and consequently to mitochondrial dysfunction (Chan et al., 2009; Surmier, 2010, 2011; Dryanovski et al., 2013). In this scenario, the impairment in the expression and activity of NCX3 in mesencephalic neurons might contribute to the selective vulnerability of these cells in the midbrain of A53T transgenic mice, due to its contribution to the perturbation of intracellular Ca<sup>2+</sup> concentration, as already hypothesized by Sirabella et al. (Sirabella et al.,

2018). The experiments performed in vivo in A53T transgenic mice further confirm that NCX3-dependent mitochondrial dysfunction occurring in mesencephalic neurons might be related to neuronal damage and PD progression. Indeed, an increase in Cyt-c and nNOS expression, both markers of mitochondrial damage and oxidative stress respectively, are already detected in the midbrain of 4 months old transgenic mice and continues to remain elevated in the late stage of the disease. Conversely, in the striatum of A53T mice, in which NCX3 expression does not change compared to WT, an increase of the two proteins expression occurs only in the late stage of the disease. Moreover, mitochondrial dysfunction in midbrain of adult transgenic mice is further confirmed by the finding that a reduction in the expression levels of MnSOD is detected in the midbrain of adult transgenic mice compared to WT, thus suggesting that a progressive impairment of the antioxidant metabolism might be claimed as pathogenic mechanism leading to dopaminergic neuronal damage occurring in PD progression. This is in line with the recent data described in the literature linking mitochondrial dysfunction to the triggering of the neuroinflammatory process in PD since, damaged mitochondria are able to release numerous pro-inflammatory factors (Hirsch et al., 2012; Tansey et al., 2010). Furthermore, that mitochondrial dysfunction has a detrimental role in PD progression is also supported by the data described in the present study, showing an increase of IBA-1, IL-1 $\beta$  and iNOS in the striatum of 16 months old A53T  $\alpha$ -synuclein transgenic mice in which an increase of Cyt-c and nNOS occurs. Moreover, the activation of microglial cells in the striatum of aged transgenic mice is associated with an increase of GFAP thus confirming a relationship between mitochondrial-induced neuroinflammation and glial activation (Thakur et al., 2015; Noh et al., 2014; Park et al., 2013; Ferger et al., 2010). Conversely, in the midbrain of 16 months old A53T  $\alpha$ -synuclein transgenic mice, the increase in Cyt-c and



nNOS protein expression is accompanied to glial proliferation as confirmed by the increase of GFAP protein levels without microglial activation. These findings, in accordance with data previously reported in 12-month-old A53T  $\alpha$ -synuclein transgenic mice (Sirabella et al., 2018), further support the hypothesis that glial cells activation might contribute to neuronal dysfunction responsible for PD progression. However, these results also suggest that the molecular mechanisms involved in the activation of microglial cells are different from those occurring in astrocytes. In fact, it is possible to hypothesize that the impairment in mitochondrial membrane permeability observed in midbrain since the early stages of the disease, and mainly related to NCX3 reduced expression and activity, can lead to neuronal damage. This causes the consequent release of neuronal toxic factors able to induce the activation of microglial cells in the striatum of A53T  $\alpha$ -synuclein transgenic adult mice. Once activated, microglial cells can release proinflammatory cytokines in adult mice that in turn promote astroglial proliferation in the striatum and in the midbrain as confirmed by the increase in NCX1 protein expression in these brain areas. Interestingly, in astrocytes obtained from A53T transgenic mice mitochondria are hyperpolarized and contain lower calcium concentration compared to WT cells. These findings let to hypothesize that the overexpression of NCX1 in transgenic astrocytes by maintaining  $[Ca^{2+}]_i$  within physiological range preserves mitochondrial function and promotes gliosis in adult mice. This is in line with data previously reported in the ischemic brain (Boscia et al., 2009) and might explain the consequent increase in dopaminergic neuronal injury observed in the midbrain of transgenic aged mice (Fig. 42).

The results obtained with mass spectrometry further support the hypothesis that mitochondrial dysfunction could play a role in the pathogenesis of neuroinflammation and neurodegeneration occurring in

PD progression. In fact, the proteomic profile obtained from whole brain of 2- and 12-month-old PDGF- $\alpha$ -synuclein mice demonstrate a trend in the impairment for proteins involved in the regulation of mitochondrial dynamics and function which mainly occurs in the early stage of the disease, as well as for proteins involved in neuronal transmission and synaptic activity in the late phase of the disease. These findings are in line with data described by Herms' group who demonstrated that the decrease in spine density and the abnormalities in spine dynamics observed in 3 months old PDGF  $\alpha$ -synuclein mice occurs in an age-dependent manner (Blumenstock et al., 2017). On the other hand, the development and morphological plasticity of spines are strictly dependent on the presence of healthy mitochondria into dendritic protrusions (Li et al., 2004; Todorova et al., 2017; Lee et al., 2018). Therefore, an impairment of dendritic mitochondria content or their dysfunction might lead to dendritic spines degeneration and synaptic loss, thus confirming that the dendritic distribution of mitochondria is essential and limiting for the support of synapses. Moreover, it is worth to underline that synaptic activity contributes to the regulation of mitochondrial function and controls mitochondrial distribution in dendrites and also, that the microglial cells play a central role in the regulation of the synaptic plasticity (Lin et al., 2019; Ronzano 2017; Yamamoto et al., 2019). As a consequence, an alteration in the structural, physiological and metabolic aspects of the mitochondrial function might hesitate into mitochondrial dysfunctions and subsequently in cellular damage occurring in neurodegenerative disorders. Another interesting aspect emerging from this proteomic study is the observation that NCX1 is down-regulated in microglia of 2 month-old PDGF- $\alpha$ -synuclein mice. This is in line with the hypothesis that NCX1 is linked to the proliferative stage of the glial cells only in late stage of the disease progression and with the findings related to the proteomic profile

described in transgenic adult mice in which only a few proteins correlated to the cell cycle are detected and, the most of them, down-regulated. However, it is worth to note that no changes in the expression profile of inflammation-related proteins have been observed in this model.

In conclusion, the results reported in the present study demonstrate that mitochondrial dysfunction described in mesencephalic neurons of A53T  $\alpha$ -synuclein transgenic mice at the early stage of the disease, promotes neuronal degeneration and activates neuroinflammation in the striatum of these mice with consequent glial activation and progressive impairment of dopaminergic neuronal plasticity in the late stage of the disease.

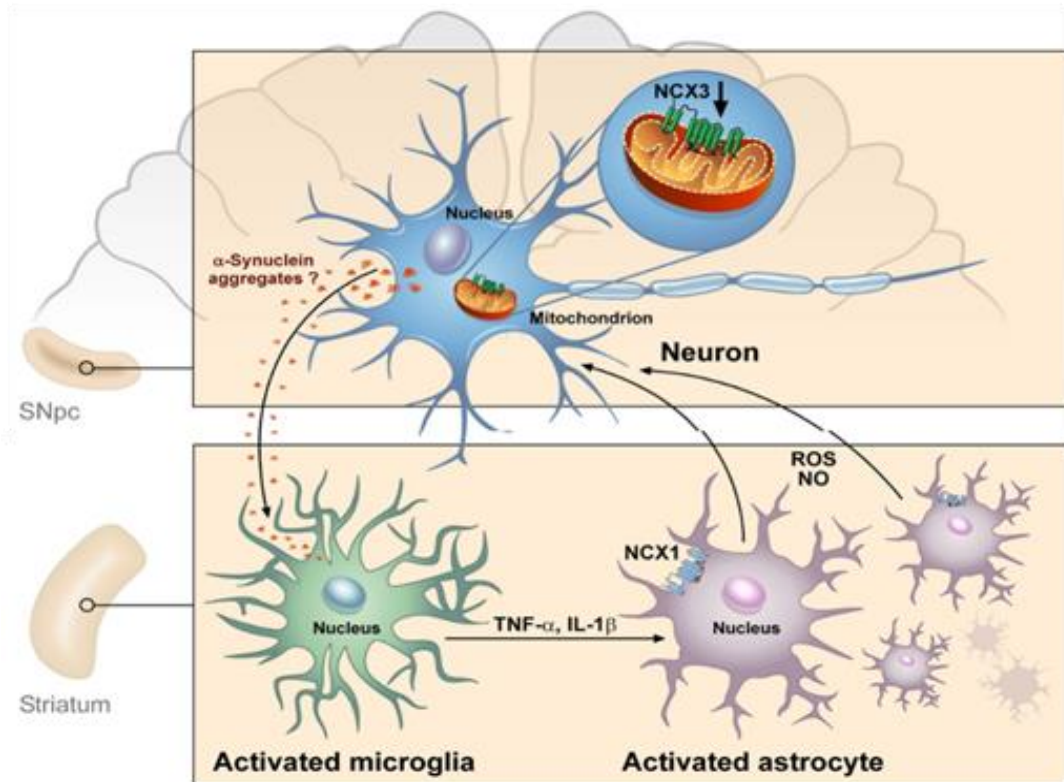


**Figure 42: Proposed Model to explain the cellular and molecular events leading to neuroinflammation in A53T  $\alpha$ -synuclein transgenic mice as a model of PD.** The reduction of NCX3 expression in dopaminergic neurons of A53T mice causes mitochondrial dysfunction and neuronal damage with the consequent release of toxic factors which activate the microglial cells in the striatum. This phenomenon might promote the release of proinflammatory cytokines that in turn activates astrocytes proliferation. The increase NCX1 expression in astrocytes preserves the mitochondrial function and promote glial proliferation which, invading the midbrain, contributes to induce DA neuronal death

## **BIBLIOGRAPHY**

Abeliovich A, Schmitz Y, Fariñas I, Choi-Lundberg D, Ho WH, Castillo PE, Shinsky N, Verdugo JM, Armanini M, Ryan A, Hynes M, Phillips H, Sulzer D, Rosenthal A. Mice lacking alpha-synuclein display functional deficits in the nigrostriatal dopamine system. *Neuron* 2000; 25: 239–52.

Abunit A, Bousset L, Loria F, Zhu S, de Chaumont F, Pieri L, Olivo-Marin JC, R Melki R, Zurzolo C. Tunneling nanotubes spread fibrillar a-synuclein by intercellular trafficking of lysosomes. *The EMBO Journal*; 2016; 35: 19

Ahn M, Kim S, Kang M, Ryu Y, Kim TD. Chaperone-like activities of alpha-synuclein: Alpha-synuclein assists enzyme activities of esterases. *Biochem. Biophys. Res. Commun.* 2006; 346: 1142–1149

Alberio T, Bondi H, Colombo F, Alloggio I, Pieroni L, Urbani A, Fasano M. Mitochondrial proteomics investigation of a cellular model of impaired dopamine homeostasis, an early step in Parkinson's disease pathogenesis. *Mol Biosyst.* 2014;10(6):1332-44.

Alvarez-Erviti L, Seow Y, Schapira AH, Gardiner C, Sargent IL, Wood MJ, Cooper JM. Lysosomal dysfunction increases exosome-mediated alpha-synuclein release and transmission. *Neurobiol Dis.* 2011; 42:360–367

Andres-Mateos E, Perier C, Zhang L, Blanchard-Fillion B, Greco TM, Thomas B, Ko HS, Sasaki M, Ischiropoulos H, Przedborski S, Dawson TM, Dawson VL. DJ-1 gene deletion reveals that DJ-1 is an atypical peroxiredoxin-like peroxidase. *Proc Natl Acad Sci USA.* 2007; 104:14807–14812.

Angelova PR, Abramov AY. Functional role of mitochondrial reactive oxygen species in physiology. *Free Radic. Biol. Med.* 2016; S0891-5849(16): 30293-3.

Angot E, Brundin P. Dissecting the potential molecular mechanisms underlying  $\alpha$ -synuclein cell-to-cell transfer in Parkinson's disease. *Parkinsonism Relat. Disord.* 2009; 15, S143–S147.

Annunziato L, Boscia F, Pignataro G. Ionic transporter activity in astrocytes, microglia, and oligodendrocytes during brain ischemia. *J Cereb Blood Flow Metab* 2013; 33:969–982.

Annunziato L, Cataldi M, Pignataro G, Secondo A, and Molinaro P. Glutamate-independent calcium toxicity: introduction. *Stroke*. 2007; 38 (Suppl 2):661–664.

Annunziato L, Pannaccione A, Cataldi M, Secondo A, Castaldo P, Di Renzo G, and Tagliatela M. Modulation of ion channels by reactive oxygen and nitrogen species: a pathophysiological role in brain aging? *Neurobiol Aging* 2002; 23:819–834.

Annunziato L, Pignataro G, and Di Renzo GF. Pharmacology of brain Na<sup>+</sup>/Ca<sup>2+</sup> exchanger: from molecular biology to therapeutic perspectives. *Pharmacol Rev.* 2004; 56:633–654.

Appel-Cresswell S, Vilarino- Guell C, Encarnacion M, Sherman H, Yu I, Shah B, Weir D, Thompson C, Szu-Tu C, Trinh J, Aasly JO, Rajput A, Rajput AH, Jon Stoessl A, Farrer MJ. Alpha-synuclein p. H50Q, a novel pathogenic mutation for Parkinson's disease. *Movement Dis.* 2013; 28:811–813

Araque A, Parpura V, Sanzgiri RP, Haydon PG. Tripartite synapses: glia, the unacknowledged partner. *Trends Neurosci.* 1999; 22:208–15.

Auluck PK, Caraveo G, and Lindquist S. alpha-Synuclein: membrane interactions and toxicity in Parkinson's disease. *Annu. Rev. CellDev. Biol.* 2010; 26, 211–233.

Austin SA, Floden AM, Murphy EJ, Combs CK. Alpha-synuclein expression modulates microglial activation phenotype. *J Neurosci*, 2006; 26, (41): 10558-10563

Bandopadhyay R, Kingsbury AE, Cookson MR, Reid AR, Evans IM, Hope AD, Pittman AM, Lashley T, Canet-Aviles R, Miller DW, McLendon C, Strand C, Leonard AJ, Abou- Sleiman PM, Healy DG, Ariga H, Wood NW, de Silva R, Revesz T, Hardy JA, Lees AJ. The expression of DJ-1 (PARK7) in normal human CNS and idiopathic Parkinson's disease. *Brain*. 2004; 127(Pt 2):420–430.

Banerjee R, Starkov AA, Beal MF, Thomas B. Mitochondrial dysfunction in the limelight of Parkinson's disease pathogenesis. *Biochim Biophys Acta* 2009; 1792(7):651-63.

Bano D, Young KW, Guerin CJ, Lefevre R, Rothwell NJ, Naldini L, Rizzuto R, Carafoli E, Nicotera P. Cleavage of the plasma membrane Na<sup>+</sup> /Ca<sup>2+</sup> exchanger in excitotoxicity. *Cell*. 2005; 120, 275–285.

Barkholt P, Sanchez-Guajardo V, Kirik D, Romero-Ramos M. Long-term polarization of microglia upon alpha-synuclein overexpression in nonhuman primates. *Neuroscience*. 2012; 19,208:85-96

Bartels AL, Willemsen AT, Doorduyn J, de Vries EF, Dierckx RA, Leenders KL (2010) [11C]-PK11195 PET: quantification of neuroinflammation and a monitor of anti-inflammatory treatment in Parkinson's disease? *Parkinsonism Relat Disord*. 20120; 16:57–59

Bean B. The action potential in mammalian central neurons. *Nat Rev Neurosci*. 2007; 8:451–465

Bellucci A, Collo G, Sarnico I, Battistin L, Missale C, Spano P. Alpha-synuclein aggregation and cell death triggered by energy deprivation and dopamine overload are counteracted by D2/D3receptor activation. *J. Neurochem*. 2008; 106: 560–577

Bellucci A, Navarria L, Falarti E, Zaltieri M, Bono F, Collo G, Spillantini MG, Missale C, Spano P. Redistribution of DAT/alpha-synuclein complexes visualized by "in situ" proximity ligation assay in transgenic mice modelling early Parkinson's disease. *PLoS ONE* 2011; 6, e27959.

Benner EJ1, Mosley RL, Destache CJ, Lewis TB, Jackson-Lewis V, Gorantla S, Nemachek C, Green SR, Przedborski S, Gendelman HE. Therapeutic immunization protects dopaminergic neurons in a mouse model of Parkinson's disease. *Proc Natl Acad Sci U S A*. 2004; 101:9435–9440.

Berberián G, Forcato D, Beaugé L. Key role of PTDIns-4,5P2 microdomain in ionic regulation of the mammalian heart Na/Ca exchanger. *Cell Calcium*. 2009; 45, 546–553.

Berg D, Schweitzer KJ, Leitner P, Zimprich A, Lichtner P, Belcredi P, Brussel T, Schulte C, Maass S, Nagele T, Wszolek ZK, Gasser T. Type and frequency of mutations in the LRRK2 gene in familial and sporadic Parkinson's disease. *Brain*. 2005; 128(Pt 12):3000–3011

Bers D, Despa S. Na<sup>+</sup>/K<sup>+</sup>-ATPase, an integral player in the adrenergic fight-or-flight response. *Trends Cardiovasc Med*. 2009; 19:111–118.

Bertler A, Rosengren E. On the distribution in the brain of monoamines and of enzymes responsible for their formation. *Experientia*. 1959; 15:382–384.

Bertoncini CW, Fernandez CO, Griesinger C, Jovin TM, Zweckstetter M. Familial mutants of alpha-synuclein with increased neurotoxicity have a destabilized conformation. *J. Biol. Chem.* 2005; 280: 30649–30652.

Birkmayer W, Hornykiewicz O. The L-3,4-dioxyphenylalanine (DOPA)-effect in Parkinson-akinesia. *Wien Klin Wochenschr.* 1961; 73:787–788.

Blackinton J, Kumaran R, van der Brug MP, Ahmad R, Olson L, Galter D, Lees A, Bandopadhyay R, Cookson MR. Post-transcriptional regulation of mRNA associated with DJ-1 in sporadic Parkinson disease. *Neurosci Lett.* 2009; 452:8–11.

Blandini F. Neural and immune mechanisms in the pathogenesis of Parkinson's disease. *J Neuroimmune Pharmacol.* 2013; 8:189–201.

Blaustein MP, Lederer WJ. Sodium/calcium exchange: its physiological implications. *Physiol. Rev.* 1999; 79: 763–854.

Blumenstock S, Rodrigues EF, Peters F, Blazquez-Llorca L, Schmidt F, Giese A, Herms J. Seeding and transgenic overexpression of alpha-synuclein triggers dendritic spine pathology in the neocortex. *EMBO Mol Med.* 2017;9(5):716-731.

Bolender N, Sickmann A, Wagner R, Meisinger C, Pfanner N. Multiple pathways for sorting mitochondrial precursor proteins. *EMBO Rep.* 2008; 9: 42–49.

Bonifati V, Rizzu P, van Baren MJ, Schaap O, Breedveld GJ, Krieger E, Dekker MC, Squitieri F, Ibanez P, Joosse M, van Dongen JW, Vanacore N, van Swieten JC, Brice A, Meco G, van Duijn CM, Oostra BA, Heutink P. Mutations in the DJ-1 gene associated with autosomal recessive early-onset parkinsonism. *Science.* 2003; 299:256–259.

Boscia F, Gala R, Pannaccione A, Secondo A, Scorziello A, Di Renzo G, Annunziato L. NCX1 expression and functional activity increase in microglia invading the infarct core. *Stroke* 2009; 40:3608–3617.

Boscia F, Gala R, Pignataro G, de Bartolomeis A, Cicale M, Ambesi-Impiombato A, Di Renzo G, Annunziato L. Permanent focal brain ischemia induces isoform-dependent changes in the pattern of Na<sup>+</sup>/Ca<sup>2+</sup> exchanger gene expression in the



ischemic core, peri-infarct area, and intact brain regions. *J. Cereb. Blood Flow Metab.* 2006; 26: 502-517

Boyman L, Hagen BM, Giladi M, Hiller R, Lederer WJ, Khananshvili D. Proton sensing  $\text{Ca}^{2+}$  binding domains regulate the cardiac  $\text{Na}^+/\text{Ca}^{2+}$  exchanger. *J Biol Chem.* 2011; 286:28811–28820.

Braak H, Bohl JR, Muller CM, Rub U, de Vos RA, Del Tredici K. Stanley Fahn Lecture 2005: The staging procedure for the inclusion body pathology associated with sporadic Parkinson's disease reconsidered. *Mov Disord.* 2006; 21:2042–2051.

Braak H, Braak E. Pathoanatomy of Parkinson's disease. *J Neurol.* 2000; 247 (Suppl 2): II3–II10.

Braak H, Del Tredici K. Invited article: nervous system pathology in sporadic Parkinson disease. *Neurology.* 2008; 70:1916–1925

Braak H, Del Tredici K, Bratzke H, Hamm-Clement J, Sandmann-Keil D, Rub U. Staging of the intracerebral inclusion body pathology associated with idiopathic Parkinson's disease (preclinical and clinical stages). *J Neurol.* 2002; 249 (Suppl 3): III/1–III/5.

Braak H, Del Tredici K, Rub U, de Vos RA, Jansen Steur EN, Braak E. Staging of brain pathology related to sporadic Parkinson's disease. *Neurobiol. Ageing.* 2003; 24:197–211

Braak H, Ghebremedhin E, Rub U, Bratzke H, Del Tredici K. Stages in the development of Parkinson's disease-related pathology. *Cell Tissue Res.* 2004; 318:121–134.

Braak H, Sastre M, Del Tredici K. Development of alpha-synuclein immunoreactive astrocytes in the forebrain parallel stages of intraneuronal pathology in sporadic Parkinson's disease. *Acta Neuropathol.* 2007; 114, (3): 231-241

Breukels V, Touw WG, Vuister GW. Structural and dynamic aspects of  $\text{Ca}^{2+}$  and  $\text{Mg}^{2+}$  binding of the regulatory domains of the  $\text{Na}^+/\text{Ca}^{2+}$  exchanger. *Biochem Soc Trans.* 2012; 40:409–414.

Brough D, Le Feuvre RA, Wheeler RD, Solovyova N, Hilfiker S, Rothwell NJ, Verkhratsky A. Ca<sup>2+</sup> stores and Ca<sup>2+</sup> entry differentially contribute to the release of IL-1 beta and IL-1 alpha from murine macrophages. *Journal of immunology*. 2003; 170(6):3029–36.

Buddhala C, Loftin SK, Kuley BM, Cairns NJ, Campbell MC, Perlmutter JS, Kotzbauer PT. Dopaminergic, serotonergic, and noradrenergic deficits in Parkinson disease. *Ann. Clin. Transl. Neurol*. 2015; 2: 949–959

Bueler H. Impaired mitochondrial dynamics and function in the pathogenesis of Parkinson's disease. *Exp. Neurol*. 2009; 218: 235–246.

Burch D, Sheerin F. (2005) Parkinson's disease. *Lancet*. 2005; 365 (9459):622-7.

Burre J, Sharma M, Tsetsenis T, Buchman V, Etherton MR, Sudhof TC.  $\alpha$ -Synuclein promotes SNARE-complex assembly in vivo and in vitro. *Science*. 2010; 329: 1663–67.

Burre J, Sharma M, Sudhof TC. Cell Biology and Pathophysiology of alpha-Synuclein. *Cold Spring Harb. Perspect. Med*. 2018; 1: 8(3)

Bussell R Jr, Ramlall TF, Eliezer D. Helix periodicity, topology, and dynamics of membrane-associated alpha-synuclein. *Protein Sci*. 2005; 14:862–872.

Butler B, Saha K, Rana T, Becker JP, Sambo D, Davari P, Goodwin JS, Khoshbouei H. Dopamine Transporter Activity Is Modulated by alpha-Synuclein. *J. Biol. Chem*. 2015; 290: 29542–29554.

Büttner S, Faes L, Reichelt WN, Broeskamp F, Habernig L, Benke S, Kourtis N, Ruli D, Carmona-Gutierrez D, Eisenberg T, D'hooge P, Ghillebert R, Franssens V, Harger A, Pieber TR, Freudenberger P, Kroemer G, Sigrist SJ, Winderickx J, Callewaert G, Tavernarakis N, Madeo F. The Ca<sup>2+</sup>/Mn<sup>2+</sup> ion-pump PMR1 links elevation of cytosolic Ca (2+) levels to  $\alpha$ -synuclein toxicity in Parkinson's disease models. *Cell Death Differ*. 2013;20(3):465-77.

Cabin DE, Gispert-Sanchez S, Murphy D, Auburger G, Myers RR, Nussbaum RL. Exacerbated synucleinopathy in mice expressing A53T SNCA on a Snca null background. *Neurobiol Aging*. 2005;26(1):25-35.

Caggiu E, Arru G, Hosseini S, Niegowska M, Sechi G, Zarbo IR, Sechi LA. Inflammation, Infectious Triggers, and Parkinson's Disease. *Front Neurol.* 2019 19;10:122.

Calì T, Ottolini D, Brini M. Calcium and endoplasmic reticulum mitochondria tethering in neurodegeneration *Cell Biol* 2013; 32: 140–146

Calì T, Ottolini D, Brini M. Mitochondrial Ca<sup>2+</sup> and neurodegeneration. *Cell Calcium* 2012; 52:73–85

Calì T, Ottolini D, Brini M. Mitochondria, calcium, and endoplasmic reticulum stress in Parkinson's disease. *Biofactors* 2011; 37:228–240

Calì T, Ottolini D, Negro A, Brini M.  $\alpha$ Synuclein controls mitochondrial calcium homeostasis by enhancing endoplasmic reticulum-mitochondria interactions. *J Biol Chem.* 2012; 287(22):17914-29.

Calì T, Ottolini D, Brini M. Calcium signaling in Parkinson's disease. *Cell Tissue Res.* 2014 ;357(2):439-54.

Calo L, Wegrzynowicz M, Santivañez-Perez J, and Spillantini G.M. Synaptic failure and a-synuclein. *Mov. Disord.* 2016; 3: 169–177.

Canitano A, Papa M, Boscia F, Castaldo P, Sellitti S, et al. Brain distribution of the Na (+)/Ca (2+) exchanger-encoding genes NCX1, NCX2, and NCX3 and their related proteins in the central nervous system. *Ann N Y Acad Sci.* 2002; 976:394–404.

Cannon JR, Geghman KD, Tapias V, Sew T, Dail MK, Li C, Greenamyre JT. Expression of human E46K-mutated  $\alpha$ -synuclein in BAC-transgenic rats replicates early-stage Parkinson's disease features and enhances vulnerability to mitochondrial impairment. *Exp. Neurol.* 2013; 240:44-56.

Canzoniero LM, Rossi A, Tagliatela M, Amoroso S, Annunziato L, Di Renzo G. The Na (+)-Ca<sup>2+</sup> exchanger activity in cerebrocortical nerve endings is reduced in old compared to young and mature rats when it operates as a Ca<sup>2+</sup> influx or efflux pathway. *Biochim. Biophys Acta.*1992; 1107(1):175-8.

Caggiu E, Arru G, Hosseini S, Niegowska M, Sechi G, Zarbo IR, Sechi LA. Inflammation, Infectious Triggers, and Parkinson's Disease. *Front Neurol.* 2019; 19: 10:122.

Capiod T. Extracellular calcium has multiple targets to control cell proliferation, *Adv. Exp. Med. Biol.* 2016; 898: 133–156

Carlsson A, Lindqvist M, Magnusson T. 3,4-Dihydroxyphenylalanine and 5-hydroxytryptophan as reserpine antagonists. *Nature.* 1957; 180:1200.

Castano A, Herrera AJ, Cano J, Machado A. Lipopolysaccharide intranigral injection induces inflammatory reaction and damage in the nigrostriatal dopaminergic system. *J Neurochem* 1998; 70(4): 1584-1592

Cavaliere F, Cerf L, Dehay B, Ramos-Gonzalez P, De Giorgi F, Bourdenx M, Bessedé A, Obeso JA, Matute C, Ichas F, Bezard E. In vitro  $\alpha$ -synuclein neurotoxicity and spreading among neurons and astrocytes using Lewy body extracts from Parkinson disease brains. *Neurobiol Dis.* 2017; 103:101-112.

Celsi F, Pizzo P, Brini M, Leo S, Fotino C, Pinton P, Rizzuto R. Mitochondria, calcium and cell death: a deadly triad in neurodegeneration. *Biochim Biophys Acta.* 2009;1787(5):335-44.

Chadchankar H, Ihalaainen J, Tanila H, Yavich L. Decreased reuptake of dopamine in the dorsal striatum in the absence of alpha-synuclein. *Brain Res.* 2011; 1382: 37–44.

Chan CS, Guzman JN, Ilijic E, Mercer JN, Rick C, Tkatch T, Meredith GE, Surmeier DJ. 'Rejuvenation' protects neurons in mouse models of Parkinson's disease. *Nature.* 2007; 447:1081–1086.

Chan CS, Gertler TS, Surmeier DJ. A molecular basis for the increased vulnerability of substantia nigra dopamine neurons in ageing and Parkinson's disease. *Mov. Disord.* 2010; 25 Suppl 1:S63-70.

Chan CS, Gertler TS, Surmeier DJ. Calcium homeostasis, selective vulnerability and Parkinson's disease. *Trends Neurosci.* 2009; 32: 249–256

Chandra S, Gallardo G, Fernandez-Chacon R, Schluter OM, Sudhof TC.  $\alpha$ -Synuclein cooperates with CSP $\alpha$  in preventing neurodegeneration. *Cell*. 2005; 123: 383–96.

Chang C, Wu G, Gao P, Yang L, Liu W, Zuo J. Upregulated Parkin expression protects mitochondrial homeostasis in DJ-1 knockdown cells and cells overexpressing the DJ-1 L166P mutation. *Mol Cell Biochem*. 2014; 387(1-2):187-95.

Chen H, Jacobs E, Schwarzschild MA, McCullough ML, Calle EE, Thun MJ, Ascherio A. Nonsteroidal anti-inflammatory drug use and the risk for Parkinson's disease. *Ann Neurol*. 2005; 58: 963-267

Chinopoulos C, Adam-Vizi V. Mitochondrial Ca<sup>2+</sup> sequestration and precipitation revisited. *FEBS J*. 2010; 277: 3637–3651.

Choi DY, Zhang J, Bing G. Aging enhances the neuroinflammatory response and alpha-synuclein nitration in rats. *Neurobiol Aging*, 2010; 31(9): 1649-1653

Chung CY, Koprach JB, Siddiqi H, Isacson O. Dynamic changes in presynaptic and axonal transport proteins combined with striatal neuroinflammation precede dopaminergic neuronal loss in a rat model of AAV alpha-synucleinopathy. *J Neurosci*, 2009; 29 (11):3365-3373

Clapham DE. Calcium signalling, *Cell*. 2007; 131: 1047–1058

Cole NB, Dieuliis D, Leo P, Mitchell DC, Nussbaum RL. Mitochondrial translocation of alpha-synuclein is promoted by intracellular acidification. *Exp. Cell Res*. 2008; 314: 2076–2089.

Colton CA, Wilcock DM. Assessing activation states in microglia. *CNS Neurol Disord Drug Targets*. 2010; 9:174–191.

Colvin RA, Davis N, Wu A, Murphy CA, Levensgood J. Studies of the mechanism underlying increased Na<sup>+</sup>/Ca<sup>2+</sup> exchange activity in Alzheimer's disease brain. *Brain Res*. 1994; 665:192–200.

Conway KA, Lee SJ, Rochet JC, Ding TT, Williamson RE, Lansbury PT Jr. Acceleration of oligomerization, not fibrillization, is a shared property of both  $\alpha$ -

synuclein mutations linked to early-onset Parkinson's disease: implications for pathogenesis and therapy. *Proc Natl Acad Sci U S A*. 2000; 97: 571-576.

Cookson MR. The biochemistry of Parkinson's disease. *Annu. Rev. Biochem.* 2005; 74: 29-52.

Costanzo M, Zurzolo C. The cell biology of prion-like spread of protein aggregates: mechanisms and implication in neurodegeneration. *Biochem. J.* 2013; 452: 1-17.

Couch Y, Alvarez-Erviti L, Sibson NR, Wood MJ, Anthony DC. The acute inflammatory response to intranigral alpha-synuclein differs significantly from intranigral lipopolysaccharide and is exacerbated by peripheral inflammation. *J Neuroinflammation*. 2011; 8:166.

Cox J, Matic I, Hilger M, Nagaraj N, Selbach M, Olsen JV, et al. A practical guide to the MaxQuant computational platform for SILAC-based quantitative proteomics. *Nat Protoc*. 2009;4(5): 698-705.)

Cox J, Neuhauser N, Michalski A, Scheltema RA, Olsen JV, Mann M. Andromeda: a peptide search engine integrated into the MaxQuant environment. *J Proteome Res*. 2011;10(4):1794-805.

Croft D, O'Kelly G, Wu G, Haw R, Gillespie M, Matthews L, Caudy M, Garapati P, Gopinath G, Jassal B, Jupe S, Kalatskaya I, Mahajan S, May B, Ndegwa N, Schmidt E, Shamovsky V, Yung C, Birney E, Hermjakob H, D'Eustachio P, Stein L. Reactome: a database of reactions, pathways and biological processes. *Nucleic Acids Res*. 2011; 39: D691-7

Crowther RA, Jakes R, Spillantini MG, Goedert M. Synthetic filaments assembled from C-terminally truncated alpha-synuclein. *FEBS Lett*. 1998; 436: 309-312.

Cuervo AM, Stefanis L, Fredenburg R, Lansbury PT, Sulzer D. Impaired degradation of mutant alpha-synuclein by chaperone-mediated autophagy. *Science*. 2004; 305:1292-1295

Czyz A, Kiedrowski L. Inhibition of plasmalemmal Na<sup>+</sup>/Ca<sup>2+</sup> exchange by mitochondrial Na<sup>+</sup>/Ca<sup>2+</sup> exchange inhibitor 7-chloro-5-(2-chlorophenyl)-1,5-

dihydro- 4,1-benzothiazepin-2(3 H)-one (CGP-37157) in cerebellar granule cells. *Biochem. Pharmacol.* 2003; 66: 2409–2411.

Danzer KM, Haasen D, Karow AR, Moussaud S, Habeck M, Giese A, Kretschmar H, Hengerer B, Kostka M. Different species of alpha-synuclein oligomers induce calcium influx and seeding. *J Neurosci* . 2007; 27:9220–9232

Danzer KM, Kranich LR, Ruf WP, Cagsal-Getkin O, Winslow AR, Zhu L, Vanderburg CR, McLean PJ. Exosomal cell-to-cell transmission of alpha-synuclein oligomers. *Mol Neurodegener.* 2012; 7:42

Danzer KM, Ruf WP, Putcha P, Joyner D, Hashimoto T, Glabe C, Hyman BT, McLean PJ. Heat-shock protein 70 modulates toxic extracellular alpha-synuclein oligomers and rescues trans-synaptic toxicity. *FASEB J.* 2011; 25:326–336

Dauer W, Przedborski S. Parkinson's disease: Mechanisms and models. *Neuron* 2003; 39: 889–909.

Davidson WS, Jonas A, Clayton DF, George JM. Stabilization of alpha-synuclein secondary structure upon binding to synthetic membranes. *J Biol Chem.*1998; 273: 9443–9449.

Dedmon MM, Christodoulou J, Wilson MR, Dobson CM. Heat shock protein 70 inhibits alpha-synuclein fibril formation via preferential binding to prefibrillar species. *J. Biol. Chem.* 2005; 280: 14733–14740.

Dehay B, Bove' J, Rodriguez-Muela N, Perier C, Recasens A, Boya P, Vila M. Pathogenic lysosomal depletion in Parkinson's disease. *J Neurosci* 2010; 30: 12535–12544.

Delgado M, Ganea D. Neuroprotective effect of the vasoactive intestinal peptide (VIP) in a mouse model of Parkinson's disease by blocking microglial activation. *FASEB J.* 2003; 17, (8): 944-946

den HJW, Bethlem J. The distribution of Lewy bodies in the central and autonomic nervous systems in idiopathic paralysis agitans. *J Neurol Neurosurg Psychiatry.* 1960; 23:283–290

Desplats P, Lee HJ, Bae EJ, Patrick C, Rockenstein E, Crews L, Spencer B, Masliah E, Lee SJ. Inclusion formation and neuronal cell death through neuron-to-neuron transmission of alpha-synuclein. *Proc Natl Acad Sci U S A*. 2009; 4, 106(31):13010-5.

Devi L, Raghavendran V, Prabhu BM, Avadhani NG, Anandatheerthavarada H.K. Mitochondrial import and accumulation of alpha-synuclein impair complex I in human dopaminergic neuronal cultures and Parkinson disease brain. *J Biol Chem*. 2008; 283: 9089–9100

Devoto VMP and Falzone TL. Mitochondrial dynamics in Parkinson's disease: a role for  $\alpha$ -synuclein? *Disease Models & Mechanisms* 2017; 10: 1075-1087

Dikiy I, Eliezer D. N-terminal acetylation stabilizes N-terminal helicity in lipid- and micelle-bound alpha-synuclein and increases its affinity for physiological membranes. *J. Biol. Chem*. 2014; 289: 3652–3665.

DiMauro S, Schon EA. Mitochondrial respiratory-chain diseases. *New Engl. J. Med*. 2003; 348:2656– 2668

DiPolo R, Beauge L. The effects of pH on  $\text{Ca}^{2+}$  extrusion mechanisms in dialyzed squid axons. *Biochim. Biophys. Acta*. 1982; 688: 237–245

Doering AE, Eisner DA, Lederer WJ. Cardiac Na-Ca exchange and pH. *Ann. N. Y. Acad. Sci*. 1996; 779: 182–198.

Doering AE, Lederer WJ. The action of  $\text{Na}^{+}$  as a cofactor in the inhibition by cytoplasmic protons of the cardiac  $\text{Na}^{+}$ - $\text{Ca}^{2+}$  exchanger in the guinea-pig. *J. Physiol*. 1994; 480: 9–20.

Doorn KJ, Lucassen PJ, Boddeke HW, Prins M, Berendse HW, Drukarch B, van Dam AM Emerging roles of microglial activation and non-motor symptoms in Parkinson's disease. *Prog Neurobiol* 2012; 98:222–238.

Dorsey ER, Constantinescu R, Thompson JP, Biglan KM, Holloway RG, Kieburtz K, Marshall FJ, Ravina BM, Schifitto G, Siderowf A, Tanner CM. Projected number of people with Parkinson disease in the most populous nations, 2005 through 2030. *Neurology*. 2007; 30,68(5):384-6.



Dryanovski DI, Guzman JN, Xie Z, Galteri DJ, Volpicelli-Daley LA, Lee VM, Miller RJ, Schumacker PT, Surmeier DJ. Calcium entry and alpha-synuclein inclusions elevate dendritic mitochondrial oxidant stress in dopaminergic neurons. *J Neurosci* 2013; 33:10154–10164

Duchen MR. Mitochondria in health and disease: perspectives on new mitochondrial biology. *Mol Aspects Med.* 2004; 25:365–451.

Ehringer H, Hornykiewicz O. Distribution of noradrenaline and dopamine (3-hydroxy-tyramine) in the human brain and their behaviour in diseases of the extrapyramidal system. *Parkinsonism Relat Disord.* 1998; 4:53–57.

El-Agnaf OM, Salem SA, Paleologou KE, Cooper LJ, Fullwood NJ, Gibson MJ, Curran MD, Court JA, Mann DM, Ikeda S, Cookson MR, Hardy J, Allsop D. Alpha-synuclein implicated in Parkinson's disease is present in extracellular biological fluids, including human plasma. *FASEB J.* 2003; 17:1945–1947

Emmanouilidou E, Melachroinou K, Roumeliotis T, Garbis SD, Ntzouni M, Margaritis LH, Stefanis L, Vekrellis K. Cell-produced alpha-synuclein is secreted in a calcium dependent manner by exosomes and impacts neuronal survival. *J Neurosci* 2010; 30:6838–6851

Emmanouilidou E, Stefanis L, Vekrellis K. Cell-produced alpha-synuclein oligomers are targeted to, and impair, the 26S proteasome. *Neurobiol Aging.* 2010; 31:953–968

Engelhardt E, Gomes MDM. Lewy and his inclusion bodies: Discovery and rejection. *Dement Neuropsychol.* 2017;11(2):198-201

Exner N, Lutz AK, Haass C, Winklhofer KF. Mitochondrial dysfunction in Parkinson's disease: molecular mechanisms and pathophysiological consequences. *EMBO J* 2012; 31:3038–3062

Fath T, Ke YD, Gunning P, Gotz J, Ittner LM. Primary support cultures of hippocampal and substantia nigra neurons. *Nature Protocols* 2009; 4(1): 78-85.

Fellner L, Irschick R, Schanda K, Reindl M, Klimaschewski L, Poewe W, Wenning GK, Stefanova N. Toll-like receptor 4 is required for alpha-synuclein dependent activation of microglia and astroglia. *Glia.* 2013; 61:349–60.

Ferger AI, Campanelli L, Reimer V, Muth KN, Merdian I, Ludolph AC, Witting A. Effects of mitochondrial dysfunction on the immunological properties of microglia. *J Neuroinflammation*. 2010; 11; 7:45

Fernagut PO, Chesselet MF. Alpha-synuclein and transgenic mouse models. *Neurobiol Dis*, 2004; 17, (2): 121-130

Fernandez-Vizarra E, Tiranti V, Zeviani M. Assembly of the oxidative phosphorylation system in humans: what we have learned by studying its defects. *Biochim. Biophys. Acta*. 2009; 1793:200–211

Ferrari CC, Pott Godoy MC, Tarelli R, Chertoff M, Depino AM, Pitossi FJ. Progressive neurodegeneration and motor disabilities induced by chronic expression of IL-1beta in the substantia nigra. *Neurobiol Dis*. 2006; 24:183–93.

Flowers A, Bell-Temin H, Jalloh A, Stevens SM Jr, Bickford PC. Proteomic analysis of aged microglia: shifts in transcription, bioenergetics, and nutrient response. *J Neuroinflammation*. 2017 3;14(1):96.

Follett J, Darlow B, Wong MB, Goodwin J, Pountney DL. Potassium depolarization and raised calcium induce alpha/synuclein aggregates. *Neurotox Res* 2013; 23:378–392

Freeman D, Cedillos R, Choyke S, Lukic Z, McGuire K, Marvin S, Burrage AM, Sudholt S, Rana A, O'Connor C, Wiethoff CM, Campbell EM. Alpha-synuclein induces lysosomal rupture and cathepsin dependent reactive oxygen species following endocytosis. *PLoS One* 2013; 8 (4) (2013)

Furukawa K, Matsuzaki-Kobayashi M, Hasegawa T, Kikuchi A, Sugeno N, Itoyama Y, Wang Y, Yao PJ, Bushlin I, Takeda A. Plasma membrane ion permeability induced by mutant alpha-synuclein contributes to the degeneration of neural cells. *J Neurochem* 2006, 97: 1071–1077

Gabellini N, Bortoluzzi S, Danieli GA, Carafoli E. The human SLC8A3 gene and the tissue specific Na<sup>+</sup>/Ca<sup>2+</sup> exchanger 3 isoforms. *Gene*. 2002; 298:1–7

Gallagher DA, Lees AJ, Schrag A. What are the most important nonmotor symptoms in patients with Parkinson's disease and are we missing them? *Mov Disord.* 2010; 25:2493–2500

Gallegos S, Pacheco C, Peters C, Opazo CM, Aguayo LG. Features of alpha-synuclein that could explain the progression and irreversibility of Parkinson's disease. *Front Neurosci.* 2015; 9; 9:59.

Gandhi S, Wood-Kaczmar A, Yao Z, Plun-Favreau H, Deas E, Klupsch K, Downward J, Latchman DS, Tabrizi SJ, Wood NW, Duchen MR, Abramov AY. PINK1-associated Parkinson's disease is caused by neuronal vulnerability to calcium-induced cell death. *Mol. Cell.* 2009; 33(5):627-38.

Gao HM, Zhang F, Zhou H, Kam W, Wilson B, Hong JS. Neuroinflammation and alpha-Synuclein dysfunction potentiate each other driving chronic progression of neurodegeneration in a mouse model of Parkinson's disease. *Environ Health Perspect,* 2011; 119(6):807-14

Gao L, Zhang Z, Lu J, Pei G. Mitochondria Are Dynamically Transferring Between Human Neural Cells and Alexander Disease-Associated GFAP Mutations Impair the Astrocytic Transfer. *Front Cell Neurosci.* 2019; 10; 13:316

Gao HM, Hong JS. Why neurodegenerative diseases are progressive: uncontrolled inflammation drives disease progression. *Trends Immuno.* 2008; 29, (8), (357-65).

Garcia-Reitboeck P, Anichtchik O, Dalley J, Ninkina N, Tofaris GK, Buchman VL, Spillantini MG. Endogenous alpha-synuclein influences the number of dopaminergic neurons in mouse substantia nigra. *Exp. Neurol.* 2013; 248, 541–545.

Gelders G, Baekelandt V, Van der Perren A. Linking Neuroinflammation and Neurodegeneration in Parkinson's Disease. *J Immunol Res.* 2018; 16: 2018:4784268.

Gerhard A, Pavese N, Hotton G, Turkheimer F, Es M, Hammers A, Eggert K, Oertel W, Banati RB, Brooks DJ. In vivo imaging of microglial activation with [11C] (R)-PK11195 PET in idiopathic Parkinson's disease. *Neurobiol Dis* 2006; 21:404–412.

Ghavami S, Shojaei S, Yeganeh B, Ande SR, Jangamreddy JR, Mehrpour M, Christoffersson J, Chaabane W, Moghadam AR, Kashani HH, Hashemi M, Owji AA, Łos MJ. Autophagy and apoptosis dysfunction in neurodegenerative disorders. *Prog. Neurobiol.* 2014; 112: 24–4910

Ghio S, Kamp F, Cauchi R, Giese A, Vassallo N. Interaction of  $\alpha$ -synuclein with biomembranes in Parkinson's disease--role of cardiolipin. *Prog Lipid Res.* 2016; 61:73-82.

Ghosh SS, Swerdlow RH, Miller SW, Sheeman B, Parker WD Jr, Davis RE. Use of cytoplasmic hybrid cell lines for elucidating the role of mitochondrial dysfunction in Alzheimer's disease and Parkinson's disease. *Ann N Y Acad Sci.* 1999; 893:176-91.

Giasson BI, Murray IV, Trojanowski JQ, Lee VM. A hydrophobic stretch of 12 amino acid residues in the middle of alpha-synuclein is essential for filament assembly. *J. Biol. Chem.* 2001, 276, 2380–2386.

Giasson BI, Duda JE, Quinn SM, Zhang B, Trojanowski JQ, Lee VM. Neuronal alpha-synucleinopathy with severe movement disorder in mice expressing A53T human alpha-synuclein. *Neuron.* 2002; 34:521–533

Giasson BI, Jakes R, Goedert M, Duda JE, Leight S, Trojanowski JQ, Lee VM. A panel of epitope-specific antibodies detects protein domains distributed throughout human alpha-synuclein in Lewy bodies of Parkinson's disease. *J. Neurosci. Res.* 2000; 59: 528–533

Glass CK, Saijo K, Winner B, Marchetto MC, Gage FH. Mechanisms underlying inflammation in neurodegeneration. *Cell.* 2010; 140:918–34.

Gleichmann M and Mattson MP. Neuronal Calcium homeostasis and dysregulation. *Antiox and Redox sig.* 2011; 7: 1261-1273.

Goers J, Manning-Bog AB, McCormack AL, Millett IS, Doniach S, Di Monte DA, Uversky VN, Fink AL. Nuclear localization of alpha-synuclein and its interaction with histones. *Biochemistry.* 2003; 42: 8465–8471

Goldwurm S, Di Fonzo A, Simons EJ, Rohe CF, Zini M, Canesi M, Tesi S, Zecchinelli A, Antonini A, Mariani C, Meucci N, Sacilotto G, Sironi F, Salani G, Ferreira J, Chien HF, Fabrizio E, Vanacore N, Dalla Libera A, Stocchi F, Diroma C,

Lamberti P, Sampaio C, Meco G, Barbosa E, Bertoli-Avella AM, Breedveld GJ, Oostra BA, Pezzoli G, Bonifati V. The G6055A (G2019S) mutation in LRRK2 is frequent in both early and late onset Parkinson's disease and originates from a common ancestor. *J Med Genet.* 2005; 42: e65

Gonzalez-Hernandez T, Cruz-Muros I, Afonso-Oramas D, Salas-Hernandez J, Castro-Hernandez J. Vulnerability of mesostriatal dopaminergic neurons in Parkinson's disease. *Front Neuroanat.* 2010; 4:140

Grace AA, Bunney BS. Intracellular and extracellular electrophysiology of nigral dopaminergic neurons. Identification and characterization. *Neuroscience.* 1983; 10:301–315

Greenbaum EA, Graves CL, Mishizen-Eberz AJ, Lupoli MA, Lynch DR, Englander SW, Axelsen PH, Giasson BI. The E46K mutation in  $\alpha$ -synuclein increases amyloid fibril formation. *J Biol Chem* 2005; 280: 7800-7807.

Greggio E, Bisaglia M, Civiero L, Bubacco L. Leucine-rich repeat kinase 2 and alpha-synuclein: intersecting pathways in the pathogenesis of Parkinson's disease? *Mol Neurodegener* 2011; 6:6.

Grozdanov V, Danzer KM. Release and uptake of pathologic alpha-synuclein. *Cell Tissue Res.* 2018 Jul;373(1):175-182

Gu XL, Long CX, Sun L, Xie C, Lin X, Cai H. Astrocytic expression of Parkinson's disease-related A53T alpha-synuclein causes neurodegeneration in mice. *Mol Brain.* 2010; 3:12

Guardia-Laguarta C, Area-Gomez E, Rub C, Liu Y, Magrane J, Becker D, Voos W, Schon EA, Przedborski S. Alpha-synuclein is localized to mitochondria-associated ER membranes. *J Neurosci.* 2014; 34:249–259

Guardia-Laguarta C, Area-Gomez E, Schon EA, Przedborski S. A new role for alpha-synuclein in Parkinson's disease: Alteration of ER-mitochondrial communication. *Mov. Disord.* 2015; 30: 1026–1033

Gurung P, Lukens JR, Kanneganti TD. Mitochondria: diversity in the regulation of the NLRP3 inflammasome. *Trends Mol Med.* 2015;21(3):193-201.

Guzman JN, Sanchez-Padilla J, Wokosin D, et al. Oxidant stress evoked by pacemaking in dopaminergic neurons is attenuated by DJ-1. *Nature* 2010; 468:696–700

Halliday GM, Stevens CH. Glia: initiators and progressors of pathology in Parkinson's disease. *Mov Disord.* 2011; 26:6–17.

Hao LY, Giasson BI, Bonini NM. DJ-1 is critical for mitochondrial function and rescues PINK1 loss of function. *Proc Natl Acad Sci USA.* 2010; 107:9747–9752.

Hashimoto M, Rockenstein E, Mante M, Mallory M, Masliah E. beta-Synuclein inhibits alpha-synuclein aggregation: a possible role as an anti-Parkinsonian factor. *Neuron.* 2001; 32: 213–223.

Hausdorff JM. Gait dynamics in Parkinson's disease: common and distinct behaviour among stride length, gait variability, and fractal-like scaling. *Chaos.* 2009; 19(2):026113.

Hilge M, Aelen J, Foarce A, Perrakis A, Vuister GW. Ca<sup>2+</sup> regulation in the Na (+)/Ca (2+) exchanger features a dual electrostatic switch mechanism. *Proc Natl Acad Sci USA.* 2009 106:14333–14338.

Hilge M, Aelen J, Vuister GW. Ca<sup>2+</sup> regulation in the Na (+)/Ca (2+) exchanger involves two markedly different Ca<sup>2+</sup> sensors. *Mol Cel.* 2006; 1 22:15–25.

Hilgemann DW, Collins A, Matsuoka S. Steady-state and dynamic properties of cardiac sodium-calcium exchange. Secondary modulation by cytoplasmic calcium and ATP. *J. Gen. Physiol.* 1992; 100: 933–961.

Hirsch EC, Vyas S, Hunot S. Neuroinflammation in Parkinson's disease. *Park. Relat. Disord.* 2012; 18 Suppl 1, S210–S212

Hoang T, Choi DK, Nagai M, Wu DC, Nagata T, Prou D, Wilson GL, Vila M, Jackson-Lewis V, Dawson VL, Dawson TM, Chesselet MF, Przedborski S. Neuronal NOS and cyclooxygenase-2 contribute to DNA damage in a mouse model of Parkinson disease. *Free Radic Biol Med* 2009; 47: 1049–1056.

Hoyer W, Antony T, Cherny D, Heim G, Jovin TM, Subramaniam V. Dependence of alpha-synuclein aggregate morphology on solution conditions. *J Mol Biol* . 2002; 322:383–393

Hu X, Li P, Guo Y, Wang H, Leak RK, Chen S, et al. Microglia/macrophage polarization dynamics reveal novel mechanism of injury expansion after focal cerebral ischemia. *Stroke*. 2012; 43:3063–70.

Huang LS, Cobessi D, Tung EY, Berry EA. Binding of the respiratory chain inhibitor antimycin to the mitochondrial bc<sub>1</sub> complex: a new crystal structure reveals an altered intramolecular hydrogen-bonding pattern. *Journal of molecular biology*. 2005; 351(3):573–97.

Hughes CS, Foehr S, Garfield DA, Furlong EE, Steinmetz LM, Krijgsveld J. Ultrasensitive proteome analysis using paramagnetic bead technology. *Molecular Systems Biology* 2014; 10: 757

Hüser J, Blatter LA. Fluctuations in mitochondrial membrane potential caused by repetitive gating of the permeability transition pore. *Biochem. J*. 1999; 343: 311–317.

Jain N, BhasneK, Hemaswasthi M, Mukhopadhyay S. Structural and dynamical insights in to the membrane-bound  $\alpha$ -Synuclein. *PLoSONE*. 2013; 8: e83752.

Jang A, Lee HJ, Suk JE, Jung JW, Kim KP, Lee SJ. Non-classical exocytosis of alpha-synuclein is sensitive to folding states and promoted under stress conditions. *J Neurochem*. 2010; 113:1263–1274

Jeannotte AM, Sidhu A. Regulation of the norepinephrine transporter by alpha-synuclein-mediated interactions with microtubules. *Eur. J. Neurosci*. 2007; 26: 1509–1520.

Jo E, McLaurin J, Yip CM, St George-Hyslop P, Fraser PE. alpha-Synuclein membrane interactions and lipid specificity. *J. Biol. Chem*. 2000; 275(44):34328–34.

Juhaszova M, Shimizu H, Borin ML, Yip RK, Santiago EM, Lindenmayer GE, Blaustein MP. Localization of the Na (+)-Ca<sup>2+</sup> exchanger in vascular smooth muscle, and in neurons and astrocytes. *Ann N Y Acad Sci*. 1996; 779:318–35.

Kahle PJ, Neumann M, Ozmen L, Muller V, Jacobsen H, Schindzielorz A, Okochi M, Leimer U, van Der Putten H, Probst A, Kremmer E, Kretschmar HA, Haass C. Subcellular localization of wild-type and Parkinson's disease-associated mutant alpha-synuclein in human and transgenic mouse brain. *J. Neurosci.* 2000; 20, 6365–6373.

Khaliq ZM, Bean BP. Pacemaking in dopaminergic ventral tegmental area neurons: depolarizing drive from background and voltage-dependent sodium conductances. *J Neurosci.* 2010; 30: 7401–7413

Khananshvili D. The SLC8 gene family of sodium-calcium exchangers (NCX)–structure, function, and regulation in health and disease. *Mol. Asp. Med.* 2012; 34(2-3):220-35

Kim B and Matsuoka S. Cytoplasmic Na<sup>+</sup>-dependent modulation of mitochondrial Ca<sup>2+</sup> via electrogenic mitochondrial Na<sup>+</sup>-Ca<sup>2+</sup> exchange. *J Physiol.*2008; 586: 1683–1697.

Kim C, Ho DH, Suk JE, You S, Michael S, Kang J, Joong Lee S, Masliah E, Hwang D, Lee HJ, Lee SJ. Neuron-released oligomeric alpha-synuclein is an endogenous agonist of TLR2 for paracrine activation of microglia. *Nat Commun.*2013; 4:1562

Kim HY, Cho MK, Kumar A, Maier E, Siebenhaar C, Becker S, Fernandez CO, Lashuel HA, Benz R, Lange A, Zweckstetter M. Structural properties of pore-forming oligomers of alpha-synuclein. *J. Am. Chem. Soc.* 2009; 131,17482–17489.

Kitada T, Asakawa S, Hattori N, Matsumine H, Yamamura Y, Minoshima S, Yokochi M, Mizuno Y, Shimizu N. Mutations in the parkin gene cause autosomal recessive juvenile parkinsonism. *Nature.* 1998; 392:605–608.

Klegeris A, McGeer EG, McGeer PL. Therapeutic approaches to inflammation in neurodegenerative disease. *Curr Opin Neurol.* 2007; 20:351–357

Klegeris A, Pelech S, Giasson BI, Maguire J, Zhang H, McGeer EG, McGeer PL. Alpha-Synuclein activates stress signaling protein kinases in THP-1 cells and microglia. *Neurobiol Aging.* 2008; 29:739–752.

Kramer ML, Schulz-Schaeffer WJ. Presynaptic alpha-synuclein aggregates, not Lewy bodies, cause neurodegeneration in dementia with Lewy bodies. *J. Neurosci.* 2007; 27:1405–10.



Kruger R, Kuhn W, Muller T, Woitalla D, Graeber M, Kosel S, Przuntek H, Eppelen JT, Schols L, Riess O. Ala30Pro mutation in the gene encoding alpha-synuclein in Parkinson's disease. *Nat Gen.* 1998; 18:106–108

Kuar A, Cookson MR. Role of LRRK2 kinase dysfunction in Parkinson disease. *Expert Rev Mol Med.* 2011; 13: e20.

Kumaran R, Vandrovicova J, Luk C, Sharma S, Renton A, Wood NW, Hardy JA, Lees AJ, Bandopadhyay R. Differential DJ-1 gene expression in Parkinson's disease. *Neurobiol Dis.* 2009; 36:393–400.

La Rovere RM, Roest G, Bultynck G, Parys JB. Intracellular Ca (2+) signalling and Ca(2+) microdomains in the control of cell survival, apoptosis and autophagy, *Cell Calcium* 2016; 60: 74–87

Langston JW, Ballard P, Irwin I. Chronic parkinsonism in humans due to a product of meperidine-analogue synthesis. *Science* 1983; 219: 979–980.

Larsen KE, Schmitz Y, Troyer MD, Mosharov E, Dietrich P, Quazi AZ, Savalle M, Nemani V, Chaudhry FA, Edwards RH, Stefanis L, Sulzer D. Alpha-Synuclein overexpression in PC12 and chromaffin cells impairs catecholamine release by interfering with a late step in exocytosis. *J Neurosci.* 2006; 26:11915–22.

Larsen NJ, Ambrosi G, Mullett SJ, Berman SB, Hinkle DA. DJ-1 knock-down impairs astrocyte mitochondrial function. *Neuroscience.* 2011; 196:251–264.

Lashuel HA, Petre BM, Wall J, Simon M, Nowak RJ, Walz T, Lansbury PT Jr. Alpha-synuclein, especially the Parkinson's disease-associated mutants, forms pore-like annular and tubular protofibrils. *J Mol Biol* 2002; 322:1089–1102

Lavedan C. The synuclein family. *GenomeRes.* 1998; 8, 871–880.

Ledeem RW, Wu G. Sodium-calcium exchangers in the nucleus: An unexpected locus and an unusual regulatory mechanism. *Ann NY Acad Sci.* 2007; 1099:494–506.

Lee A, Hirabayashi Y, Kwon SK, Lewis TL Jr, Polleux F. Emerging roles of mitochondria in synaptic transmission and neurodegeneration. *Curr Opin Physiol.* 2018; 3:82-93.

Lee E. J., Woo MS, Moon PG, Baek MC, Choi IY, Kim WK, Junn E, Kim HS. Alpha-synuclein activates microglia by inducing the expressions of matrix metalloproteinases and the subsequent activation of protease-activated receptor-1. *J Immunol*, 2010; 185, (1): 615-623

Lee FJ, Liu F, Pristupa ZB, Niznik HB. Direct binding and functional coupling of alpha-synuclein to the dopamine transporters accelerate dopamine-induced apoptosis. *FASEB J.* 2001; 15: 916–926.

Lee HJ, Khoshaghideh F, Patel S, Lee SJ. Clearance of alpha synuclein oligomeric intermediates via the lysosomal degradation pathway. *J Neurosci.* 2004; 24:1888–1896

Lee HJ, Patel S, Lee SJ. Intravesicular localization and exocytosis of alpha-synuclein and its aggregates. *J Neurosci.* 2005; 25:6016–6024

Lee HJ, Suk JE, Bae EJ, Lee JH, Paik SR, Lee SJ. Assembly dependent endocytosis and clearance of extracellular alpha-synuclein. *Int J Biochem Cell Biol.* 2008; 40:1835–1849

Lee HJ, Suk JE, Bae EJ, Lee SJ. Clearance and deposition of extracellular alpha-synuclein aggregates in microglia. *Biochem Biophys Res Commun.* 2008; 372:423–428.

Lee HJ, Suk JE, Patrick C, Bae EJ, Cho JH, Rho S, Hwang D, Masliah E, Lee SJ. Direct transfer of alpha-synuclein from neuron to astroglia causes inflammatory responses in synucleinopathies. *J Biol Chem.* 2010 19;285(12):9262-72.

Lee HM, Yuk JM, Kim KH, Jang J, Kang G, Park JB, Son JW, Jo EK. Mycobacterium abscessus activates the NLRP3 inflammasome via Dectin-1-Syk and p62/SQSTM1. *Immunology and cell biology.* 2012; 90(6):601–10.

Lee JK, Tran T, Tansey MG. Neuroinflammation in Parkinson's disease. *J Neuroimmune Pharmacol.* 2009; 4:419–429.

Lees AJ, Selikhova M, Andrade LA, Duyckaerts C. The black stuff and Konstantin Nikolaevich Tretiakoff. *Mov Disord.* 2008; 23:777–783

Lesage S, Anheim M, Letournel F, Bousset L, Honoré A, Rozas N, Pieri L, Madiona K, Dürr A, Melki R, Verny C, Brice A; French Parkinson's Disease Genetics Study Group. G51D alpha-synuclein mutation causes a novel parkinsonian-pyramidal syndrome. *Ann Neurol.* 2013; 73(4):459-71

Li L, Nadanaciva S, Berger Z, Shen W, Paumier K, Schwartz J, Mou K, Loos P, Milici AJ, Dunlop J, Hirst WD. Human A53T  $\alpha$ -synuclein causes reversible deficits in mitochondrial function and dynamics in primary mouse cortical neurons. *PLoS One.* 2013; 31:8(12): e85815.

Li N, Ragheb K, Lawler G, Sturgis J, Rajwa B, Melendez JA, Robinson JP. Mitochondrial complex I inhibitor rotenone induces apoptosis through enhancing mitochondrial reactive oxygen species production. *The Journal of biological chemistry.* 2003; 278(10):8516–25.

Li WW, Yang R, Guo JC, Ren HM, Zha XL, Cheng J.S., Cai D.F. Localization of alpha-synuclein to mitochondria within midbrain of mice. *Neuroreport.* 2007; 18:1543–1546

Li Z, Matsuoka S, Hryshko LV, Nicoll DA, Bersohn MM, Burke EP, Lifton RP, Philipson KD. Cloning of the NCX2 isoform of the plasma membrane Na (+)/Ca (2+) exchanger. *J Biol Chem.* 1994; 269:17434–17439.

Li Z, Okamoto K, Hayashi Y, Sheng M. The importance of dendritic mitochondria in the morphogenesis and plasticity of spines and synapses. *Cell.* 2004; 17;119(6):873-87

Li W, West N, Colla E, Pletnikova O, Troncoso JC, Marsh L, Dawson TM, Jakala P, Hartmann T, Price DL, Lee MK. Aggregation promoting C-terminal truncation of alpha-synuclein is a normal cellular process and is enhanced by the familial Parkinson's disease-linked mutations. *Proc. Natl. Acad. Sci. USA* 2005, 102, 2162–2167.

Lin L, Chen X, Zhou Q, Huang P, Jiang S, Wang H, Deng Y. Synaptic structure and alterations in the hippocampus in neonatal rats exposed to lipopolysaccharide. *Neurosci Lett.* 2019; 14,709:134364.

Lindgren RM, Zhao J, Heller S, Berglind H, Nister M. Molecular cloning and characterization of two novel truncated isoforms of human Na<sup>+</sup>/Ca<sup>2+</sup> exchanger 3, expressed in the fetal brain. *Gene*. 2005; 348:143–155.

Liu J, Hong Z, Ding J, Liu J, Zhang J, Chen S. Predominant release of lysosomal enzymes by newborn rat microglia after LPS treatment revealed by proteomic studies. *J Proteome Res*. 2008; 7(5):2033-49.

Liu J, Shi M, Hong Z, Zhang J, Bradner J, Quinn T, Beyer RP, McGeer PL, Chen S. Identification of ciliary neurotrophic factor receptor alpha as a mediator of neurotoxicity induced by alpha-synuclein. *Proteomics* 2010; 10:2138–2150

Liu J, Zhou Y, Wang Y, Fong H, Murray TM, Zhang J. Identification of proteins involved in microglial endocytosis of alpha-synuclein. *J Proteome Res*. 2007; 6(9):3614-27.

Liu G, Zhang C, Yin J, Li X, Cheng F, Li Y, Yang H, Ueda K, Chan P, Yu S. alpha-Synuclein is differentially expressed in mitochondria from different rat brain regions and dose-dependently down-regulates complex I activity. *Neurosci. Lett*. 2009; 454(3):187-92.

Livigni A, Scorziello A, Agnese S, Adornetto A, Carlucci A, Garbi C, Castaldo I, Annunziato L, Avvedimento EV, Feliciello A. Mitochondrial AKAP121 links cAMP and src signalling to oxidative metabolism. *Mol. Biol. Cell* 2006; 17(1):263-71

Long-Smith CM, Sullivan AM, Nolan YM. The influence of microglia on the pathogenesis of Parkinson's disease. *Prog Neurobiol*. 2009; 89:277–287

Lowe R, Pountney DL, Jensen PH, Gai WP, Voelcker NH. Calcium(II) selectively induces alpha-synuclein annular oligomers via interaction with the C-terminal domain. *Protein Sci* 2004; 13:3245– 3252

Luther PW, Yip RK, Bloch RJ, Ambesi A, Lindenmayer GE, et al. Presynaptic localization of sodium/ calcium exchangers in neuromuscular preparations. *J Neurosci*. 1992; 12:4898–4904.

Marongiu R, Spencer B, Crews L, Adame A, Patrick C, Trejo M, Dallapiccola B, Valente EM, Masliah E. Mutant Pink1 induces mitochondrial dysfunction in a neuronal cell model of Parkinson's disease by disturbing calcium flux. *J Neurochem* 2009; 108: 1561–1574

Maroteaux L, Campanelli JT, Scheller RH. Synuclein: a neuron-specific protein localized to the nucleus and presynaptic nerve terminal. *J Neurosci.*1998; 8: 2804–2815.

Martin LJ, Pan Y, Price AC, Sterling W, Copeland NG, Jenkins NA, Price DL, Lee MK. Parkinson's disease alpha-synuclein transgenic mice develop neuronal mitochondrial degeneration and cell death. *J Neurosci* 2006; 4,26(1):41-50.

Martinez-Vicente M, Talloczy Z, Kaushik S, Massey AC, Mazzulli J, Mosharov EV, Hodara R, Fredenburg R, Wu DC, Follenzi A, Dauer W, Przedborski S, Ischiropoulos H, Lansbury PT, Sulzer D, Cuervo AM. Dopamine-modified alpha synuclein blocks chaperone-mediated autophagy, *J. Clin. Invest.* 2008; 118 (2): 777–78810.

Masliah E, Rockenstein E, Veinbergs I, Mallory M, Hashimoto M, Takeda A, Sagara Y, Sisk A, Mucke L. Dopaminergic loss and inclusion body formation in alpha-synuclein mice: implications for neurodegenerative disorders. *Science.* 2000 18;287(5456):1265-9.

Matsuda T, Arakawa N, Takuma K, Kishida Y, Kawasaki Y, Sakaue M, Takahashi K, Takahashi T, Suzuki T, Ota T, Hamano-Takahashi A, Onishi M, Tanaka Y, Kameo K, Baba A. SEA0400, a novel and selective inhibitor of the Na<sup>+</sup>-Ca<sup>2+</sup> exchanger, attenuates reperfusion injury in the in vitro and in vivo cerebral ischemic models. *J Pharmacol Exp Ther* 2001; 298:249–256.

Matsuoka S, Nicoll DA, He Z, Philipson KD. Regulation of cardiac Na<sup>+</sup>/Ca<sup>2+</sup> exchanger by the endogenous XIP region. *J Gen Physiol.* 1997; 109:273–286.

Mattson MP, Gleichmann M, Cheng A. Mitochondria in neuroplasticity and neurological disorders. *Neuron.* 2008; 60: 748–766.

McCoy MK, Martinez TN, Ruhn KA, Szymkowski DE, Smith CG, Botterman BR, et al. Blocking soluble tumor necrosis factor signaling with dominant negative tumor necrosis factor inhibitor attenuates loss of dopaminergic neurons in models of Parkinson's disease. *J Neurosci.* 2006; 26:9365–75.

McGeer PL, Itagaki S, Boyes BE, McGeer EG. Reactive microglia are positive for HLA-DR in the substantia nigra of Parkinson's and Alzheimer's disease brains. *Neurology*. 1988; 38:1285–1291

McGeer PL, McGeer EG. Glial reactions in Parkinson's disease. *Mov Disord*. 2008; 23(4):474–483

McLean PJ, Ribich S, Hyman BT. Subcellular localization of alpha-synuclein in primary neuronal cultures: effect of missense mutations. *J Neural Transm*. 2000; 58(Suppl):53–63

Mehra S, Sahay S, Maji SK.  $\alpha$ -Synuclein misfolding and aggregation: Implications in Parkinson's disease pathogenesis. *Biochim Biophys Acta Proteins Proteom*. 2019: S1570-9639(19)30045-7

Melachroinou K, Xilouri M, Emmanouilidou E, Masgrau R, Papazafiri P, Stefanis L, Vekrellis K. Deregulation of calcium homeostasis mediates secreted alpha-synuclein-induced neurotoxicity. *Neurobiol Aging* 2013, 34:2853–2865

Michaelis ML, Johe K, and Kito TE. Age-dependent alterations in synaptic membrane systems for Ca<sup>2+</sup> regulation. *Mech. Ageing Dev*. 1984; 25:215–225.

Michel LY, Hoenderop JG, Bindels RJ. Towards Understanding the Role of the Na<sup>2+</sup>-Ca<sup>2+</sup> Exchanger Isoform 3. *Rev Physiol Biochem Pharmacol*. 2015; 168:31-57.

Molinaro P, Cuomo O, Pignataro G, Boscia F, Sirabella R, Pannaccione A, Secondo A, Scorziello A, Adornetto A, Gala R, Viggiano D, Sokolow S, Herchuelz A, Schurmans S, Di Renzo G, Annunziato L. Targeted disruption of Na<sup>+</sup>/Ca<sup>2+</sup> exchanger 3 (NCX3) gene leads to a worsening of ischemic brain damage. *J. Neurosci*. 2008; 28, 1179–1184

Mollenhauer B, Cullen V, Kahn I, Krastins B, Outeiro TF, Pepivani I, Ng J, Schulz-Schaeffer W, Kretschmar HA, McLean PJ, Trenkwalder C, Sarracino DA, Vonsattel JP, Locascio JJ, El-Agnaf OM, Schlossmacher MG. Direct quantification of CSF alpha/synuclein by ELISA and first cross-sectional study in patients with neurodegeneration. *Exp Neurol*. 2008; 213:315–325

Mor DE, Ugras SE, Daniels MJ, Ischiropoulos H. Dynamic structural flexibility of alpha-synuclein. *Neurobiol. Dis.* 2016; 88: 66–74.

Munishkina LA, Phelan C, UverskyVN, FinkAL Conformational behaviour and aggregation of alpha-synuclein in organic solvents: modelling the effects of membranes. *Biochemistry* 2003; 42:2720–2730

Murata H, Hotta S, Sawada E, Yamamura H, Ohya S, et al. Cellular Ca<sup>2+</sup> dynamics in urinary bladder smooth muscle from transgenic mice overexpressing Na (+)/Ca (2+) exchanger. *J Pharmacol Sci.* 2010; 112:373– 377.

Nagano T, Kawasaki Y, Baba A, Takemura M, Matsuda T. Up-regulation of Na<sup>+</sup>-Ca<sup>2+</sup> exchange activity by interferon-gamma in cultured rat microglia. *J Neurochem* 2004, 90:784–791.

Nakamura K. alpha-Synuclein and mitochondria: partners in crime? *Neurotherapeutics.* 2013; 10 (3) 391–39910.

Narendra DP, Jin SM, Tanaka A, Suen DF, Gautier CA, Shen J, Cookson MR, Youle RJ. PINK1 is selectively stabilized on impaired mitochondria to activate Parkin. *PLoS Biol.* 2010; 8: e1000298.

Narhi L, Wood SJ, Steavenson S, Jiang Y, Wu GM, Anafi D, Kaufman SA, Martin F, Sitney K, Denis P, Louis JC, Wypych J, Biere AL, Citron M. Both familial Parkinson's disease mutations accelerate  $\alpha$ -synuclein aggregation, *J Biol Chem*, 1999; 274; 9843-9846.

Nath S, Goodwin J, Engelborghs Y, Pountney DL. Raised calcium promotes alpha-synuclein aggregate formation. *Mol Cell Neurosci* 2011, 46:516–526

Neupert W., J.M. Herrmann, Translocation of proteins into mitochondria. *Annu. Rev. Biochem.* 2007; 76: 723 749.

Newell EW, Stanley EF, Schlichter LC. Reversed Na<sup>+</sup>/Ca<sup>2+</sup> exchange contributes to Ca<sup>2+</sup> influx and respiratory burst in microglia. *Channels (Austin)* 2007; 1:366–376.

Ni Y, Malarkey EB, Parpura V. Vesicular release of glutamate mediates bidirectional signaling between astrocytes and neurons. *J Neurochem* 2007; 103: 1273–1284.

Nicholls DG. Mitochondria and calcium signaling. *Cell Calcium*.2005; 38: 311–317.

Nicoll DA, Quednau BD, Qui Z, Xia YR, Lusi AJ, et al. Cloning of a third mammalian Na (+)/Ca (2+) exchanger, NCX3. *J Biol Chem*. 1996; 271:24914–24921

Nicoll DA, Ren X, Ottolia M, Phillips M, Parades AR, Abramson J, Philipson KD. What we know about the structure of NCX1 and how it relates to its function. *Ann. NY Acad. Sci.*2007; 1099:1–6.

Noh H, Jeon J1, Seo H. Systemic injection of LPS induces region-specific neuroinflammation and mitochondrial dysfunction in normal mouse brain. *Neurochem Int*. 2014 ;69:35-40

Obeso JA, Rodriguez-Oroz MC, Goetz CG, Marin C, Kordower HJ, Rodriguez M, Hirsch EC, Farrer M, Schapira AHV, Halliday G. Missing pieces in the Parkinson's disease puzzle. *Nature Medicine*. 2010; .16(6): 653-661

Obeso JA, Rodriguez-Oroz MC, Rodriguez M, Lanciego JL, Artieda J, Gonzalo N, Olanow CW. Pathophysiology of the basal ganglia in Parkinson's disease. *Trends Neurosci*. 2000; 23, S8-S19.

Olson JK. Immune response by microglia in the spinal cord. *Ann NY Acad Sci*. 2010; 1198:271–278.

Orr CF, Rowe DB, Mizuno Y, Mori H, Halliday GM. A possible role for humoral immunity in the pathogenesis of Parkinson's disease. *Brain*. 2005; 128:2665–2674.

Ouchi Y, Yoshikawa E, Sekine Y, Futatsubashi M, Kanno T, Ogusu T, Torizuka T. Microglial activation and dopamine terminal loss in early Parkinson's disease. *Ann Neurol* 2005; 57:168–175.



Pahwa R, Lyons KE. Early diagnosis of Parkinson's disease: recommendations from diagnostic clinical guidelines. *Am J Manag Care*. 2010; 16 Suppl Implications: S94-9.

Pannaccione A, Secondo A, Molinaro P, D'Avanzo C, Cantile M, Esposito A, Boscia F, Scorziello A, Sirabella R, Sokolow S, Herchuelz A, Di Renzo G, Annunziato L. A new concept: A $\beta$ 1-42 generates a hyper-functional proteolytic NCX3 fragment that delays caspase-12 activation and neuronal death. *J. Neurosci*. 2012; 32, 10609–10617.

Papa M, Canitano A, Boscia F, Castaldo P, Sellitti S, Porzig H, Tagliatela M, and Annunziato L. Differential expression of the Na-Ca<sup>2+</sup> exchanger transcripts and proteins in rat brain regions. *J. Comp. Neurol*. 2003; 461:31–48.

Parihar MS, Parihar A, Fujita M, Hashimoto M, Ghafourifar P. Mitochondrial association of alpha-synuclein causes oxidative stress, *Cell. Mol. Life Sci*. 2008; 65 (7-8) 1272–128410

Parihar MS, Parihar A, Fujita M, Hashimoto M, Ghafourifar P. Alpha-synuclein overexpression and aggregation exacerbates impairment of mitochondrial functions by augmenting oxidative stress in human neuroblastoma cells. *Int.J.Biochem.Cell Biol*. 2009; 41,2015–2024.

Park JY, Choi H, Min JS, Park SJ, Kim JH, Park HJ, Kim B, Chae JI, Yim M, Lee DS. Mitochondrial dynamics modulate the expression of pro-inflammatory mediators in microglial cells. *J Neurochem*. 2013;127(2):221-32.

Park JY, Paik SR, Jou I, Park SM. Microglial phagocytosis is enhanced by monomeric alpha-synuclein, not aggregated alpha synuclein: implications for Parkinson's disease. *Glia*. 2008; 56:1215–1223.

Parker WD Jr, Boyson SJ, Parks JK. Abnormalities of the electron transport chain in idiopathic Parkinson's disease. *Ann Neurol*. 1989 ;26(6):719-23.

Parker WD Jr, Parks JK, Swerdlow RH. Complex I deficiency in Parkinson's disease frontal cortex. *Brain Res*. 2008; 1189:215-8.

Paulsen F, Pufe T, Conradi L, Varoga D, Tsokos M, Papendieck J, et al. Antimicrobial peptides are expressed and produced in healthy and inflamed human synovial membranes. *J Pathol.* 2002; 198:369–77.

Perea G, Araque A. Astrocytes potentiate transmitter release at single hippocampal synapses. *Sci.* 2007; 317:1083–1086.

Perfeito R, Cunha-Oliveira T, Rego AC. Reprint of: revisiting oxidative stress and mitochondrial dysfunction in the pathogenesis of Parkinson disease-resemblance to the effect of amphetamine drugs of abuse. *Free Radic. Biol. Med.* 2013; 62:186-201

Perier C, Tieu K, Guegan C, Caspersen C, Jackson-Lewis V, Carelli V, Martinuzzi A, Hirano M, Przedborski S, Vila M. Complex I deficiency primes Bax-dependent neuronal apoptosis through mitochondrial oxidative damage. *Proc Natl Acad Sci* 2005; 102: 19126 19131

Perier C. and Vila M. Mitochondrial biology and Parkinson's disease. *Cold Spring Harb Perspect Med.* 2012; 2(2): a009332

Periquet M, Fulga T, Myllykangas L, Schlossmacher MG, Feany MB. Aggregated alpha-synuclein mediates dopaminergic neurotoxicity in vivo. *J. Neurosci.* 2007; 27: 3338–3346.

Philipson KD, Nicoll DA. Sodium-calcium exchange: a molecular perspective. *Annu. Rev. Physiol.* 2000; 62:111-33.

Pignataro G, Gala R, Cuomo O, Tortiglione A, Giaccio L, Castaldo P, Sirabella R, Matrone C, Canitano A, Amoroso S, Di Renzo G, Annunziato L. Two sodium/calcium exchanger gene products, NCX1 and NCX3, play a major role in the development of permanent focal cerebral ischemia. *Stroke.* 2004; 35: 2566–2570.

Pinho R, Paiva I, Jercic KG, Fonseca-Ornelas L, Gerhardt E, Fahlbusch C, Garcia-Esparcia P, Kerimoglu C, Pavlou MA, Villar-Pique A, Szego É, Lopes da Fonseca T, Odoardi F, Soeroes S, Rego AC, Fischle W, Schwamborn JC, Meyer T, Kügler S, Ferrer I, Attems J, Fischer A, Becker S, Zweckstetter M, Borovecki F, Outeiro TF. Nuclear localization and phosphorylation modulate pathological effects of Alpha-Synuclein. *Hum. Mol. Genet.* 2019; 1; 28 (1):31-50.

Pisanu A, Lecca D, Mulas G, Wardas J, Simbula G, Spiga S, et al. Dynamic changes in pro- and anti-inflammatory cytokines in microglia after PPARgamma agonist

neuroprotective treatment in the MPTPp mouse model of progressive Parkinson's disease. *Neurobiol Dis.* 2014; 71:280–91.

Politis M, Su P, Piccini. Imaging of microglia in patients with neurodegenerative disorders. *Front Pharmacol* 2012; 3:96.

Polymeropoulos MH, Lavedan C, Leroy E, Ide SE, Dehejia A, Dutra A, Pike B, Root H, Rubenstein J, Boyer R, Stenroos ES, Chandrasekharappa S, Athanassiadou A, Papapetropoulos T, Johnson WG, Lazzarini AM, Duvoisin RC, Di Iorio G, Golbe LI, Nussbaum RL. Mutation in the alpha-synuclein gene identified in families with Parkinson's disease. *Science.* 1997;276(5321):2045-7.

Pozner A, Xu B, Palumbos S, Gee JM, Tvrdik P, Capecchi MR. Intracellular calcium dynamics in cortical microglia responding to focal laser injury in the PC: G5-tdT reporter mouse. *Front Mol Neurosci* 2015; 8:12.

Preterre C, Corbillé AG, Balloy G, Letournel F, Neunlist M, Derkinderen P. Optimizing Western Blots for the Detection of Endogenous  $\alpha$ -Synuclein in the Enteric Nervous System. *J Parkinsons Dis.* 2015;5(4):765-72.

Proukakis C, Dudzik CG, Brier T, MacKay DS, Cooper JM, Millhauser GL, Houlden H, Schapira AH. A novel alpha-synuclein missense mutation in Parkinson disease. *Neurology.* 2013; 80:1062– 1064.

Przedborski S. Neuroinflammation and Parkinson's disease. *Handb Clin Neurol.* 2007; 83:535-51

Quednau BD, Nicoll DA, and Philipson KD. Tissue specificity and alternative splicing of the Na<sup>1</sup>/Ca<sup>21</sup> exchanger isoforms NCX1, NCX2, and NCX3 in rat. *Am. J. Physiol.* 1997; 272:C1250–C1261.

Rees K, Stowe R, Patel S, Ives N, Breen K, Clarke CE, Ben-Shlomo Y. Non-steroidal anti-inflammatory drugs as disease modifying agents for Parkinson's disease: evidence from observational studies. *Cochrane Database Syst Rev* 2011 ;9, (11):CD008454

Reeve AK, Krishnan KJ, Turnbull D. Mitochondrial DNA mutations in disease, aging, and neurodegeneration. *Ann. N. Y. Acad. Sci.* 2008; 1147: 21–29.

Reeves J, Condrescu M. Ionic regulation of the cardiac sodium-calcium exchanger. *Channels (Austin)*; 2008; 2: 322–328

Ren X, Philipson KD. The topology of the cardiac Na (+)/Ca (2+) exchanger, NCX1. *J Mol Cell Cardiol* .2013; 57:68–71.

Reyes JF, Olsson TT, Lamberts JT, Devine MJ, Kunath T, Brundin P (2015) A cell culture model for monitoring alpha-synuclein cell to- cell transfer. *Neurobiol Dis*. 2015; 77:266–275

Reyes RC, Verkhratsky A, Parpura V. Plasmalemmal Na<sup>+</sup>/Ca<sup>2+</sup> exchanger modulates Ca<sup>2+</sup>-dependent exocytotic release of glutamate from rat cortical astrocytes. *ASN Neuro* 2012; 4: e00075.

Rideout HJ, Dietrich P, Wang Q, Dauer WT, Stefanis L Alpha-synuclein is required for the fibrillar nature of ubiquitinated inclusions induced by proteasomal inhibition in primary neurons. *J Biol Chem*. 2004; 279:46915–46920.

Rizzuto R, Bernardi P, Pozzan T. Mitochondria as all-round players of the calcium game. *J. Physiol*. 2000; 529: 37–47.

Rizzuto R, Pozzan T. Microdomains of intracellular Ca<sup>2+</sup>: molecular determinants and functional consequences. *Physiol. Rev* 2006; 86:369–408.

Rodrigues e Silva AM, Geldsetzer F, Holdorff B, Kielhorn FW, Balzer-Geldsetzer M, Oertel WH, Hurtig H, Dodel R. Who was the man who discovered the “Lewy bodies”? *Mov Disord*. 2010; 25:1765–1773

Ronzano R. Astrocytes and microglia: active players in synaptic plasticity *Med Sci (Paris)*. 2017 Dec;33(12):1071-1078

Rostami J, Holmqvist S, Lindström V, Sigvardson J, Westermark GT, Ingelsson M, Bergström J, Roybon L, Erlandsson A. Human Astrocytes Transfer Aggregated AlphaSynuclein via Tunneling Nanotubes. *J Neurosci*. 2017 Dec 6;37(49):11835-11853.

Ruf VC, Nübling GS, Willikens S, Shi S, Schmidt F, Levin J, Bötzel K, Kamp F, Giese A. Different Effects of  $\alpha$ -Synuclein Mutants on Lipid Binding and Aggregation Detected by Single Molecule Fluorescence Spectroscopy and ThT Fluorescence-Based Measurements. *ACS Chem Neurosci*. 2019;10(3):1649-1659.

Saijo K, Winner B, Carson CT, Collier JG, Boyer L, Rosenfeld MG, et al. A Nurr1/CoREST pathway in microglia and astrocytes protects dopaminergic neurons from inflammation-induced death. *Cell*. 2009; 137:47–59.

Sanchez-Guajardo V, Febbraro F, Kirik D, Romero-Ramos M. Microglia acquire distinct activation profiles depending on the degree of alpha-synuclein neuropathology in a rAAV based model of Parkinson's disease. *PLoS One*. 2010; 5: e8784.

Sanchez-Pernaute R, Ferree A, Cooper O, Yu M, Brownell AL, Isacson O. Selective COX-2 inhibition prevents progressive dopamine neuron degeneration in a rat model of Parkinson's disease. *JNeuroinflammation*,2004; 1, (1): 6

Sandebring A, Dehvari N, Perez-Manso M, Thomas KJ, Karpilovski E, Cookson MR, Cowburn RF, Cedazo-Minguez A. Parkin deficiency disrupts calcium homeostasis by modulating phospholipase C signalling. *FEBS J*. 2009; 276, 5041–5052.

Scalzo P, Kümmer A, Bretas TL, Cardoso F, Teixeira AL. Serum levels of brain-derived neurotrophic factor correlate with motor impairment in Parkinson's disease. *J. Neurol*. 2010; 257(4):540-5.

Schapira AH. Mitochondrial pathology in Parkinson's disease. *Mt Sinai J Med* 2011; 78:872–881

Schapira AH, Cooper JM, Morgan-Hughes JA, Landon DN, Clark JB. Mitochondrial myopathy with a defect of mitochondrial-protein transport. *N Engl J Med*. 1990; 5, 323(1):37-42.

Schiess, M. C., Barnes JL, Ellmore TM, Poindexter BJ, Dinh K, Bick RJ. CSF from Parkinson disease patients differentially affects cultured microglia and astrocytes. *BMC Neurosci*, 2010; 11: 151

Schmidt F, Levin J, Kamp F, Kretzschmar H, Giese A, Botzel K. Single-channel electrophysiology reveals a distinct and uniform pore complex formed by alpha-synuclein oligomers in lipid membranes. *PLoS One* 2012; 7: e42545

Schroder K, Tschopp J. The inflammasomes. *Cell* 2010; 140: 821–832

Schulze DH, Muqhal M, Lederer WJ, Ruknudin AM. Sodium/calcium exchanger (NCX1) macromolecular complex. *J. Biol. Chem.* 2003; 278:28849–28855.

Schwaller M.J. Berridge, Neuronal calcium signaling, *Neuron* 1998; 21: 13–26.

Scorziello A, Santillo M, Adornetto A, Dell'aversano C, Sirabella R, Damiano S, Canzoniero LM, Renzo GF, Annunziato L. NO-induced neuroprotection in ischemic preconditioning stimulates mitochondrial Mn-SOD activity and expression via Ras/ERK1/2 pathway. *J Neurochem* 2007; .103 (4):1472-80.

Scorziello A, Savoia C, Sisalli MJ, Adornetto A, Secondo A, Boscia F, Esposito A, Polishchuk EV, Polishchuk RS, Molinaro P, Carlucci A, Lignitto L, Di Renzo G, Feliciello A, Annunziato L. NCX3 regulates mitochondrial Ca (2+) handling through the AKAP121-anchored signaling complex and prevents hypoxia-induced neuronal death. *J Cell Sci.* 2013 Dec 15;126(Pt 24):5566-77.

Secondo A, Esposito A, Petrozziello T, Boscia F, Molinaro P, Tedeschi V, Pannaccione A, Ciccone R, Guida N, Di Renzo G, Annunziato L. Na<sup>+</sup>/Ca<sup>2+</sup> exchanger 1 on nuclear envelope controls PTEN/Akt pathway via nucleoplasmic Ca<sup>2+</sup> regulation during neuronal differentiation. *Cell Death Discov.* 2018;4:12.

Secondo A, Staiano IR, Scorziello A, Sirabella R, Boscia F, Adornetto A, Canzoniero LM, Di Renzo G, Annunziato L. The Na<sup>+</sup>/Ca<sup>2+</sup> exchanger isoform 3 (NCX3) but not isoform 2 (NCX2) and 1 (NCX1) singly transfected in BHK cells plays a protective role in a model of in vitro hypoxia. *Ann N Y Acad Sci.* 2007; 1099:481-5.

Sevcsik E, Trexler AJ, Dunn JM, Rhoades E. Allostery in a disordered protein: Oxidative modifications to alpha-synuclein act distally to regulate membrane binding. *J. Am. Chem. Soc.* 2011; 133: 7152–7158.

Sharma V, O'Halloran DM. Recent structural and functional insights into the family of sodium calcium exchangers. *Genesis.* 2014;52(2):93-109.

Shendelman S, Jonason A, Martinat C, Leete T, Abeliovich A. DJ-1 is a redox-dependent molecular chaperone that inhibits alpha-synuclein aggregate formation. *PLoS Biol.* 2004; 2: e362.

Shimura H, Hattori N, Kubo S, Mizuno Y, Asakawa S, Minoshima S, Shimizu N, Iwai K, Chiba T, Tanaka K, Suzuki T. Familial Parkinson disease gene product, parkin, is a ubiquitin-protein ligase. *Nat Genet.* 2000; 25:302–305.

Shtifman, A., Zhong, N., Lopez, J. R., Shen, J., and Xu, J. Altered Ca<sup>2+</sup> homeostasis in the skeletal muscle of DJ-1 null mice. *Neurobiol. Aging.* 2011; 32:125–132.

Shulman LM, Taback RL, Rabinstein AA, Weiner WJ. Non-recognition of depression and other non-motor symptoms in Parkinson's disease. *Parkinsonism Relat Disord.* 2002; 8:193–197

Sirabella R, Secondo A, Pannaccione A, Scorziello A, Valsecchi V, Adornetto A, Bilo L, Di Renzo G, and Annunziato L. Anoxia-induced NF-kappaB-dependent upregulation of NCX1 contributes to Ca<sup>2+</sup> refilling into endoplasmic reticulum in cortical neurons. *Stroke.* 2009; 40:922–929.

Sirabella R, Sisalli MJ, Costa G, Omura K, Ianniello G, Pinna A, Morelli M, Di Renzo GM, Annunziato L, Scorziello A. NCX1 and NCX3 as potential factors contributing to neurodegeneration and neuroinflammation in the A53T transgenic mouse model of Parkinson's Disease. *Cell Death Dis.* 2018;9(7):725.

Sisalli MJ, Secondo A, Esposito A, Valsecchi V, Savoia C, Di Renzo GF, Annunziato L, Scorziello A. Endoplasmic reticulum refilling and mitochondrial calcium extrusion promoted in neurons by NCX1 and NCX3 in ischemic preconditioning are determinant for neuroprotection. *Cell Death Differ.* 2014 ;21(7):1142-9.

Smith, W. W., Jiang, H., Pei, Z., Tanaka, Y., Morita, H., Sawa, A., et al. Endoplasmic reticulum stress and mitochondrial cell death pathways mediate A53T mutant alpha-synuclein-induced toxicity. *Hum.Mol.Genet.* 2005; 14: 3801–3811

Sokolow S, Luu SH, Headley AJ, Hanson AY, Kim T, Miller CA, Vinters HV, Gylys KH. High levels of synaptosomal Na (+)-Ca (2+) exchangers (NCX1, NCX2,

NCX3) co-localized with amyloid-beta in human cerebral cortex affected by Alzheimer's disease. *Cell Calcium* 2011; 49:208–216.

Spillantini MG, Crowther RA, Jakes R, Hasegawa M, Goedert M. alpha-Synuclein in filamentous inclusions of Lewy bodies from Parkinson's disease and dementia with Lewy bodies. *Proc Natl. Acad. Sci. USA*.1998; 95: 6469–6473

Spillantini MG, Schmidt ML, Lee VM, Trojanowski JQ, Jakes R, Goedert M. Alpha-synuclein in Lewy bodies. *Nature*. 1997; 388:839–840

Starkov AA, Polster BM, Fiskum G. Regulation of hydrogen peroxide production by brain mitochondria by calcium and Bax. *J Neurochem*.2002; 83(1):220-8.

Stockl MT, Zijlstra N, Subramaniam V.  $\alpha$ -Synuclein oligomers: an amyloid pore? Insights into mechanisms of  $\alpha$ -synuclein oligomer-lipid interactions. *Mol. Neurobiol*.2013; 47, 613–621.

Su X, Federoff HJ, Maguire-Zeiss KA. Mutant alpha-Synuclein overexpression mediates the early proinflammatory activity. *Neurotox Res*. 2009; 16:238–254.

Su X, Maguire-Zeiss KA, Giuliano R, Prifti L, Venkatesh K, Federoff HJ. Synuclein activates microglia in a model of Parkinson's disease. *Neurobiol Aging*. 2008; 29:1690–1701.

Surmeier DJ. Calcium, aging, and neuronal vulnerability in Parkinson's disease. *Lancet Neurol* .2007, 6:933–938

Surmeier DJ, Guzman JN, Sanchez-Padilla J. Calcium, cellular aging, and selective neuronal vulnerability in Parkinson's disease. *Cell Calcium* 2010; 47, 175–182

Surmeier DJ, Guzman JN, Sanchez-Padilla J, Schumacker PT. The role of calcium and mitochondrial oxidant stress in the loss of substantia nigra pars compacta dopaminergic neurons in Parkinson's disease. *Neuroscience* 2011; 198, 221–231

Surmeier DJ, Guzman JN, Sanchez J, Schumacker PT. Physiological phenotype and vulnerability in Parkinson's disease. *Cold Spring Harb Perspect Med*, 2012; 2: a009290



Surmeier DJ, Plotkin J, Shen W. Dopamine and synaptic plasticity in dorsal striatal circuits controlling action selection. *Curr. Opin. Neurobiol.* 2009; 19(6):621-8.

Surmeier DJ, Schumacker PT. Calcium, bioenergetics, and neuronal vulnerability in Parkinson's disease. *J Biol Chem.* 2013; 288:10736– 10741

Szklarczyk D, Gable AL, Lyon D, Junge A, Wyder S, Huerta-Cepas J, Simonovic M, Doncheva NT, Morris JH5, Bork P, Jensen LJ, Mering CV. STRING v11: protein-protein association networks with increased coverage, supporting functional discovery in genome-wide experimental datasets. *Nucleic Acids Res.* 2019 8;47(D1): D607-D613.

Taira T, Saito Y, Niki T, Iguchi-Ariga S M, Takahashi K, Ariga H. DJ-1 has a role in antioxidative stress to prevent cell death. *EMBO 2004; Rep. 5: 213–218.*

Tanaka T, Kai S, Matsuyama T, Adachi T, Fukuda K, Hirota K. General anaesthetics inhibit LPS-induced IL-1beta expression in glial cells. *PLoS One.* 2013; 8: e82930.

Tang Y, Li T, Li J, Yang J, Liu H, Zhang XJ, et al. Jmjd3 is essential for the epigenetic modulation of microglia phenotypes in the immune pathogenesis of Parkinson's disease. *Cell Death Differ.* 2014; 21:369–80.

Tanji K., Mori F, Nakajo S, Imaizumi T, Yoshida H, Hirabayashi T, Yoshimoto M, Satoh K, Takahashi H, Wakabayashi K. Expression of beta-synuclein in normal human astrocytes. *Neuroreport*, 2001; 12, (13): 2845-2848

Tansey MG and Goldberg MS. Neuroinflammation in Parkinson's disease: its role in neuronal death and implications for therapeutic intervention. *Neurobiol.Dis* 2010; 37, 510–518

Tansey MG and Romero-Ramos M. Immune system responses in Parkinson's disease: Early and dynamic. *Eur J Neurosci.* 2019 ;49(3):364-383.

Terada S., Ishizu H, Yokota O, Tsuchiya K, Nakashima H, Ishihara T, Fujita D, Uéda K, Ikeda K, Kuroda S. Glial involvement in diffuse Lewy body disease. *Acta Neuropathol*, 2003; 105, (2): 163-169

Thakur P, Nehru B. Inhibition of neuroinflammation and mitochondrial dysfunctions by carbenoxolone in the rotenone model of Parkinson's disease. *Mol Neurobiol.* 2015; 51(1):209-19

Theillet FX, Binolfi A, Bekei B, Martorana A, Rose HM, Stuiiver M, Verzini S, Lorenz D, van Rossum M, Goldfarb D, Selenko P. Structural disorder of monomeric alpha-synuclein persists in mammalian cells. *Nature* 2016; 530: 45–50.

Theodore S, Cao S, McLean PJ, Standaert DG. Targeted overexpression of human alpha-synuclein triggers microglial activation and adaptive immune response in a mouse model of Parkinson disease. *J Neuropathol Exp Neurol*,2008; 67, (12): 1149-1158

Thomas KJ, McCoy MK, Blackinton J, Beilina A, van der Brug M, Sandebring A, Miller D, Maric D, Cedazo-Minguez A, Cookson MR. DJ-1 acts in parallel to the PINK1/parkin pathway to control mitochondrial function and autophagy. *Mol Genet.* 2011; 20(1):40-50.

Todorova V, Blokland A. Mitochondria and Synaptic Plasticity in the Mature and Aging Nervous System. *Curr Neuropharmacol.* 2017;15(1):166-173.

Torres-Odio S, Key J, Hoepken HH, Canet-Pons J, Valek L, Roller B, Walter M, Morales-Gordo B, Meierhofer D, Harter PN, Mittelbronn M, Tegeder I, Gispert S, Auburger G. Progression of pathology in PINK1-deficient mouse brain from splicing via ubiquitination, ER stress, and mitophagy changes to neuroinflammation. *J Neuroinflammation.* 2017; 2: 14(1):154.

Tosatto L, Andrighetti AO, Plotegher N, Antonini V, Tessari I, Ricci L, Bubacco L, Dalla Serra M. Alpha-synuclein pore forming activity upon membrane association. *Biochim. Biophys. Acta.* 2012; 1818: 2876–2883.

Toth AB, Shum AK, Prakriya M. Regulation of neurogenesis by calcium signalling, *Cell Calcium* 2016; 59: 124–134.

Trexler AJ, Rhoades E. N-terminal acetylation is critical for forming alpha-helical oligomer of alpha-synuclein. *Protein Sci.* 2012, 21, 601–605.

Troncoso-Escudero P, Parra A, Nassif M, Vidal RL. Outside in: Unraveling the Role of Neuroinflammation in the Progression of Parkinson's Disease. *Front Neurol.* 2018 Oct 15; 9:860.

Tsigelny IF, Sharikov Y, Wrasidlo W, Gonzalez T, Desplats PA, Crews L, Spencer B, Masliah E. Role of  $\alpha$ -synuclein penetration into the membrane in the mechanisms of oligomer pore formation. *FEBS J.* 2012; 279: 1000–1013.

Twelves D, Perkins KS, Counsell C. Systematic review of incidence studies of Parkinson's disease. *Mov Disord.* 2003; 18:19–31.

Ueda K, Fukushima H, Masliah E, Xia Y, Iwai A, Yoshimoto M et al., Molecular cloning of cDNA encoding an unrecognized component of amyloid in Alzheimer disease. *Proc Natl Acad Sci USA.* 1993; 90: 11282–11286.

Ulmer TS, Bax A. Comparison of structure and dynamics of micelle-bound human alpha-synuclein and Parkinson disease variants. *J. Biol. Chem.* 2005; 280: 43179–43187.

Valente EM, Abou-Sleiman PM, Caputo V, Muqit MM, Harvey K, Gispert S, Ali Z, Del Turco D, Bentivoglio AR, Healy DG, Albanese A, Nussbaum R, Gonzalez-Maldonado R, Deller T, Salvi S, Cortelli P, Gilks WP, Latchman DS, Harvey RJ, Dallapiccola B, Auburger G, Wood NW. Hereditary early-onset Parkinson's disease caused by mutations in PINK1. *Science.* 2004; 304:1158–1160.

Vamvaca K, Volles MJ, Lansbury PTJr. The first N-terminal amino acids of alpha-synuclein are essential for alpha-helical structure formation in vitro and membrane binding in yeast. *J. Mol. Biol.* 2009; 389: 413–424.

Van Den Eeden SK, Tanner CM, Bernstein AL, Fross RD, Leimpeter A, Bloch DA, Nelson LM. Incidence of Parkinson's disease: variation by age, gender, and race/ethnicity. *Am J Epidemiol.* 2003; 157:1015–1022.

Verkhatsky A, Rodriguez JJ, Parpura V. Calcium signalling in astroglia. *Mol Cell Endocrinol.* 2012, 353:45–56.

Verkhatsky A. Physiology and pathophysiology of the calcium store in the endoplasmic reticulum of neurons. *Physiol Rev.* 2005; 85:201–279.

Vila M, Jackson-Lewis V, Guégan C, Wu DC, Teismann P, Choi DK, Tieu K, Przedborski S. The role of glial cells in Parkinson's disease. *Curr Opin Neurol*, 2001; 14, (4):483-489.

Vives-Bauza C, Przedborski S. Mitophagy the latest problem for Parkinson's disease. *Trends MolMed*. 2011 ;17(3):158-65.

Wakabayashi K1, Hayashi S, Yoshimoto M, Kudo H, Takahashi H. NACP/alpha-synuclein-positive filamentous inclusions in astrocytes and oligodendrocytes of Parkinson's disease brains. *Acta Neuropathol*, 2000; 99, (1):14-20

Wang Q, Liu Y, Zhou J. Neuroinflammation in Parkinson's disease and its potential as a therapeutic target. *Transl Neurodegener*. 2015; 12: 4-19.

Wang X, Bukoreshtliev NV, Gerdes HH. Developing neurons form transient nanotubes facilitating electrical coupling and calcium signalling with distant astrocytes. *PLoS One*. 2012;7(10): e47429.

Weber CR, Ginsburg KS, Philipson KD, Shannon TR, Bers DM. Allosteric regulation of Na/Ca exchange current by cytosolic Ca in intact cardiomyocytes. *J. Gen. Physiol*. 2001; 117: 119-131.

Weissman BA, Raveh L. Peripheral benzodiazepine receptors: on mice and human brain imaging. *J Neurochem*. 2003; 84:432-437.

Wersinger C, Jeannotte A, Sidhu A. Attenuation of the norepinephrine transporter activity and trafficking via interactions with alpha-synuclein. *Eur. J. Neurosci*. 2006a; 24: 3141-3152.

Wersinger C, Prou D, Vernier P, Sidhu A. Modulation of dopamine transporter function by alpha-synuclein is altered by impairment of cell adhesion and by induction of oxidative stress. *FASEB J*. 2003; 17: 2151-2153

Wersinger C, Rusnak M, Sidhu A. Modulation of the trafficking of the human serotonin transporter by human alpha-synuclein. *Eur. J. Neurosci*. 2006b; 24, 55-64.

Wiesner J, Vilcinskas A. Antimicrobial peptides: the ancient arm of the human immune system. *Virulence*. 2010; 1:440-64.

Williams AJ, Fry CH. Calcium-proton exchange in cardiac and liver mitochondria. *FEBS Lett.* 1979; 97: 288–292.

Wilms H, Rosenstiel P, Romero-Ramos M, Arlt A, Schafer H, Seegert D, Kahle PJ, Odoy S, Claasen JH, Holzknicht C, Brandenburg LO, Deuschl G, Schreiber S, Kirik D, Lucius R. Suppression of MAP kinases inhibits microglial activation and attenuates neuronal cell death induced by alpha-synuclein protofibrils. *Int J Immunopathol Pharmacol* 2009; 22:897–909.

Wilson CJ and Callaway JC. Coupled oscillator model of the dopaminergic neuron of the substantia nigra. *J. Neurophysiol.* 2000; 83: 3084–3100.

Winkfein RJ, Szerencsei RT, Kinjo TG, Kang K, Perizzolo M, Eisner L, Schnetkamp PP. Scanning mutagenesis of the alpha repeats and of the transmembrane acidic residues of the human retinal cone Na/Ca-K exchanger. *Biochemistry.* 2003; 42:543–552.

Winner B, Jappelli R, Maji SK, Desplats PA, Boyer L, Aigner S, Hetzer C, Loher T, Vilar M, Campioni S, Tzitzilonis C, Soragni A, Jessberger S, Mira H, Consiglio A, Pham E, Masliah E, Gage FH, Riek R. In vivo demonstration that alpha-synuclein oligomers are toxic. *Proc Natl Acad Sci U S A* 2011; 108:4194–4199

Winslow AR, Rubinsztein DC. The Parkinson disease protein alpha-synuclein inhibits autophagy. *Autophagy.* 2011; 7 (4): 429–431.

Winslow AR, Chen CW, Corrochano S, Acevedo-Arozena A, Gordon DE, Peden AA, Lichtenberg M, Menzies FM, Ravikumar B, Imarisio S, Brown S, O’Kane CJ, Rubinsztein DC. Alpha-Synuclein impairs macroautophagy: implications for Parkinson’s disease. *J. Cell Biol.* 2010; 190 (6): 1023–37.

Wong YC, Holzbaur EL. Autophagosome dynamics in neurodegeneration at a glance. *J. Cell. Sci.* 2015; 128 (7) 1259–126710.

Wu DC, Jackson-Lewis V, Vila M, Tieu K, Teismann P, Vadseth C, Choi DK, Ischiropoulos H, Przedborski S. Blockade of microglial activation is neuroprotective in the 1-methyl- 4-phenyl-1,2,3,6-tetrahydropyridine mouse model of Parkinson disease. *J Neurosci,* 2002; 22, (5):1763-1771.

Wyss-Coray T, Mucke L. Inflammation in neurodegenerative disease--a double-edged sword. *Neuron* 2002; 35, (3): 419-432

Xu W, Lipscombe D. Neuronal Ca(V)1.3alpha (1) L-type channels activate at relatively hyperpolarized membrane potentials and are incompletely inhibited by dihydropyridines. *J Neurosci* .2001; 21:5944–5951

Yamaguchi Y, Nagase T, Tomita T, Nakamura K, Fukuhara S, Amano T, et al. Beta-defensin overexpression induces progressive muscle degeneration in mice. *Am J Physiol Cell Physiol*. 2007; 292:C2141–9.

Yamamoto M, Kim M, Imai H, Itakura Y, Ohtsuki G. Microglia-Triggered Plasticity of Intrinsic Excitability Modulates Psychomotor Behaviors in Acute Cerebellar Inflammation. *Cell Rep*. 2019; 28(11):2923-2938

Yavich L, Tanila H, Vepsäläinen S, Jakala P. Role of alpha-synuclein in presynaptic dopamine recruitment. *J Neurosci*. 2004; 24: 11165–11170.

Yu L, Colvin RA. Regional differences in expression of transcripts for Na<sup>+</sup>/Ca<sup>2+</sup> exchanger isoforms in the rat brain. *Brain Res Mol Brain Res*.1997; 50(1-2):285-92.

Zarranz JJ, Alegre J, Gomez-Esteban JC, Lezcano E, Ros R, Ampuero I, Vidal L, Hoenicka J, Rodriguez O, Atares B, et al. The new mutation, E46K, of alpha-synuclein causes Parkinson and Lewy body dementia. *Ann Neurol*. 2004; 55:164–173

Zhang W, Wang T, Pei Z, Miller DS, Wu X, Block ML, et al. Aggregated alpha-synuclein activates microglia: a process leading to disease progression in Parkinson's disease. *FASEB J*. 2005; 19:533–42.

Zhang W, Wang T, Pei Z, Miller DS, Wu X, Block ML, Wilson B, Zhou Y, Hong JS, Zhang J. Aggregated alpha-synuclein activates microglia: a process leading to disease progression in Parkinson's disease. *Faseb J*. 2005; 19:533–542.

Zhao W, Xu Z, Cao J, Fu Q, Wu Y, Zhang X, Long Y, Zhang X, Yang Y, Li Y, Mi W. Elamipretide (SS-31) improves mitochondrial dysfunction, synaptic and memory impairment induced by lipopolysaccharide in mice. *J Neuroinflammation*. 2019; 20;16(1):230.

Zhou R, Yazdi AS, Menu P, Tschopp J. A role for mitochondria in NLRP3 inflammasome activation. *Nature*. 2011; 469(7329):221–5.

Zhou RM, Huang YX, Li XL, Chen C, Shi Q, Wang GR, Tian C, Wang ZY, Jing YY, Gao C, Dong XP. Molecular interaction of alpha-synuclein with tubulin influences on the polymerization of microtubule in vitro and structure of microtubule in cells. *Mol. Biol. Rep.* 2010; 37: 3183–3192.

Zhu M, Fink AL. Lipid binding inhibits alpha-synuclein fibril formation. *J. Biol. Chem.* 2003; 278: 16873–16877.